PETROGENESIS OF THE BANDED GNEISSIC COMPLEX AROUND MASUDA, RAJASTHAN : IMPLICATIONS FOR THE PRECAMBRIAN CRUSTAL EVOLUTION OF THE ARAVALLI CRATON, NW INDIA

A THESIS

submitted in fulfilment of the
requirements for the award of the degree
of
DOCTOR OF PHILOSOPHY
in
EARTH SCIENCES

By

JAYARAM SAHOO

DEPARTMENT OF EARTH SCIENCES
UNIVERSITY OF ROORKEE
ROORKEE-247 667 (INDIA)

NOVEMBER, 1996

Gratis

CANDIDATE'S DECLARATION

I hereby, certify that the work which is being presented in this thesis entitled **" PETROGENESIS OF THE BANDED GNEISSIC COMPLEX AROUND MASUDA, RAJASTHAN: IMPLICATIONS FOR THE PRECAMBRIAN CRUSTAL EVOLUTION OF THE ARAVALLI CRATON, NW INDIA"** in fulfilment of the requirement for the award of the Degree of **Doctor of Philosophy**, submitted in the **Department of Earth Sciences** of the University, is an authentic record of my own work carried out during a period from November, 1990 to November, 1996 under the supervision of Dr. S. Balakrishnan.

The matter embodied in this thesis has not been submitted by me for the award of any other degree.

Jayaram Sahoo

JAYARAM SAHOO

This is to certify that the above statement made by the candidate is correct to the best of my knowledge.

S. Balakrishnan

DR. S. BALAKRISHNAN

Assistant Professor
Department of Earth Sciences
University of Roorkee
Roorkee -247667, U.P
INDIA

Date : Nov. 4, 1996

The Ph.D. viva-voce examination of **Mr. Jayaram Sahoo** Research Scholar, has been held on ...12-4-1997.....

S. Balakrishnan — Signature of Supervisor

Signature of H.O.D.

Signature of External Examiner

ACKNOWLEDGEMENT

I take this opportunity to express my heartiest thanks to my Supervisor **Dr. S. Balakrishnan** for his expert guidance throughout the present work. I learnt the different analytical techniques in geochemistry due to his constant and vigilant guidance. Eversince, he introduced the world of geochemistry to me in a profound way, I found the analytical work more fascinating, challenging and innovative in due course. His constructive criticism and encouragement from time to time enabled me to bring the thesis to the present form.

I am indebted to the present Head of the Department **Prof. S.K. Upadhyay** and former Heads, late **Prof. R.K. Goel** and **Prof. A.K. Jain** for extending various facilities for carrying out research work in the department.

The help, advice, suggestions and guidance from **Prof. V. Rajamani**, JNU, New Delhi during the various stages of research work is gratefully acknowledged.

I am grateful to **Directors,** University Science Instrumentation Centre and Atomic Mineral Division, Hyderabad for extending the analytical facilities for certain key elements on the rocks.

I gratefully acknowledge the discussions with **Prof. V.K.S. Dave** and **Prof. B.B.S. Singhal** which helped in improving the quality of my work and understanding.

My heartfelt thanks goes to **Dr. S.K.Arora**, BARC, Mumbai for his constant encouragement and advice.

I would thank **Dr. D.C. Srivastava** for his valuable guidance in the field, **Dr. D.K. Mukhopadhyay** and **Dr. R.M. Manickavasagam** in the thin section study.

I would also like to thank **Dr. T. Ahmad**, Wadia Institute of Himalayan Geology, Dehradun for his help, valuable suggestions and thought provoking discussions which I had with him during the preparation of the thesis. I feel obliged to **Dr. N.S. Shivasiddaiah** and **Dr. J.K. Zachariah** for their scientific help which was quite helpful in understanding the subject of geochemistry.

The help and hospitality provided by **Mr. Jagmohan Singh Meena,** the then BDO of Masuda Block during the geologial field works carried out in and around Masuda is gratefully acknowledged. I enjoyed the field trip with friends like **Pradhan**, **Nag**, **Yadav**, **Panigrahy** and

Bodo during the field works in Rajasthan. I also thank **Ram Karan**, **Bhim Singh** for their valuable help during the field work.

Seniors like **Manoj Mahanta** and friend **Giritharan** were very cooperative in developing the preconcentration procedure for effective determination of REEs by ICP-AES at JNU and Roorkee.

Any attempt to thank friends like **Tarun, Sanjeev** and **Tinku** will be a droplet in the ocean. The help and moral support from them particularly during the last stage of thesis preparation is memorable and unforgettable. They were instrumental in boosting up my sagging morale and made me sail through the most difficult times of the thesis.

The help extended by **Sri Nair**, **Sri Nandan Singh**, **Sri Ramdal Mishra** and **Sri Amar Singh** during different stages of thesis work is duly acknowledged.

The moral strength received from the senior friends like **Manas Mohanty**, **Drs. R.C. Patel, G.J. Chakrapani**, **Sandeep Singh**, **Kamal Pruseth**, **B.K. Bhadra**, **Tamal Ghosh**, **L.P. Singh**, **Pankaj Srivastava**, **A. Asokan**, **H.N. Sihna**, **A.K.seth**, **Mr. Anurag Khanna**, **Mr. Dinesh Tewari** and **Mr. Alok Sahai** at various stages of their stay at Roorkee are unforgettable.

I would like to thank my lab mates **Basir**, **Mandal**, **Tarun**, **Jyoti**, **Diganta** and **Prasanjit** for their help and discussions during different stages of work.

I would also like to acknowledge the help received from fellow colleagues **Thomas**, **Puspender**, **Premananda**, **Sundaram**, and **Ajay** from time to time. I am grateful to **Piyush** and **Binod** who helped me at the difficult times. Young friends like **Kaushik**, **Tanmay** and **Prasanjit** were very useful in the preparation of the document.

I am equally thankful to **Dr. Bikash Mohanty** and **Mrs. Pratima Mohanty** who have always supported me in personal as well as academic front. The **little Debjyoti** made my stay at Roorkee more pleasant.

I am obliged to my **parents**, **uncles**, **brothers**, **sisters** and **family members** who provided the much needed moral support during the Ph.D. work. I am deeply obliged to my **mother** who had to stay with me for one and half year at Roorkee during the preparation of the thesis. The help, encouragement received from my cousin **Manas** and his wife **Sunita**, who never failed to inquire about my Ph.D is warmly thanked .

The financial assistance received from Bhaba Atomic Research Centre, Mumbai in the form of **Dr. K.S. Krishnan DAE Research Fellowship** for carrying out the present work is gratefully acknowledged.

Jayaram Sahoo

JAYARAM SAHOO

ABSTRACT

The Precambrian Banded Gneissic Complex in the northern part of Aravalli Craton, Rajasthan, is lithologically heterogeneous. Both meta-igneous and meta-sedimentary lithologies constitute the Banded Gneissic Complex. The meta-igneous rocks are classified as amphibolites, diorite-monzodiorite-quartz diorite gneisses and granodiorite gneisses with small volumes of granophyres and aplites. The meta-sedimentary components are defined by cherts, calc-silicate rocks, garnet-biotite-schist and migmatized mica schist. Mineral chemistry data on amphibolites indicate that the rocks of Banded Gneissic Complex had attained amphibolite grade of metamorphism. The rocks had been subjected to four phases of folding and two episodes of shearing. They are inter banded and co-folded in all scales. Contact relationships between the different litho-units appear to be tectonic.

The amphibolites are silica undersaturated Fe-enriched tholeiites and they have higher K_2O and lower Ni than Archaean tholeiites. They exhibit a flat to slightly light REE enriched chondrite normalized REE patterns. The REE and other less mobile trace element characteristics of the amphibolites are very much comparable to the marginal sea basalts. Quantitative geochemical modelling suggests that they are derived by 5-20% partial melting of flat to slightly light REE depleted mantle sources, but had higher [Fe]/[Mg] ratio than garnet lherzolite.

The diorite-monzodiorite-quartz diorite rocks occur both as volcanic flows and plutonic bodies in the field. On the basis of geochemistry, they are classified as sanukitoids. Further, on the basis of TiO_2/MgO ratio they are classified as low-Ti and high-Ti sanukitoids. The sanukitoids have light REE and large ion lithophile elements enriched characteristics. The low-Ti sanukitoids have higher mg#, lower Ba, Sr, Zr, Nb and light REE abundances than the high-Ti sanukitoids.

On the basis of geochemical modelling, it is suggested that magmas represented by the sanukitoids could not have derived by partial melting of tholeiitic amphibolites occurring in the Masuda area. Further, neither fractional crystallization nor assimilation cum fractional

crystallization of tholeiitic parental magmas could produce the observed elemental abundances in the sanukitoids. [Mg]-[Fe] modelling suggests that magmas represented by two sanukitoid suites could have been derived from mantle sources with high but variable [Fe]/[Mg] ratios and at different pressure and temperature conditions. High-Ti sanukitoids could not be related to low-Ti sanukitoids either by fractional crystallization or by assimilation cum fractional crystallization.

It is suggested that the sanukitoid magmas were derived from enriched sources. Such enrichment could have occurred by addition of fluids or melts derived from deeper sources prior to melting. The sources for the high-Ti sanukitoid magmas were relatively more enriched in LILEs, LREEs and Nb compared to the sources for the low-Ti sanukitoid magma.

The granodiorite suite of rocks form chemical continuum with sanukitoids. On the basis of REE and other trace element abundances, they are classified into two different suites. The suite-I has higher LREE, HREE and large negative Eu anomalies compared to the second suite. The granodiorite suite-I might have been derived by partial melting of a source similar to the sanukitoids. The parental magma thus derived could have undergone variable extents of fractional crystallization of plagioclase, alkali-feldspar and allanite which gave rise to residual magmas representing samples of this suite.

The suite-II of granodiorites have chondrite normalized REE patterns sub-parallel to that of the low-Ti sanukitoids, but have lower REEs and large ion lithophile elements compared to the latter. Furthermore, granodiorites and sanukitoids have overlapping biotite compositions. The magmas represented by the granodiorite suite-II might have fractionated from parental sanukitoid magmas by processes including magma unmixing.

Granophyres and aplite veins, occupy a small volume proportion of the study area. The foliated granophyres could have crystallized from residual fluids formed during last stages of crystallization of sanukiotids and granodiorite magmas. The post-tectonic aplite veins could have crystallized from hydrothermal fluids formed during high grade metamorphism.

Petrogenetic considerations of sanukitoids and granodiorite suites indicate that they were emplaced in an arc related tectonic setting. Whereas, the amphibolites are suggested to represent magmas emplaced in marginal basin environment.

These geochemically diverse suite of rocks with distinct petrogenetic histories which were emplaced in different tectonic settings are closely associated in space and make up the Banded Gneissic Complex in the study area. They must have been brought together by accretionary processes. Subsequently, the amphibolites and granodiorite gneisses were co-folded and sheared to give rise to present - day character of the Banded Gneissic Complex in the northern Aravalli Craton.

LIST OF TABLES

LIST OF FIGURES

CHAPTER V

CHAPTER VI

LIST OF PLATES

CHAPTER I

INTRODUCTION

The continental crust consists of more than 80% of the Precambrian rocks (Condie,1981; Radhakrishna and Naqvi, 1986; Naqvi and Rogers, 1987). Hence, studies on Precambrian rocks are important in understanding growth and evolution of the continental crust. It is considered that by the end of Archaen (2500 Ma ago) the continental crust stabilized and during post Archaen epochs, igneous activities were characterized by reworking of Archaean continental crust (e.g. Hofmann, 1988; Taylor, 1989; Rapp and Watson, 1995). This hypothesis is also supported by distinct changes in REE characteristic of shales. The geochemistry of shales is considered to represent average composition of the continenetal crust at the time of its formation. The Archaean shales are reported by Taylor and McLennan (1985) to have chondrite normalized REE patterns without Eu anamolies. Whereas, post-Archaean shales have more fractionated chondrite normalized REE patterns with significant negative Eu anamolies (Taylor and McLennan, 1985).

Whereas, Taylor (1967) and Moorbath and Taylor (1982) susggested that the post-Archaean continental growth is pre-dominantly by newer additions from mantle. Thus, it is essential to find out whether continental reworking or juvenile additions from mantle was the dominant process in evolution of continents during early Proterozoic (2500 - 1000 Ma).

The mechanism of continental growth during early Proterozoic is also not clear. Accretion of rocks generated at arcs to continental margin is considered as the dominant tectonic process responsible for Phanerozoic crustal evolution (Saleeby, 1983; Allegre et al., 1984). Whether the continental growth during Precambrian is dominated by accretionary tectonic process or by vertical tectonics (underplating of magmas) needs to be addressed.

Kay and Kay (1988) observed that at the convergent plate margins the crust-mantle recycling gives rise to formation of new continental crust. At the subduction zones, when altered basaltic crust goes back to the mantle it releases hydrous fluids by dehydration reactions which enrich and cause partial melting of the mantle wedge (Thompson, 1992). Whereas, Rudnick (1990)

and Voshage et al. (1990) argued that underplating of mantle derived basaltic magma plays an important role in thickening and growth of continental crust on the basis of study of xenoliths from the lower crust (Rudnick and Taylor, 1987) and sub-continental lithospheric mantle (MacGregor and Manton, 1986). Therefore, geochemical studies will be useful to identify the mechanism of continental crustal growth in a given terrane.

Archaean terranes are considered to be predominantly made up of tonalite-trondhjemite-granodiorite (TTG) suite (Barker and Arth, 1976; Barker, 1981). The magmas of TTG suite are considered to have been derived by partial melting of subducted basaltic oceanic crust during the Archaean. It is assumed that the Archaean geothermal gradient was steeper, subduction was faster, which resulted in subduction of young and hot basaltic oceanic crust (Parson and Sclater, 1977). This has facilitated partial melting of hot subducting slab yielding magmas parental to the Archaean TTG suite (Drummond and Defant, 1990).

However, in the present day, the source for arc magmas are considered to be the mantle wedge rather than the subducting slab (Kay et al., 1993). Because, the subducting slab in the present day is considered to be older and colder than their Archaean analogs and the modern geothermal gradient in the subduction zone is also not high enough to cause significant partial melting of the slab.

Whereas, Shirey and Hanson (1984), Balakrishnan and Rajamani (1987) and Stern and Hanson (1991) reported that sanukitoid-granodiorite suite of rocks predominantly constitute the Late Archaean terranes studied by them. They also suggested that the magmas representing the sanukitoid-granodiorite suites were derived from enriched shallow mantle sources.

Therefore, it is important to assess the relative roles of subducted slab and mantle wedge as sources for granitoid rocks which predominate Precambrian terranes, such as, the Banded Gneissic Complex, in northern Aravalli Craton.

The study area consists of rocks of early Proterozoic (Chaudhury et al., 1984; Sarkar et al., 1989) and forms part of the northern Banded Gneissic Complex of the Aravalli Craton, NW India. The igneous suite in the study area have wide mineralogical and geochemical variations. The predominant rock types include amphibolites, diorite, monzodiorite, quartz diorite (sanukitoids) and granodiorite gneisses with small volume of aplite and granophyres. The rocks of the area have undergone amphibolite facies of metamorphism and several episodes of deformations, including, a minimum of four phases of folding and two episodes of shearing (Srivastava et al., 1995).

Heron (1953) considered the Banded Gneissic Complex as the oldest and lithologically heterogeneous unit. Whereas, Naha et al. (1967) considered the Banded Gneissic Complex to be

the migmatization product of Aravalli Supergroup of rocks. One of the objectives of this study is to know the geochemical characteristics of the different components that constitute the BGC in northern Aravalli Craton and compare it with the rocks of the Banded Gneissic Complex exposed around Nathdwara and Udaipur (southern Aravalli Craton) using the data from published literature (Ahmad and Rajamani, 1991; Ahmad and Tarney, 1994; Gopalan et al., 1990).

The geochemical approach is an important tool in understanding the crustal evolution through time. From the major, trace and rare earth element abundances of the rocks, it is possible to place constraints on the models for source characteristics, magmatic processes and the tectonic conditions of their emplacement. Such studies have been carried out by Rajamani et al. (1985), Krogstad et al. (1989), Peucat et al. (1989), Jayananda et al. (1995) in south India and Ahmad and Rajamani (1991) and Ahmad and Tarney (1994) in southern Aravalli Craton. Here, an attempt is made to understand the early Proterozoic crustal evolution in the northern Aravalli Craton by placing constraints on models for petrogenesis of igneous rocks using geochemical data.

CHAPTER II

GEOLOGY OF THE ARAVALLI CRATON

2.1 ARAVALLI CRATON

Indian peninsula is considered as a mosaic of Dharwar, Bhandara, Singhbhum and Aravalli Cratons (Radhakrishna & Naqvi, 1986). The Dharwar Craton makes up the southern part of the Indian Peninsula and it has been extensively studied for the past two decades (Janardan et al., 1982; Rajamani et al., 1985; Krogstad et al., 1989; Jayananda et al., 1995). Bhandara Craton occupies the central portion of peninsula (Naqvi & Rogers, 1987). Singhbhum Craton represents the eastern part of the peninsula. The western part of the peninsula is known as Aravalli Craton (Fig. 2.1).

The Aravalli Craton is bounded by the Himalayas in the north, the Cambay graben on the south-west and the Narmada-Son lineament on the south and Vindhyans as well as Deccan Traps on the east. In the west the Aravalli Craton is covered with recent alluvial deposits (Naqvi & Rogers, 1987). The exposures are along the Aravalli Mountain Ranges and in the Bundelkhand massif and the Son valley region. The Aravalli Craton is separated from Vindhyan sedimentary basin by a major lineament, known as the Great Boundary Fault.

The Aravalli Craton is approximately 700 Km in length from Delhi in the north to the plains of Gujarat in the south. The Aravalli Craton is predominantly exposed in the state of Rajasthan with the thinnest part towards south of Ajmer. However, sporadic occurrences of rocks of the Craton are found in the states of Haryana, Delhi, Gujarat and Madhya Pradesh. Three major fundamental geological formations/units constitute the Aravalli Craton. The oldest and lithologically diverse unit is termed as Banded Gneissic Complex (BGC) which is followed by metasedimentary units of the Aravalli and Delhi Supergroup of rocks in the younging order (Heron, 1953).

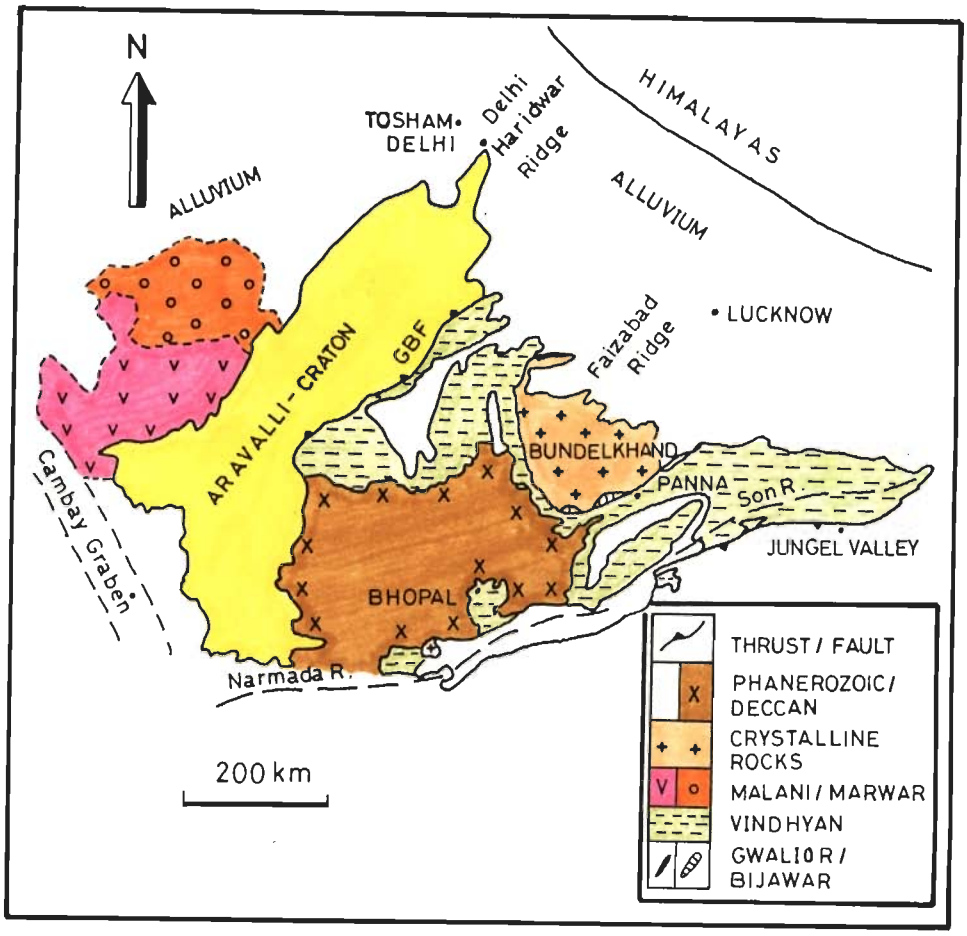

Fig. 2.1 **Generalized geological map of northern part of the Indian peninsula showing the Aravalli Craton and major litho units around it (after Naqvi and Rogers, 1987).**

2.1.1 BANDED GNEISSIC COMPLEX

Heron (1917) introduced the terminology "Banded Gneissic Complex" (BGC) to describe what he considered as stratigraphically the oldest group of rocks (Pre-Aravalli rocks) in Rajasthan. The BGC occurs mainly in three areas in the Aravalli Craton (Fig. 2.2) and they are:

(i) Southern BGC rocks are best exposed around Nathdwara, Parsola and south of Salumbar. They are bounded by the Aravalli Supergroup of rocks and Deccan Flood basalts (Fig.2.2).

(ii) Central BGC rocks are mainly confined to the area west of Chittaurgarh. They are bounded by rocks of the Aravalli and Vindhyan Supergroup in the east and west respectively (Fig.2.2).

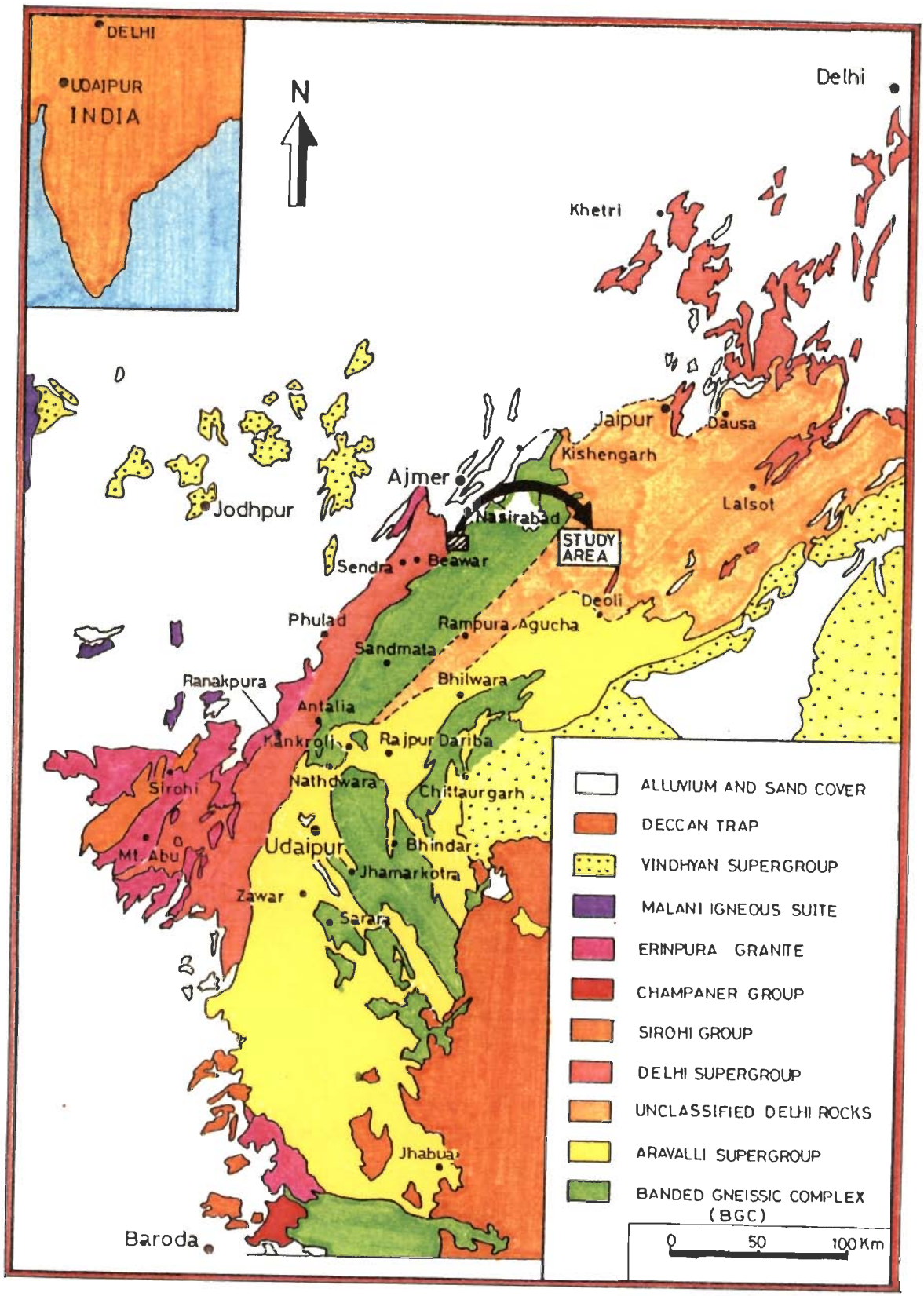

FIG.2.2 Generalized Geological Map of Aravalli Craton (after Roy, 1988)

(iii) Continuous exposure of northern BGC rocks are located between south of Ajmer and Sandmata. It is bounded by alluvium in the north and by the Aravalli Supergroup of rocks in the south as well as east whereas, the western boundary is marked by a continuous linear belt of the Delhi Supergroup of rocks (Fig. 2.2).

Foliated biotite and chlorite schists, hornblende-schist, epidiorites, granitic gneisses, calc-schists/gneisses and unfoliated granitoids make up the BGC which is also known as composite gneiss (Heron, 1953). Aplites, pegmatites and numerous quartz veins occur as intrusives. Migmatites and amphibolites also occur in different proportions within the BGC. Granulites are reported from the northern BGC terrane. However, the predominant group of rocks are granitoids (foliated and unfoliated) which frequently alternate with schistose rocks such as, amphibolites and biotite-muscovite-schists, giving a banded appearance to it.

2.1.2 ARAVALLI SUPERGROUP

The Aravalli Supergroup consists of rocks of the Aravalli System and Raialo series of Heron (1953). Subsequent workers found no evidence of an unconformity between rocks of the Raialo Series and the Aravalli System in the Pur-Banera and Zahazpur belts (Sen, 1970, 1983). Therefore, it is justifiable to include both groups of rocks in the Aravalli Supergroup (Roy, 1988).

Predominantly, it consists of slates, phyllites, mica schist + garnet + magnetite, quartzites and garnet bearing hornblende schists. Nathdwara-Udaipur-Jhabua section is considered as the type locality for the Aravalli Supergroup where the complete succession of all the formations have been observed. Poddar (1966) and Roy & Paliwal (1981) reported the presence of shelf facies and deep water facies in the type area. The rocks were metamorphosed to greenschist to middle amphibolite facies conditions. The basal part of the Aravalli Supergroup is represented by chert/quartzite and mafic meta-volcanics (Roy et al., 1984).

2.1.3 DELHI SUPERGROUP

The Delhi Supergroup of rocks occur as a linear belt in the central Rajasthan. The northern end of this belt extends from Haryana in the north to Gujarat in the south. The Delhi Supergroup is bounded by the BGC in the east and Erinpura granite with discontinuous patches of Vindhyan rocks in the west. Further, alluvial covers occupy the greater part in the north.

Rocks of lower Alwar and Upper Ajabgarh Group constitute the main body of Delhi Supergroup. The Alwar group of rocks are arenaceous in nature characterized by arkosic grits and conglomerates with quartzite occurring in the basal part whereas, the Ajabgarh Group rocks,

which are argillaceous in nature, is dominated by phyllites, calc-gneisses, calc-schists and biotite schist.

Sinha Roy (1988) classified the Delhi Supergroup of rocks into North Delhi Belt and South Delhi Belt on the basis of contrasting sedimentary facies assemblages. According to him, the North Delhi Belt contains an older, shallow water sedimentary facies of rocks with volcanics. Whereas, younger, deep water carbonate facies of rocks with volcanics and mafic-ultramafic rock assemblages make up the south Delhi Belt. However, the Delhi Belt as a continuous sequence of rocks from north to south was advocated by Naha et al. (1984) based on structural similarity. Similarity in metamorphic imprints and continuous lithostratigraphy at northern and southern extremeties have been substantiated by Sharma (1988) and Singh (1988) respectively. Hence, it can be inferred that Delhi Supergroup of rocks occurring in the north and south are indistinguishable with respect to structures present and grade of metamorphism.

2.2 STRUCTURE OF THE ARAVALLI CRATON

2.2.1 BANDED GNEISSIC COMPLEX

Structural history of the Banded Gneissic Complex (BGC) exposed in central and southern Rajasthan have been well documented by Naha et al. (1966, 1967, 1969), Naha and Chaudhury (1968) and Naha and Majumdar (1971a). They reported two phases of deformation in the rocks of the BGC. The first phase of structures are reclined, inclined isoclinal folds with dominantly westerly trend. The second set of structures are upright folds with north-northeast (N-NE) trending axial planes. Further, Naha et al. (1973) and Naha (1983) reported coaxial refolding of F_1 structures in the BGC at some places. As a result of coaxial folding the inclined and reclined nature of the F_1 folding was developed. The interference of F_1 and F_1' (co-axially refolded F_1) with F_2 gave rise to superposed folds.

The superimposition of the second phase upright folds on the first phase isoclinal, reclined folds led to the development of a number of fold interference patterns due to variable orientation of axial planes and fold axes. As a result, the hook shaped, mushroom and eyed folds with dome and basin structures developed. Naha et al. (1967) considered the outcrop patterns of the hammer head and hook syncline (Heron, 1953) as a result of interference of F_1 with F_2 folds.

Further, more detailed structural investigations in southern Rajasthan by Naha (1983), Naha et al. (1984) and Naha and Mohanty (1988, 1990) revealed the presence of two phases of deformation (F_3 and F_4) in addition to the earlier two phases of deformation ($F_1$and F_2). The third

and fourth generation structures are mainly confined to schistose rocks and occur as kink bands and conjugate folds.

In the northern part of Rajasthan, structural studies in the exposed BGC rocks were carried out by Sharma and Upadhyay (1975), Sharma (1977) and Pyne and Bandopadhyay (1985). Sharma and Upadhyay (1975) showed two phases of deformation while the work of Sharma (1977) suggested three phases of deformation. The first generation structures (F_1) developed in the axial surfaces in the small scale. They are isoclinal in nature and the fold axes trend in the NE direction. The second generation folds (F_2) are tight to open asymmetric folds best developed in the limbs or axial plane surfaces of the first folds (F_1). The third deformational structures considered by Sharma (1977) as the pre-Delhi orogeny are recumbent to reclined folds with fold axes plunging towards W to WNW.

Further, investigations by Mukhopadhyay and Dasgupta (1978) in Badnor, Gangopadhyay and Lahiri (1988) in Deogarh and Guha and Bhattacharya (1993) in Sandmata Complex, reported three folding events. According to Mukhopadhyay and Dasgupta (1978), the development of schistosity took place due to F_1 folding and subsequently F_2 folded F_1 schistosity producing crenulation cleavage pattern. They also reported dextral nature of the F_2 folds. The third generation structures are sinistral folds with dipping axial planes striking E-W to ENE-WSE. In addition to polyphase folding, Guha and Bhattacharya (1993) reported two phases of ductile deformation in the high grade rocks of the Sandmata complex.

The recumbent, reclined folds of Sharma (1977), tight to isoclinal minor folds with stripping lineation, well developed gneissic foliation (locally mylonitic) with steeply dipping stretching lineations (west of Beawar) of Tobisch et al. (1994) are absent in the cover rocks of the Delhi Supergroup in northern BGC.

Structure of the Study Area

The study area falls under northern BGC of Aravalli Craton. On the basis of detailed structural mapping, Srivastava and Yadav (1994) and Srivastava et al. (1995) have demonstrated four phases of folding in the basement rocks (F_1-F_4). The F_1 phase of folding comprised of three different sub groups designated as F_{1A},F_{1B},F_{1C} which are co-axial and co-planar in nature. F_2 folds contain F_1 deformed lineations on their folded surfaces and hence differ from the F_1 group of folds. The F_3 folds show recumbent geometry, whereas, the F_4 folds have steep axial plane and are orthogonal to the regional foliation in the basement.

F_1 and F_2 group of folds control the outcrop pattern and structural geometry of the basement rocks and are non cylindrical in nature and exihibit sheath like geometry. According to them, the noncylindricity and sheath like geometry may be attributed to repeated events of ductile shearing. These authors have also reported the presence of abundant meso scale ductile shear zones in the basement. The predominant ductile shear zones are those which are developed along the axial planes of the F_1 and F_2 folds. On the basis of sense of movements, they are classified as dextral and sinistral. The large scale structure in the study area is a northerly closing fold attributed to the interference of F_1 and F_2 phases of folding Srivastava and Yadav (1994) and Srivastava et al. (1995)

2.2.2 ARAVALLI SUPERGROUP

Record of the complex structural pattern of the Aravalli Supergroup due to multiple deformational events in different parts of the Aravalli Craton have been worked out by Naha et al. (1966), Roy et al. (1971, 1980, 1985), Sengupta (1976), Naha and Halyburton (1977b), Roy and Bejarniya (1984), Mohanty and Naha (1986), Naha and Mohanty (1988) and Roy and Nagori (1990). In general, the Aravalli Supergroup of rocks have undergone at least, four phases of folding. Out of these, AF_1, AF_2 & AF_3 phases are prominently developed while AF_4 folds are developed only sporadically (Roy, 1973; Naha and Halyburton, 1977b; Mohanty and Naha, 1986; Paliwal, 1988; Naha and Mohanty, 1988).

By and large, the deformation pattern of the Aravalli Supergroup (AF_1, AF_2, AF_3 & AF_4) are comparable with that of the Delhi Supergroup of rocks (Naha and Mukherjee, 1969; Naha and Halyburton, 1974a). However, the steeply plunging reclined folds and down dip linear structures characteristic of the Aravalli rocks are absent in the Delhi rocks (Naha and Halyburton, 1977b; Mukhopadhyay and Dasgupta, 1978).

2.2.3 DELHI SUPERGROUP

Polyphase deformations have affected the Delhi Supergroup of rocks (Mukhopadhyay and Dasgupta, 1978; Roday, 1979; Roy, 1983; Naha et al., 1984; Gangopadhyay and Mukhopadhyay, 1987). Sharma (1977) reported two deformational in the Delhi Supergroup of rocks around Ajmer-Beawar region. Naha et al. (1984) and Naha and Mohanty (1988) have reported four phases of deformational episodes in the north and central parts of the Aravalli Craton. Naha and Halyburton (1977b) demonstrated the absence of the first phase of deformational structures of BGC in the Delhi Supergroup of rocks in central Rajasthan. Mukhopadhyay and Dasgupta (1978) also recorded similar observation within the Delhi Supergroup of rocks in northern part of the

Aravalli Craton around Badnor and reported three phases of deformation affecting the Delhi rocks. Further, they have shown that earlier structure in the BGC (F_1 folds) predate the deposition of Delhi Supergroup of rocks and attributed the outcrop pattern of Delhi Supergroup of rocks to the second phase of deformation.

2.3 BASEMENT - COVER RELATIONSHIP

2.3.1 BGC-ARAVALLI SUPERGROUP

Crookshank (1948) considered the rocks of the Banded Gneissic Complexe as the granitized equivalents of the Aravalli-Raialo rocks. However, Heron (1953) suggested that the BGC acted as the basement for rocks of the Aravalli Supergroup on the basis of angular unconformities observed south-east of Nathdwara and an erosional unconformity at Rajnagar, north-east of Nathdwara.

Raja Rao (1970) and Raja Rao et al. (1971) supported Heron's observation and suggested that the metasedimentary rocks in the eastern part of the Aravalli Craton, including the rocks of Chittaurgarh and Bhilwara regions were older than the rocks around Udaipur, which is considered as the type area for the Aravalli Supergroup (Roy et al., 1981).

Naha and Majumdar (1971b) considered the conglomerates at the base of the Aravallis to be of non-sedimentary origin which had originatined from folding and stretching of vein quartz and quartzitic layers in the mica schists. Furthermore, Naha and Halyburton (1974a) reported that both the metasedimentary enclaves and their host rocks within the BGC as well as the metasedimentary rocks outside BGC have similar structural style. Hence, they concluded that the BGC lying between Nathdwara and Amet regions are the migmatized product of the rocks of the Aravalli Supergroup. On the contrary, Sharma (1983a) held the view that rocks of the BGC have experienced several episodes of metamorphism in contrast to the single event of metamorphism to which the Aravalli Supergroup of rocks have been subjected to. Therefore, the BGC seems to be older than the Aravallis and might not be a migmatized product of the latter.

2.3.2 BGC - DELHI SUPERGROUP

According to Heron (1935, 1953) the BGC acted as the basement for the Delhi Supergroup of rocks in the Aravalli Craton. The two stratigraphic entities were separated by an unconformity represented by feldspathic quartzite in the northern part of the Craton. However, Crookshank (1948) and Niyogi (1965) questioned the basement status of the BGC and correlated them with the rocks of the Aravalli Supergroup and their granitoid equivalents. In the southern sector, an erosional unconformity between the Delhi and the BGC is reported by Sen (1970).

In the central part of the Craton, Sen (1970) reported a faulted contact between the BGC and the Delhi Supergroup of rocks. Sharma and Upadhyay (1975) also suggested that the Delhi rocks had slid over the BGC. Further, Sen (1981) suggested a paleosuture between the BGC and the Delhi Supergroup of rocks. Bhattacharya et al. (1995) observed that the Delhi-BGC contact is highly sheared and represents a melange zone.

2.3.3 ARAVALLI - DELHI SUPERGROUP

Based on the regional study, Heron (1953) considered that the rocks of the Delhi Supergroup were laid unconformably over the Aravalli Supergroup of rocks. Gupta et al. (1980) reported the presence of a major lineament along the western boundary of the Delhi Supergroup. This inference is supported by Sugden and Windley (1984), Sinha Roy (1988) and Sugden et al. (1990) that the contact zone between the Aravalli and the Delhi Supergroups is a major suture. The mafic and ultramafic rocks of the Barotiya sequence within Delhi Supergroup characterize the rock assemblages of the lineament or suture. Volpe and McDougall (1990) observed that such a sequence of rocks might have been formed due to closure of an oceanic crust or disrupted island arc or a rift related basin.

2.4 METAMORPHISM

2.4.1 BANDED GNEISSIC COMPLEX

The BGC in the northern sector have been affected by two distinct episodes of metamorphism (Sharma and Narayan, 1975; Sharma, 1977; Sharma and Roy, 1979; Sharma, 1983b). The first episode of metamorphism M1 is represented by staurolite-kyanite zone of the middle amphibolite facies whereas, the second episode which is more regional in nature is characterised by sillimanite-K-feldspar + muscovite zone of the upper amphibolite facies. Similarly, polymetamorphic nature of the BGC rocks around Rampura-Agucha has been documented by Gandhi et al. (1984), Sharma (1988) and Deb and Sarkar (1990).

Occurrences of charnockite and granulites have been reported from the Bhim-Karera region (Rode et al., 1969), Bandanwara (Pandya and Gyani, 1970) and Sandmata area (Sharma, 1983b; Sharma and Joshi, 1984; Joshi, 1985). The high grade rocks in the Bandanwara region are sillimanite-garnet gneiss, diopside bearing amphibole gneiss and granites whereas, the Sandmata rocks are represented by pelitic granulite, basic granulite and olivine norite (hypersthene dolerite). The metamorphic mineral assemblages in the Sandmata area are different from the charnockites of the Bhim-Karera region (Sharma, 1988). Pyne and Bandopadhyay (1985) considered the dolerite of Heron (1953) as mafic granulite based on the presence of hypersthene.

Sharma (1988) estimated pressure of 5.5-6 kb and temperature of 600-700^{0}C on the BGC rocks around Ajmer-Beawar region. Whereas, higher pressure and temperature (8-11 kb and 650-850^{0}C, respectively) conditions of metamorphism have been reported from Sandmata Complex (Sharma, 1990).

In the southern sector, upper amphibolite facies condition prevailed in the BGC rocks around Nathdwara. Biotite-rich layers alternate with predominant granitic materials. The mineral assemblages studied from dark biotite-rich layers and quartzo-feldspathic materials by Sharma (1988) indicated that the granite gneisses and granitoids were metamorphosed up to upper amphibolite facies at various localities (Berach, Chittaurgarh and Amet) in southern and eastern part of the Aravalli Craton.

2.4.2 ARAVALLI SUPERGROUP

On the basis of mineral paragenetic study around Amet-Lawa Sardargarh, Sharma (1988) suggested that the rocks were metamorphosed up to middle amphibolite facies. However, the Aravalli Supergroup of rocks had been reported to be of greenschist facies in the Raialo syncline of Heron (1953) and the Nathdwara group of Gupta et al. (1980). The greenschist facies condition also extends to the west of the Raialo syncline (Mohanty, 1982). The Aravalli metasediments overlying the Berach granites show greenschist facies condition of metamorphism (cf. Sharma, 1988).

2.4.3 DELHI SUPERGROUP

Two distinct metamorphic series are the characteristic features of the Delhi Supergroup of rocks (Dasgupta, 1964, 1968; Lal and Shukla, 1975). The earlier metamorphism was regional in nature which produced the regional schistosity whereas, the later low-pressure thermal metamorphism is localised around plutonic intrusives (Sarkar, 1973; Sharma, 1988). The Delhi rocks were subjected to middle amphibolite facies of regional metamorphism where granitic intrusives are absent (Sharma, 1988).

Sharma and Narayan (1975) and Sharma (1977) proposed an amphibolite facies of metamorphism for rocks of the Delhi Supergroup around the Ajmer-Beawar region from the mineral assemblage garnet + staurolite + biotite + kyanite. Gangopadhyay and Lahiri (1988) reported similar metamorphic grade in Barr to Phulad area in contrast to high-pressure garnet-pyroxene (grospydite) from the same area (Sychanthavang and Desai, 1977). The southern Delhi fold belt (north of Ajmer to Abu Road in south) rocks have undergone amphibolite facies condition of metamorphism (Sharma, 1988).

2.5 GEOCHEMISTRY

2.5.1 AMPHIBOLITES AND MAFIC META-VOLCANICS

The presence of ortho-amphibolite in the BGC between Ajmer in the north and Udaipur in the south had been reported by Pandya (1967), Kataria (1981) and Sharma (1983a). The origin of ortho-amphibolites is attributed to the recrystallization of tholeiitic rocks under amphibolite to upper amphibolite facies of metamorphism. Based on trace element constraints, Kataria et al. (1988) suggested an oceanic affinity for the amphibolites of the Amet region. Khandelwal and Pandya (1988) classified the amphibolites of the Masuda - Ramgarh region as massive and schistose types. They reported that massive amphibolites occurs as intrusives whereas, the schistose amphibolites as volcanic flows. Further, Goel (1988) considered the derivation of the metabasites from metamorphism of basic igneous rocks and pyroclastic materials under low P and T conditions around the region east of Udaipur.

Geochemical studies by Ahmad and Rajamani (1988) of mafic enclaves within the BGC southeast of Nathdwara indicated light REE enriched pattern in the enclaves sampled away from the BGC-Aravalli contact and depletion of light REE at the contact. Further, investigations by Ahmad and Rajamani (1991) of Aravalli basic volcanics around Nathdwara indicated that they are picritic as well as tholeiitic in nature. The tholeiitic amphibolites are enriched in LREE (40 - 70 X chondrite) with sloping REE patterns. Picritic amphibolites have lower REE abundances compared to the tholeiitic counterparts. Based on the trace element characteristics, source for their magmas was attributed to sub-continental mantle variably enriched in incompatible elements. More detailed work by Ahmad and Tarney (1994) showed similar results for the tholeiites with pronounced Sr and Nb anomalies in spider diagrams whereas, the mafic enclaves showed only strong Sr anomaly.

Gopalan et al. (1990) reported that the mafic enclaves in the BGC around Nathdwara are predominantly Fe-enriched tholeiites with a few samples as basaltic andesites. They have a flat to slightly LREE (5-20X) enriched REE patterns with a slight negative Eu anomaly. Deb and Sarkar (1990) found that the amphibolites of Bhilwara and Aravalli Supergroup are similar to low-K tholeiites and calc-alkaline basalts. They are characterized by variable REE fractionation and near chondritic ratio of TiO_2/Zr, Zr/Nb and Ce/Zr which led the above authors to suggest a primitive mantle source for magmas represented by the amphibolites.

Deb and Sarkar (1990) reported similarity of mafic rocks of the Delhi Supergroup with the low-K tholeiites and considered them to have an origin similar to that of the mafic magmatism of modern island arcs. The work of Volpe and McDougall (1990) on mafic rocks (Phulad ophiolites of Gupta et al., 1980) has shown two independent rock suites. Phulad-Barr-Jetgarh (PBJ) metabasalts

resemble the Mid Oceanic Ridge Basalts (MORBs) as indicated by transition element ratios whereas, the other rock suite Ranakpur-Desuri metabasalts bear a resemblance to intra-oceanic island arc basalts characterized by low REE, Zr and Y, and high Rb, Ba and K abundances.

2.5.2 GRANITOIDS

The gneisses around Udaipur are tonalitic to granitic in composition (Srivastava, 1988). They have low potash and are chemically classified as andesites and dacites. Further, Srivastava (1988) reported that the Ahar river granites occurring south of Udaipur range in composition from trondhjemite-tonalite-potassic granite. Similar affinities for biotite gneisses around Jhamarkotra was reported by Gopalan et al. (1990). Based on the alkali contents, the BGC in the area are well comparable with the average Archaean tonalite of Barberton Craton (Viljoen and Viljoen, 1969), Karnataka (Bhaskar Rao et al., 1983) and the Singhbhum region (Saha and Roy, 1984). Some of the gneisses have low alumina and silica. Biotite-gneisses are strongly enriched in LREE (100 - 300 X) with depleted heavy rare earths (2 - 40X) (Gopalan et al., 1990; Ahmad and Tarney, 1994). The REE patterns are similar to that of low alumina Archaean tonalite-trondhjemite suites from other areas (Fig. 5-14, in Condie, 1981).

Samples of granitic rocks near Rampura-Agucha and Berach have major element abundances similar to upper continental crust (cf. Deb, 1992). The Rampura-Agucha sample is highly enriched in LREE compared to the moderate to high LREE enrichment in the Berach granite. On the basis of rare earth element modelling, Deb (1987) suggested that magmas parental to felsic gneisses (migmatitic) of the BGC around Rampura-Agucha and Berach had originated by partial melting of the upper crust.

2.6 GEOCHRONOLOGY

2.6.1 BANDED GNEISSIC COMPLEX

Vinogradov and Tugarinov (1964) reported Uranium-lead isochron age of 3500±200 Ma on detrital zircons collected from the Aravalli schists near Udaipur. Untala and Gingala granites occurring east of Udaipur in the BGC gave a whole rock Rb-Sr isochron age of 2950±150 Ma and a mineral Rb-Sr isochron age of 900 Ma (Crawford, 1970; Chaudhury et al., 1984).

The Rb-Sr whole rock dates of the Amet granite (1870±200 Ma) and the Darwal granite (1900±80 Ma) determined by Chaudhury et al. (1984) contradicts Heron's classification of these rocks as part of BGC, whereas the Berach granite of BGC gave a scattered but consistent Rb-Sr whole rock age of 2600±150 (Chaudhury et al., 1984). Based on the isotopic age data of the

Berach, Untala and Gingla granite, Chaudhury et al. (1984) suggested that the Cratonization of the BGC might have occurred before 2500 Ma.

The schistose amphibolite enclaves within BGC (SE of Nathdwara) gave an age of 2828±46 Ma based on whole rock Sm-Nd isochron whereas, biotite gneisses (around Jhamarkotra) gave an age of 3307±65 Ma (Gopalan et al., 1990). They compared the formation of schistose amphibolites to that of intrusive period of Untala and Gingala granites (2860±55Ma, Chaudhury et al., 1984). Further, a garnet-whole rock Sm-Nd age of 2450±170 Ma from the gneissses around Jhamarkotra was compared with the Berach granite (2.5 Ga, Crawford, 1970). On the basis of isotope dates they recognized at least three phases of thermal events in the area. Based on Pb-Pb isotopic study on zircons from the ortho-gneisses of Jhamarkotra, Wiedenbeck and Goswami (1994), reported 3281±3 Ma and attributed this age as the minimum period for crystallization igneous protolith of gneiss.

Sarkar et al. (1989) dated the charnockite-granodiorite suites within the granulite facies metasediments of the Bhilwara Supergroup (Gupta et al., 1980) by U-Pb technique. They found the crystallization age to be 1723+14/-7 Ma for the above suites.

Tobisch et al. (1994) carried out Sm-Nd and Rb-Sr isotope studies on the felsic and mafic gneisses which they considered to be BGC equivalents around Govindgarh (west of Ajmer). They reported that the samples do not define an isochron either in Sm-Nd or Rb-Sr isotope evolution diagram. The geochronological data of the rocks of BGC are shown in Table 2.1 and Fig. 2.3.

2.6.2 ARAVALLI SUPERGROUP

Aravalli Supergroup of rocks that underlie the Berach granites unconformably are considered to be younger than 2500 Ma, the Rb-Sr isochron age of the Berach granites (Crawford, 1970). Whereas, the granites that are intrusive into the Aravalli Supergroup (Ahar river granite, Kishengarh granodiorite) gave younger Rb-Sr whole rock ages of 1900-2000 Ma (Crawford, 1970). Chaudhury et al. (1984) confirmed such a relationship by providing age data of Darwal granites (1900±80 Ma) and Amet granites (1870±200 Ma). The geochronological data of the rocks of Aravalli Supergroup are given in Table 2.1 and are also shown in Fig. 2.3.

2.6.3 DELHI SUPERGROUP

Chaudhury et al. (1984) carried out Rb-Sr whole rock isochron of the granites from the Delhi Supergroup of rocks in the north to north-eastern Rajasthan. Based on Rb-Sr whole rock technique Chaudhury et al. (1984) reported an age range of 1500-1700 Ma for the Bairat, Dadikar, Harsora,

Table 2.1 Geochronological Data of BGC and Aravalli Rocks

S.No	Location & Rock Type	Method	Age in Ma	Reference
1.	Near Udaipur, Aravalli Schists	Pb-Pb isochron detrital Zircon	**3500 ± 200**	Vinogradov & Tugarinov, 1964
2.	Near Udaipur, Aravalli Schists	Extracted Pb from Rocks	**1500**	Vinogradov et al., 1964
3.	Chittaurgarh, Berach Granite	Rb-Sr WR	**2550**	Crawford, 1970
3b.	Chittaurgarh, Berach Granite	Rb-Sr WR	**2600± 150**	Chaudhary et al., 1984
4.	SE of Udaipur, Gingla Granite	Rb-Sr WR	**2950± 150**	Chaudhary et al., 1984
5.	SE of Udaipur, Untala Granite	Rb-Sr mineral	**900± 150**	Crawford, 1970 & Chaudhary et al., 1984
6.	SE of Nathdwara, Amphibolite Enclave	Sm-Nd WR	**2828± 46**	Gopalan et al., 1990
7a.	Jhamarkotra, Biotite Gneiss	Sm-Nd WR, Sm-Nd Garnet-WR	**3307± 65** **2450±170**	Gopalan et al., 1990 Gopalan et al., 1990
7b.	Jhamarkotra, Ortho Gneiss	Pb-Pb Zircon	**3281± 3**	Wiedenbeck & Goswami, 1994
8.	SE Udaipur, Gneisses/Metabasic	Sm-Nd WR Rb-Sr	**~ 3500**	McDougall et al., 1983
9.	Gyangarh, Charnockite/Granod.	U-Pb Zircon	**1723+14/-7**	Sarkar et al., 1989
10.	Darwal Granite	Rb-Sr	**1900± 80**	Chaudhary et al., 1984
11.	Amet Granite	Rb-Sr	**1870± 200**	Chaudhary et al., 1984
12.	Zawar/Sulphides	Model Age of Galena Pb	**1440± 170**	Balasubrahmanyam & Chandy, 1976
13.	Udaipur, Ahar River Granite Kishengarh Granodiorite	Rb-Sr WR Rb-Sr WR	**1900-2000** **1900-2000**	Crawford, 1970 Crawford, 1970
14.	Govindgarh, Felsic & Mafic Gneisses	Sm-Nd	**2830?**	Tobisch et al., 1994

Seoli, Saladipura, Chapoli, Ajitgarh and Annasagar granites from Ajmer on the basis of two reference isochrons at corresponding ages. Crawford (1970) estimated 950 Ma for the Ajmer granite whereas, the Chapoli gave an age of 1000 Ma. On the contrary, in the western part of the Aravalli Craton the granite suites from Sendra, Sadri Ranakpur, Sai, Ambaji (south of Ajmer) and from Jhunjhunu, Pali, Erinpura yielded a much more younger Rb-Sr whole rock age of 800±50 Ma.

Gupta et al. (1980) suggested syntectonic origin for Sai, Sendra and Sadri Ranakpura granites to Delhi orogeny whereas, the relationship of Ajitgarh and Bairat granites to the Delhi orogeny is not conclusively drawn (Chaudhury et al., 1984). Subsequently, Volpe and McDougall (1990) reported whole rock Sm-Nd isochron age of 1012±78 Ma for the Ranakpur diorites. Based on Sm-Nd mineral isochron they determined the age of Ranakpur meta-gabbro as 838±36Ma, Ranakpur diorite 835±43Ma and Ranakpur quartz-diorite 791±43 Ma. Tobisch et al. (1994) reported the age of Sendra granites to be of 966±250 Ma. Such a contrasting age data of 1500-

1700 Ma (northern Delhi Supergroup) with 750-850 Ma in southern Delhi Supergroup can be attributed to two distinct magmatic events in the Delhi fold belt. The geochronological data of the rocks of Delhi Supergroup are given in Table 2.2 and Fig. 2.3.

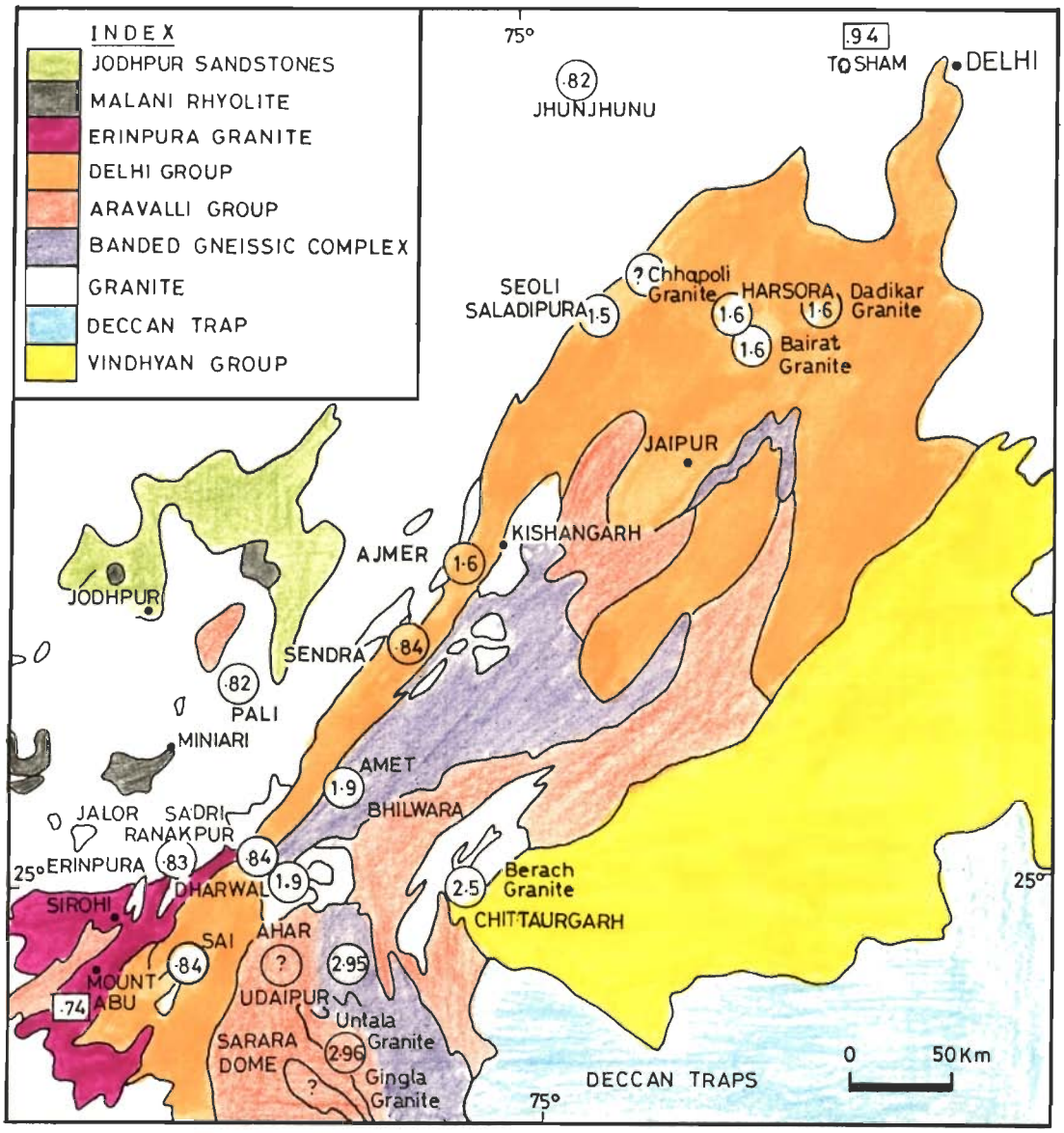

Fig. 2.3 **Geochronological map of Rajasthan (after Chaudhury et al., 1984). The figures within circles are in b.y. and the references are given in Table 2.1 & 2.2.**

2.7 CRUSTAL STRUCTURES FROM GEOPHYSICAL INVESTIGATIONS

Gravity, magnetic and seismic studies were carried out by various workers along Nagaur-Jhalawar geo-transect which passes through the Marwar Supergroup (MSG), Delhi Supergroup (DSG), BGC/Aravalli Supergroup and Vindhyans in the Aravalli Craton. The gravity study by Mishra et al. (1995) indicated a high Bouguer anomaly of ~60 mgal in the central region represented by the Delhi Supergroup of geo-transect (Fig. 2.4) whereas, very low Bouguer anomalies were

observed on both sides of DSG. They reported larger magnetic anomalies M2 and M3 (Fig. 2.4). M2 anomaly was reported at the junction of MSG and DSG whereas, M3 magnetic anomaly

Table 2.2 Geochronology Data on Delhi Supergroup of Rocks

S.No.	Location & Rock Type	Method	Age in Ma	Reference
1.	Bairat Granite	Rb-Sr Single Model Age	**1650**	Crawford, 1970
2.	Ajmer Granite	Rb-Sr Single Model Age	**950?** **1600**	Crawford, 1970 Chaudhary et al., 1984
3.	Chapoli Granite	Rb-Sr Single Model Age	**1000**	Chaudhary et al., 1984
4.	Bairat Granite, Dadikar Granite, Harsara Granite, Ajitgarh Granite Seoli, Saladipura Granite	Rb-Sr WR Rb-Sr WR Rb-Sr WR Rb-Sr WR Rb-Sr WR	**1600** **1600** **1600** **1600** **1500**	Chaudhary et al., 1984 Chaudhary et al., 1984 Chaudhary et al., 1984 Chaudhary et al., 1984 Chaudhary et al., 1984
5.	Bairat Granite, Dadikar Granite, Harsara Granite, Ajitgarh Granite Seoli, Saladipura Granite	Rb-Sr Mineral Rb-Sr Mineral Rb-Sr Mineral Rb-Sr Mineral Rb-Sr Mineral	**800± 50** **800± 50** **800± 50** **800± 50** **800± 50**	Chaudhary et al., 1984 Chaudhary et al., 1984 Chaudhary et al., 1984 Chaudhary et al., 1984 Chaudhary et al., 1984
6.	Mount Abu & Idar Granite	Rb-Sr Wr	**740**	Crawford & Compston, 1970 Crawford, 1975
7.	Ranakpur Diorites, Ranakpur Metagabbro, Ranakpur Diorite, Ranakpur Quartz-Diorite Ranakpur Granite/Granodiorite	Sm-Nd WR Sm-Nd Mineral Sm-Nd Mineral Sm-Nd Mineral Rb-Sr WR	**1012± 78** **838± 36** **835± 43** **791± 43** **800± 50**	Volpe & McDougall, 1990 Volpe & McDougall, 1990 Volpe & McDougall, 1990 Volpe & McDougall, 1990 Chaudhary et al., 1984
8.	Phulad Metabasalts	Model Sm-Nd	**1300-1700**	Volpe & McDougall, 1990
9.	Sendra, Sai, Ambaji, Jhunjhunu, Pali, Erinpura Granite	Rb-Sr WR	**800± 50**	Chaudhary et al., 1984
10.	Sendra Foliated Granite	Rb-Sr Model II Isochron	**966±250**	Tobisch et al., 1994

between DSG and BGC. They inferred the junctions as faulted contacts and attributed the variations in magnetic susceptibility to the presence of basic intrusives present in the faulted contacts. The small wavelength gravity anomalies (G1-G4, Fig. 2.4) were attributed to the crustal inhomogeneities at the shallower levels of the upper crust. The high magnetic nature and susceptibility of the granulite facies rocks of Sandmata Complex were characteristically observed by large magnetic anomalies. They inferred a thicker lower crust under the DSG and BGC and attributed this to the magmatic activity. They envisaged a thinner crust under the Vindhyan Supergroup. The seismic reflection studies in the same geo-transect were carried out by Reddy et al. (1995). They observed poor reflectivity in DSG, north west part of the Bhilwara granitic region and in the Vindhyan region. The possible explanation of this may be, according to them, was distinct evolutionary processes for each of these segments of the Aravalli Craton. They inferred a possible

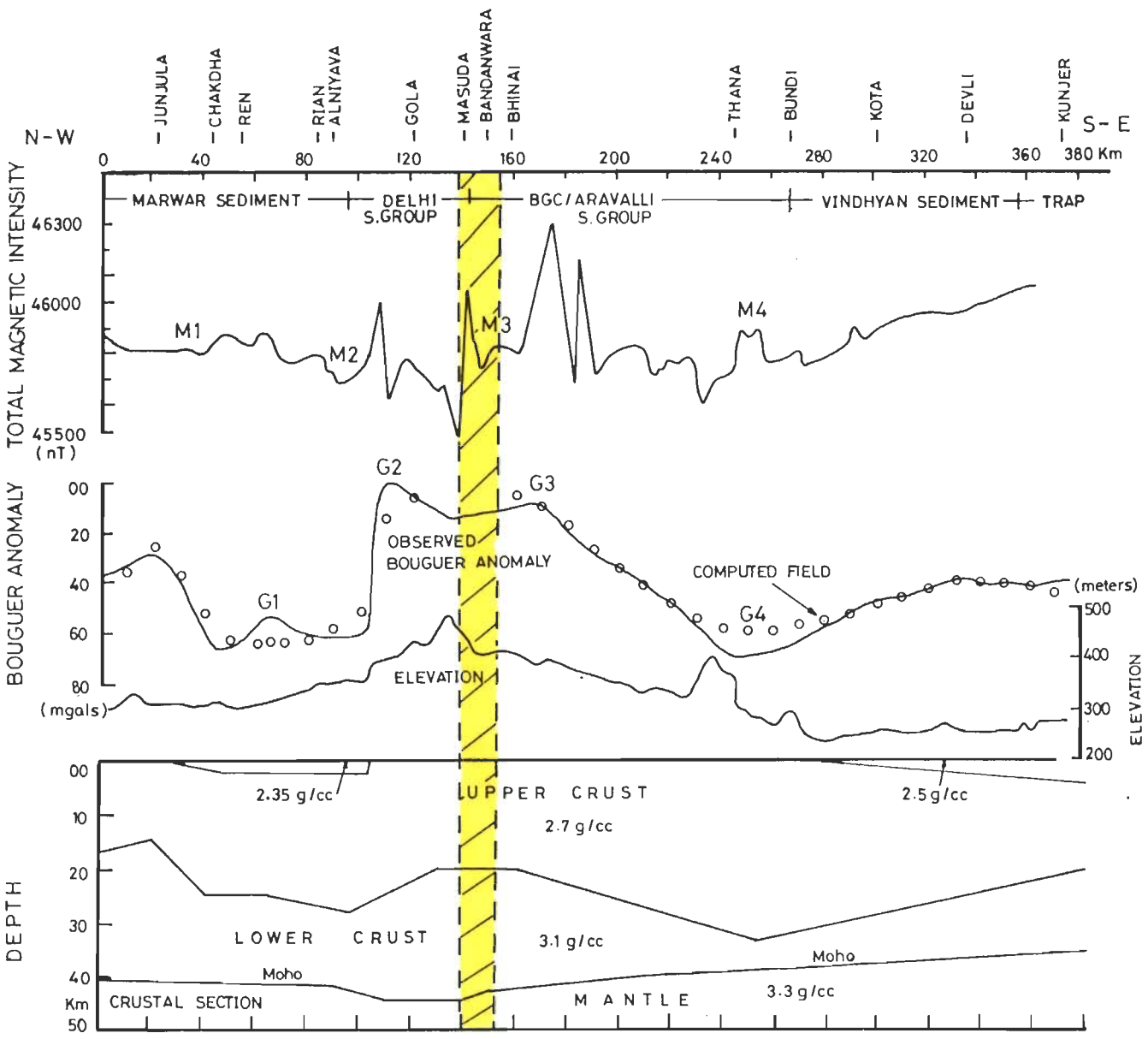

Fig. 2.4 **Gravity and magnetic data along Nagaur - Jhalawar Geotransect and the crustal section modelled from the observed Bouger anomaly constraining it from deep seismic reflection along the same profile which passes through the study area represented by shaded bar (after Mishra et al., 1995).**

rift zone in the lower crust in the MSG and in the southeastern Bhilwara region. Further, they suggested a compressive and collision related regime on the basis of highly reflective lower crust with southeasterly down dip of rocks at mid to sub-crustal levels within the terrane occurring within DSG and Vindhyan sedimentary basin. On the basis of structure of Moho along the transect, they have indicated presence of deep crustal shear zone below BGC. They have also inferred that the crust mantle boundary lies at 45-50 km depth below the BGC terrane, which includes the study area.

2.8 MINERALIZATION

Except the lone occurrence of Pb-Zn deposits around Rampura-Agucha, BGC rocks do not contain any viable mineral deposits. The associated rock types with the Pb-Zn mineralized zone are garnet-graphite-sillimanite bearing biotite schists, gneisses, calc-granulites and amphibolites. Galena and sphalerite are the two major characteristic minerals in the stratiform and stratabound Pb-Zn deposits. The localization of ore mineralization is mainly structurally controlled (Ranawat et al., 1988). The grade of metamorphism varies from the upper amphibolite to granulite facies condition for the ores as well as the associated rocks. Ranawat et al. (1988) estimated ~6 kb pressure and 680^0C temperature for rocks , as well as, the ores.

In contrast to basement mineralization, a number of economically viable base metal deposits are found in the Aravalli Supergroup of rocks. The most important and economic ores are that of Pb-Zn deposits of Zawar, multimetal deposits of Rajpura-Dariba and the Pb-Zn deposits of Pur-Banera belt. Apart from the base metal occurrences, a moderate phosphorite deposit at Jhamarkotra (near Udaipur) was reported by Banerjee (1971).

Like the Aravalli supergroup, a number of mineral deposits also enrich the Delhi Supergroup of rocks. The prominent ones are found as pyrite-pyrrhotite deposits in Saladipura, copper deposits in Khetri and Kho-Dariba, and polymetallic sulphide deposits in Ambaji-Deri and Basantgarh. Pyrite-pyrrhotite deposits of Saladipura belong to the Ajabgarh group whereas, Kho-Dariba deposits are confined to intercalated bands of gray phyllites of the Alwar group (Deb and Sarkar, 1990).

Deb (1982) advocated an exhalative mechanism for the stratiform base metal deposits of Aravalli Craton. Based on stable isotopic studies, Deb and Sarkar (1990) stated that sea water hydrothermal ore fluids widely circulated through a variety of mixed sources. The Rajpura-Dariba and Pur-Banera deposits were reported to have been formed from volcanic exhalations with contributions from biologic activities along trough regions (Deb and Sarkar, 1990). Similarity

between the Rampura-Agucha and the Rajpura-Dariba deposits was established on the basis of stable isotopic ratios and model Pb isotope ages (Deb et al., 1989).

2.9 STRATIGRAPHY

Over the years the Precambrian stratigraphy of the Aravalli Craton has evolved with more detailed studies using newer techniques. A comprehensive account on the stratigraphy of Aravalli Craton given by prominent workers is presented in Table 2.3. Gupta (1934) and Heron (1953)

Table 2.3 General Stratigraphy of the Aravalli Craton

B.C.Gupta (1934) & Heron (1953)	Raja Rao et al. (1971)	Naha & Halyburton (1974a)	Gupta et al. (1980)	A.B.Roy (1988)
Erinpura Granite			Erinpura Granite	Erinpura Granite
Delhi System	**Delhi System**	**Delhi Group**	**Delhi Supergroup**	Mafic & ultramafic
Ajabgarh Series			*Pali Group*	intrusives into
Alwar Series			*Sindereth Group*	Delhi fold belt
			Sirohi Group	
			Kumbhalgarh Group	Champaner Group
			Gogunda Group	Sirohi Group(?)
—Unconformity—				
Raialo Series		**Post Aravalli Granite**		**Delhi Supergroup**
				Ajabgarh Group
—Unconformity—				Alwar Group
				*Rayanahala Group
Aplo Granites		**BGC by migmatization**		
				—Unconformity—
Aravalli System	**Aravalli Group**	**Aravalli Group**	**Aravalli Supergroup**	**Aravalli Supergroup**
			Champret Group	
			Lunavada group	Upper Aravalli
			Jharol Group etc.	Group
	Bhilwara Group		*Bari lake Group etc.*	
			Udaipur Group	Lower Aravalli
			Debari Group	Group
Banded Gneissic Complex		**Banded Gneissic Complex**	**Bhilwara Supergroup**	**-- Unconformity—**
			Ranthambhor Goup,	
			Rajpura Group,	
			Pur-Banera Group etc.	
			Hindoli Group,	**Mewar Gneiss**
			Mangalwar Complex (?),	
			Sandmata Complex (?)	
Berach Granite = Bundelkhand Gneiss	**Berach Granite**	**Berach Granite = Sarara Granite**		

** Heron's Raialo Series in Alwar District*

considered Berach Granite as equivalent of Bundelkhand Gneiss and considered Banded Gneissic Complex as a distinct lithological unit. Raja Rao et al. (1971) also proposed Banded

Gneissic Complex as different from Berach Granite. On the other hand, Naha and Halyburton (1974a) equated Berach Granite as the equivalent of Sarara Granite and considered the formation of Banded Gneissic Complex by migmatization of Aravalli Group of rocks and placed the BGC above the Aravalli Group (Table 2.3).

However, Gupta et al. (1980) designated Bhilwara Supergroup to the rocks formed more than 2500 Ma. in Aravalli Craton. Further, they subdivided Bhilwara Supergroup into lower and upper divisions. The upper division comprised of Ranthambhor Group, Rajpura-Dariba Group, Pur-Banera Group, Zahazpur Group, and Sawar Group. The lower division comprised of Hindoli Group, Mangalwar Complex (?) and Sandmata Complex (?) (Table 2.3). Roy (1988) designated the oldest unit in the Aravalli Craton as Mewar Gneiss which are older than the Aravalli Supergroup of rocks.

CHAPTER III

FIELD STUDY & PETROGRAPHY

3.1 FIELD STUDY

3.1.1 Location & Accessibility:

The study area around Masuda falls in the Ajmer district of Rajasthan. It is ca. 400 km southwest of Delhi and 50 km sout-south-west of Ajmer city. The area under investigation falls between 26°3′ to 26°13′ N Latitude and 74°30′ to 79°42′ E Longitude on Survey of India Toposheet no. 45J/12.

The rocks of the study area are classified as Banded Gneissic Complex by Heron (1953) and reclassified as Sandmata Complex forming part of Bhilwara Supergroup of Aravalli Craton by Gupta et al. (1980). The study area is bounded by rocks of Delhi Supergroup to the west and by high grade rocks (BGC) to east and south.

Meta-igneous and meta-sedimentary rocks, which have been subjected to several episodes of deformation and mylonitization, constitute the lithology of the study area. Hence, primary igneous and sedimentary structures are rarely preserved. The regional foliation strikes NE-SW with a steep dip towards southeast. A detailed account of the structural and deformational history of rocks of the study area is given in Chapter-II sub-section "Structure of the study area" (section 2.2.1).

3.1.2 Rock Types

The study area consists of diverse lithologies which are classified into the following categories :

1. Metabasites
2. Intermediate to granitoid gneisses
3. High grade rocks
4. Mica-schist and migmatized mica-schist
5. Calc-silicate and chert/quartzite bands
6. Dykes and quartz veins

The study area has been mapped by Srivastava et al. (1995) and a modified version of this map is given in Fig. 3.1. The major litho-unit is represented by intermediate to granitoid gneisses which is flanked by migmatized mica-schist. The meta-basites are found within and at the margins of the intermediate to granitoid gneisses. They occur as discontinuous folded bands in association with calc-silicate rocks.

Elongated granitic bodies occur near Jamola and Jipiya. At places these are fine grained and give aplitic appearance. Numerous quartzite bands occur within migmatized mica-schist and high grade rocks which are folded and boudinaged.

Metabasites

The meta-basites include components of amphibolites, meta-gabbro and meta-diabase. The amphibolites are the predominant rock type in this group. These groups of rocks are medium to coarse grained, melanocratic consisting of predominantly amphiboles and plagioclase feldspars and schistose in nature. Preferred orientation of prismatic amphiboles define the schistosity. The mylonitized variety of meta-basites are fine to medium grained and epidotized at places. The amphibolites are inter banded and cofolded with calc-gneiss and intermediate to granitoid gneisses.

A vesicular variety of fine to medium grained inter banded with calc-gneiss occurs near Jhunton ka Bariya on Masuda-Bandanwara road. The vesicles are stretched (Plate 3.1a). The presence of vesicles possibly indicate that this rock type must have been of volcanic origin.

Only the mappable units of meta-basite along with calc-silicate gneiss are shown in the map. However, there are numerous thin bands of meta-basites that occur within intermediate to granitic gneisses which could not be shown in the map (Fig. 3.1).

The dark coloured, medium to coarse grained, highly weathered calc-gneiss consists of calcareous, as well as, resistant silicate bands. Folds are better observed in this rock type as there is contrast in colour and mineralogy between the calcareous and silicate bands. The silicate bands consist of quartz, feldspars, amphiboles, epidote and sphene whereas, calcareous bands are essentially composed of carbonate minerals (Plate 3.1b).

Intermediate Rocks

These rocks are medium to coarse grained and leucocratic to mesocratic and foliated in nature and in some outcrops gneissic bandings (alternate felsic & mafic layers) are well developed. The felsic layers are represented by quartz and feldspars whereas, the mafic layers are defined by biotite and hornblende. The rock composition varies from diorite to monzodiorite to

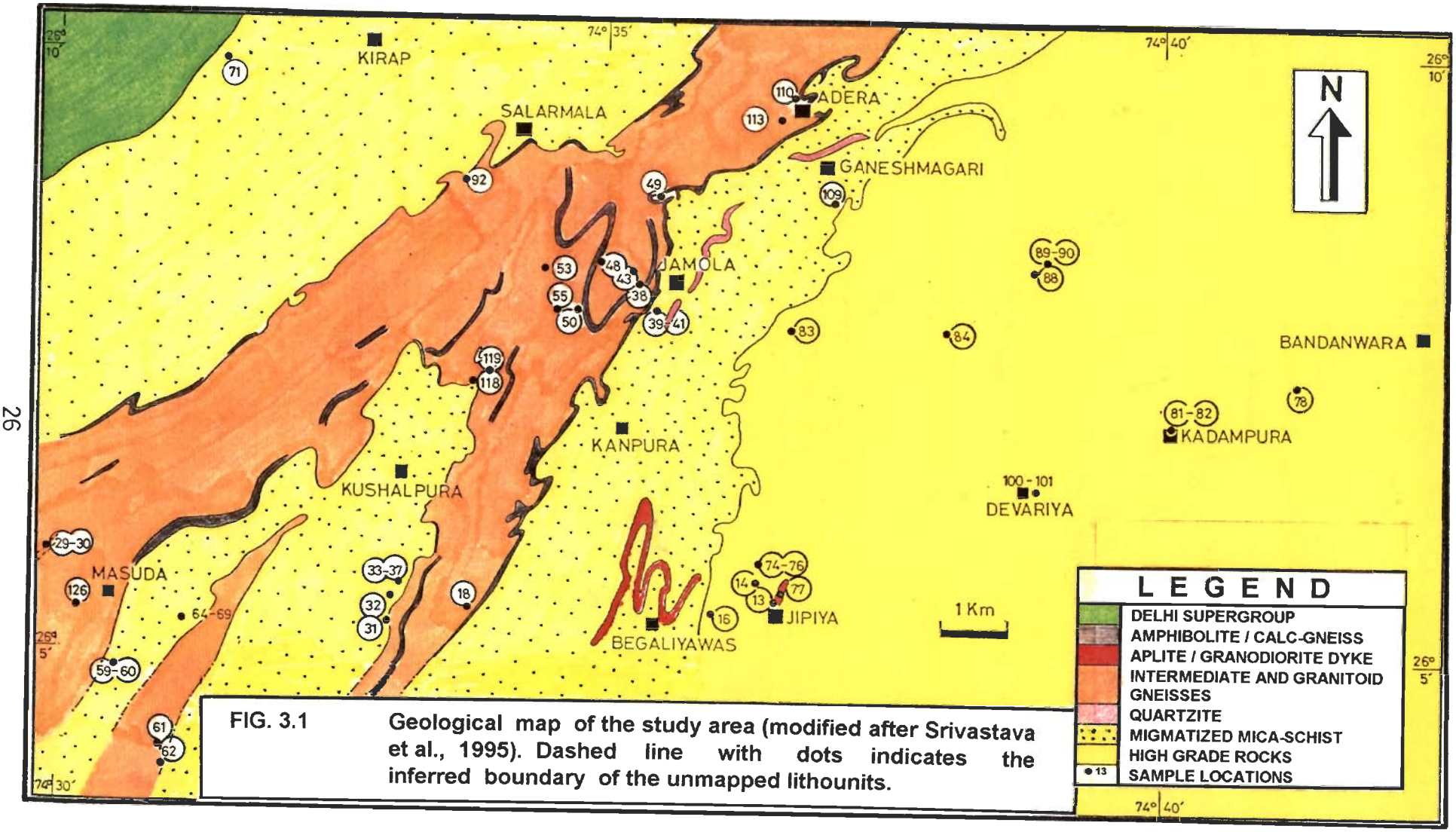

FIG. 3.1 Geological map of the study area (modified after Srivastava et al., 1995). Dashed line with dots indicates the inferred boundary of the unmapped lithounits.

quartz diorite based on the abundances of quartz, alkali and plagioclase feldspars. Garnets are found in a few samples.

In an outcrop ~ 2 km east of Masuda, granite mylonite, amphibolite, diorite to quartzdiorite gneisses are inter banded and cofolded (Plate 3.1c). The rocks have been mylonitized and the contact relationship amongst them appear to be tectonic (cf. Srivastava et al., 1995). The quartzo-feldspathic veins within the intermediate suite of rocks are co-folded (Plate 3.1d).

A number of ductile shear zones both sinistral and dextral in nature are ubiquitous in the study area and are well observed in the intermediate, as well as granitoid gneisses. Several generations of small scale quartzo-feldspathic veins of variable width are found to occur within the intermediate to granitoid gneisses. One such example, can be seen behind Masuda Fort, where at least three generations of quartz veins are observed and some of them show ptygmatic folding (Plate 3.2a).

Porphyritic rocks

A dark coloured porphyritic rock with alkali feldspar as phenocrystic phase is observed at an outcrop west of Jamola (Plate 3.2b). The size of the phenocryst varies from 0.3 to 0.7 cm in diameter. The orientation of these phenocrysts are random. Most of the phenocrysts are tabular and euhedral in shape where the rock is least deformed. The matrix is fine grained. This rock possibly represents a volcanic flow.

In another outcrop near Ganeshmagari, a similar rock type is found. The feldspar phenocrysts are augen shaped and stretched (Plate 3.2c). The matrix is fine to medium grained. This rock also could have been a flow and was more deformed relative to the phenocrystic rock occurring west of Jamola.

Granitoid Gneisses

The granodiorites and granite gneisses constitute this group. They are leucocratic, medium to coarse grained and mainly consist of felsic minerals, such as, quartz, alkali feldspar and plagioclase feldspars. The mafic minerals are represented by muscovite, biotite and amphiboles. The gneissic banding of the felsic and mafic minerals are seen in meso to microscopic scales. Granodiorite gneisses have biotite and amphiboles as the mafic minerals whereas, granites contain amphibole, biotite and muscovite. Near Begaliyawas a highly mylonitized outcrop of granodiorite gneiss occurs. In this outcrop, porphyroclasts of feldspar with garnet inclusions are seen (Plate 3.2d).

In the mylonitized felsic gneisses, the feldspar augens have undergone extreme stretching (Plate 3.3a). Variable degree of mylonitization are best observed at the contact between granitic

gneiss and mica-schist and near shear zones. The augen shaped alkali feldspars progressively stretched and finally become ribbons as one approaches the contact (Plate 3.3b)

A number of elongated bodies with long axis parallel to regional foliation plane occur within the intermediate to granitic gneisses. Such linear bodies of granodioritic composition is observed near Jipiya (Plate 3.3c) and Jamola.

Mica-Schist

This unit includes both migmatized and non-migmatized variety of rocks. The non-migmatized variety is soft, friable, highly fissile and schistose in nature. It contains predominantly muscovite followed by biotite, garnet and quartz. Unmigmatized mica-schist is not prominently observed as that of migmatized mica-schist.

The migmatized mica-schist contains both distinct mafic and felsic layers. The width of bands vary in meso to microscopic scale. Mafic rich layers are predominantly biotite with minor proportion of muscovite. Well developed garnet porphyroblasts (10 X 13 cm) are observed. One such augen shaped garnet porphyroblasts is surrounded by mafic, as well as, felsic rich layers (Plate 3.3d). The migmatized mica-shist occur as 1-2 km wide bands forming small mounds and hillocks, as seen around Kushalpura, Lalwas and Kirap villages.

High Grade Rocks

These rocks are leuco to mesocratic and coarse grained in nature. Mineralogically the rock is composed of quartz, alkali & plagioclase feldspars, garnet, pyroxene, amphiboles and biotite. Compositionally they fall in the intermediate to granodioritic suite of rocks. The high grade rocks have distinct texture (Plate 3.4a) from that of amphibolite grade rocks. The high grade rocks are massive and weakly foliated in the contact zone with the amphibolite grade rocks. Mega-crysts of plagioclase feldspars (>2 cm diameter) are widespread in these rocks.

Enclaves

Enclaves of different size, shape and composition are found within intermediate to granodiorite gneisses and high grade granolitic rocks. From the field occurrences, the enclaves are classified as : (a) tectonic enclaves and (b) stratigraphically older enclaves (Srivastava et al. 1995).

Further, on the basis of textural criteria, the enclaves are classified as massive, foliated and porphyritic varieties. A dark, massive, medium to coarse grained square shaped enclave occurs in a weakly foliated coarse grained granolitic host rock (Plate 3.4b).

In an outcrop near Kadampura, medium dark coloured, unfoliated and coarse grained enclave occurs within the granolitic host rock (Plate 3.4c). Randomly oriented mega-crysts of

feldspars of different size and shape occur within the enclave and other identifiable minerals are quartz, feldspars, amphiboles, biotite and garnet. The host granolitic rock has similar mineralogy and is weakly foliated.

South of Devariya, well foliated enclave occurs within weakly foliated granolitic country rock. This enclave has quarto-feldspathic light coloured bands that alternate with meso-cratic gneiss. From the field observations, it may be noted that the gneissosity found within the enclave terminates abruptly against the host rock (Plate 3.4d). Therefore, based on the structural discordance the enclave must be older than the country rock.

Dykes and Quartz Veins

The dykes of both mafic and felsic composition intrude the different rock types along with the quart veins and define the last phase of magmatic activity in the area. A late aplitic dyke cross cuts the foliation in a granodioritic country rock.

3.2 PETROGRAPHIC OBSERVATION

Thin sections were prepared for all the rock types to decipher the texture, mineralogy, alteration and grade of metamorphism. As the rocks of the study area have been subjected to multi phase deformation and metamorphism, the thin section study would help in identifying the original nature of the rock, whether igneous or sedimentary, from the textural study. Further, petrographic study can be useful in classifying the rocks and its correlation with the whole rock chemical data.

3.2.1 AMPHIBOLITES

Hornblende schist, meta-gabbro and meta-diabase constitute the amphibolite group. Hornblende schist is the predominant rock type followed by meta-gabbro and meta-diabase.

Hornblende-Schist

They are fine to medium grained with hornblende and plagioclase as major mineral phases. The modal abundance of hornblende is around 65 vol.%, whereas, that of plagioclase is 20 to 25 vol.%. and quartz is 5-8 vol%. The remaining 5 to 10 vol.% constituted by epidote, ± biotite, ± clinozoisite and ± sphene which occur in minor volumes. The opaque minerals (sulphides and magnetite) constitute up to 3 vol.% The prismatic hornblende crystals are oriented parallel or sub-parallel to each other and define the schistosity (Plate 3.5a). Plagioclase occurs as lath shaped crystal and its composition varies from oligoclase to andesine. Plagioclase crystals show polysynthetic twinning. Actinolites are found in some samples, usually at the margins of hornblende due to retrogression. Apatite occurs in accessory amounts. Garnet occurs in a few

samples of amphibolites collected close to the granolites (Plate 3.5b) and relict clinopyroxene is observed in one of the samples of hornblende schist (Plate 3.5c).

During retrograde metamorphism certain minerals recrystallize to form different minerals of smaller grain size. Recrystallization of hornblende in hornblende schist is seen, possibly, because of retrograde metamorphism. Epidotes occur as sub-hedral to well developed euhedral crystals and characteristically show anomalous interference colours whereas, zoisite show typical inky-blue interference colour. Sub-hedral to anhedral quartz grains occur as inclusions in the hornblende. Interestingly myrmekitic intergrowth of quartz-epidote and quartz-zoisite are observed (Plate 3.5d). These intergrowths are mainly confined to the margin of amphiboles.

Sphenes are developed at the margin of hornblende and plagioclase. Biotite is observed in one of the hornblende schist (# J-68) which is interbanded with intermediate and granitic rocks. Presence of biotite is perhaps due to introduction of potassium (K) into hornblende schist from granitic rocks during metamorphism and deformation.

Meta-Gabbro

The rock is medium to coarse grained principally composed of augite and plagioclase (Plate 3.6a). The plagioclase composition is that of labradorite. Actinolites are developed at the margins of clinopyroxene due to retrogression. Poikilitic igneous texture is preserved at places. K-feldspar, sphene and epidotes occur in subordinate amount. Calcite is found within interstitial spaces of the grain boundaries and fractures. Grain size reduction at the margin of diopside and augite are observed. Microscopic shear zones have been observed in thin sections.

Meta-Diabase

The rock is medium to coarse grained essentially composed of plagioclase, clinopyroxene and minor amount of quartz. Plagioclase crystals are lath shaped, randomly oriented and ophitic texture is preserved. Clinopyroxenes are altered to hornblende and at the margins actinolites are observed. The reduction in grain size of quartz and plagioclase due to shearing is seen. The plagioclase lamallae have been bent due to deformation. The extensive development of epidote and zoisite and grain size reduction are observed along microscopic shear zones.

3.2.2 INTERMEDIATE ROCKS

The intermediate suite of rocks usually exhibit either porphyritic or gneissic texture. Diorite-monzodiorite-quartzdiorite, porphyritic rocks and mylonites constitute the intermediate suite.

Diorite-Monzodiorite-Quartz Diorite-Gneisses

This suite of rocks are medium to coarse grained and mineralogically characterized by the presence of plagioclase, K-feldspar, microcline, perthites. Biotite and hornblende are the

ferromagnesian minerals and garnet is rarely present. The texture is mainly gneissic with alternate bands of mafic and felsic minerals. Porphyroclasts of plagioclase have been wrapped by hornblende and biotite that define the foliation (Plate 3.6b). Accessory phases are zircon, sphene, apatite and epidote group of minerals. Alterations of K-feldspar and plagioclase feldspars by sericitisation and saussuritization respectively, are observed in some samples. Hornblende crystals have altered to zoisite in large scale in a few samples. Chlorites are developed at the expense of hornblende. Myrmekitic intergrowth of quartz and plagioclase and graphic intergrowth of quartz-K-feldspar are usually seen. The perthite is wrapped by quartz and biotite (Plate 3.6c). Zoning in the epidotes are also observed. In some sections sphene aggregates are found within biotite (Plate 3.6d). There are two generations of biotite. One generation is found along the fracture of garnet and the other generation surrounds the garnet. The intermediate suite has a variable modal proportion of different minerals. The modal abundances of quartz varies from 5 to 20%, plagioclase 25 to 33%, alkali-feldspar 20-25%, hornblende ca.20%, biotite 10-12% and rest of the mode is occupied by sphene, zircon, apatite, epidote and chlorite. Using modal abundances of quartz, alkali and plagioclase feldspars in QAP classification diagram of LeBas and Streckeisen (1991), the intermediate suite of rocks are classified as diorite, monzodiorite and quartz-diorites.

Porphyritic Rocks

Petrographically, the porphyritic rocks are classified into two different varieties based on the grain size.

i) fine grained with K-feldspar-phenocryst (Plate 3.7a)
ii) relatively coarser grained with feldspar phenocrysts

(i) The fine grained porphyritic rock shows inequigranular texture consisting of fine grained matrix and with coarse grained euhedral phenocrysts of alkali feldspar and K-feldspar.The matrix is predominantly composed of quartz, feldspars and biotite (Plate 3.7b). The groundmass also contains muscovite, chlorite, epidote, sphene, zircon, apatite and opaques. Plagioclase is observed at the margins of K-feldspar phenocryst. Biotite and plagioclase feldspar as inclusions in alkali-feldspars are also seen (Plate 3.7c). Very fine lamellae of albite is seen in K-feldspar (Plate 3.7c). The orientation of alkali feldspar phenocrysts are random in least deformed samples. In these samples, the alkali-feldspar is augen shaped and tends to become streaky in relatively intensively mylonitized samples. These features can be observed in mesoscopic as well as microscopic scale. K-feldspars have been sericitised. At high magnification (500X) the muscovite and apatite (?) show acicular habit (Plate 3.7d). This rock may be classified as trachyte on the basis of petrography.

(ii) In the relatively coarse grained variety, the mineralogy is quite similar to that of fine grained rock. However, the groundmass minerals are medium to grained. Alkali-

feldspar shows corroded margin which may be due to resorption. Biotite is developed as the alteration product of hornblende (Plate 3.8a). Occurrence of radiating skeletal plagioclase feldspar crystals in one of the samples indicate that the magma representing this sample might have undergone rapid cooling at the time of its emplacement. Presence of K - feldspar phenocrysts and biotite, quartz and plagioclase feldspar in fine grained groundmass indicate that the porphyritic variety of intermediate rocks might have crystallized from magmas emplaced as flows or as shallow intrusives.

3.2.3 GRANITOIDS

These suite of rocks are petrographically distinguished into granodiorite gneisses, granophyres and aplites.

Granodiorite Gneiss

They are holocrystalline, medium to coarse grained and non-porphyriytic in nature. Quartz, orthoclase, microcline, perthite are the felsic minerals present in the rock. The mafic phases are dominated by hornblende and biotite that occur in subordinate amount. In one of the cases, biotite is the predominant mafic mineral. The typical granodiorite sample has modal abundances of quartz 21%, plagioclase 40%, orthoclase 18%, amphibole 12%, biotite 7% and rest of the mode is occupied by accessory phases. The amphiboles are usually alkali rich. The texture is usually gneissic and when it is intensely mylonitized, it grades into aplitic (Plate 3.8b). Epidote, sphene, apatite and zircon occur as accessory phases. In one of the samples, sphene occurs in the form of a string. Apatites have perfectly hexagonal shape. Allanite is identified in one of the samples. Epidotes are observed in places where granodiorites are intensely sheared. Vermicular quartz is often found within k-feldspar (Plate 3.8c). The intergrowth of alkali-feldspar and quartz (granophyric texture) and myrmekitic intergrowth of quartz and palgiocalse are found at the margin of plagioclase (Plate 3.8d). Alterations of K-feldspar into sericites and plagioclase into saussurites are widely observed.

Granophyres and Aplite

The granophyres are holocrystalline and coarse grained. The predominant minerals are quartz, perthite, microcline with subordinate amount of plagioclase. Predominantly biotite mica and lesser amount of muscovite constitute the ferromagnesian minerals. The texture is usually granophyric (quartz-K-feldspar intergrowth). Sphene, zircon, epidotes and apatites occur as the accessory mineral phases. Biotite occurs as minor inclusions within K-feldspars. Sericites are developed as the alteration product of K-feldspar. The aplite has an anhedral fine garined granular texture. Biotite is the only mica found in the sample. Biotite swerves around porpyroclasts.

Mylonites

Rock compositions of mylonites vary from intermediate suite of rocks to granodiorite to granite suite. The basic rocks have also been affected by mylonitization process but, the effect of mylonitization is better displayed by intermediate and granite suite of rocks. The plagioclase porphyroclasts are surrounded by a narrow zone of fine grained quartz and feldspar (Plate 3.9a). K-feldspar porphyroclasts are wrapped by mainly quartz and biotite (Plate 3.9b). Myrmekitic intergrowth between plagioclase and quartz are common. Different extents of mylonitization can be observed. When extensively mylonitized, granite and granodiorite gneisses become fine grained and show aplitic appearance. Strain free quartz in the from of quartz ribbons, formed due to dynamic recrystallisation during progressive mylonitization occur in highly mylonitized samples (Plate 3.9c) .

3.2.4 GRANOLITIC ROCKS

The rocks are very coarse grained and mineralogically composed of quartz, orthoclase, microcline, plagioclase ± cpx ± opx ± hb ± biotie and ± garnet. The rock composition varies from quartzdiorite to quartz monzonite to granodioirte. The texture is granular to inequigranular. Alkali-feldspar porphyroclasts with 3-5 cm diameter are prominently seen. Biotite and hornblende constitute the predominant mafic phases. Myrmekitic texture is common. Plagioclase and K-feldspars are altered to saussurite and sericites, respectively. Zircon, sphene and apatite occur as accessory minerals. Quartz very often shows undulose extinction. The pleochroic halos around zircon are observed.

Enclaves

Petrographically the enclaves and the host rocks are similar. Quartz, perthite, microcline and plagioclase occur as coarse grained porphyroclasts. Medium grained garnet, hornblende, biotite and epidote occur in the matrix. Myrmekitic intergrowths between quartz and plagioclase and sieve textures are commonly observed (Plate 3.9d). The bending of the cleavage of biotite gives rise to mottled extinction (Plate 3.10a). Zircon and apatite are common accessory minerals. The modal abundances of the major minerals indicates that enclave rock samples are of intermediate compositions.

3.2.5 CALC-SILICATE ROCKS

The coarse grained rock consists of predominantly orthoclase, microcline, plagioclase, calcite, quartz, diopside and actinolite (Plate 3.10b). The texture is granular to gneissic. K-feldspars are sericitised and the epidotes are developed at the margin of plagioclase. Sphene occurs as

accessory phase. Because of the presence of abundant calcite and occurrence of dark and light coloured minerals as alternating bands, the rock is named as calc-gneiss.

3.2.6 MICA-SCHIST/ MIGMATIZED MICA-SCHIST

Mica-schist is composed of muscovite, biotite, quartz, k-feldspar and plagioclase. The texture is schistose and the schistosity is defined by biotite and muscovite. Muscovite is much more abundant than the biotite. It grades into migmatized mica-schist because of development of bands of quartzo-feldspathic minerals along foliation. As a result, it shows gneissic texture; bands of quartz-feldspar layers alternate with biotite and muscovite layers. Garnets are abundant in these rocks. Therefore, the rock is named as garnet-biotite-muscovite schist. Pelitic granulites are found as the high grade variety. It contains both hypersthene and augite and also fibrous sillimanite (Plate 3.10c). Acicular apatite crystals are found in a narrow zone (Plate 3.10d). Inclusion of muscovite and biotite are seen in K-feldspar. The allanites are also seen in some of the migmatites.

PLATE 3.1

a Fine grained vesicular amphibolite. The body occurs as intrusive within composite gneiss(Jhunton ka Bariya).

b Folded calc-gneiss near Jhunton ka Bariya.

c Different rock types occurring within composite gneiss. The contact is sheared.

d F1 fold in composite gneiss. East of Jamola.

PLATE 3.1

PLATE 3.2

a Ptygmatic folding in composite gneiss defined by quartzo-feldspathic layers (Behind Masuda fort).

b Massive and dark fine-grained trachytic rocks with variably oriented feldspar megacrysts.

c Fine to medium-grained trachyte with stretched megacrysts of alkali-feldspar, south of Ganeshmagari.

d Granodioritic dyke within mica-schist near Begaliyawas. Note that, the garnets are growing out of feldspars.

PLATE 3.2

PLATE 3.3

a Sheared augen gneiss with stretched feldspar porphyroclasts.

b Contact of mica-schist and augen gneiss. Note that the contact is sheared and parallel to the foliation. The feldspar augen becomes very fine grained towards the contact. Pen is kept parallel to the contact as well as foliation.

c Granodioritic dyke near Jipiya.

d Comparatively less migmatized mica-schist with large garnet porphyroblast. Paleosomes are thick, Salarmala.

PLATE 3.3

PLATE 3.4

a Granolitic rocks near Kadampura.

b Massive mafic enclave in granolites. Pen is kept parallel to weakly developed foliation in the country rock. Feldspar augens are randomly oriented, Kadampura.

c Intermediate type of enclave in a granolite country rock. Megacryst of feldspar are present, Kadampura.

d Granodiorite gneiss enclave in a granolite country rock, south of Devariya.

PLATE 3.4

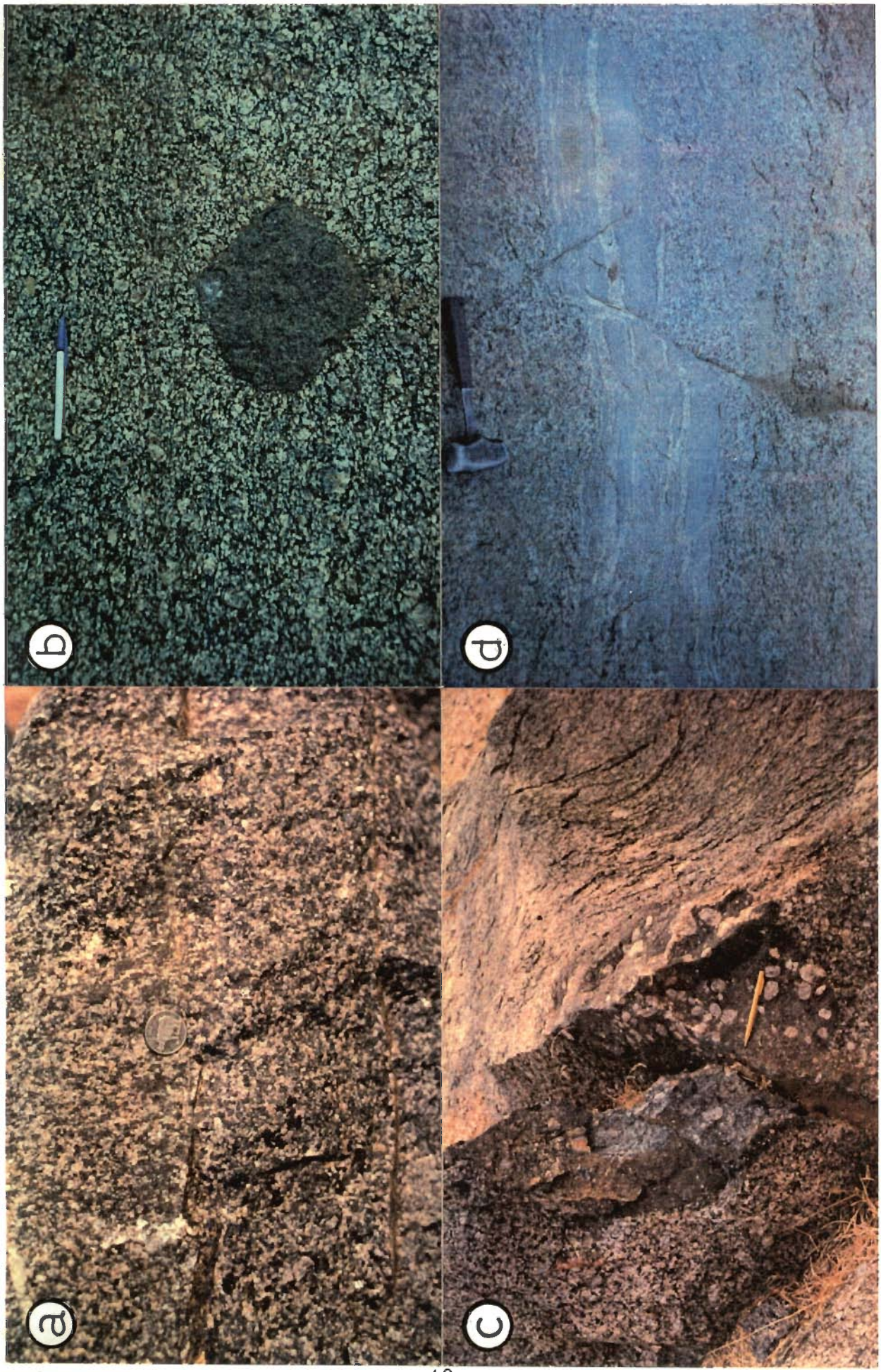

PLATE 3.5

a Amphibolites showing the schistose structure. The schistosity is defined by parallel to sub parallel arrangement of hornblende. Crossed polars.

b Garnets are found in amphibolite in association with hornblende and plagioclase. Plane polars.

c Relict clinopyroxene observed in amphibolite occurring within granolite grade of rocks. Crossed polars.

d Quartz-epidote/zoisite intergrowth in amphibolites. Crossed polars.

PLATE 3.5

PLATE 3.6

a Metagabbro showing the marginal reduction in grain size at the margin of clinopyroxene.

b Plagioclase is wrapped by micas and pretectonic to deformation. Crossed polars.

c Perthite is wrapped by faintly developed biotite. Crossed polars.

d Sphene aggregate occurring within biotite. Crossed polars.

PLATE 3.6

PLATE 3.7

a Phenocrysts of microcline or perthite found in a fine grained matrix of the porphyritic rock. Crossed polars.

b The matrix composed of mainly biotite, quartz and appears to be directional in nature. Crossed polars.

c Fine lamellae of albite in the K-feldspar phenocryst. Note that within the bigger phenocryst albitic plagioclase with muscovite is seen. Crossed polars.

d Fine grained needles of muscovite and possibly apatite(?) in the matrix of the porphyritic rock. Plane polars.

PLATE 3.7

PLATE 3.8

a Biotites are forming at the core of an amphibole. Euhedral apatite crystal is also seen. Plane polars.

b Aplitic texture. Crossed polars.

c Vermicular quartz found within K-feldspar. Note that zircon also shows zoning. Crossed polars.

d Widespread myrmekitisation of quartz and plagioclase intergrowth. Crossed polars.

PLATE 3.8

PLATE 3.9

a Plagioclase shows deformational effect in twin lamella and note that fine grained quartz occur at the left margin of plagioclase. Quartz shows undulose extinction. Crossed polars.

b Orthoclase wrapped by mainly strain free quartz with some amount of biotite. Crossed polars.

c Quartz ribbons formed because of mylonitization. Crossed polars.

d Sieve texture found in granolitic rocks. Plane polars.

PLATE 3.9

PLATE 3.10

a Lamellae of biotite is bent due to deformation. Plane polars.

b Calc-silicate rock showing actinolite, calcite, clinopyroxene, feldspar, epidote and quartz. Crossed polars.

c Sillimanite (fibrous) found in granolites. Crossed polars.

d Needle of muscovite and possibly apatite arranged in a narrow zone. Crossed polars.

PLATE 3.10

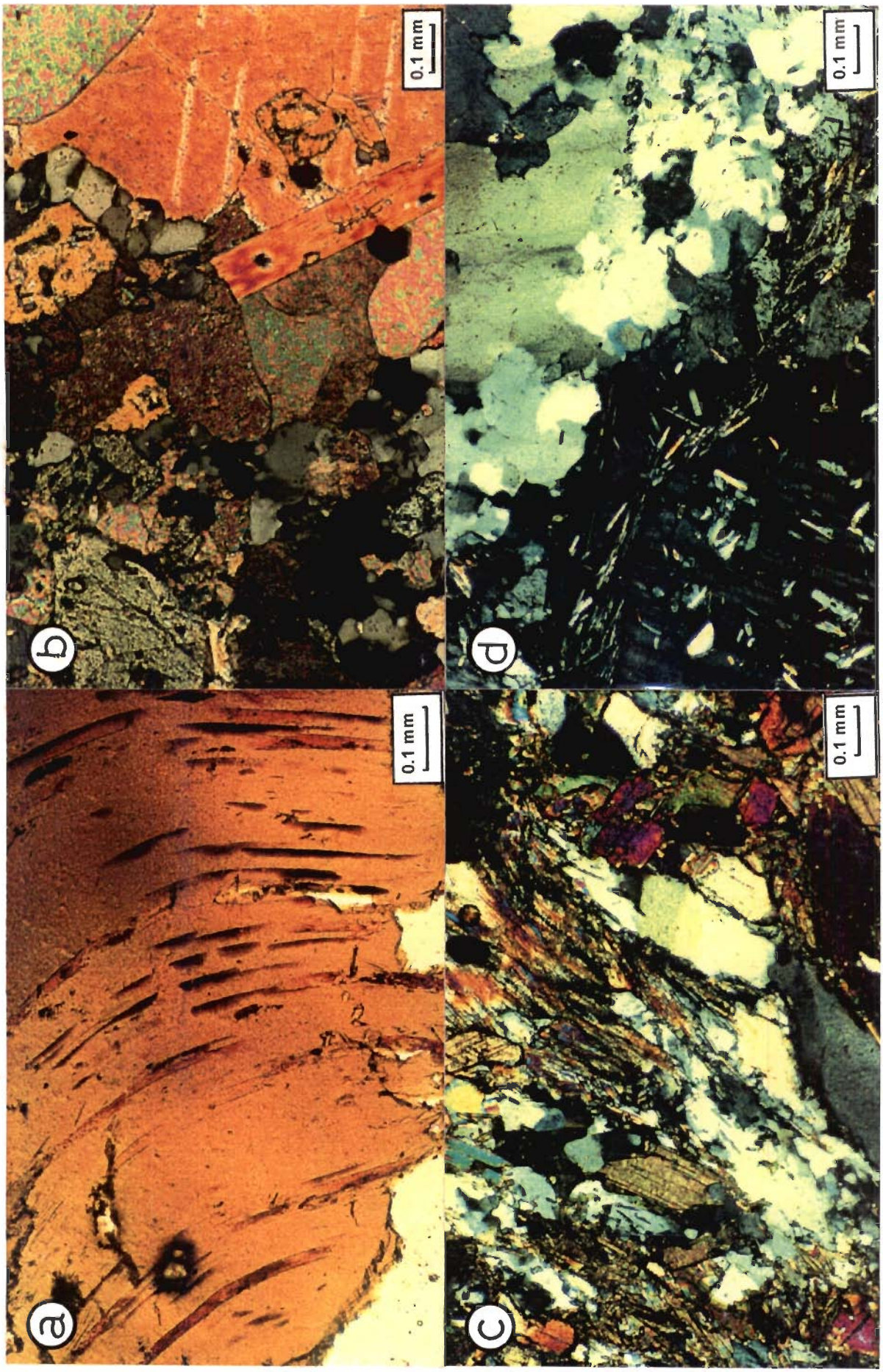

CHAPTER IV

GEOCHEMISTRY

4.1 ANALYTICAL METHODS

4.1.1 Sample Processing

The samples were processed in three different stages. (i) The rock samples weighing approximately 5 kg were broken into small chips of about 0.5 cm size. The chips were cleaned with single distilled water to wash off dust and impurities. They were air dried on a sheet of brown paper in a dust free environment. (ii) The rock chips were crushed into powders using rendered steel mortar and pestle and the entire sample powder was homogenized and coning and quartering was done. (iii) Then about 100 gm of sample was crushed using a mechanized steel mortar, followed by an agate mortar to -200 mesh size. In all the above steps, care was taken to avoid cross contamination.

4.1.2 Sample Digestion

The procedure followed for sample digestion was modified version of Shapiro and Brannock (1962), using two solutions. Solution 'A' was used for the determination of silica only whereas, from solution 'B' all major and trace elements were determined. The samples were digested in a pressure vessel (teflon lined steel bomb) to determine major and trace elements other than rare earth elements. For REEs analysis the samples were fused using a mixture of NaOH and Na_2O_2 fluxes.

'A' Solution

Silica was determined by gravimetric technique. 0.5 gm of rock powder was taken in a 75 ml nickel crucible with the fluxes NaOH and Na_2O_2 in the proportion of 2:9. The mixture was heated in a Meker burner for about 10 minutes in an oxidizing flame till the nickel crucibles turned red and a homogeneous melt formed. The melt was swirled repeatedly to get the sample and flux

homogenized and subsequently it was allowed to cool down. 50 ml of double distilled water was added approximately to the crucible and left overnight. The next day contents of the crucibles were transferred quantitatively to 500 ml teflon beakers and gently heated. 10 ml of 6N HCl was added step by step until the solution became clear. Once the solution became clear, the solution was subjected to incipient dryness followed by re-dissolution in 1N HCl. A gelatinous mass was precipitated and settled at the bottom of the beaker. The solution was filtered to separate filtrate from residue using Whatman # '41' ashless filter paper. The white gelatinous mass in the filter paper was dried down in an oven at low temperature of 70^0C. The residue was put into a pre-weighed platinum dish and ignited using muffle furnace and first charred around 800^0C and ashed around 1050^0C. After cooling to about 150^0C it was removed and kept in a dessicator. The weight of the crucible with filter paper was taken once the crucible attained room temperature and the difference in weight of the crucible gave the amount silica present in 0.5 gm of sample which was converted into percentage. The weighing procedure was repeated twice or thrice till a constant reading was obtained. Accuracy of this procedure was established by analyzing several rock standards.

'B' Solution

0.5 gm of sample was taken in 70 ml teflon beaker. 10 ml of HF, 5 ml of HNO_3 and 1 ml of $HClO_4$ were added to the teflon beaker. It was covered and kept over the hot plate overnight for closed digestion for about 12 hours. However, for the granitoids and the samples containing refractory phases such as, zircon, sphene, rutile etc. the samples were digested in a teflon lined stainless steel pressure bomb for 48 hours. Then the beakers were uncovered and evaporated to incipient dryness. Further 10 ml of HNO_3 was added and evaporated to complete dryness. When the fumes stopped coming, 10 ml of 6N HCl and 20 ml of distilled water was added to the residue in the teflon beaker and gently warmed till the solutions became clear. It was then transferred to 100 ml volumetric flasks and made up to volume.

4.1.3 Determination of Rare Earth Elements

Rare earth elements occur in ppb to ppm levels in the rocks. Many workers have suggested different procedures for sample digestion and effective determination of REEs by ICP-AES after pre-concentration (Walsh et el.,1981; Crock et al.,1984; Satynarayan et al.,1989; Rathi et al.,1991; Zackariah, 1992 and Sahoo and Balakrishnan, 1994) in different laboratories. However, a suitable procedure for REE analysis needs to be developed taking into account one's own laboratory and instrumental conditions and nature of samples to be analyzed.

Complete sample digestion is important to obtain the true abundances of the REEs present in the rock. Because, refractory minerals such as, rutile, zircon, monazite contain high concentration of REEs (Gromet & Silver, 1983). Initially, teflon lined bomb digestion technique was

tried as described in 'B' solution procedure. It was found that in replicate analysis of the samples, the values obtained in different analyses were inconsistent, as the refractory minerals may not have been completely digested. Therefore, fusion technique was adopted as described in 'A' solution procedure for the dissolution of the samples, which gave consistent results in successive analyses.

For clean separation of REE as a group adopting two columns procedure was necessary. Because, Fe and Ca & Sr could not be removed completely in HNO_3 and HCL columns respectively (Fig. 4.1). Presence of these matrix elements affected the REE analysis by ICP-AES. After the columns were calibrated they were used for the separation of REEs as a group from the unknown samples. After fusion of the samples, the silica was filtered out and the filtrate was collected. It was dried down completely and traces of silica, if any, was got rid of by adding HF and evaporated to dryness. The residue was dissolved in 1N HCl which contained all the elements barring silica.

A few drops of phenol red, pH indicator was added to the above solution. Subsequently, ammonium hydroxide was added drop by drop till the pH became 7 and a thick gelatinous precipitate was formed. The solution was centrifuged for about 30 minutes at 6000 rpm and the supernatant solution containing mono & divalent ions was decanted. The precipitate was dissolved in 2N HCl and evaporated to complete dryness. Subsequently, it was dissolved in 30 ml of 1N HNO_3 which was used for group separation of REEs using cation exchange resin columns.

Column Calibration

The separation of REEs as a group were done using cation exchange resins (Biorad AG 50 X-8, 100-200 mesh size) in quartz columns (24 cm long x 1 cm inner diameter). The columns were calibrated using multi-element solution containing matrix elements (Fe, Ca, Sr, Al, Mn, Na, K, Zr and Ba) and Rare Earth Elements. 30 ml of the multi-element solution dissolved in 1N HNO_3 initially loaded into the (cation exchange resin) HNO_3 column. To elute the matrix elements, 1.8 HNO_3 was passed through column which was collected at 10 ml intervals and subsequently analyzed by ICP-AES. From the analytical data it was noted that by passing 110 ml of 1.8 HNO_3, all the matrix elements were eluted except Fe (Fig. 4.1a, b) and all REEs were eluted using 120 ml of 6N HNO_3 (Fig. 4.2).

Similar type of column calibration exercise was followed for HCl column also. By passing 70 ml of 1.8N HCl (Fig. 4.1c) through the HCl column, Fe and other matrix elements were removed and REEs were eluted by passing 200 ml of 6N HCl (Fig. 4.2). The procedural details of pre concentration of REEs and subsequent determination by ICP-AES is provided in the form of a flow chart (Fig. 4.3). Each column was further used after regeneration.

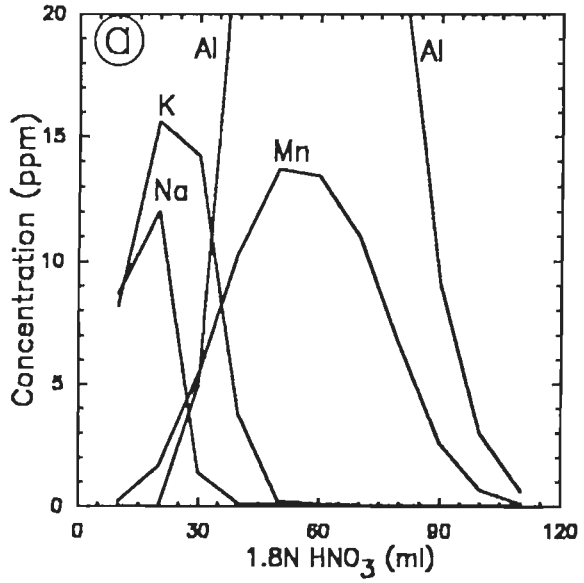

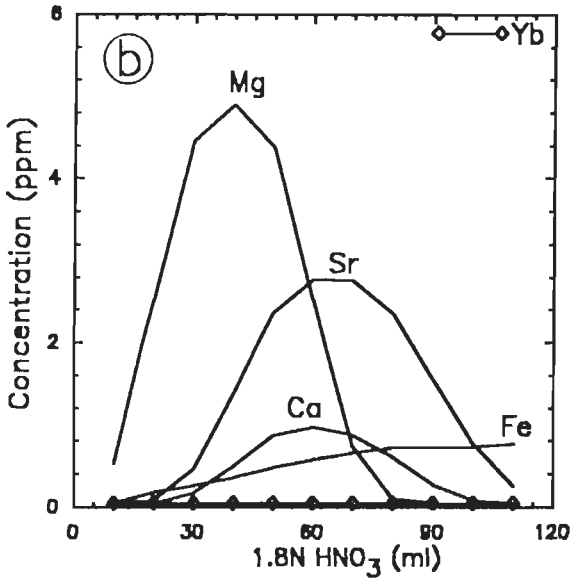

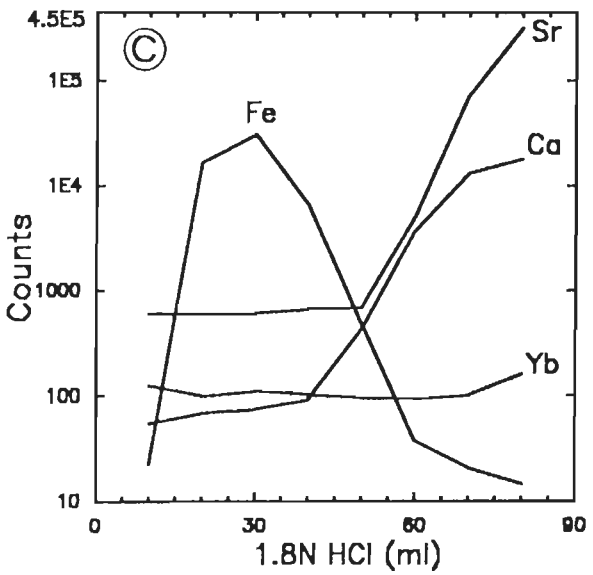

FIG. 4.1 Elution patterns for matrix elements at 1.8N HNO_3 and HCl acid.

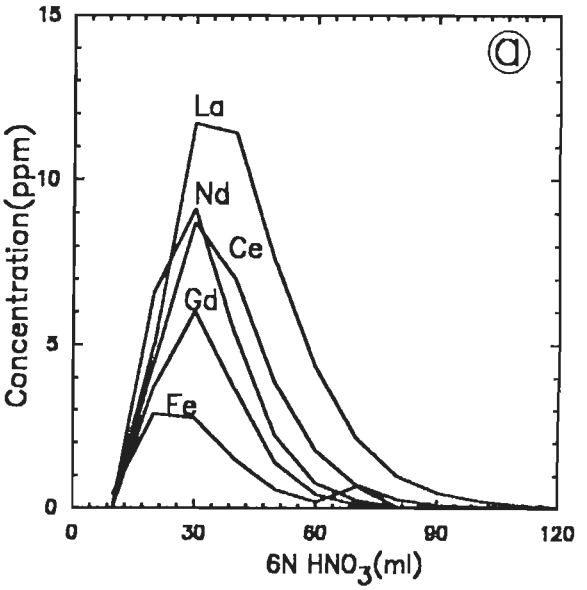

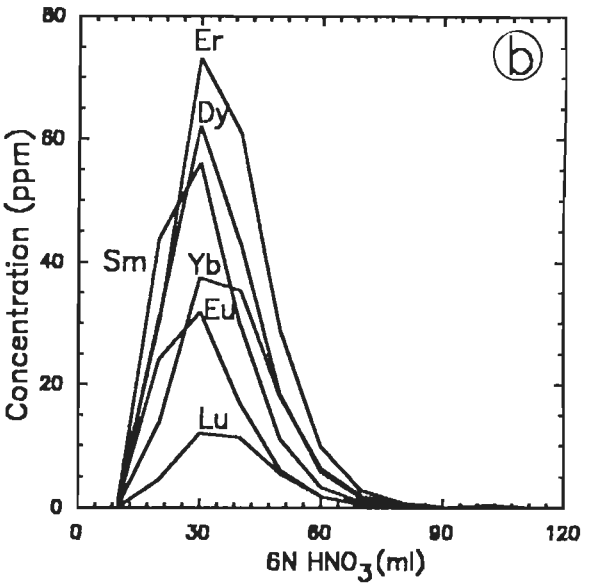

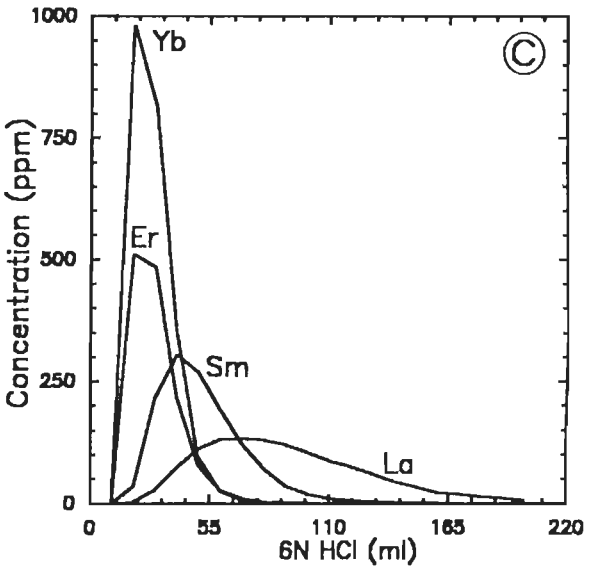

FIG. 4.2 Rare Earth Element elution patterns for 6N HNO_3 and HCl acid.

4.1.4 Analyses of Sample

The samples were analyzed for major and trace elements after calibrating the instruments using USGS rock standards BHVO, STM-1, RGM-1 and DNC-2 (Govindaraju, 1989). MB-H an International standard developed by Wadia Institute of Himalayan Geology, Dehradun, India (Rathi et al., 1994) was run as unknown to check the accuracy of the analysis. The major elements Al_2O_3, FeO, MgO, MnO, CaO, TiO_2 and P_2O_5 and trace elements Ba, Sr, Ni, Cr and Zr were analyzed by ICP-AES (LABTAM-8440) from 'B' solution. Only Na_2O and K_2O were analyzed by flame photometer. Nb and Y analysis on a few selected samples were carried out by XRF (at Atomic

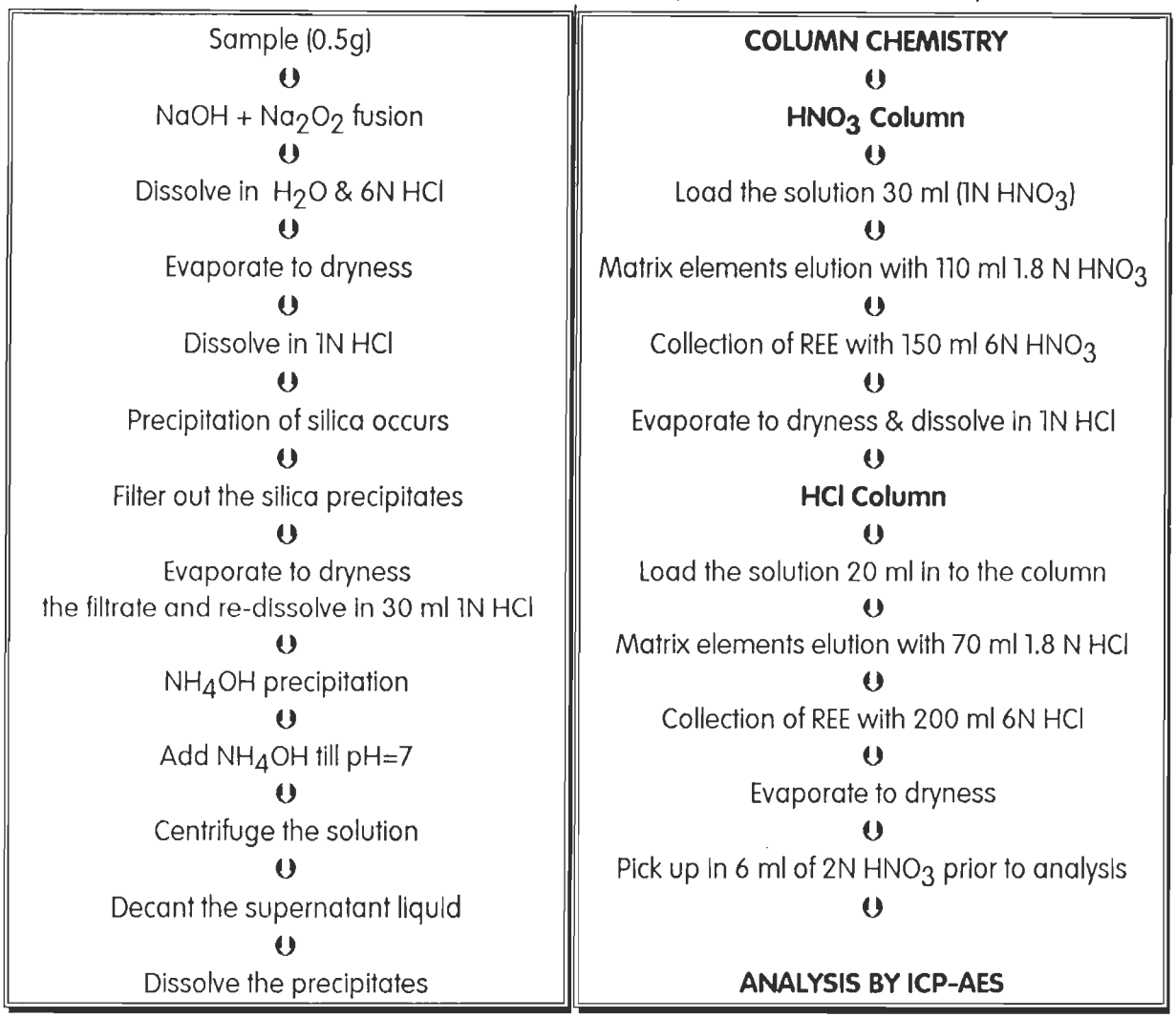

Figure 4.3 Preconcentration procedure for REEs & their Determination by ICP-AES

Mineral Division, Hyderabad) and ICP-AES respectively.

For analyses of REEs as a group the multi-element standards of high purity were prepared from salts obtained from Johnson & Mathey and Spex Inc. and used for calibration. Internal standard 90-57 (Zackariah,1992) on which the REE data is available by isotope dilution technique and MB-H (Rathi et al., 1994) were used to evaluate the instrumental, as well as, procedural

performance. Consistent values obtained on replicate analyses of these reference materials and samples, reflect the accuracy and precision of the REE analysis (Table 4.1).

Table 4.1 Replicate analysis of the samples for major, trace and Rare Earth Element abundances.

Replicate analysis of the samples for major and trace element abundances. SDM indicates standard deviation from the mean values

Sample #	J-88	J-88D	Mean ± SDM	J-109	J-109D	Mean ± SDM	J-113	J-113D	Mean ± SDM
SiO_2	77.89	76.35	77.12 ± 0.77	59.83	57.93	58.88±0.95	78.97	77.1	78.035±0.935
TiO_2	0.149	0.149	----	1.34	1.36	1.35±0.01	0.139	0.143	0.141±0.002
Al_2O_3	12.2	12.7	12.45±0.25	15.6	15.7	15.65±0.05	11	11.4	11.2±0.2
FeOt	1.46	1.46	----	7.7	7.8	7.75±0.05	0.69	0.67	0.68±0.01
MnO	0.011	0.011	----	0.148	0.149	0.1485±0.0005	0.013	0.014	0.0135±0.0005
MgO	0.352	0.393	0.3725±0.02	2.18	2.21	2.195±0.015	0.194	0.198	0.196±0.002
CaO	0.37	0.4	0.385±0.015	4.74	4.73	4.735±0.005	1.95	2.01	1.98±0.03
Na_2O	1.69	1.67	1.68±0.01	2.88	2.82	2.85±0.03	3.07	3.1	3.085±0.015
K_2O	5.07	4.8	4.335±0.135	4.07	4.07	----	2.07	2.2	2.135±0.065
P_2O_5	0.24	0.23	0.235±0.015	0.54	0.52	0.53±0.01	0.15	0.145	0.1475±0.0025
Ba	520	540	530±10	1650	1560	1605±45	1830	1860	1845±15
Sr	35	38	36.5±1.5	272	258	265±7	355	365	360±5
Cr	79	71	75±4	111	115	113±2	31	29	30±1
Ni	16	14	15±1	45	41	43±2	14	16	15±1
Zr	91	87	89±2	104	114	109±5	38	37	37.5±0.5
Y	30.56	31.29	30.925±0.365	24	23.27	23.635±0.365	1.71	1.8	1.755±0.045

Replicate analysis of the samples for Rare Earth element abundances. D1, D2 refers to successive replicate analysis of the samples

Sample #	J-69	J-69D	Mean ± SDM	J-82	J-82D	Mean ± SDM	J-109	J-109D1	J-109D2	Mean ± SDM
Ce	6.51	6.34	6.425 ± .085	132.39	133.25	132.82 ± 0.43	64.23	66.42	63.55	64.985 ± 1.435
Nd	2.07	1.97	2.02 ± 0.05	65.31	66.68	65.995 ± 0.685	37.63	38.91	36.12	37.515 ± 1.395
Sm	0.26	0.29	0.275 ± 0.015	14.43	14.54	14.485 ± 0.055	8	8.22	8.03	8.11 ± 0.11
Eu	0.77	0.71	0.74 ± 0.03	2.51	2.55	2.53 ± 0.01	3.88	4.01	3.72	3.865 ± 0.145
Gd	0.55	0.6	0.575 ± 0.025	11.3	11.11	11.205 ± 0.095	6.36	6.5	6.28	6.39 ± 0.11
Dy	0.64	0.7	0.67 ± 0.03	9.64	9.1	9.37 ± 0.27	4.94	4.98	4.58	4.78± 0.20
Er	0.46	0.49	0.475 ± 0.015	5.18	4.82	5.0 ± 0.18	2.24	2.02	1.94	2.09 ± 0.15
Yb	0.68	0.7	0.69 ± 0.01	4.53	4.35	4.44 ± 0.09	1.82	1.42	1.6	1.62 ± 0.2

Accuracy of the analysis for the Rare Earth Elements. 90-57 values by isotope dilution technique (Zachariah, 1992) and MB-H* values (from Rathi et al., 1994). A, A1 and A2 refers to successive analyses carried out

Sample #	90-57 ID value	90-57 A1	90-57A2	Accuracy %	MB-H*	MB-H A	Accuracy %
Ce	38.5	35.07	35.48	8.37	73.6	68.31	7.19
Nd	21.8	21.61	22.53	1.24	39.4	37.95	3.68
Sm	4.89	5.38	5.49	11.14	9.69	9.165	5.42
Eu	1.58	1.72	1.76	10.13	2.77	2.86	3.24
Gd	4.75	5.14	5.12	8.0	9.28	10.06	8.40
Dy	4.6	4.88	5.01	7.50	9.35	9.83	5.13
Er	2.6	3.21	3.21	23.46	5.23	5.205	0.48
Yb	2.3	2.42	2.44	5.65	5.02	4.87	2.99

Table 4.1 Contd.

Accuracy of the analysis for major and trace elements using MB-H standard			
Std.Name	MB-H *	MB-H A	Accuracy %
SiO_2	49.55	49.28	0.54
TiO_2	2.77	2.82	1.8
Al_2O_3	13.1	13.01	0.69
FeO_T		13.81	
Fe_2O_{3T}	15.39		
Mno	0.22	0.22	0
MgO	5.07	5.12	0.99
CaO	6.38	6.26	1.89
Na_2O	2.76	2.72	1.45
K_2O	2.66	2.59	2.63
P_2O_5	0.39	0.4	2.56
Ba	482	459	4.78
Sr	147	145	1.36
Ni	18	20	11.11
Zr	233	223	4.3
Y	52.8	54.4	3.03
V	300	314	4.67
Zn	136	136	0

* Indicates working values for MB-H standard (after Rathi et al.,1994)

4.2 RESULTS

4.2.1 Amphibolites

The amphibolites have a very narrow range in SiO_2 & TiO_2, FeO, MnO, CaO and Na_2O contents (Table 4.2). The MgO abundances range from 5.7 to 8.6 wt.%. The amphibolites of Masuda have higher K_2O contents compared to the amphibolites from the Archaean Dharwar Craton (Rajamani et al., 1985). The high K_2O contents of Masuda amphibolites may be due to its close spatial association with intermediate and granitoid suites in the study area which have higher K_2O contents compared to amphibolites. Sample J-38 has the lowest K_2O content among the amphibolite samples studied (Table 4.2).

Variation in Ba contents is quite large (36 to 581 ppm) among the amphibolites. Ni contents vary from 50 to 102 ppm and that of Sr from 111-203 ppm. Nb contents vary from 3-11 ppm and Zr from 49 to 137 ppm.

Rare Earth Elements show a flat to light rare earth element enriched pattern (Fig. 4.4). Ce_N values in amphibolites vary from 8 to 25 and Yb 10 to 14 relative to chondrite. These samples do not show any significant Eu anomaly (Fig. 4.4). Chondrite normalized factors are taken from Masuda et al. (1973). The REE data for all the rock types including amphibolites of study area are presented in Table 4.7.

4.2.2 Intermediate rocks

Geochemically, the intermediate suite of rocks are comparable to the sanukitoids (see section 6.1, Chapter VI). Based on TiO_2/MgO ratio the rock suite can be classified into two different categories. If the TiO_2/MgO ratio is greater than 0.404 the rocks may be classified as high-Ti sanukitoid suites and as low-Ti sanukitoids when the ratio is less than 0.404. The intermediate group of rocks have a wide range of silica contents (51 to 69 wt.%). The intermediate rocks also have a wide variation in total FeO contents (3.5 to 12 wt.%). Two of the samples show low MgO contents (J - 83 = 0.57 and J - 84 = 1.04 wt.%) although they have SiO_2 contents of 64.2, 61.38

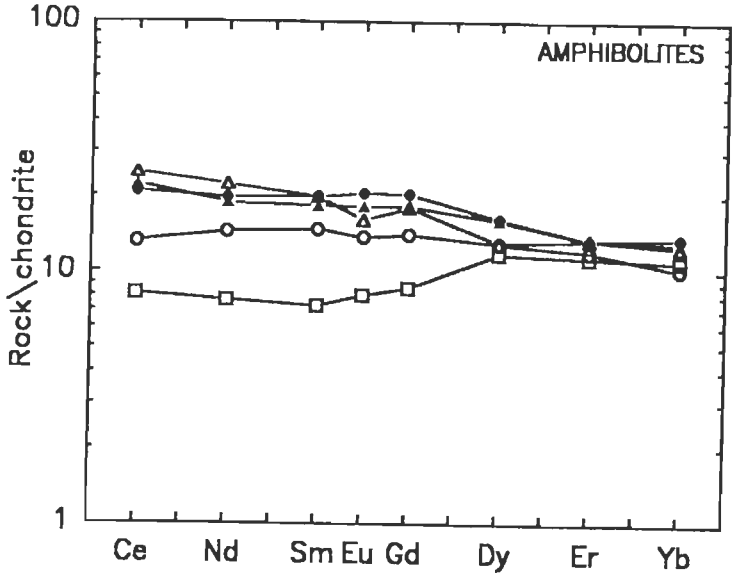

FIG 4.4 **Chondrite normalized rare earth element patterns for amphibolites which show flat to slightly enriched LREE pattern.**

Table 4.2 Major & Trace element data of amphibolites of BGC around Masuda

Sample #	J-18A	J-29	J-31	J-35	J-37	J-38	J-68	J-71
SiO_2	46.75	42.7	42.99	43.6	44.4	48.3	43.9	43.93
TiO_2	1.18	1.56	1.87	1.67	1.22	1.97	1.53	1.36
Al_2O_3	15.27	15.08	14.52	14.68	15.48	14.19	15.2	15.29
FeO_T	11.43	13.21	13.60	14.47	11.93	14.73	13.12	14.54
MnO	0.19	0.23	0.24	0.22	0.2	0.23	0.29	0.24
MgO	7.44	6.96	6.81	5.68	7.53	6.82	8.59	6.83
CaO	12.03	14.23	14.68	12.65	12.48	8.31	9.98	11.1
Na_2O	3.15	2.8	2.77	3.12	3.15	3.23	3.0	3.3
K_2O	1.28	1.82	1.26	1.34	1.36	0.24.	2.34	1.24
P_2O_5	0.12	0.12	0.14	0.1	0.1	0.15	0.17	0.13
Total	98.84	98.71	98.88	97.53	97.85	98.17	98.12	97.96
mg #	0.58	0.53	0.50	0.45	0.57	0.49	0.58	0.50
Ba	81	581	79	89	100	326	345	36
V	224	317	354	342	250	373	379	318
Rb	26	22	25	13	42	162	136	12
Sr	147	203	180	202	158	144	179	111
Ni	50	80	69	98	51	80	102	122
Cr	151	203	58	153	172	134	273	204
Cu	43	59	16	11	64	79	145	76
Zn	39	121	119	85	61	105	120	105
Zr	54	49	74	81	70	137	96	49
Nb	5	3	nd	11	10	10	8	nd
[Fe]%	11.98	12.76	13.31	14.89	12.14	16.39	13.39	14.9
[Mg]%	17.58	16.48	15.72	13.8	17.84	15.56	19.92	16.04
Ol T °C	1204	1188	1177	1151	1210	1196	1257	1194
Eq.Ol	80.0	78.12	76.39	71.32	80.50	72.60	81.24	74.87
Al_2O_3/TiO_2	12.94	9.67	7.76	8.80	12.69	7.20	9.93	11.24
Zr/Nb	11	16.33	___	7.36	7.0	13.70	12.0	___
Ce/Yb	___	5.05	___	6.0	7.72	___	6.70	2.91

Oxides are in wt.% and trace elements are in ppm.

wt.% and FeO_t contents of 5.88, 5.3 wt.% respectively (Table 4.3). The sample # J-126 shows the highest MgO content of 7.2 wt.% amongst the intermediate rocks sampled. CaO contents of the sanukitoids have a range from 3 to 7.4 wt.% except for the two of the samples that have less than 3 wt.% CaO (sample # J-76 and J-119).

Ba contents have a very wide range from 324-2436 ppm (Table 4.3). Excepting one sample (J-126) all others have more than 500 ppm Ba. Quite a few samples have greater than 1000 ppm of Ba abundances. Two of the samples (J-53 & J-53A) have high Zr concentration (446 & 558 ppm). The Sr abundances range from 215 to 888 ppm and most of the samples have Sr abundances more than 300 ppm. Samples (J-39 & J-53A) with high Ba, K, Sr and TiO_2 contents also show high Nb concentrations (Table 4.3).

Samples with higher Ba, Sr, Nb abundances and TiO_2/MgO ratio (high-Ti sanukitoids) are also enriched in light rare earth elements (Ce=64-309 ppm) and the heavy rare earth element (HREE) abundances vary from 1.5 to 2 ppm (Table 4.7). They have a sloping chondrite normalized REE patterns without significant Eu anomaly (Fig. 4.5).

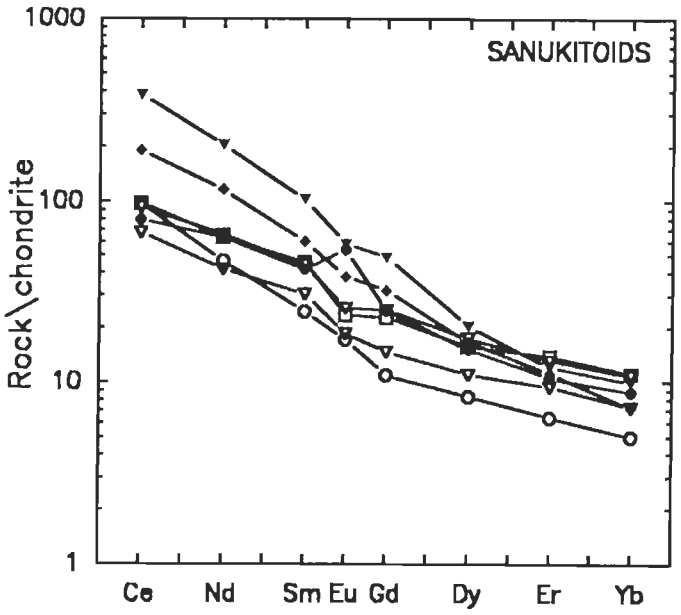

FIG 4.5 **Chondrite normalized rare earth element patterns for the two suites of sanukitoids. Filled and open symbols represent high- and low-Ti sanukitoids respectively. Note that the high-Ti sanukitoids have higher LREE abundances than low-Ti sanukitoids.**

Low-Ti sanukitoids are comparatively less light REE enriched (Ce=55-80 ppm) relative to the high-Ti sanukitoid suite (Fig. 4.5). However, both low- and the high-Ti suite sanukitoids have comparable HREE abundances (Table 4.7) and are devoid of Eu anomaly excepting sample # J-109 which has a slight positive Eu anomaly (Fig. 4.5).

4.2.3 Granodiorite gneisses

Granodiorites invariably have greater than 68 wt.% and less than 73 wt.% of SiO_2 (Table 4.4). The granodiorites have a range of TiO_2 contents from 0.1 to 0.81 wt.%, however, a large number of samples have more than 0.3 wt.% TiO_2. They also have ca. 3 wt.% of total FeO contents. The low-TiO_2 samples also have lower FeO (Table 4.4). The MgO content in the granodiorite samples is ca.1 wt.% excepting a few samples. Similarly, average CaO content is ca. 1.8 wt.% and they have higher total alkali contents than the sanukitoid suite of rocks. However, one of the granodiorite sample (J-30) shows much higher CaO content (8.6 wt.%) compared to other samples. This sample is highly altered and has about 15 vol.% of epidote group of minerals which might have contributed to the high CaO contents in the sample.

Ba contents are more than 400 ppm and the Sr abundances range from 113-479 ppm except two samples. Two of the granodiorite samples (J-13 & J-77) have low Ba (92 & 145) and Sr (29 & 35) concentrations compared to other samples in the suites (Table 4.4). Sample # J-77, for which REE data is available, has a prominent negative Eu anomaly in chondrite normalized REE diagram (Fig. 4.6).

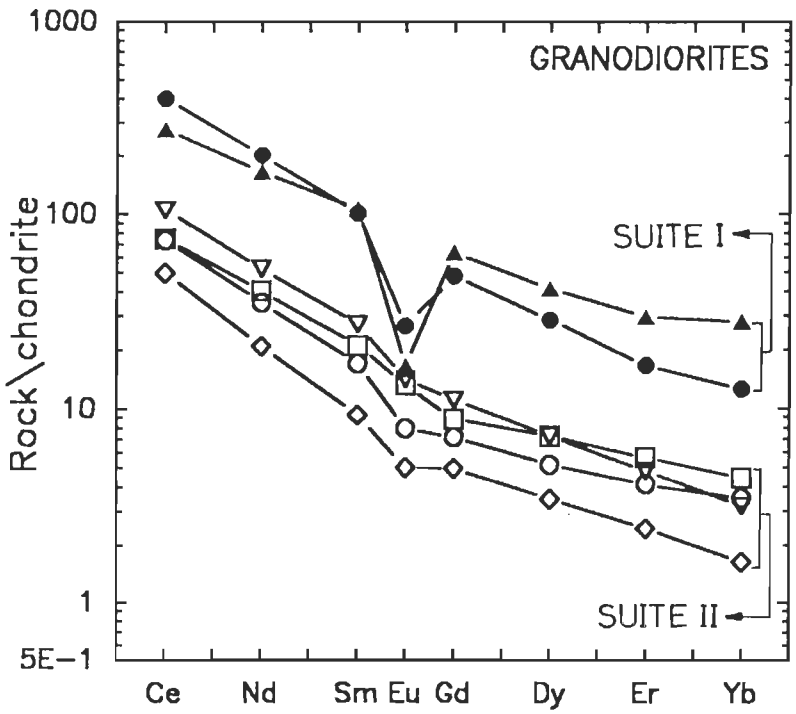

FIG 4.6 **Chondrite normalized rare earth element patterns for granodiorite suite of rocks. Filled symbols represented by granodiorite suite I and open symbols by granodiorite suite II. The first suite has higher REE abundances, prominent negative Eu anomalies than the suite II.**

Table 4.4 Major& Trace element data of granodioritic rocks of BGC around Masuda.

Rock types	Granodiorite Suite I			Granodiorite Suite II										
Samples #	J-13	J-74	J-77	J-16	J-30	J-32	J-33	J-41	J-43	J-50	J-59	J-64	J-75	J-89
SiO_2	73.0	66.23	70.0	68.50	73.55	69.60	71.78	72.65	73.5	72.11	73.92	69.45	70.06	71.01
TiO_2	0.45	0.73	0.38	0.81	0.14	0.27	0.13	0.46	0.11	0.33	0.15	0.32	0.4	0.6
Al_2O_3	13.0	17.62	14.72	14.83	10.33	15.29	14.33	13.81	13.33	14.08	14.26	15.41	16.03	14.5
FeO_t	3.53	4.97	4.32	4.45	1.79	2.45	1.65	3.74	1.42	3.21	1.62	3.43	4.1	4.55
MnO	0.07	0.05	0.67	0.06	0.04	0.05	0.04	0.04	0.02	0.05	0.02	0.06	0.04	0.04
MgO	0.11	0.87	0.3	0.87	0.56	1.08	0.69	0.93	0.62	1.37	0.64	1.75	1.23	0.85
CaO	1.28	1.81	1.72	1.82	7.61	4.72	2.79	1.56	2.58	2.8	1.17	2.48	1.93	1.45
Na_2O	3.4	3.62	4.3	3.65	1.90	3.98	3.88	3.55	4.0	3.98	4.3	4.5	4.04	2.64
K_2O	3.32	3.7	3.92	3.22	3.02	2.80	3.26	3.40	3.4	2.30	3.92	2.6	2.9	2.71
P_2O_5	0.06	0.15	0.12	0.19	0.06	0.12	0.04	0.11	0.04	0.09	0.09	0.14	0.04	0.28
Total	98.22	99.75	100.45	98.4	99.00	100.36	98.59	100.25	99.02	100.32	100.09	100.14	100.77	98.63
Ba	145	622	92	805	1271	977	831	639	929	745	739	940	412	1020
V	8	22	9	21	34	36	16	34	17	48	20	45	31	nd
Rb	117	225	186	101	72	44	246	500	216	72	142	87	219	nd
Sr	35	143	29	153	217	479	253	113	253	345	183	321	169	177
Ni	bdl	bdl	bdl	4	35	3	123	49	28	86	41	11	bdl	32
Cr	bdl	58	40	bdl	495	149	376	246	227	339	201	219	149	290
Cu	bdl	13	bdl	16	3	1	1	2	bdl	13	3	9	bdl	nd
Zn	25	34	34	27	bdl	bdl-	bdl	2	bdl	bdl-	bdl-	3	24	nd
Zr	354	336	473	384	97	172	137	283	125	193	261	184	289	nd
Y	nd	nd	nd	nd	nd	nd	nd	nd	nd	nd	nd	nd	nd	25

Based on the REE abundances the granodiorite suite of rocks are classified into two categories. The first suite defined by samples (J-74 & J-77) have high light (Ce=274 to 398 ppm) and heavy REE (Yb=12.5 to 27.5 ppm) abundances shown in Table 4.7. These rocks show LREE enriched chondrite normalized REE patterns with prominent negative Eu anomalies (Fig.4.6).

The second suite of granodiorite rocks have lower REE abundances (Ce=50-105 and Yb=1.6-4.4 ppm) than the Suite I (Table 4.7) and have subparallel fractionated chondrite normalized REE patterns with no significant Eu anomaly (Fig. 4.6).

4.2.4 Granolitic Rocks

Granolitic rocks have comparable major and trace element characteristics similar to that of sanukitoids, as well as, granodiorite suite of rocks. Based on the SiO_2 contents they can be grouped into two categories. The first suite has a silica range from 59 to 63 wt.%. and the second suite has more than 67 wt.% of SiO_2 (Table 4.5). The first suite is broadly comparable with the sanukitoids and the second suite with the granodiorites. The granolites invariably have more than 1 wt.% TiO_2 except a few samples having ca. 0.6 wt.% TiO_2. The average Al_2O_3 content is greater than 14 wt.% and FeO_t more than 6 wt.%. The MgO contents have a range from 0.93 to 2.83 wt.% (Table 4.5).

Table 4.5 Major and trace element abundances of granolites

Rock types	Granolite Suite I					Granolite Suite II			
Sample #	J-62	J-78	J-81	J-82	J-118	J-100	J-101A	J-101B	J-124
SiO_2	61.7	59.8	59.25	60.46	62.7	67.97	70.92	69.98	70.93
TiO_2	1.61	1.65	0.97	1.12	0.6	0.97	0.54	0.6	0.99
Al_2O_3	14.92	15.26	15.43	15.36	14.7	13.8	13.4	12.9	12.8
FeO_t	8.61	10.26	9.11	7.43	4.13	5.8	4.55	5.5	6.4
MnO	0.12	0.12	0.12	0.09	0.08	0.08	0.06	0.68	0.1
MgO	1.98	2.69	2.83	1.7	3.16	1.35	1.39	1.66	0.93
CaO	4.35	2.36	5.7	4.4	7.7	3.78	2.96	2.78	2.91
Na_2O	3.12	2.75	3.05	3.05	3.05	1.86	2.05	1.63	1.78
K_2O	2.68	2.45	3.02	2.98	3.93	3.5	3.36	3.78	3.36
P_2O_5	0.45	0.35	0.21	0.27	0.33	0.34	0.25	0.3	0.3
Total	99.54	97.69	99.69	96.86	100.38	99.45	99.48	99.81	100.5
Ba	1088	885	1254	1224	1100	1030	970	1090	1230
V	128	151	119	97	nd	nd	nd	nd	nd
Rb	142	131	145	200	nd	nd	nd	nd	nd
Sr	244	221	191	184	374	162	154	147	185
Ni	2	20	39	10	39	37	37	42	23
Cr	93	76	112	94	101	60	145	188	4
Cu	16	28	42	7	nd	nd	nd	nd	nd
Zn	63	82	75	41	nd	nd	nd	nd	nd
Zr	109	71	66	79	nd	nd	nd	nd	nd
Nb	nd	nd	24	nd	nd	nd	nd	nd	nd
Y	nd	nd	nd	nd	23.14	51	20.4	52.17	51.86

Among the trace element abundances the average Ba and Sr contents are 1000 and 200 ppm respectively. Nb (24ppm) and Y (20-52 ppm) abundances are also high on a few samples. The granolites have distinctly lower Zr abundances than the sanukitoids and granodiorites.

Both, granolitic host (J-81) and enclave (J-82) have similar abundances of major and trace elements (Table 4.5). The host as well as enclave have subparallel chondrite normalized REE patterns with negative Eu anomalies (Fig. 4.7). The enclave sample has higher REE abundances than the host (Table 4.7). The other set of granolitic host (J-101A) and enclave (J-101B) are also indistinguishable from each other in major and trace element abundances (Table 4.5).

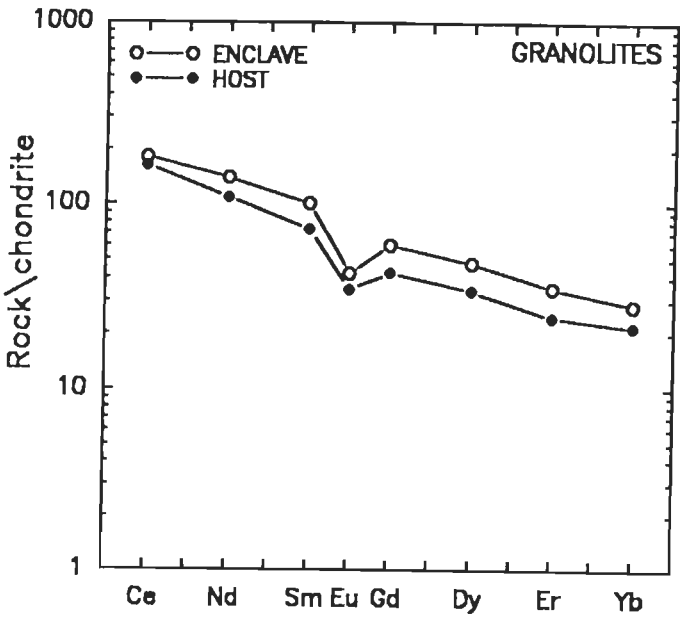

FIG 4.7 **Chondrite normalized rare earth element patterns for granolites. The granolitic enclave has higher REE abundances than the granolitic host.**

4.2.5 Granophyres and aplite

The granophyres have more than 77 wt.% SiO_2 whereas, the aplite has 73 wt.% SiO_2. The aplite sample has high FeO, MgO, Zr and have lower Ba than the granophyres (Table 4.6). The rocks of this suite are typically low in TiO_2, FeO, CaO abundances than the granodiorite suite of rocks. Two of the granophyre samples (J-69 & J-113) have high Ba (1735 & 1830 ppm) and Sr (203 & 355 ppm) compared to the other granophyre and aplite samples. One of the granophyre sample # J-88 has very high Y content (30 ppm) in the group (Table 4.6).

The aplite has higher REE (Ce=86 and Yb=2.5) abundances than the granophyres (Table 4.7). They have a light REE enriched sloping chondrite normalized concave upward REE pattern with prominent positive Eu anomalies (Fig. 4.8). The sample # J-69 has the least REE abundances among the group.

Table 4.6 Major & Trace element abundances of granophyres, aplite and miscellaneous samples of BGC around Masuda.

Rock types	Granophyres				Aplite	Miscellaneous rocks				
Sample #	J-69	J-88	J-110	J-113	J-65	J-14	J-40	J-48	J-90	J-92
SiO_2	77.25	77.89	78.35	78.97	72.85	47.23	67.35	35.3	59.21	66.95
TiO_2	0.01	0.15	0.14	0.14	0.26	0.86	0.51	0.18	0.65	0.45
Al_2O_3	14.81	12.2	11.8	11.0	14.62	23.1	15.45	7.35	20.7	15.6
FeO_t	0.7	1.46	1.15	0.69	2.85	5.63	4.92	2.37	8.30	3.49
MnO	0.002	0.01	0.03	0.01	0.04	0.08	0.04	0.06	0.08	0.05
MgO	0.22	0.35	0.4	0.19	0.79	4.84	1.63	1.76	2.6	1.65
CaO	0.7	0.37	1.52	1.95	1.61	11.76	2.99	35.40	0.3	8.70
Na_2O	3.07	1.69	1.52	3.07	3.62	3.18	3.75	2.45	0.69	1.46
K_2O	3.84	5.07	4.25	2.07	3.24	1.34	2.14	3.38	4.5	0.21
P_2O_5	0.05	0.24	0.17	0.15	0.11	0.21	0.11	0.09	0.26	0.27
Total	100.65	99.43	99.33	98.24	99.99	98.23	98.89	88.34	97.29	98.53
Ba	1735	520	750	1830	730	502	339	418	900	60
V	8	nd	nd	nd	29	102	55	39	nd	nd
Rb	175	nd	nd	nd	117	31	231	177	nd	nd
Sr	203	35	173	355	189	743	241	246	57	883
Ni	bdl	16	16	14	bdl	64	16	63	80	46
Cr	147	79	38	31	147	224	172	153	384	76
Cu	2	nd	nd	nd	1	26	2	4	nd	nd
Zn	bdl	nd	nd	nd	bdl	bdl	19	bdl	nd	nd
Zr	51	nd	nd	nd	249	45	251	72	174	nd
Nb	nd	nd	nd	nd	nd	4	nd	nd	nd	nd
Y	nd	30.56	9.24	1.71	nd	26	nd	nd	27.68	18

Oxides are in wt.% and trace elements are in ppm, bdl is below detection limit and nd is not determined. J-14; highly epidotized sample; J-40: migmatized mica-schist; J-48: Calc-silicate; J-90: pure mica-schist; J-92: mixed rock

4.2.6 Miscellaneous Rocks

A few samples presumably of meta-sedimentary origin occurring within the study area were analyzed for major, trace and Rare Earth Element abundances. A typical calc-silicate rock (J-48) has 35.3 wt.% of SiO_2, 35.4 wt.% of CaO and total major element oxides in this sample add up to 88 wt.% and the rest could be CO_2 as this sample has abundant calcite. A sample of pure mica-schist shows high alumina content of 20.7 wt.% (Table 4.6). The migmatized mica-schist is chemically comparable with granodiorite suite of rocks. It has a LREE enriched (Table 4.7) sloping chondrite normalized REE pattern with negative Eu anomaly (Fig. 4.9).

One of the sample (J-92) has a very unusual chemistry having high CaO (8.7 wt.%), low Ba (60 ppm), low K_2O (0.92 wt.%) and high Sr (883 ppm) contents. Similarly, J-14 a basic to intermediate in composition is highly mylonitized and epidotized. It contains high Al_2O_3 (23.1 wt.%), CaO (13.76 wt.%) and low SiO_2, 49.2 wt.% (Table 4.6). The unusual chemistry is perhaps due to alteration during shearing and mylonitization. Hence, these rocks are not being considered for petrogenetic modelling.

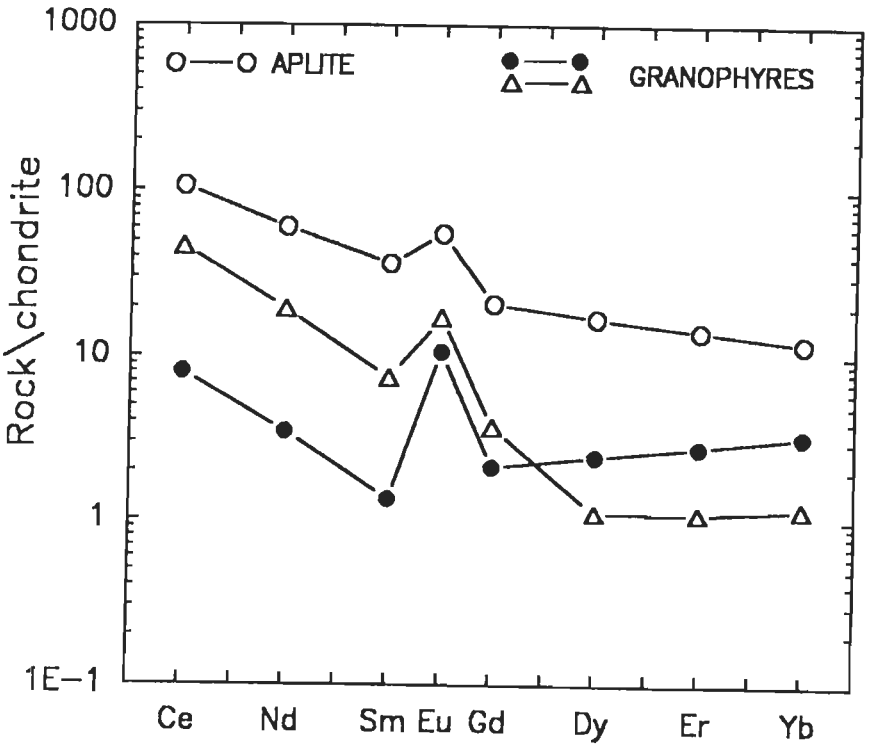

FIG 4.8 Chondrite normalized rare earth element patterns for granophyres and aplite. The aplite has higher REE abundances than the granophyres.

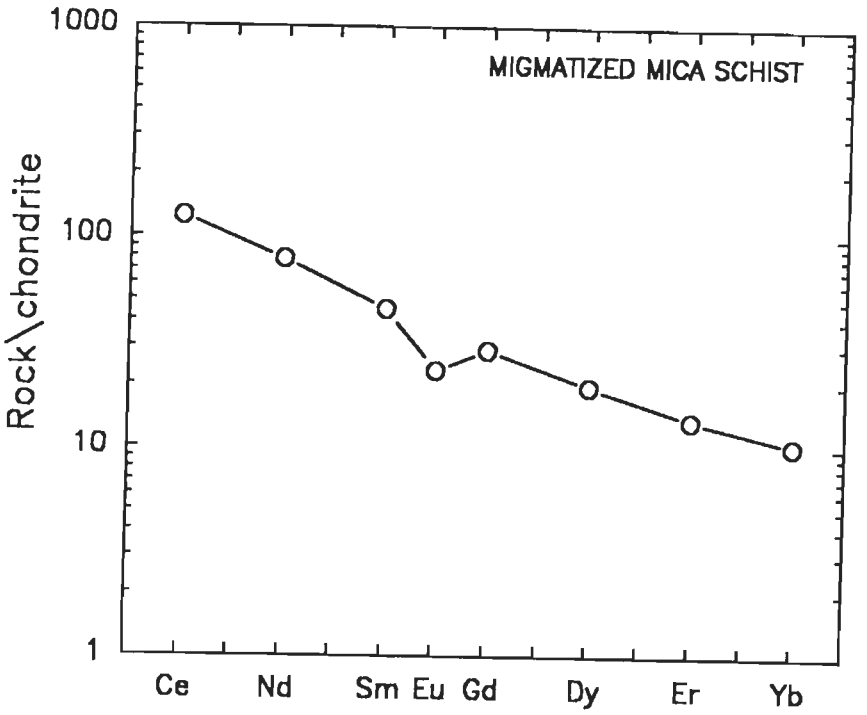

FIG 4.9 Chondrite normalized rare earth element pattern for migmatized mica schist

Table 4.7 Rare Earth Element abundances on representative samples of different rock types of BGC around Masuda

Rock types	Tholeiitic Amphibolites					High-Ti Sanukitoids			Low-Ti Sanukitoids			
Sample #	J-29	J-35	J-37	J-68	J-71	J-39	J-53A	J-109	J-55	J-60	J-66	J-67
Ce	10.7	16.93	20.07	18.09	6.64	154.05	309.6	64.23	79.23	79.516	75.3	54.59
Nd	8.58	11.75	13.27	11.19	4.58	69.38	121.2	37.63	27.76	37.70	39.1	24.926
Sm	2.82	3.82	3.81	3.5	1.4	11.52	19.8	8.0	4.69	8.796	8.42	5.85
Eu	0.98	1.47	1.15	1.31	0.58	2.74	4.18	3.88	1.24	1.689	1.84	1.339
Gd	3.62	5.26	4.63	4.68	2.22	8.23	12.6	6.36	2.81	5.871	6.45	3.817
Dy	4.18	5.26	4.22	5.18	3.81	5.39	6.6	4.94	2.7	5.109	5.66	3.504
Er	2.55	2.84	2.85	2.84	2.42	2.38	2.57	2.24	1.35	2.946	2.79	1.998
Yb	2.12	2.82	2.6	2.7	2.28	1.49	2.05	1.82	1.04	2.307	2.24	1.503

Rock type	Granodiorite Suite I		Granodiorite Suite II			
Sample #	J-74	J-77	J-30	J-32	J-43	J-59
Ce	324	223.2	60.51	40.34	59.78	85.56
Nd	120	98.4	24	12.46	20.97	31.25
Sm	19.32	20.28	4.02	1.78	3.25	5.19
Eu	1.91	1.19	0.95	0.36	0.57	1.02
Gd	12.36	16.32	2.29	1.28	1.85	2.88
Dy	9.23	13.32	2.35	1.12	1.68	2.34
Er	3.53	4.13	1.2	0.52	0.87	1.02
Yb	2.6	5.76	0.92	0.34	0.72	0.66

Rock type	Granolite Enclave	Granolite Host	Granophyres		Aplite	Migmatized Mica Schist
Sample #	J-81	J-82	J-69	J-113	J-65	J-40
Ce	147	132	6.51	37.29	86.0	101.15
Nd	83	65	2.07	11.53	35.99	46.7
Sm	19.4	14	0.26	1.42	7.0	8.69
Eu	3.04	2.5	0.77	1.24	4.0	1.68
Gd	15.5	11	0.55	0.96	5.4	7.5
Dy	14.3	9.6	0.8	0.36	5.5	6.35
Er	7.46	5.2	0.6	0.23	3.03	2.88
Yb	5.9	4.5	0.68	0.245	2.5	2.14

4.2.7 Classification

No primary minerals are preserved as the amphibolites have recrystallized from their igneous precursors during metamorphism. Hence, the modal mineralogy can not be used for classification of these rocks. Therefore, the rocks are classified using elemental abundances. Two of the amphibolites fall in the basalt field and rest of the samples plot very close to the basalt field in silica vs total alkali diagram (Fig. 4.10; after LeBas & Streckeisen, 1991).

In Jenson's (1976) cation mole percent AFM diagram the amphibolites plot in Fe-enriched tholeiites field (Fig. 4.11). Using the tectonic discriminant diagram Zr-Ti/100-Sr/2 of Pearce & Cann (1973) it was found that the amphibolite samples fall in the ocean floor basalt field (Fig. 4.12). In TiO_2-K_2O-P_2O_5 diagram also these samples plot in ocean basalt field. Thus, in classification and

tectonic discrimination diagrams the amphibolites plot consistently in the basaltic field having oceanic affinity.

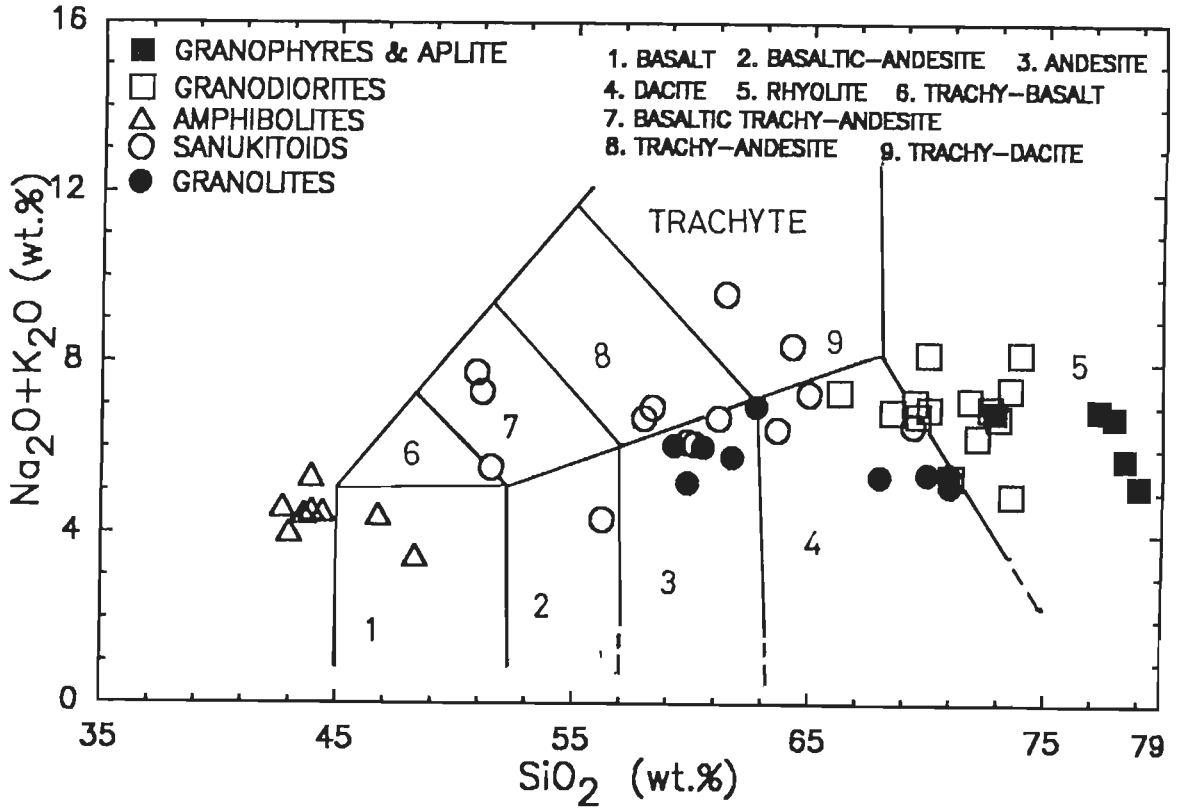

FIG. 4.10 **Silica vs total alkali classification diagram (after LeBas & Streckeisen, 1991) for the rocks of the study area. Symbols indicate the different rock types.**

In the SiO_2-(Na_2O+K_2O) diagram the intermediate suite of rocks fall in the basaltic andesite, andesite, basaltic trachy-andesite, trachyte, trachy-dacite and dacite fields. The granodiorites plot in the dacite and rhyolite fields and the granophyres and aplite in the rhyolite field (Fig. 4.10). In the AFM diagram (after Barker and Arth, 1976) the sanukitoids and granodiorites fall in the calc-alkaline to alkali field (Fig. 4.13a). Further, in the Na-K-Ca diagram (after Barker and Arth, 1976) the sanukitoids and granodiorites define calc-alkaline to trondhjemitic trend (Fig. 4.13b). Therefore, broadly the sanukitoids and the granodiorites are calc-alkaline in nature.

4.2.8 Mineral Chemistry

The mineral chemistry of equilibrium assemblage of hornblende and plagioclase in amphibolites can be useful in deciphering the grade of matamorphism. In addition to that, the mineral chemistry data can be used in quantitative modelling of petrogenetic processes, such as, fractional crystallization and liquid immiscibility. In order to achieve these objectives mineral chemistry of certain selected samples representing different rock types occurring in the study area were carried out using Electron Probe Micro Analyzer (JXA - 8600M JEOL).

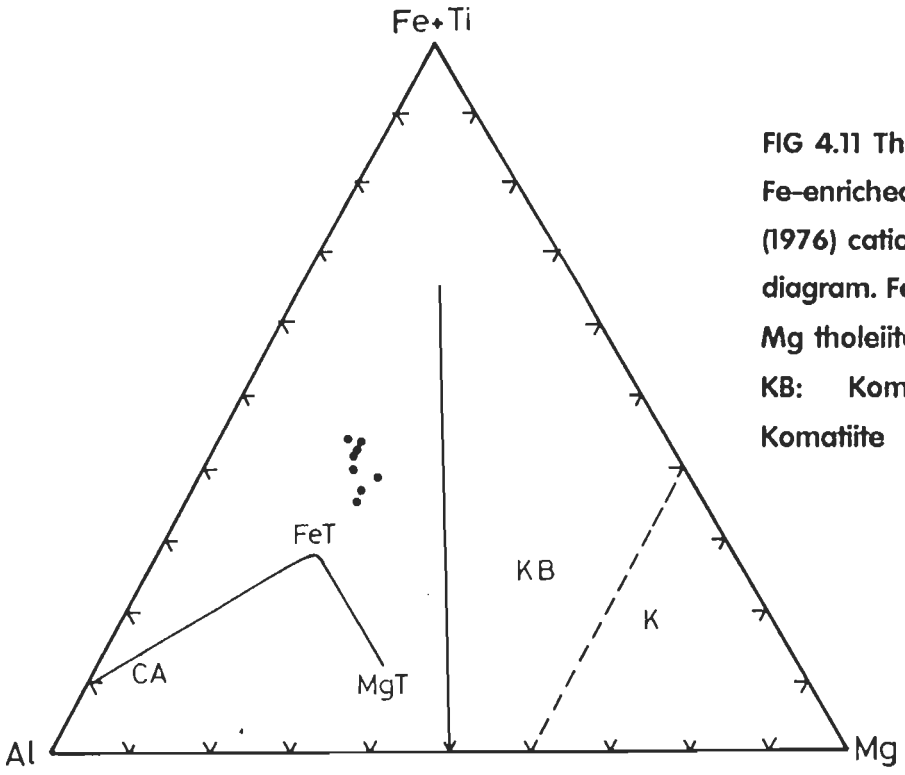

FIG 4.11 The amphibolites show Fe-enriched trend in Jenson's (1976) cation mole percent AFM diagram. FeT: Fe tholeiites; MgT: Mg tholeiites; CA: Calc-alkaline; KB: Komatiitic basalt; K: Komatiite

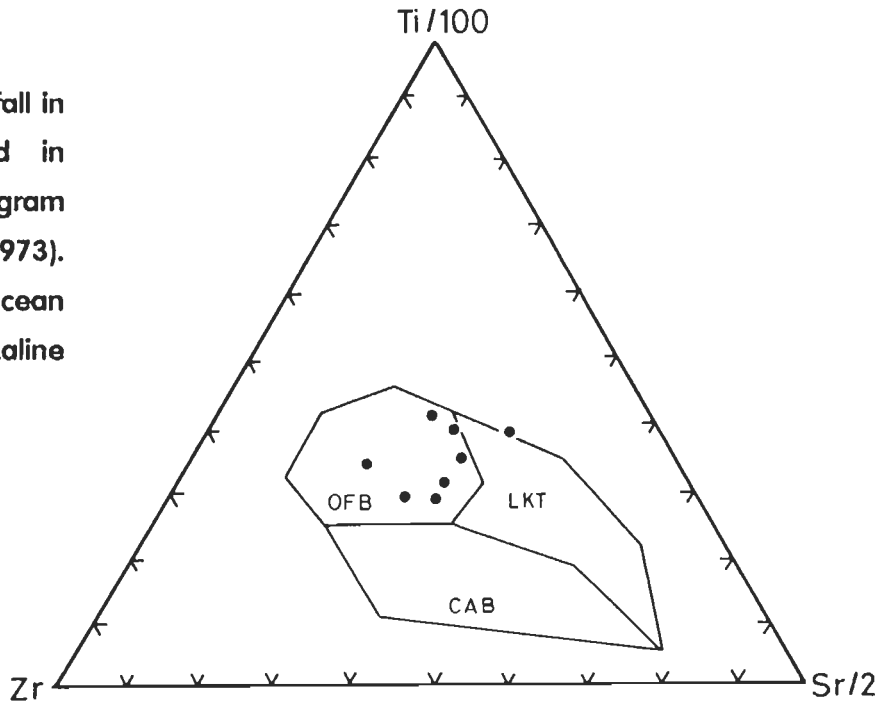

FIG 4.12 The amphibolites fall in ocean floor basalt field in tectonic discrimination diagram (after Pearce & Cann, 1973). LKT: low K tholeiites; OFB: ocean floor basalt; CAB: calc-alkaline basalt

Amphibolites

Three coexisting pairs of amphibole and plagioclase in each samples were analyzed. Only the representative analyses of each pair is given in the Appendix-I. From the data, it can be observed that there is no significant variation in the elemental abundances of amphiboles between rim and core. The amphiboles are classified as hornblende as they plot in hornblende field in $[Al]^{+4}$ - (Na+K) atom classification diagram.

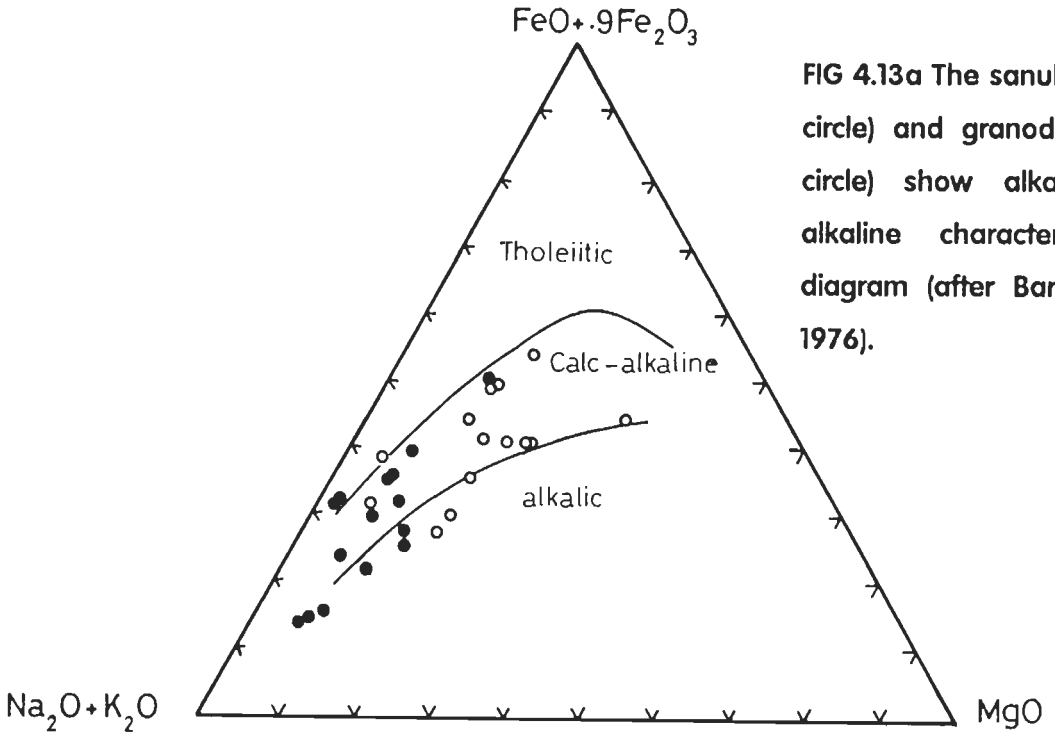

FIG 4.13a The sanukitoids (open circle) and granodiorites (filled circle) show alkali to calc-alkaline character in AFM diagram (after Barker & Arth, 1976).

There is no compositional zoning observed in the clinopyroxene grains of metagabbro sample (Appendix-I). In the pyroxene quadrilateral the clinopyroxene fall in the diopside field.

The plagioclase chemistry indicates that absence of any chemical variation between rim and core (Appendix-I). The plagioclase composition varies from oligoclase to andesine (an=24 to 38 mole %). On the basis of coexisting plagioclase composition with the hornblende, the grade of metamorphism can be inferred to be within amphibolite facies of metamorphism (Yardely, 1990).

Sanukitoids

The porphyritic variety of sanukitoid samples have feldspar phenocrysts of different size, shape and composition. Three phenocrysts of different sizes are analyzed by EPMA for their mineral chemistry (Appendix-II). The mineral chemistry of these phenocrysts indicates that

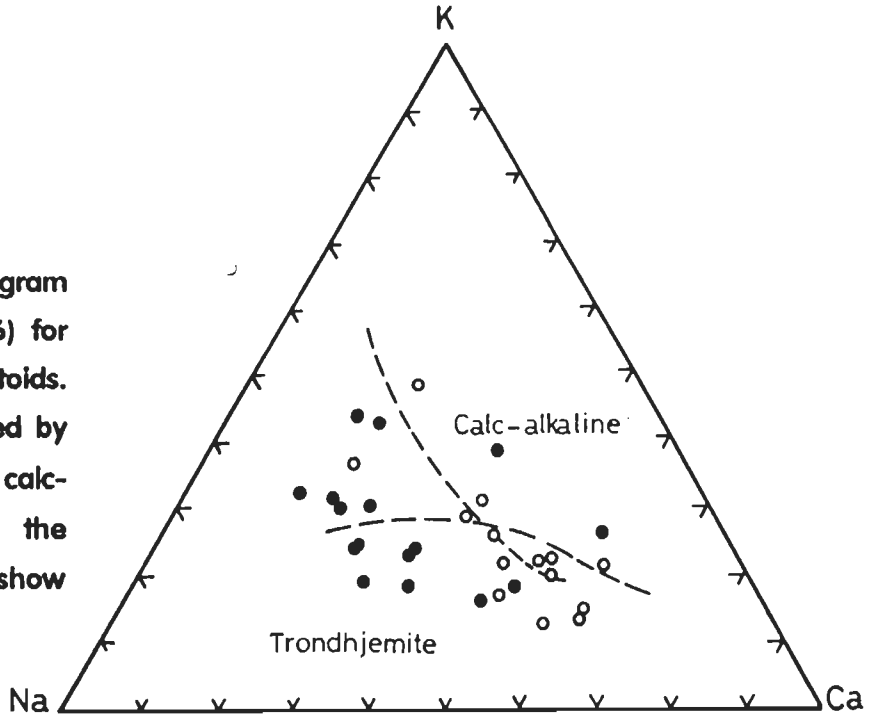

FIG 4.13b Na-K-Ca diagram (after Barker & Arth, 1976) for granodiorites and sanukitoids. Sanukitoids are represented by open circles and show calc-alkaline trend whereas, the granodiorites (filled circle) show trondhjemitic trend.

there are two types of feldspars. The phenocrystic phases I and II (first category) have a range of 38 to 41 mole % of albite, 10 to 11 mole % of anorthite and 47 to 52 mole % orthoclase component.

The second category of phenocryst have orthoclase (95 mole %) and albite (5 mole %) components (Appendix-II). Further, analysis along a line with very closely spaced points on this alkali feldspar phenocryst indicates that albite occurs as fine lamallae.

The mineral chemistry of biotites in the groundmass of high-Ti sanukitoid sample J-53A indicate higher FeO, TiO_2 and lower MgO abundances compared to biotites from low-Ti sanukitoid sample # J-66 (Appendix-III).

When the amphibole chemistry of high-Ti sanukitoid J-53A is compared with low-Ti sanukitoid sample J-66, it is observed that the high-Ti sanukitoid has higher Al_2O_3, comparable FeO and lower MgO and TiO_2 abundances compared to the low-Ti sanukitoid (Appendix-III).

The mineral chemistry of biotite occurring within granodiorites and sanukitoids have been carried out. The data indicates that there is no chemical variation from rim to core within a grain. However, the biotite chemistry of sanukitoid sample has higher TiO_2 and lower Al_2O_3 contents compared to granodiorite sample (Appendix-III). The Fe/[Fe+Mg] ratio of granodiorite as well as sanukitoids are overlapping and have a value ranging from 0.43 to 0.45.

CHAPTER V

PETROGENESIS OF AMPHIBOLITES

The evolutionary history of Precambrian continental crust can be evaluated by petrogenetic study of igneous rocks. The Petrogenetic study of igneous rocks attempts to characterize the sources of their magmas in terms of chemical composition and mineralogy, extent of partial melting required to generate the parental magmas, extent of fractional crystallization that the parental magmas might have undergone to give rise to magmas represented by the igneous rocks. Further, such a study can yield information on the pressure and temperature conditions of melting of source rocks. It may also be possible to evaluate whether the magma composition had been changed by zone refining or crustal contamination before it solidified. Thus, using the petrogenetic information it is possible to place constraints on various models applicable to Precambrian magmatism and crustal evolution.

The Precambrian rocks have been subjected to several episodes of deformation and metamorphism. Their primary textures and mineralogy are seldom preserved. Hence, geochemical data on these rocks is extensively used to understand their petrogenesis.

To evaluate Petrogenesis, the geochemical modelling of the elemental abundances on rocks with best possible accuracy and precision are needed. For quantitative modeling, appropriate equilibrium mineral melt distribution coefficient (K_d) values are required. The K_d values vary as a function of pressure, temperature and composition of the melt. The pressure, temperature and fO_2 condition in which the magmatic processes were operative are precisely not known. Therefore, it is not possible to choose the exact K_d values while modelling the petrogenetic processes. Thus, the inadequacy of our knowledge on K_d values at different pressure, temperature conditions for various rocks under study makes it difficult to quantitatively model the geochemical data for petrogenetic study. Hence, the geochemical modelling carried out here is semi-quantitative in nature while evaluating the petrogenetic processes.

5.1 MOBILITY OF THE ELEMENTS

Post crystallization processes such as metamorphism, deformation and alteration might have affected the Precambrian crustal rocks to varying extents. Therefore, it is important to evaluate whether the elements behaved in a closed system from the time of crystallization till the analysis, within the scale of sampling.

Various workers have attempted to determine the relative mobility of the different elements (Beswick, 1982; Pearce, 1983; Tatsumi et al., 1986; Bienvenu et al., 1990) The relative mobility or immobility of an element depends upon crystal chemistry and environmental conditions. During post crystallization processes some of the elements tend to be relatively more mobile while others remain essentially unaffected. For example, during low temperature alteration such as, that of sea water-rock interaction K, Rb, Sr and Ba are known to be mobile (Thompson, 1984).

To identify elemental mobility during water-rock interactions, Pearce (1983) suggested the usefulness of ionic potential (ionic charge/ionic radius) values to identify the relative elemental mobility. His study indicated that the mobile elements are those whose ionic potential values are less than three and greater than twelve and the immobile elements are those having ionic potential values between three and twelve.

Pearce (1983) suggested that the trace elements Nb, Ta, Zr, Hf, Ti, Y and Yb are immobile. Vocke et al. (1979) suggested that the REEs behave as immobile elements during metamorphism up to amphibolite grade in basic and granitoid rocks. More recent studies by Bienvenu et al. (1990) have brought out relative mobility of rare earth and non rare earth elements in fresh and altered basaltic samples recovered from the Atlantic Ocean. They have shown that sea water alteration does not affect Nb/Zr ratio and insignificantly modify the chondrite normalized REE patterns.

To find out the relative mobility of different major elements in metamorphosed ultrabasic rocks, Beswick (1982) suggested molecular proportion ratio plots. An attempt has been made to test relative mobility of the major elements of the amphibolite samples. Initially, the weight percent of oxides were converted to mole percent oxides and they were plotted against other elemental ratios. As TiO_2 behaved as an incompatible element and is considered to be least mobile, it was kept in the denominator in all the plots. A linear trend is expected in these variation diagrams for immobile elements because, magmatic processes cause systematic variation in abundances of these elements from a cogenetic suite of rocks (Fig. 5.1). It was found that all the elements show a linear trend except Ca and K. Therefore, Ca and K might have been mobilized during post-crystallization processes.

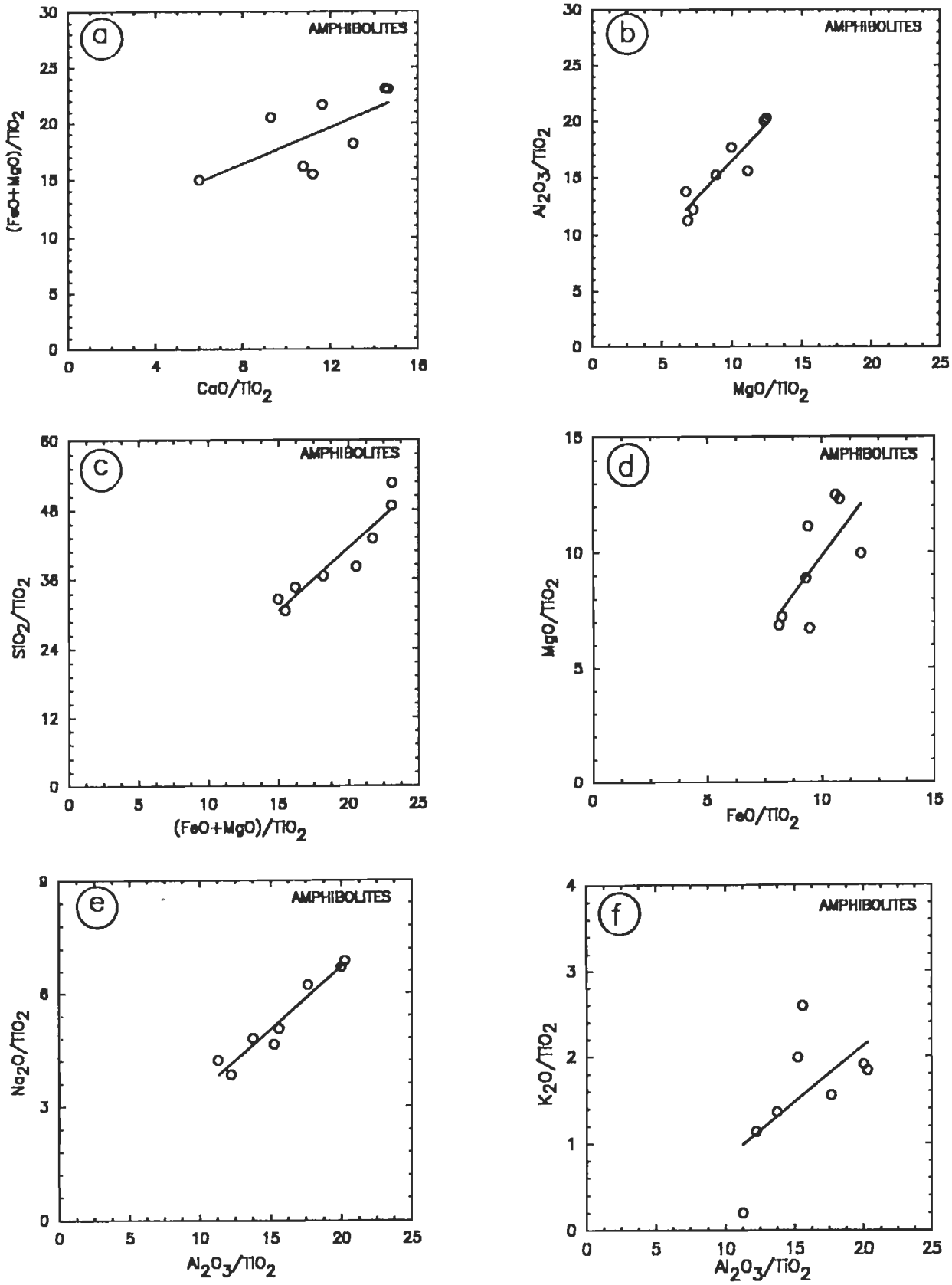

Fig. 5.1 Mole percent oxide ratio plots to distinguish the relative mobility of the elements (after Beswick, 1982). Note that all oxide ratios show linear trends and are therefore, less mobile, except CaO and K_2O (a & f) which are considered to be relatively more mobile compared to other oxides plotted.

For amphibolites all the elements are plotted against Zr and TiO_2 as both of these elements are considered to be relatively immobile. It was found that Na, K and V are mobile whereas, Ca and Ba are selectively mobile in a few samples. Therefore, immobile elements are only considered for quantitative modelling. The mobile and relatively less and selectively mobile elements have been treated more cautiously while evaluating the petrogenesis.

Chondrite normalized Rare Earth Element abundances do not show selective depletion or enrichment of a particular element relative to its neighbour. Hence, the smoothness of the chondrite normalized REE pattern can be considered as an indicator of relative immobile nature of REEs (Bienvenu et al., 1990). Eu and sometimes Ce are exception to this as they exhibit positive or negative anomalies for a variety of reasons such as, source characteristics, fractional crystallization of minerals like plagioclase, pyroxene and oxygen fugacity of parental magmas (Hanson, 1980; Bienvenu et al., 1990).

In the study area, the amphibolites are intimately associated with intermediate and granitoid rocks. Amphibolites are more prone to post crystallization processes than the intermediate and granitoid rocks as it contains higher proportion of minerals recrystallized during metamorphism. Similar mobility tests were carried out for intermediate as well as, granitoid rocks and the results obtained are well comparable to the amphibolites in terms of characterization of mobile and immobile elements.

In this chapter, an attempt has been made to place constraints on various petrogenetic models using major, trace and Rare Earth Element abundances in conjunction with field and petrographic observations. More emphasis is given on elements that have remained least mobile (e.g. REEs). An attempt has also been made to find out the inter relationship amongst the suites of amphibolites intermediate and granitoid rocks to test whether these suites were derived from similar sources and magmatic processes (Chapter-VI).

5.2 MAGMATIC PROCESSES

Partial melting and fractional crystallization are the two important magmatic processes which govern the evolution of a variety of rocks from different sources. Out of different kinds of melting batch melting or equilibrium fusion is the simplest melting model. During batch melting of a source the concentration of an element in the melt can be defined by the following relation:

$$C_l / C_0 = 1/ D(1-F) + F$$

where, C_l and C_0 are the concentrations of an element in the liquid and source respectively

D is the bulk distribution coefficient ($D= \sum K_{di}$, where i=1 to n), F is the fraction of melting

From the above relation, C_l can be determined if C_0, D and F are known. The relative enrichment or depletion of the elements is a function of D. For example, when D=0, the melt is highly enriched in abundances of incompatible elements at low extent of melting. As the melting proceeds, the abundances of incompatible elements in the melt decreases (Fig. 5.2a) and at higher extents of melting the variation in the elemental abundances become negligible. As D increases (at 0.3 and 0.6) the abundances of incompatible elements are less enriched in the melt. When D>1, the element behaves as a compatible element and the variation in the abundances of the compatible element is not pronounced at the low extents of melting (<40%; Fig. 5.2a).

When a magma undergoes fractionation, the concentration of an element in the liquid can be given by the following relation:

$$C_l / C_0 = F^{D-1}$$

where, F is the fraction of melt remaining and the extent of fractinal crystallization is 1-F. Other parameters are same as defined above.

As D approaches zero, C_l/C_0 becomes 1/F which becomes the equation of melting at the same D. Therefore, it may not be possible to distinguish between melting and crystallization when $D \approx 0$. When D<1, the abundances of an element in the melt relative to the source ($C_l=C_0$) do not show much variation at low extent of fractional crystallization. At D=3, even at the low extent of fractional crystallization, the depletion of element in the melt with respect to the parent magma is quite prominent (Fig. 5.2b).

These basic principles of batch melting and fractional crystallization have been used while modelling the petrogenetic processes using trace element data.

5.3 CMAS DIAGRAM

O' Hara (1968) constructed a natural basalt phase diagram by projecting natural rock analysis into a modification of the CaO-MgO-Al_2O_3 -SiO_2 (CMAS) tetrahedron showing a variety of boundary curves for pressures up to 3 GPa (30 Kbar). Subsequently, Herzberg & O'Hara (1985) extended the O'Hara's (1968) phase relations projected from diopside into part of CA-M-S plane to 15 GPa (150 Kbar). The C, A, M and S values are calculated as follows:

C = (mol. prop. CaO - 3 1/3 P_2O_5 + 2Na_2O + 2K2O) x 56.08

M = (mol. prop. FeO + MnO + NiO + MgO - TiO2) x 40.31

A = (mol. prop. Al_2O_3 + Cr_2O_3 +Fe_2O_3 + Na_2O + K_2O + TiO_2) x 101.96

S = (mol. prop. SiO_2 - 2Na_2O - 2K_2O) x 60.09

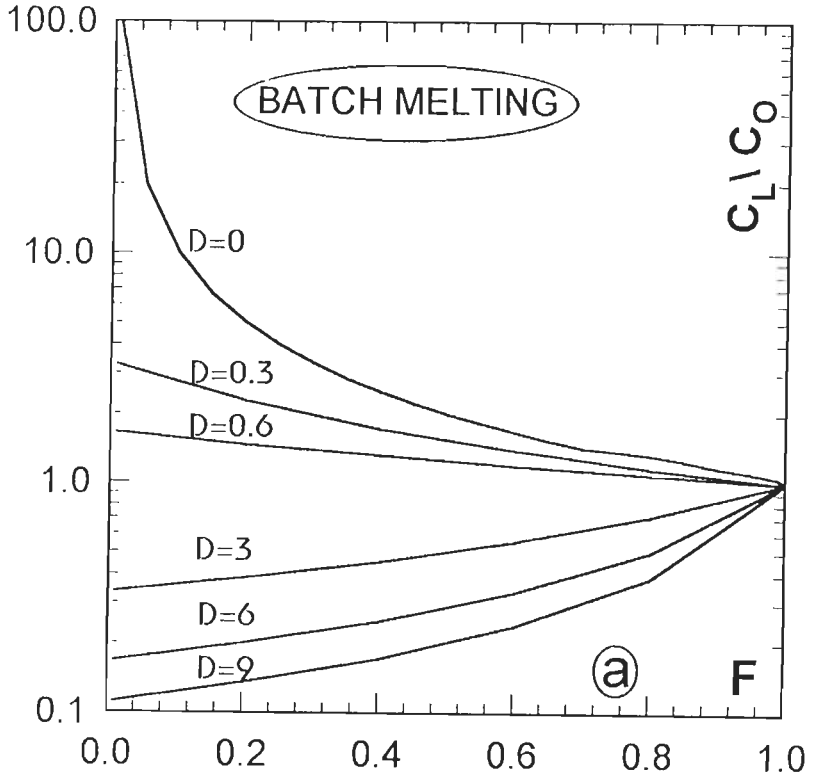

Fig. 5.2a Hypothetical curve for batch melting for a range of D values. 'F' represents the fraction of melting; 'D' is the bulk distribution coefficient; C_l is the concentration of an element in the liquid and C_0 is the concentration of an element in the parent.

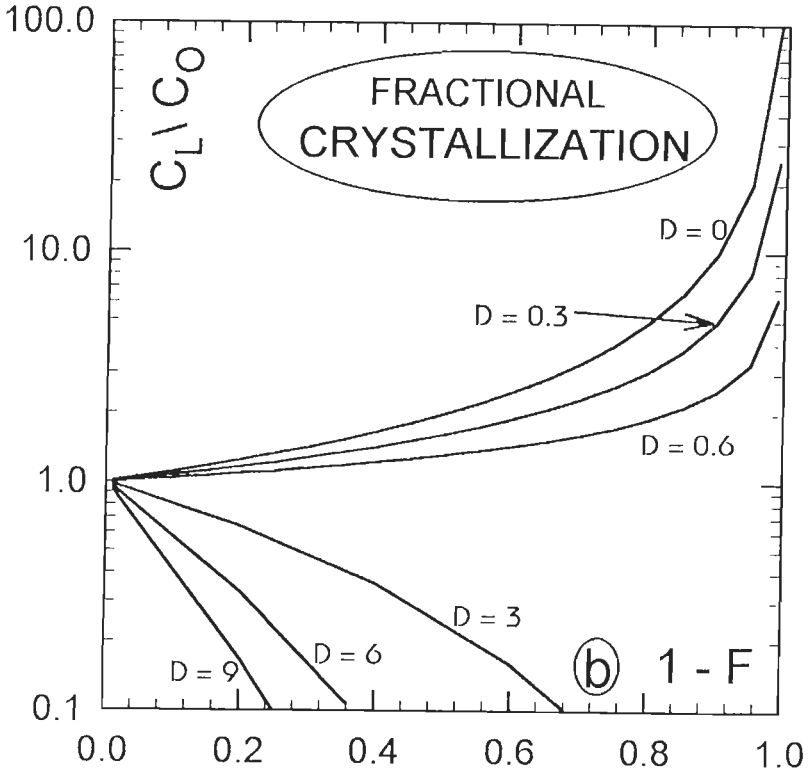

Fig. 5.2b Hypothetical curve for fractional crystallization for a range of D values. (1-F) represents the extent of fractional crystallization, C_l, C_0 and D as defined above.

The plotted parameters CA, M and S are calculated using the procedure as discussed in Cox et al. (1987). In this projection all albite and orthoclase molecules plot as the equivalent weight of anorthite (CAS_2) molecule.

In the CAMS projection Herzberg and O'Hara (1985) have shown that during melting of olivine rich peridotite at 1 atmosphere pressure olivine, plagioclase and pigeonite-orthopyroxene are the liquidus phases and as the pressures increases to 30 Kbar garnet appears as the liquidus phase. Whereas, at 40 Kbar pressure garnet, olivine and orthopyroxene are the only liquidus phases.

The amphibolite samples of Masuda area fall below olivine-anorthite-orthopyroxene plane except sample J-38. However, these samples show a linear trend parallel to S-CA join (Fig. 5.3),

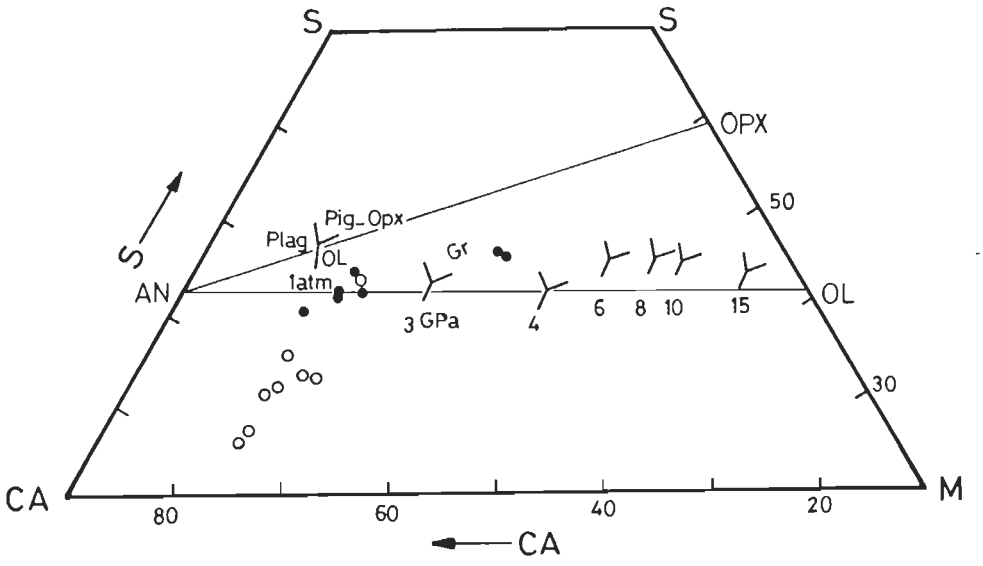

Fig. 5.3 **Some predicted extensions of O'Hara's (1968) phase relations projected from diopside into part of the plane CA-M-S to 15 GPa (after Herzberg and O'Hara, 1985). Compositions of solidus melts at various preesures (1 atm. P to 15 Gpa) are also shown. Amphibolites of the Masuda area have been shown as open and filled triangles (Data for the filled triangles are from Dr. S. Balakrishnan, personnel communication) which plot between 1 atm. P and 3Gpa pressures. If the amphibolites represent magmas generated by low extents of partial melting of mantle sources, then they could have been formed at about 1.5 Gpa. Plag = plagioclase; Opx = orthopyroxene; Pig. = pigeonite; Ol. = olivine; Gr. = garnet ($Py_{80}Gr_{20}$-Py_{100}).**

because, they are variably silica depleted and enriched in CaO and K_2O compared to J-38 which fall above the olivine-anorthite join. Enrichment of CaO and K_2O in these amphibolite samples could have been caused by post-crystallization processes. Some of the amphibolite samples (data from Dr. S. Balakrishnan, personnel communication) from the study area also fall along with J-38 plotting between solidus melt composition for 1 atm. pressure and 3 GPa melting of peridotite. From this, it can be inferred that their magmas could have been generated by partial melting of mantle sources at 1 to 1.5 GPa.

5.4 [Mg]-[Fe] MODELLING

Hanson & Langmuir (1978) proposed [Mg]-[Fe] melt field based on olivine saturation concept of Roeder & Emsile (1971). As long as olivine is in equilibrium with melt, the MgO and FeO contents of the melt are determined by equilibrium distribution coefficients of MgO and FeO between olivine and melt. The equilibrium distribution coefficients is affected by temperature, pressure and composition of the melt. Using Ford et al.'s (1983) experimental data, Rajamani et al. (1985) modified the melt field by applying the correction for pressure and composition effects on the equilibrium distribution coefficient for MgO and FeO. This diagram is very useful to understand the nature of source, extents of melting of mafic and ultramafic magmas that could have been equilibrated with olivine. Details to these diagram are given in Rajamani et al. (1989, 1993).

In Fig. 5.4, a garnet lherzolite (Takahasi and Scarfe, 1985), a primitive ultramafic rock is considered as the source for olivine saturated magmas. Using Ford et al.'s (1983) equation '3', cation mole percent of [Fe] & [Mg] were calculated for melts generated at 1 atmospheric pressure. As the pressure increases, solidus temperature of melting and [Mg] content of solidus melt increases and the melt field contracts (see. Rajamani et al., 1989).

For the melt field shown in the Fig. 5.4, the lower curve (S) represents 1 atmosphere pressure solidus (zero percent melting) and upper curve (L) represent olivine only liquidus. As the extent of partial melting increases, the melt composition would plot to the left of the solidus curve (i.e. within the melt field). However, amphibolites from Masuda area fall to the right of the 1 atmosphere pressure solidus. Therefore, partial melting of a garnet lherzolite source cannot generate the magma for BGC amphibolites at any pressures.

Another possibility is that the low pressure fractional crystallization of phases such as, olivine and clinopyroxene from a magma generated by partial melting of garnet lherzolite at 1 atmospheric pressure may give rise to residual magmas similar to the amphibolites. For this, a high MgO sample G-27 from the study area which falls within the melt field was considered as the potential parental magma. For fractional crystallization of olivine, the composition of olivine was taken from the most primitive magma amongst the amphibolite samples. Initially, 20% fractional crystallization of olivine was considered at the five percent intervals. Subsequently, clinopyroxene

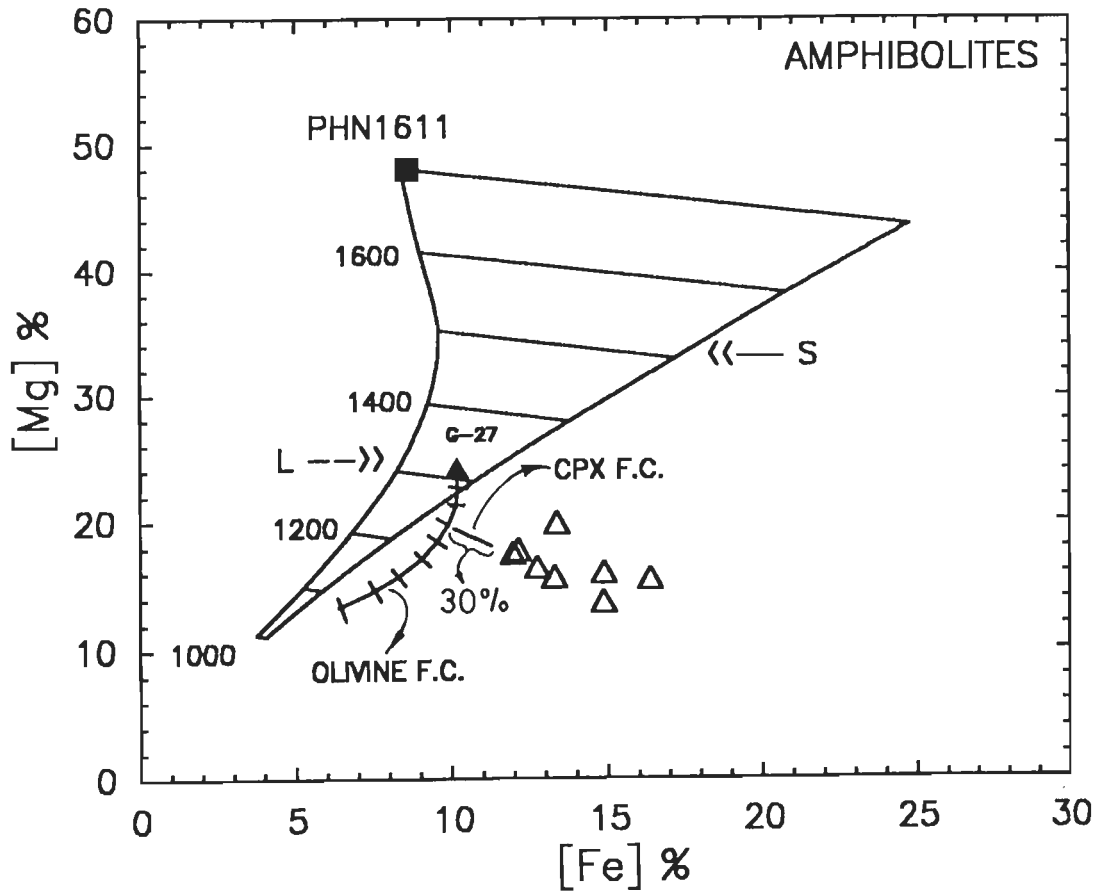

Fig. 5.4 **[Mg]-[Fe] systematic for the amphibolites of Masuda area. [Mg]-[Fe] values are in cation mole percent which were calculated using the Ford et al's (1983) equation. The calculated melt field is for 1 atmospheric pressure from a garnet lherzolite source; PHN1611 (Takahasi and Scarfe, 1985). Different isotherms are also shown in the diagram; 'S' and 'L' represents solidus and liquidus (olivine) curves respectively. G-27 is a high-Mg amphibolite, from Masuda (data from Dr. S. Balakrishnan, personnel communication) which plots inside the melt field. Fractional crystallization (F.C.) curve is drawn from G-27 up to 45% olivine only fractional crystallization with ticks indicating 5% olivine F.C. Clinopyroxene F.C. curve (upto 30%) is drawn from the residual liquid which formed after 20% of olivine only F.C.**

joined as the fractionating phase. Even after 20% of olivine fractional crystallization and 30% of clinopyroxene fractional crystallization could not generate the amphibolite suite magma.

Third possibility is that it may be possible that the most primitive magma in terms of high MgO and mg # might have undergone fractional crystallization of clinopyroxene to produce residual magmas similar to other amphibolite samples. Amongst the amphibolites, the most primitive sample is J-18A. If magma represented by sample J-18A had undergone clinopyroxene fractional crystallization then one would expect the decrease in Ni and Cr contents in magmas

represented by samples plotting to the right of J-18A. However, it is observed that there is no systematic decrease in the concentration of Cr and Ni amongst the amphibolite samples that plot to right of J-18A (Fig. 5.4).

The fourth possibility is that whether assimilation coupled with fractional crystallization (AFC) had played any role in generating magmas represented by the amphibolites. If the composition of average continental crust is considered for assimilation, it will lower both [Fe] and [Mg] in residual magma undergoing assimilation coupled with fractional crystallization. Therefore, the observed trend in figure 5.4 can not be explained if the amphibolites magma have variably contaminated by continental crust coupled with or without fractional crystallization of olivine and pyroxenes.

In summary, it may be worth mentioning that a garnet lherzolite source can not generate the magma for amphibolites by partial melting at different pressures or by fractional crystallization of olivine and olivine+clinopyroxene or by assimilation of continental crust. Therefore, the source for amphibolites might have had a higher [Fe]/[Mg] ratio than the garnet lherzolite.

5.5 Ni-Zr MODELLING

In the mantle melt systems, Ni behaves as a compatible element whereas, Zr behaves as an incompatible element. During magmatic processes such as, partial melting or fractional crystallization systematic variations in abundances of these two elements are expected. Because the incompatible elements are preferentially concentrated in the melt phase and the compatible elements are preferentially retained in the solids during partial melting and fractional crystallization respectively.

Rajamani et al. (1985) suggested the use of Ni-Zr diagram to constrain the source composition and magmatic processes for the basic and ultra basic rocks. In a series of melts representing increasing extents of melting of a homogeneous source, Zr abundances vary by several order of magnitude while, Ni contents remain nearly constant. During the different extents of fractional crystallization, the Ni abundances in the melt vary by 7 to 8th order of magnitude. Whereas, Zr abundances vary less dramatically.

To constrain the source mineralogy three different mantle sources are considered. The source S1 has 60% olivine and 40% pyroxene, source S2 has 40% olivine and 60% pyroxene and source S3, a Bulk Silicate Earth, having residual mineralogy 57.5% olivine, 27.5% orthopyroxene, 12.5% clinopyroxene and 2.5% spinel as suggested by Kostopoulous, (1991) are being used to model the partial melt compositions.

2000 ppm and 8.3 ppm are considered as abundances of Ni and Zr respectively in the primitive mantle source (Taylor & McLennan, 1985). The Ni-olivine distribution coefficient

($K_{dNi}^{ol\text{-}melt}$) = 8 is taken from Irving (1978) and the bulk distribution coefficients (D_{Zr}) is assumed to be zero for calculations for partial melting and the curves have been drawn with tic marks at 5% intervals.

To evaluate whether partial melting or fractional crystallization played the dominant role for the generation of tholeiitic magma that represent the amphibolite samples, they are plotted in the Ni-Zr diagram (Fig. 5.5). All the amphibolite samples, as a group, do not show any distinct trend in the figure 5.5.

In Fig. 5.5, the amphibolite samples plot to the left of the sources S1, S2 and S3 partial melting curves. The four samples J-38, J-68, J-35 and J-71 which show a negative correlation plot parallel to different extents of partial melting curves.

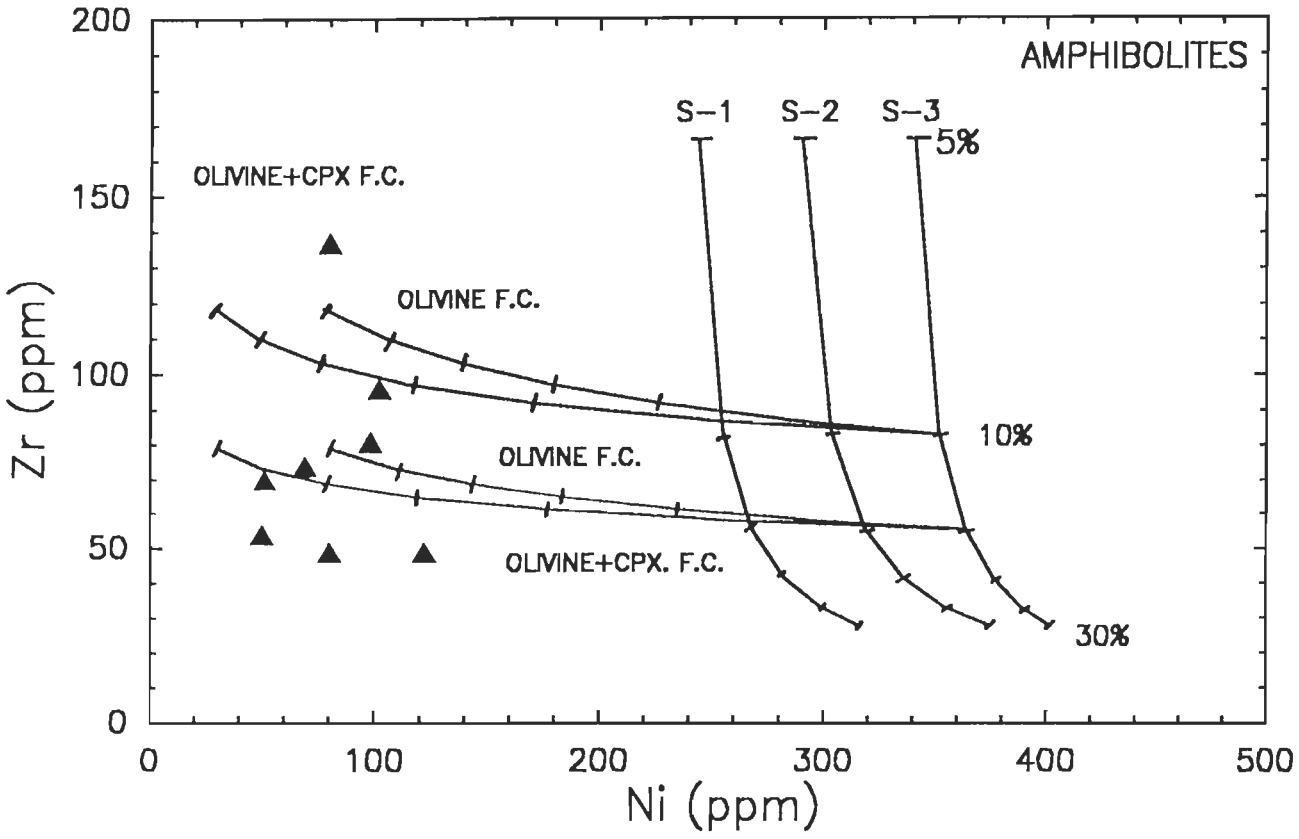

Fig. 5.5 **Ni-Zr relation for the amphibolites of Masuda. S1 represents a calculated partial melting (PM) curve defined by magmas formed at different extents of partial melting of a source leaving 60% olivine, 40% pyroxene; S2 represents a calculated PM curve leaving 40% olivine and 60% pyroxene; S3 represents a calculated PM curve leaving 57.5% olivine, 27.5% orthopyroxene, 12.5% clinopyroxene 2.5% spinel. Each tick mark is drawn at 5% intervals. Olivine only and olivine + clinopyroxene (CPX) fractional crystallization curves are drawn from the magmas formed by 10% and 20% partial melting on S3 curve .**

Another possibility which can be tested is that whether fractional crystallization of only olivine or olivine and clinopyroxene can give rise to the liquid compositions similar to amphibolites from a low percent (~ 10%) melt of the Bulk Silicate Earth source (S3). The fractional crystallization curves are drawn at 5% tic intervals assuming 10% and 15% partial melts as parental magmas (Fig. 5.5). Forty percent olivine only fractional crystallization is required to generate residual melts with Ni and Zr abundances similar to sample # 68. However, the MgO contents of the residual melt on 40% olivine fractional crystallization would be much lower than what is observed in sample # J-68. Similarly, olivine+clinopyroxene fractional crystallization can not explain the observed MgO and CaO contents of the amphibolite samples.

Therefore, the assumed Bulk Silicate Earth (BSE) which is equivalent to spinel lherzolite composition can not generate the magmas similar in Ni and Zr abundances to the amphibolites, either by different extents of partial melting or by fractional crystallization of olivine and clinopyroxene from primary magmas generated by 10-15% partial melting.

To determine the concentrations of Ni and Zr in the source the liquid composition of sample # J-68 was assumed to represent the 10% partial melt. This sample has the highest mg#. By using the batch melting equation [$C_l/C_0 = 1/D(1-F)+F$], the Ni concentration in the source was found to be 600-900 ppm for a range of D_{Ni} (6-12) and that of Zr from 7-10 ppm ($D_{Zr}=0$). Therefore, it may be inferred that the partial melting of a source having an average of 900 ppm Ni and 8 ppm Zr may give rise to the magmas representing amphibolites.

It may be possible that amphibolite samples may be interrelated by different extents of melting. To test this hypothesis, these four sample #'s (J-35, J-38, J-68, J-71) showing the partial melting trend were considered. Sample no. J-38 having highest Zr abundances may represent the lowest percentage of melting and J-71 having lowest Zr abundances may represent highest percent of partial melting in the group. Amphibolite sample #'s J-68 and J-35 plot in between J-38 & J-71 and may represent intermediate percent of partial melting.

In the [Mg]-[Fe] diagram, sample # J-71 which represents highest extents of melting should have lower [Fe] than samples J-68 and J-35. Whereas, sample # J-68 has lower [Fe] than J-71. Thus, it is not possible to relate the samples plotting along a partial melting trend in the Ni-Zr diagram as well as in [Mg]-[Fe] diagram. It is quite likely that their source could have been heterogeneous with respect to [Fe]/[Mg] ratio, Ni and Zr abundances.

5.6 TRACE ELEMENT VARIATION DIAGRAMS

These diagrams, called as Spider Plots use the trace elements which behaved as incompatible elements during partial melting and fractional crystallization. A range of incompatible elements are plotted in the X-axis in the decreasing order of incompatibility and in Y-axis their

abundances are normalized to estimated abundances in the primordial earth. The concept of spider diagrams were put forward by Wood et al. (1979), Sun (1980), Thompson (1982) and Thompson et al. (1984) and they can be used to compare trace element characteristics of basalts formed at different tectonic settings with the samples being studied.

The peaks, troughs, slopes and curvature defined by different elements may provide useful petrogenetic information concerning crystal-liquid equilibria. For example, troughs at Sr probably result from the fractional crystallization of plagioclase from basalts whereas, troughs at Th and Rb combined with Nb-Ta may suggest contamination of a magma by continental crustal rocks (Wilson, 1989).

The data for N-MORB, P-MORB, Ocean Island Basalt (OIB), Island Arc Basalts (IAB) and Island Arc calc-alkaline basalts are taken from Sun (1980) and Sun & McDonough (1989) to plot the spider diagrams (Fig. 5.6a). The data are normalized to primordial mantle (Sun & McDonough, 1989). The N-MORB shows a depleted smooth multi-element pattern whereas, P-MORB shows an enriched smooth multi-element pattern. OIB has a smooth pattern and has higher primitive mantle normalized abundances than all basalts. IABs have a marked trough at Nb, peak at Sr with slight trough at Zr. The normalized abundances of the IA-calc-alkaline basalt falls in between OIB and IAB and has a slight peak at Sr.

The Masuda amphibolites have variable primordial mantle normalized trace element abundances. Out of four primitive mantle normalized patterns three patterns have trough at Ba and Nb to a lesser extent at P with an insignificant peak at La. One of the samples shows prominent trough at Nb, slight trough at Zr and a peak at Sr (Fig. 5.6b). The average normalized abundances fall between IAB and OIB. All of them have a marked peak at K. From this diagram it is not possible to conclusively infer about the tectonic settings. However, with some reservations it may be inferred that the trace element characteristics of the magma are transitional to that of IAB and OIB.

5.7 REE GEOCHEMISTRY

The chondrite normalized REE patterns for the tholeiitic amphibolite samples of Masuda area are compared with those of tholeiitic basalt samples from various tectonic settings. The chondrite normalized Rare Earth Element (REE) plots for amphibolites show flat to slight light REE (LREE) enriched patterns relative to chondrites. The REE patterns are sub-parallel to parallel with each other. Amongst the amphibolite samples, J-71 shows slight LREE depleted REE pattern relative to other samples. Sample # J-37 has the highest LREE abundances and shows a slight negative Eu anomaly.

The chondrite normalized REE patterns for N-type Mid Ocean Ridge Basalts (MORB) is depleted in LREE (Ce_N=3-8) and have unfractionated HREE (Yb_N=10) abundances and P-type

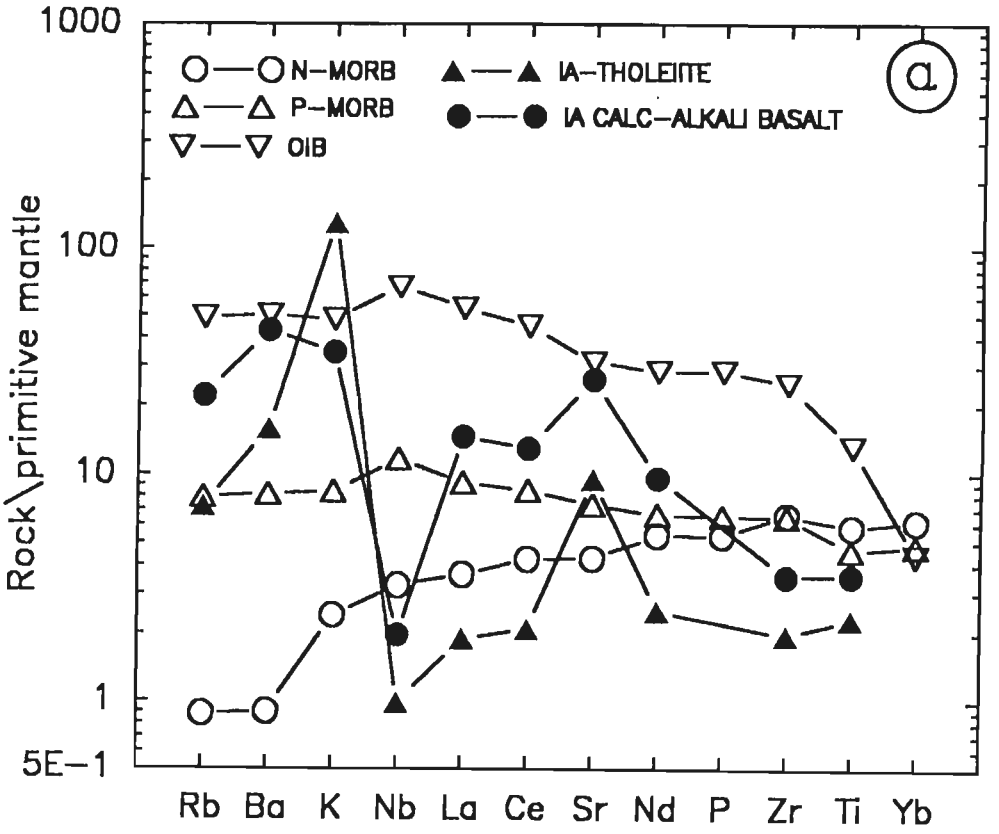

Fig. 5.6a **Multi element plots for basalts emplaced in different tectonic settings. MORB = Mid Ocean Ridge Basalts; OIB = Ocean Island Basalts; IA-Thol = Island arc tholeiites; IA - Calc Alkali Basalts = Island Arc Calc - Alkaline basalts. Data sources Sun (1980) and Sun and McDonough (1989).**

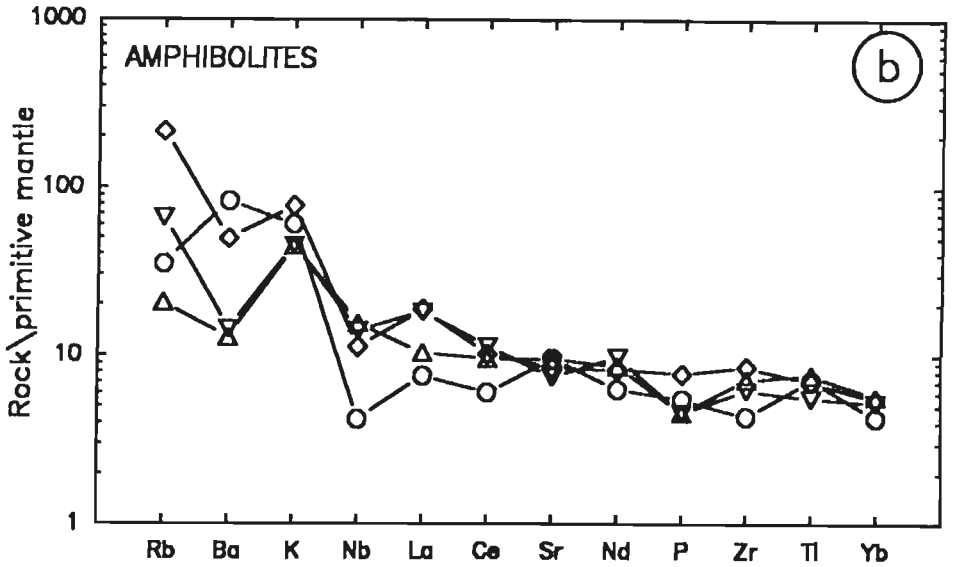

Fig. 5.6b **Multi-element plot for the amphibolites of Masuda area.**

MORB have enriched LREE (Ce_N=20-70) and unfractionated HREE abundances (Yb_N=25; data from Schilling et al., 1983). The tholeiitic amphibolites of Masuda area are neither similar to N-MORB nor P-MORB in terms of chondrite normalized REE patterns. However, they plot within the field for Mid Ocean Ridge Basalts defined by N & P MORB and thus fall in Transitional type of Mid Ocean Ridge Basalts field (Fig. 5.7a).

The ocean island tholeiitic basalts show a typical LREE enriched patterns (C_N=20-90) and a fractionated HREE patterns (Yb_N=8-20) shown in figure 5.7b (Basaltic volcanism study project, 1981). The oceanic island alkali basalts are variably LREE enriched (Ce_N=60-220) and have highly fractionated HREE abundances which give rise to sloping chondrite normalized REE patterns (Fig. 5.7c). However, the tholeiitic amphibolites of Masuda area do not have HREE fractionated REE patterns and thus are unlike the ocean island basalts as well as oceanic island alkali basalts (Fig. 5.7b & c).

The Continental Flood Basalts (CFB) have a very wide range in chondrite normalized LREE enriched patterns (Ce_N=20-200) with fractionated HREEs (Yb_N=10-50, Basaltic volcanism study project, 1981). The REE patterns of Masuda amphibolites are quite different from the continental flood basalts as they have lower REE abundances and unfractionated HREE patterns (Fig. 5.7d).

The chondrite normalized REE patterns for island arc basalts range from LREE depleted to slight LREE enriched patterns with unfractionated HREEs (Fig. 5.7e). They show variable Eu anomaly. The marginal basin basalts have a range of REE abundances. They are flat (Ce_N=6) to slightly enriched in LREE (Ce_N=~25) with unfractionated HREE (Yb_N=6-18; FIG. 5.7f, Basaltic volcanism study project, 1981). The tholeiitic amphibolites fall well within the field defined by marginal basin basalts, as well as, island arc basalts (Fig. 5.7e & f).

In summary, it can be inferred that the chondrite normalized REE patterns of amphibolites of Masuda area fall within the field defined by MORB and are akin to island arc tholeiitic basalts. They are also quite similar to the REE patterns and abundances to that of marginal basin basalts.

5.8 COMPARISON OF REE PATTERNS OF MASUDA AMPHIBOLITES WITH THOLEIITIC ROCKS OF DHARWAR AND ARAVALLI CRATON

The chondrite normalized REE patterns for the tholeiites from Archaean Kolar Schist Belt, Dharwar Craton are of two types. The first type has LREE enriched and HREE fractionated sloping REE patterns and the second type is depleted in light REE abundances (Ce_N=12-6) with nearly flat HREE patterns (Rajamani et al. 1985, 1989). The tholeiitic amphibolites of the study area are unlike

the light REE depleted tholeiites as well as the HREE fractionated and LREE enriched tholeiites of the Kolar Schist Belt.

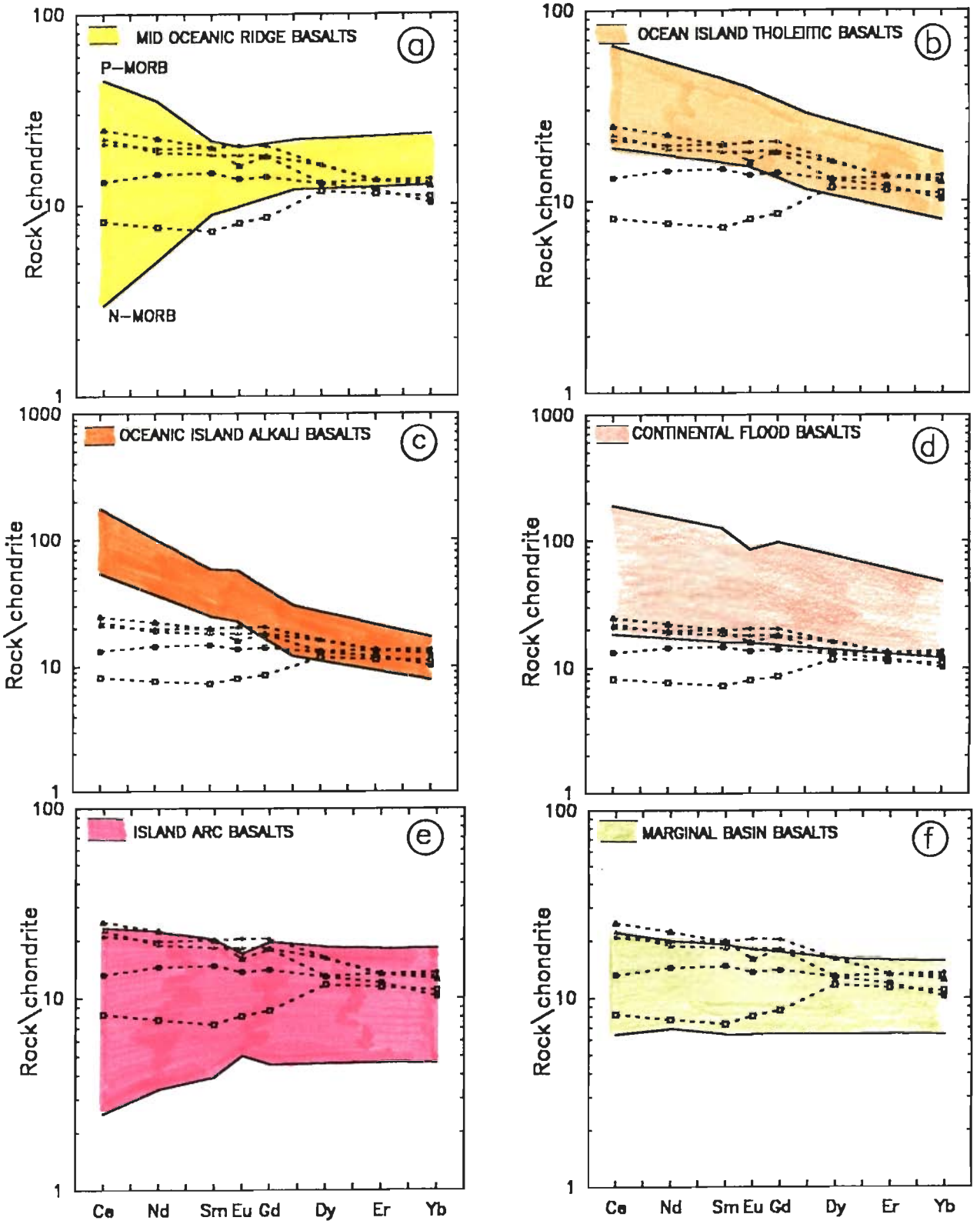

Fig. 5.7 **Comparison of chondrite normalized REE patterns of Masuda amphibolites with the fields for basalts from different tectonic settings. Data sources for each tectonic settings are referred in the text.**

Zachariah (1992) reported three different suites of meta-tholeiites from Ramagiri gold fields on the basis of chondrite normalized REE patterns. The light REE enriched suites are also highly fractionated in HREEs and have sloping REE patterns. The tholeiitic amphibolites of BGC are comparable to the some of the samples of Flat-Suite from the Ramagiri Schist Belt.

The basal Aravalli meta-volcanics have been studied by Ahmad & Rajamani (1991) and Ahmad and Tarney (1994). The tholeiitic basalt of the basal Aravallis have LREE enriched and HREE depleted chondrite normalized REE patterns. The LREE abundance vary from 15-80 times chondrite for Ce whereas, HREE abundances may vary from 4-20 times chondrite for Yb. The amphibolites of Masuda area (northern BGC) has REE patterns quite different from that of basal Aravalli volcanics with respect to LREE enrichment and overall REE abundances (Fig. 5.8a).

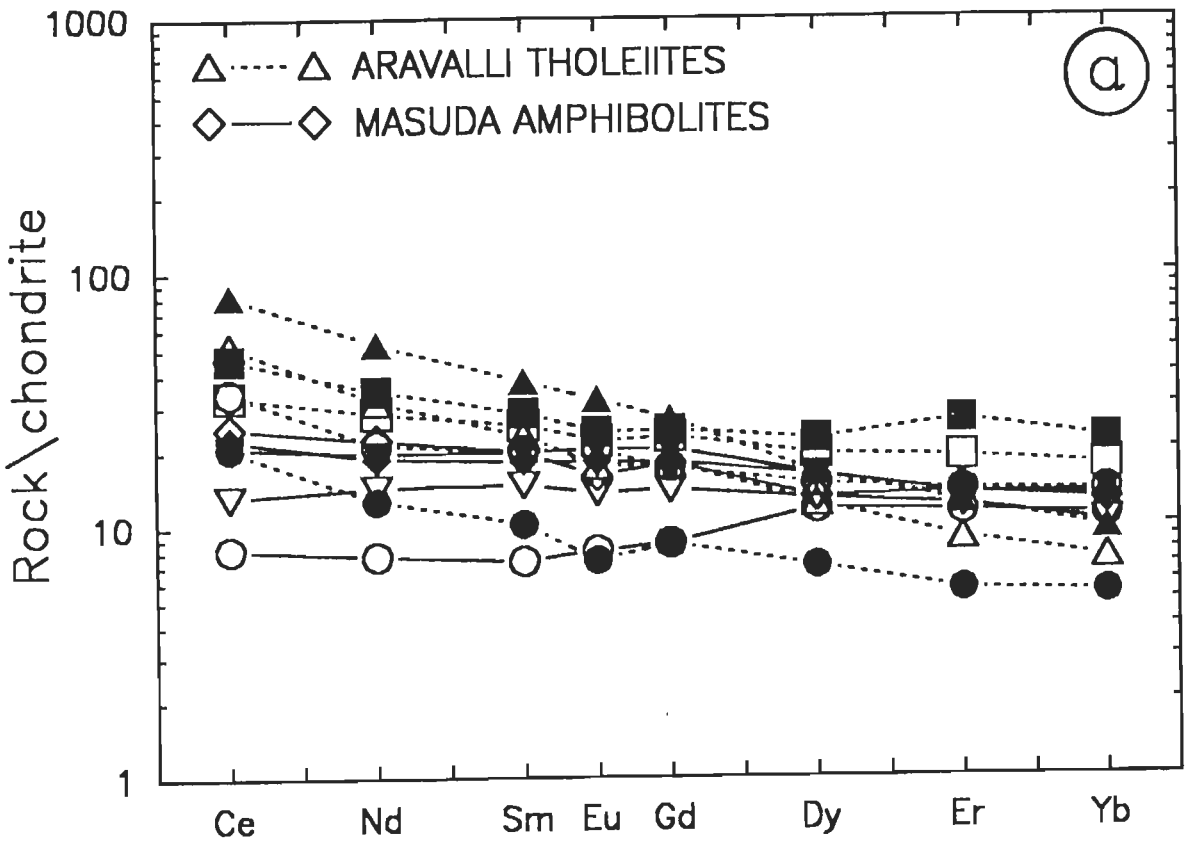

Fig. 5.8a **Chondrite normalized REE patterns (short dashed line) for basal Aravalli tholeiites (Ahmad and Rajamani, 1991). Note that the Aravalli tholeiites have LREE enriched characteristics whereas, Masuda amphibolites (solid line) have flat to slight LREE enriched characteristics.**

The amphibolites occur as enclaves in different dimensions within southern BGC (east of Nathdwara & Udaipur). The REE abundances of these enclaves have been given in Ahmad and Rajamani (1988), Gopalan et al. (1990) and Ahmad & Tarney (1994). The amphibolite enclaves within BGC have variable REE abundances. Their chondrite normalized REE patterns can be

grouped into three categories. Enclaves collected near BGC-Aravalli contact have very high REE abundances with convex upward REE patterns. The second type of enclaves are light REE enriched, HREE depleted and have sloping REE patterns. The LREE abundances vary from Ce_N=15-200 and HREE from Yb_N=5-15. The third type of mafic bodies have nearly flat chondrite normalized REE patterns with REE abundances varying from 10-25 times relative to chondrite. The amphibolites of the study area (northern BGC) have chondrite normalized REE patterns which are somewhat similar to that of the third type of enclaves (Fig. 5.8b).

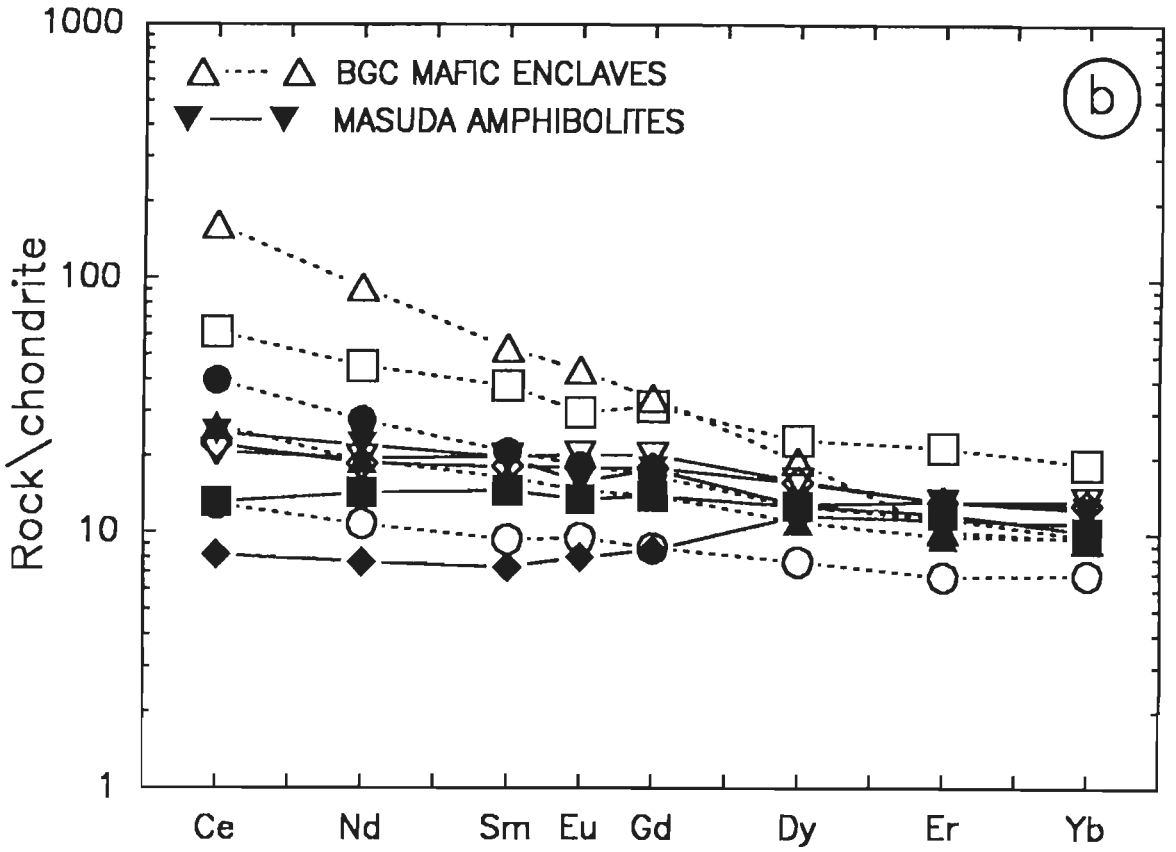

Fig. 5.8b **Chondrite normalized REE patterns for mafic enclaves of the Banded Gneissic Complex occurring to the east of Nathdwara (Ahmad and Tarney, 1994). These enclaves have variable light REE and fractionated patterns (short dashed line) as compared to the amphibolites of Masuda.**

Deb (1992) reported LREE enriched and HREE fractionated chondrite normalized REE patterns for the amphibolites from Rampura-Agucha which lies ~60 km south-east of Masuda. Except for one sample other samples have more than 24 times Ce and 10 times Yb relative to chondrite and these are unlike the Masuda amphibolites. Whereas, one of the samples from Rampura-Agucha has REE pattern quite similar to that of the Masuda amphibolites.

In summary, the amphibolites around Masuda in the northern part of the BGC are comparable to that of REE abundances and chondrite normalized REE patterns of type-3 mafic bodies of southern BGC (east of Nathdwara) which also have flat REE patterns.

5.9 RARE EARTH ELEMENT MODELLING

The amphibolites are inter banded with sanukitoids to granodiorite-granite gneisses in the Masuda area. Therefore, it is important to test whether the magmas parental to the amphibolites had undergone crustal contamination during its emplacement. Ce-Nd plot can be used to test whether the amphibolite magma had undergone any crustal contamination (cf. Horan et al., 1987; Balakrishnan et al., 1990). The Ce and Nd abundances in the upper crust (Taylor and McLennan, 1985) is also plotted in the diagram (Fig. 5.9) along with the amphibolites. The average Ce and Nd abundances of the sanukitoids and granodiorite samples (Granitoids) of the Masuda area are also shown (Fig. 5.9).

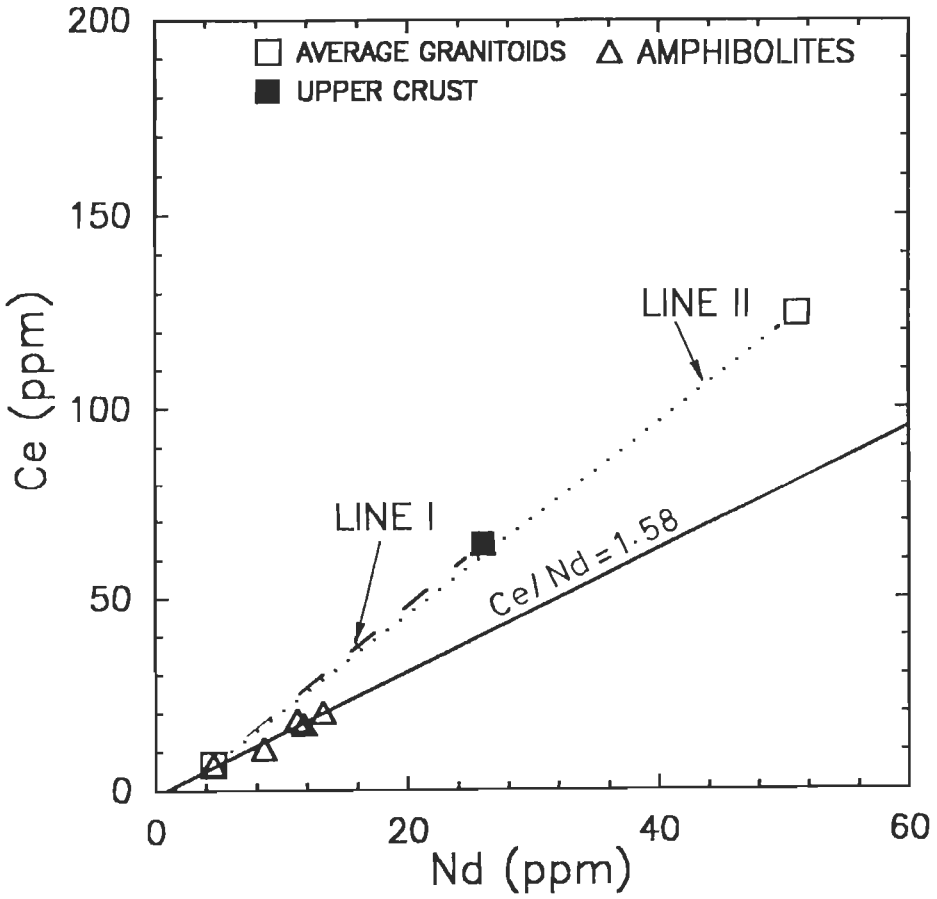

Fig. 5.9 **Ce-Nd plot for the amphibolites to test the possi-bility of crustal contamination (after Horan et al., 1987 and Balakrishnan et al., 1990). The amphibolites define a linear array which is different from hypothetical mixing trends between sample # J-71 (lowest Ce and Nd abundances) and upper crust (line I) as well as with the average composition of the granitoids (line II) occurring in the study area. The reference line for Masuda amp-hibolites may represent Ce/Nd ratio of their sources.**

If, magmas represented by the amphibolite samples have been crustally contaminated then a linear mixing trend between upper crustal composition and amphibolites are expected. The amphibolite samples define a linear array which is quite different from that of mixing line constructed (line I & II) for reference (Fig. 5.9). Thus, the tholeiitic magmas represented by amphibolites were not contaminated by upper crustal rocks. Ce and Nd being incompatible elements, the linear array defined by the samples possibly reflects Ce and Nd ratio of their sources (cf. Balakrishnan et al., 1990).

When a homogeneous source is subjected to different extents of partial melting, the melts will have chondrite normalized REE patterns that are sub-parallel to each other but varying in abundances . Whereas, a series of residual magmas formed by different extents of fractional crystallization of olivine along with clinopyroxene or plagioclase would have crossing chondrite normalized REE patterns with Eu anamolies. The amphibolite samples of Masuda area, have sub-parallel REE patterns without significant Eu anamolies (Fig. 5.10). Hence, it is likely that they represent magmas generated by different extents of partial melting from a parent magma. [Mg]-[Fe] and Ni-Zr modelling also do not support the premise that the magmas representing amphibolites could be derived by fractional crystallization from a parent magma.

The upper mantle; likely source for the tholeiitic magmas consists of olivine, pyroxene, garnet, plagioclase and spinel. It is important to take appropriate modal abundances of the minerals while modelling trace element abundances in the magmas generated by partial melting of upper mantle sources. The modal proportions of the above mantle minerals that possibly equlibrated with partial melts, as suggested by Kostopoulous (1991), is used for trace element modelling.

The REE data of the primitive mantle (Taylor & McLennan, 1985) is used as the source concentrations for the calculation. The source (spinel lherzolite) has modal mineralogy consisting of 57.5% olivine, 27.5% orthopyroxene, 12.5% clinopyroxene and 2.5% spinel. In a chondrite normalized plot the REE pattern for primitive mantle is almost flat and the abundances are ~1.8 times the chondrite. Using batch melting equation the melt composition for different extents of partial melting have been calculated. Bulk distribution coefficients for REE were calculated using the K_d values for olivine, clinopyroxene, orthopyroxene as reported in Hanson (1980) and for spinel from Kostopoulos and James (1992) for the mantle-melt system.

The calculated abundances of eight REEs for 5 to 20% partial melt compositions are plotted in the chondrite normalized diagram (Fig. 5.10). It can be observed that a flat to slightly LREE enriched pattern is observed for 20 to 5 % partial melts. The HREE abundances show unfractionated REE patterns with a very narrow range in their abundances. The amphibolites of the study area fall within the 5-20 % partial melting of the primitive mantle (Fig. 5.10). Thus, it is poslible

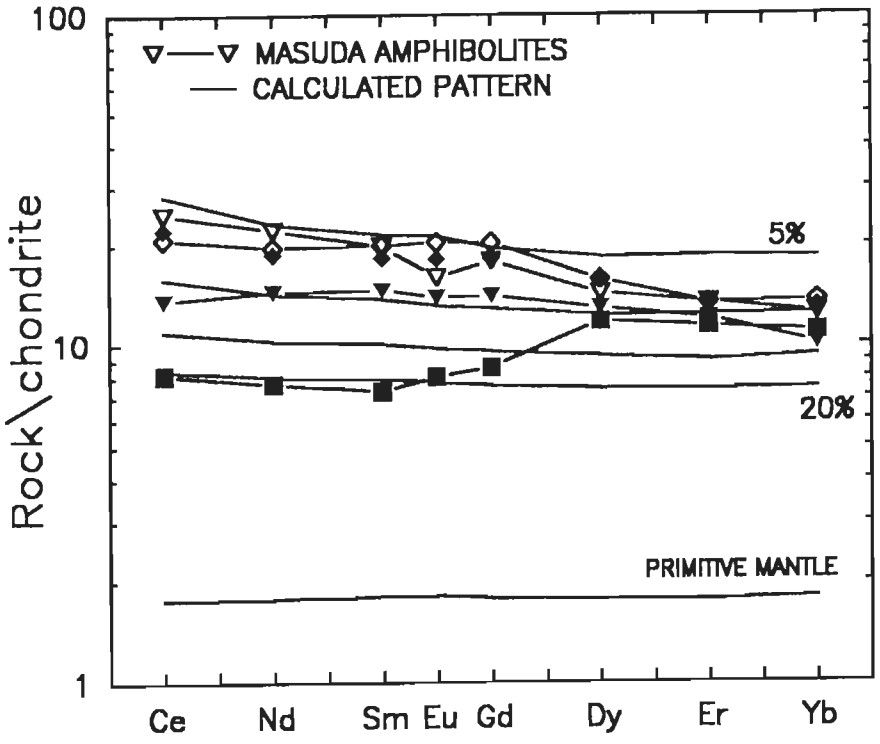

Fig. 5.10 **Calculated chondrite normalized REE patterns for 5, 10, 15 & 20% partial melting of a spinel lherzolite leaving a residue consisting of 57.5% olivine, 12.5% orthopyroxene, 27.5% clinopyroxene and 2.5% spinel. The assumed residual mineralogy for the spinel lherzolite source is after Kostopoulos (1991). The REE abundances of the primitive mantle are taken from Taylor and McLennan (1985). The REE patterns for Masuda amphibolite are shown for comparison. Note that the REE patterns for Masuda amphibolites fall between the calculated curves for 5 to 20% partial melting of spinel lherzolite source.**

to generate magmas representing amphibolites from sources similar to the primitive mantle in terms of REE abundances.

In summary, the amphibolites of the study area have REE abundances and chondrite normalised patterns similar to that of marginal sea basalts. They have REE abundances similar to some of the mafic enclaves occurring in southern BGC (north-east of Udaipur) and are quite different from that of Basal Aravalli Volcanics of Nathdwara. The source might have been a lherzolite having higher but variable [Fe]/[Mg] ratio than a garnet lherzolite (Takahasi and Scarfe, 1985) with ca.900 ppm Ni. This source upon 5-20% partial melting could have given rise to amphibolites occurring in the BGC of Masuda area.

CHAPTER VI

PETROGENESIS OF GRANITOIDS

Petrogenetic modelling of granitoids are very complex. Because they can be formed by a variety of petrogenetic processes such as, partial melting, fractional crystallization, magma mixing, liquid immiscibility and crustal contamination and also from a variety of sources, such as, by partial melting of basaltic rocks leaving amphibolite, granulite or eclogite residue, by partial melting of ultramafic rocks of upper mantle and by fractional crystallization of mantle derived magmas, anatexis of crustal rocks or combination of these (Skjerlie and Johnston, 1996).

The granitoid rocks that occur in the Masuda area can be classified as intermediate (diorite-monzodiorite-quartz diorite), granodiorite and granite suites. Petrogenesis of the intermediate suite is considered first followed by granodiorites, granophyres and aplite in this chapter. Geochemical modelling is carried out using the least mobile elements, such as, the REEs. For quantitative modelling of partial melting and fractional crystallization processes appropriate K_d values for different source and melt systems, as suggested by Hanson (1980), Henderson (1982), Stern and Hanson (1991) and Kostopoulos and James (1992) have been used.

In the study area, the intermediate suite of rocks, comprising of diorite-monzodiorite-quartz dioritic gneisses are associated with amphibolites, granodiorite and calc-silicate gneisses. To such a rock association of intermediate rocks and their derivatives in the Rainy Lake region the term sanukitoids was used by Shirey and Hanson (1984) to describe it as a group. The terminology sanukitoid derived its name from the Sanuki region of south west Japan. Tatsumi and Ishizaca (1982a, 1982b) described the sanukitoids as relatively aphyric, plagioclase free andesites and basalts. The sanukite is a volcanic rock andesitic in composition with phenocrystic phases such as, olivine, clinopyroxene or orthopyroxene. The term sanukitoid is used here on the basis of chemical characteristics rather than the mineralogical and it may occur in the field as extrusive or intrusive igneous bodies (Stern et al., 1989).

6.1 GEOCHEMICAL CHARACTERISTICS OF THE INTERMEDIATE SUITE

The sanukitoids in the type area (Sanuki area, Japan) have 55-60 wt.% SiO_2, mg#'s near 0.7, Ni contents near 200 ppm and olivine of Fo_{87-89} on their liquidii. One of the intermediate samples (J-60) from the study area has SiO_2=59.8 wt.%, mg# =0.56, Ni=247 ppm, Cr=544 ppm and olivine Fo_{79} composition on its liquidus. The other samples of this suite have similar or slightly more evolved geochemical features (Table 4.3, Chapter IV). Thus, the sample J-60 of the intermediate suite is geochemically comparable with the sanukitoids from Archaean Superior Province and from other parts of the world (Table 6.1; Stern et al., 1989).

Relative to the sanukitoids from Archaean Superior Province, sample # J-60 has a similar TiO_2, total alkalis and FeO. However, it has higher SiO_2, Al_2O_3, Ni, Cr and Rb/Sr ratio and lower Ba, Sr, mg#, $(Ce/Yb)_N$ and K/Rb ratio than the sanukitoids from Superior Province. When compared with high-Mg andesite of Japan (column 3; Table 6.1), it has higher FeO, Al_2O_3, Sr, Rb, Ni, Cr, total alkalis and lower MgO, CaO. Similarly, when compared with high Mg andesite of Aleutian ridge (column 4; Table 6.1), it has higher SiO_2, Al_2O_3, Ba and lower TiO_2, MgO, CaO and Sr. When compared with sanukitoids from Andes and Cascades and the Appinite and Shosonite rocks it has higher SiO_2, Ni, Rb, Cr and lower Ba, Sr, MgO and CaO (column 5,6,7and 8).

The intermediate rocks for the Masuda area have lower MgO, CaO and Sr and higher SiO_2, Al_2O_3 than other sanukitoids, and therefore, could represent magmas more evolved than the typical sanukitoids. However, they have broadly similar abundances of major and trace elements to that of the sanukitoid suite. Hence, they are referred as sanukitoid suites in the following discussion.

The sanukitoids of Masuda area can be classified as low-Ti and high-Ti suites on the basis of their TiO_2/MgO ratio. The low-Ti suite has TiO_2/MgO ratio less than 0.404 and that of high-Ti suite greater than 0.404 (Fig. 6.1a). The high-Ti suite also has higher Ba/Sr ratio (> 2) compared to low -Ti suite (Fig. 6.1b).

The low-Ti and high-Ti suites show two parallel trends in SiO_2 ~ TiO_2 plot (Fig. 6.2a). The low-Ti suite has TiO_2 abundances similar to that of andesites which usually have less than 1.3 wt.% TiO_2 (Pearce and Cann, 1973). In general the low-TiO_2 suite has higher mg#, MgO, Cr and lower K_2O and Ba abundances than the high-TiO_2 suite.

The high-Ti suite has higher K_2O contents than the low-TiO_2 suite for similar SiO_2 values. The K_2O abundances in low-TiO_2 suite of intermediate rocks show a positive correlation with SiO_2 (Fig.6.2b) and this indicates that 'K' perhaps behaved as an incompatible element during partial melting and fractional crystallization of their magmas.

Table 6.1 Comparison of BGC Sanukitoids with the Sanukitoids from other areas

S.No.	1	2	3	4	5	6	7	8	9
Elements	Masuda Sanukitoids J-60	Archaean Sanukitoids	Japan Sanukitoids	Aleutians Sanukitoids	Andes Sanukitoids	Cascades Sanukitoids	Appinite	Shoshonite	Melt
SiO_2	59.80	56.07	57.35	58.5	52.6	54.06	55.36	55.46	55.5
TiO_2	0.7	0.71	0.66	0.94	1.16	1.43	0.92	0.93	2.5
Al_2O_3	16.22	14.88	15.56	15.2	16.6	16.66	15.75	16.75	12.3
Fe_2O_3				2.4		3.63	1.77	2.55	0.5
FeO	6.9	7.08	6.27	1.5	7.59	4.7	5.48	4.01	6.8
MnO	0.1	0.12	0.13	0.06	0.12	0.13	0.15	0.11	0.1
MgO	4.21	6.85	8.59	5.0	8.16	5.42	5.87	4.81	9.3
CaO	3.95	7.65	6.80	7.6	7.66	7.64	7.15	6.71	10.4
Na_2O	3.62	4.04	2.81	3.7	3.3	3.65	2.81	2.94	2.0
K_2O	2.52	2.23	1.68	2.2	1.72	2.15	2.25	3.66	0.5
P_2O_5	0.27	0.36	0.14	0.54		0.54	0.21	0.6	
Total	98.29	99.99	99.99	97.64	98.91	100.01	97.72	98.53	99.9
Rb	217	60	78	17	49	46.7	64	63	
Sr	378	1229	276	2600	650	1194	433	956	
Ba	578	1214		343	482	1015	529	567	
Zr	177	111		170		189	173	121	
Ce	79.52	97.0	24.65	88.5	47	107	29		
Yb	2.307	1.6	1.57	0.633	1.83	3.5			
Ni	247	154	203	150	139	83.2	71	53	
Cr	544	352	451		395	189	229	141	
Mg#	0.561	0.63	0.71	0.71	0.66	0.55	0.6	0.58	0.7
$(Ce/Yb)_n$	8.82	15.5	4.02	35.8	25.7	7.8			
K/Rb	96.4	309	179	1074	291	382	292	482	
Rb/Sr	0.57	0.05	0.28	0.01	0.08	0.04	0.15	0.07	

(Compiled from Stern et al., 1989 and the references therein)

Sanukitoids show a decreasing trend in FeO, MgO and TiO_2 with increasing SiO_2 (Fig.6.2c,d&a). This could be as a result of equilibration of their magmas with ferromagnesian minerals such as, Fe-Mg and Fe-Ti bearing phase(s).

Narrow variation of Al_2O_3 contents with silica (Fig. 6.2e) indicate that the Al_2O_3 abundances in their magmas could have been buffered by phases in which Al is an essential structural constituent (Hanson and Langmuir, 1978). CaO along with P_2O_5 abundances decrease with increasing silica (Fig. 6.2f & g). This implies that probably the magma might have equilibrated with clinopyroxene, plagioclase and possibly apatite.

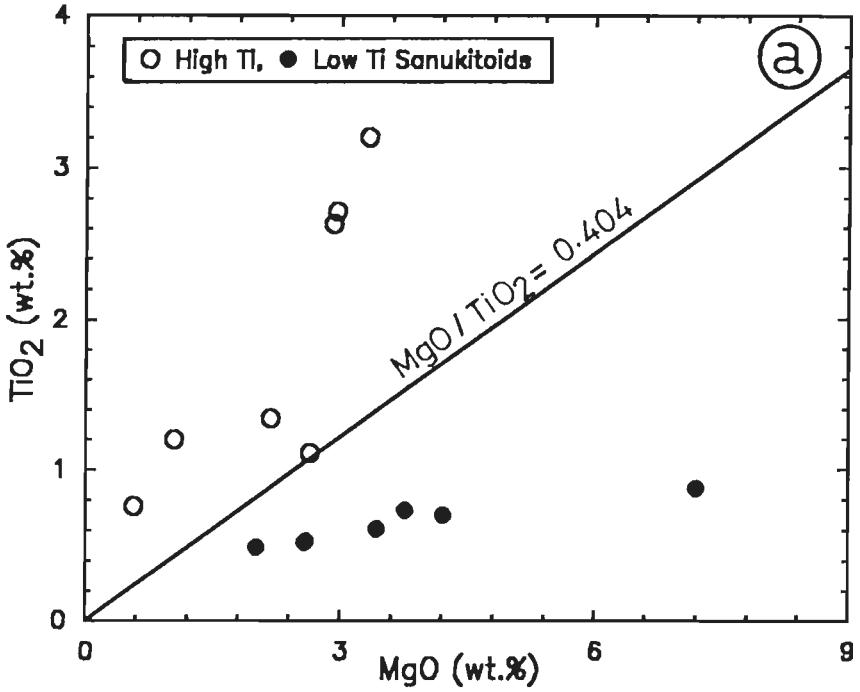

Fig. 6.1a MgO-TiO_2 relation for the Masuda sanukitoids. The low-Ti sanukitoids have TiO_2/MgO ratio less than 0.404 whereas, high-Ti sanukitoids have greater than 0.404.

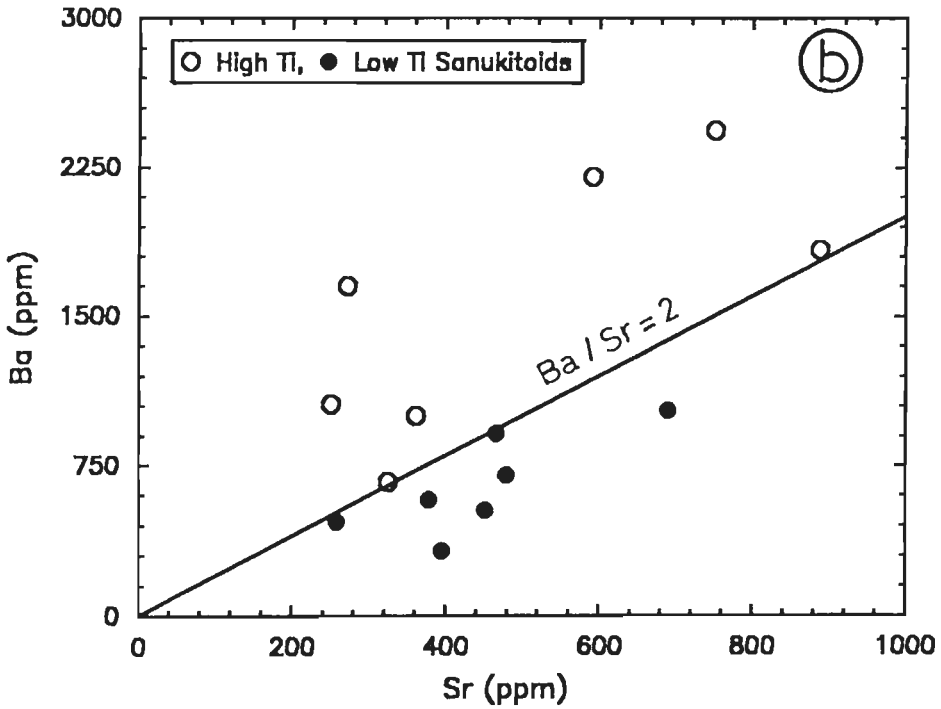

Fig. 6.1b Ba-Sr relation shows that the high-Ti sanukitoid suite also has higher Ba/Sr ratio greater than 2 than the low-Ti sanukitoid suite (less than 2).

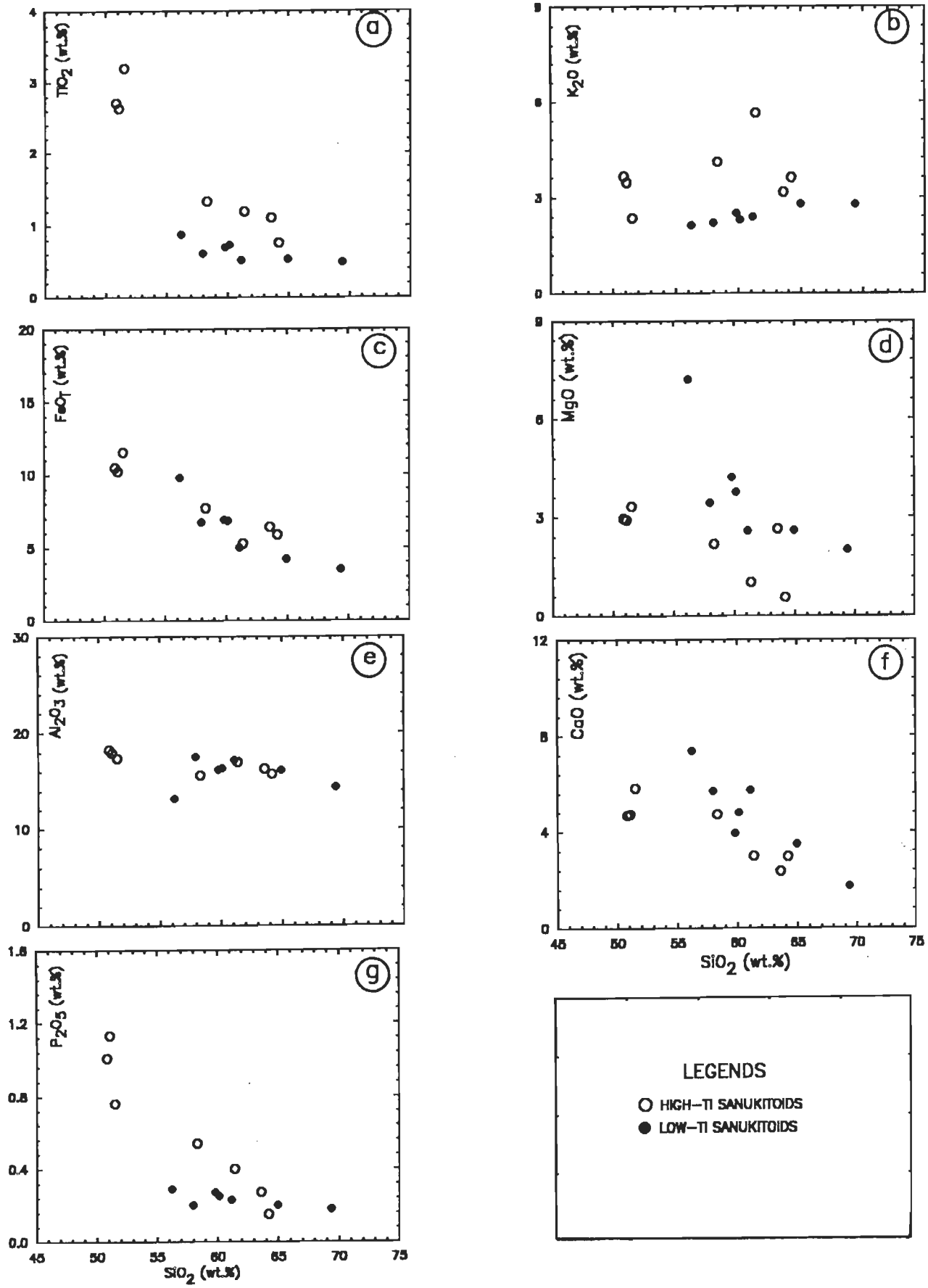

Fig. 6.2 Harker's variation diagram showing the behaviour of different major element oxides with silica. The symbols are defined in the legend.

6.1.1 FRACTIONAL CRYSTALLIZATION MODEL

The generation of trachyte-trachy-andesite magma by fractional crystallization of plagioclase and ferro-magnesian minerals from basic magma (wet & dry) is proposed by Arth et al. (1978) and Wilson et al. (1995). In the study area, the sanukitoids are closely associated with amphibolites of tholeiitic composition. It is possible that the magmas represented by sanukitoid suites could have been derived by fractional crystallization from a parental tholeiitic magma undersaturated with water.

To test this hypothesis, J-68, a tholeiitic amphibolite (mg# 0.58) is assumed as the parent magma. The fractional crystallization of clinopyroxene and plagioclase are considered in various proportions. Using the Rayleigh's equation for fractional crystallization, $C_l/C_0 = F^{D-1}$, the residual liquid compositions for 5% and 40% fractional crystallization of clinopyroxene are calculated and plotted in the chondrite normalized REE diagram (Fig. 6.3a). The calculated patterns show flat REE patterns with slight Ce enrichment for 5% (Ce_N=23) and 40% (Ce_N=31). The LREE abundances calculated for residual liquids for fractional crystallization of clinopyroxene are much lower than the abundances observed in the samples.

A combination of plagioclase (80%) and clinopyroxene (20%) fractional crystallization is also considered. The fractionally crystallizing minerals will have 56 wt.% SiO_2 content while the parent magma has 43.9 wt.% SiO_2. Therefore, fractional crystallization of such an assemblage can not increase the SiO_2 content of residual magma as would be required.

When 70% clinopyroxene and 30% hornblende are considered as the fractionally crystallizing phases, on 10% fractional crystallization, they produced a nearly flat REE pattern (Ce_N=23 and Yb_N=11). As the fractionation proceeded to 30% Ce abundances increased (Ce_N=32) whereas, abundances of all other REEs decreased (Fig. 6.3b). At 70% fractionation Ce_N increased to 78 whereas, HREEs were depleted giving rise to a concave upward pattern with a prominent positive Eu anomaly. However, the REE patterns of the sanukitoids are unlike the calculated REE patterns in residual melts on 10%, 30% and 70% fractional crystallization of hornblende+clinopyroxene.

Similarly, when 80% clinopyroxene and 20% garnet are considered as the fractionally crystallizing phases, on 10% fractionation, the residual melt has a chondrite normalized REE pattern with slight enrichment in Ce abundances (Ce_N=24). At 20% and 30% fractional crystallization of clinopyroxene+garnet, the HREEs are drastically depleted and LREEs are also depleted in the residual magmas (Fig. 6.3c). Again, as the calculated REE patterns in these residual liquids do not match with that of the sanukitoids, therefore, clinopyroxene and garnet fractional crystallization from tholeiitic parental magma can not give rise to magmas represented by the sanukitoids.

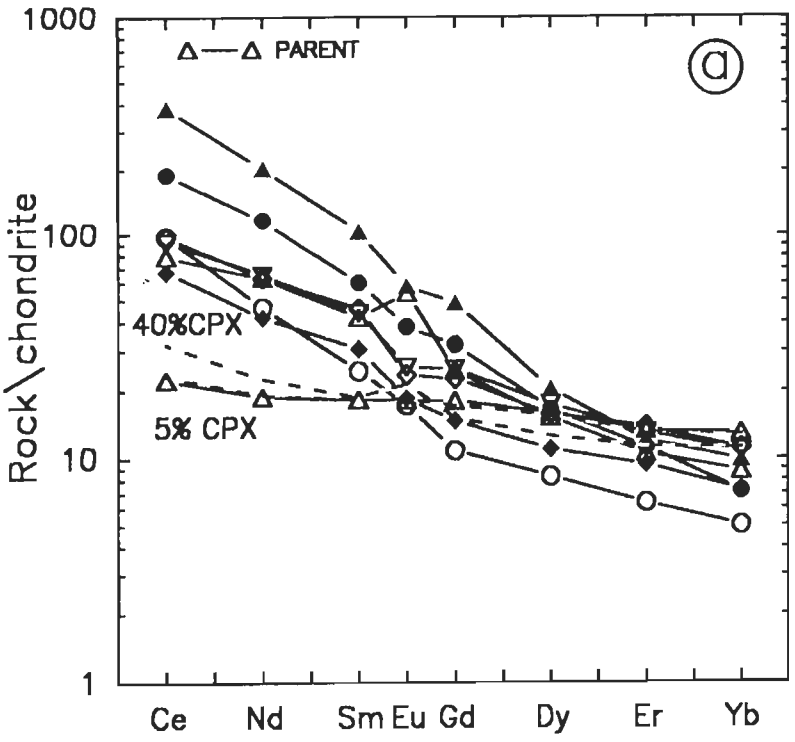

Fig. 6.3a Calculated chondrite normalized REE patterns (medium dashed lines) for 5 and 40% clinopyroxene fractional crystallization from a tholeiite parent (J-68). REE patterns of the sanukitoids are quite different from that of the calculated REE patterns.

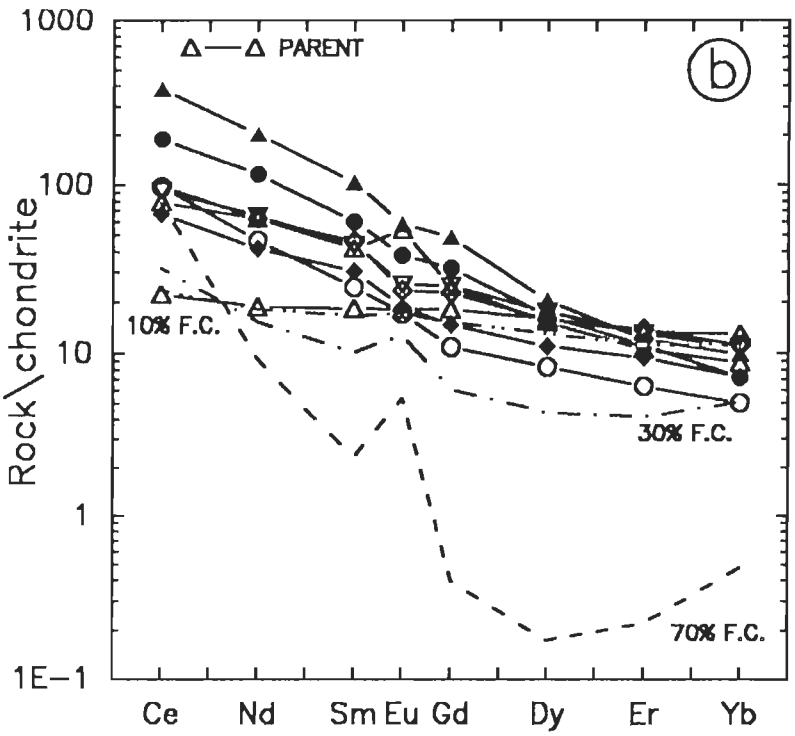

Fig. 6.3b Calculated chondrite normalized REE patterns (medium dashed lines) for 10, 30 and 70% fractional crystallization of clinopyroxene and hornblende in 7:3 proportion from a tholeiite parent (J-68). The REE patterns of the sanukitoids are also shown for comparison.

Arth et al. (1978)) and Kramers (1988) suggested that on fractional crystallization of hornblende and plagioclase from wet basic magmas can also generate the residual liquid similar in chemical composition to that of tonalite-trondhjemite suite. The REE contents of amphibolite sample # J-68 from the study area is assumed as the chemical equivalent of wet basic magma.

5% hornblende fractional crystallization from the wet magma results in a flat REE pattern while subsequent fractional crystallization of hornblende up to (40%) results in a sloping LREE pattern with positive Eu anomaly (Fig. 6.3d). The HREE abundances show a concave upward REE pattern (Yb_N =1.2 to 2). Plagioclase fractionation increases both HREE and LREE and gives rise to negative Eu anomaly (not shown) as the fractionation proceeds. However, in the sanukitoid samples no such REE pattern is observed.

When 40% fractional crystallization of hornblende and plagioclase in equal proportion is considered, the residual liquid has slight LREE enrichment (Ce_N =20) and concave upward chondrite normalized HREE pattern (Fig. 6.3d). Mass balance calculations are carried out using amphibole and plagioclase compositions data of J-68, a tholeiite (see Appendix - I) for SiO_2, Al_2O_3 and CaO. After 40% fractionation of hornblende and plagioclase in 1:1 proportion from the tholeiitic magma the residual melt had 38% SiO_2, 13.67% Al_2O_3 and 10.86% CaO. In contrast to this, the samples have SiO_2>50 wt.%, Al_2O_3>16 wt.% and CaO <6 wt.%. Therefore, fractional crystallization of hornblende and plagioclase can not produce the residual liquid having REE and major element abundances similar to that of sanukitoid magma.

6.1.2 CONTAMINATION MODEL

Stern et al. (1989) reported that the sanukitoids of southwestern Superior Province can not be generated either by fractionation or by contamination of lamprophyres based on the mg#, [Mg]-[Fe] systematic and Ni & Cr contents. They contended that mg# of lamprophyres are similar to the sanukitoids and also have similar Ni and Cr contents. Therefore, mixing or contamination of lamprophyres by the upper crust would generate a magma with lower mg # than sanukitoids.

Spark (1986) suggested that crustal contamination of komatiite magma can give rise to sanukitoid magma, as it may explain high abundances of ferromagnesian elements and evolved silica content coupled with higher LILE abundances. Detailed quantitative modelling by Stern et al. (1989) for Roaring River Complex sanukitoids suggested that it is possible to explain mg# in the melt but lower abundances of Na_2O, K_2O, Ba, and Sr in the contaminated melt rule out the effectiveness of komatiite contamination as a viable mechanism. As some of the sanukitoids from the study area are comparable with Roaring River Complex, it is unlikely that the assimilation of upper continental crust by lamprophyric and komatiitic magmas could have generated the

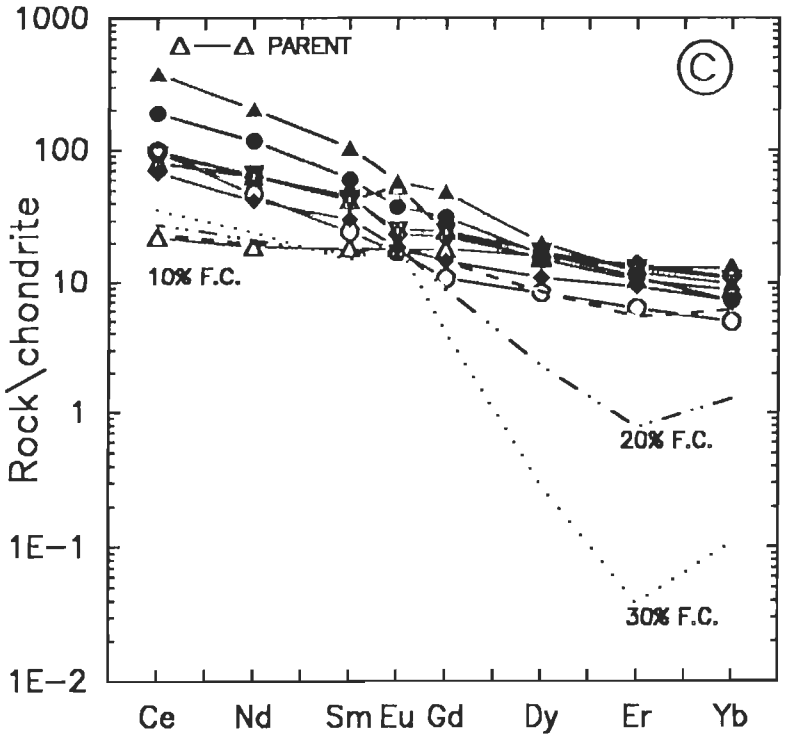

Fig. 6.3c Calculated chondrite normalized REE patterns for 10, 20 & 30% fractional crystallization of clino-pyroxene and garnet in 4:1 proportion from a tholeiitic parent J-68. REE patterns of the sanukitoids are quite different from that of the calculated REE patterns.

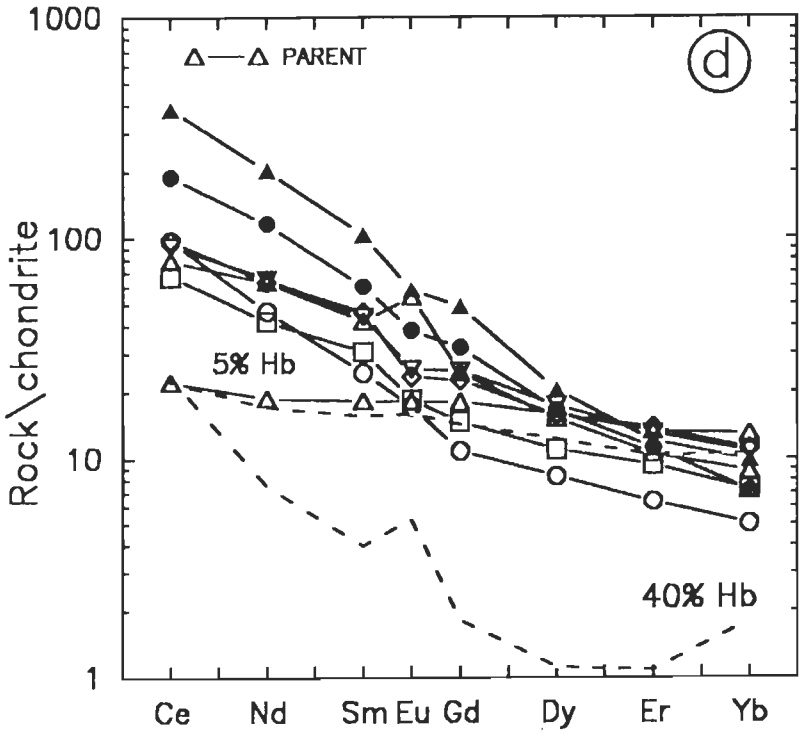

Fig. 6.3d Calculated chondrite normalized REE patterns for 5 & 40% fractional crystallization of hornblende only (medium dashed lines) and for 40% fractional crystallization of hornblende and plagi-oclase in equal proportion from the tholeiitic parent J-68. All the calculated patterns are unlike the REE patterns of the sanukitoid samples.

magmas represented by the sanukitoids of the study area. The lamprophyres and komatiitic rocks are also not reported from the study area.

Therefore, the only possibility is that the sanukitoids magmas might have resulted due to assimilation of upper continental crust by tholeiitic magmas. This possibility is tested using Ce vs Nd diagram proposed by Horan et al. (1987). In Fig. 6.4, the average of composition of upper crust (Taylor and McLennan, 1985), tholeiitic amphibolites and granodiorite gneisses from the study area are also plotted. It is evident from the plot that all sanukitoid samples plot well above the upper crust and they do not fall along a mixing trend between tholeiite and upper crust. Crustal contamination of tholeiitic magmas with granodiorite gneisses of Masuda area also can not explain the higher abundances Ce and Nd observed in the sanukitoids. Therefore, the contamination model can not be a possible mechanism for the generation of sanukitoid magmas.

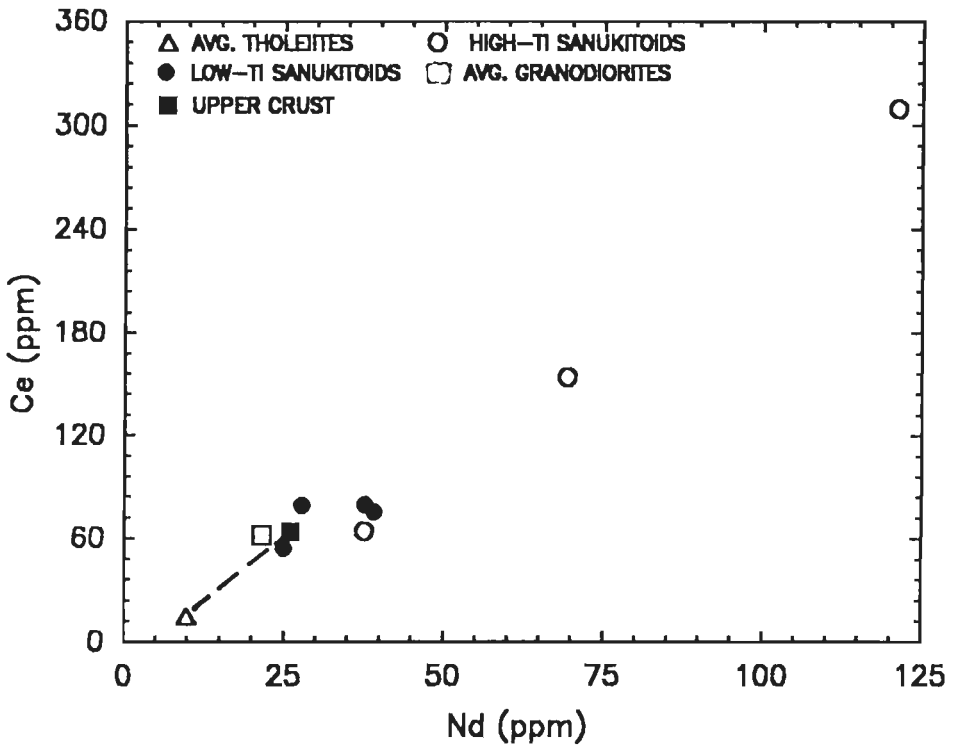

Fig. 6.4 **Ce - Nd relation for the sanukitoids of the Masuda area. Both the suites of sanukitoids plot well above the hypothetical mixing lines between amphibolites (from the study area) and upper crust.**

Residual liquids formed on 40% fractional crystallization of clinopyroxene + plagioclase, clinopyroxene + hornblende and clino pyroxene + garnet have Ce and Nd abundances much less than the sanukitoids. Assimilation of the upper continental crust or granodiorites can not also give rise to magmas with Ce and Nd abundances similar to that of the sanukitoids (Fig. 6.4). Thus, fractional crystallization, assimilation and assimilation coupled with fractional crystallization of tholeiitic magmas can not give rise to magmas compositionally similar to that of the sanukitoids.

6.1.3 PARTIAL MELTING MODEL

Several workers consider that the partial melting of amphibolite ± garnet can give rise to magmas of intermediate composition (Barker & Arth, 1976; Condie, 1986; Rudnik & Taylor, 1986; Martin, 1987; Arkani-Hamed and Jolly, 1989; Rapp et al., 1991). Further, Arth (1972), Arth & Hanson (1975) and Rudnick & Taylor (1986) favoured the generation of tonalite and trondhjemite suite magma by partial melting of tholeiitic basalts under granulite and eclogite metamorphic facies condition.

In the study area, the sanukitoids are associated with amphibolites and meta-gabbroic rocks. Therefore, it is possible that the monzodiorite to granodioritic magmas could have been generated by partial melting of tholeiitic rocks. Using rare earth elements and other incompatible trace element abundances quantitative modelling of the partial melting of the amphibolites is carried out.

Burnham (1979b) and Arculus & Wills (1980) have observed from the experimental investigations that high P_{H2O} leads to the instability of plagioclase. Further, Beard and Lofgren (1991) found that in water saturated experiments ($P_{H2O}=P_{Total}$) at 3 kb the plagioclase breaks down and enrich the melt in Al_2O_3 and Ca while the abundances of FeO, MgO, TiO_2 and K_2O are lowered in the melt. This is considered to be the result of greater stability of mafic minerals particularly amphibole, relative to the plagioclase under the above conditions of melting. Whereas, during dehydration melting, plagioclase is relatively stable and the melts formed by break down of amphibole+quartz are low in Al_2O_3 and enriched in FeO, MgO and TiO_2 (Beard and Lofgren, 1991). Thermal stability limit of amphibole increases with P_{H2O} whereas, pyroxene stability increases with increased temperature and decreased P_{H2O} (Spear, 1981; Gilbert et al., 1982). Thus, the residual mineralogy and their relative abundances are determined by P_{H2O} condition during melting of tholeiitic rocks.

Rapp et al. (1991) from the experimental investigations found that basaltic rocks at 8, 16 and 22 kb pressures (on 10-40% partial melting) can produce tonalite to trondhjemitic liquid. They observed that dehydration partial melting of basalt ($P_{fluids} < P_{Total}$) at 8 kb and 1000^0C are dominated by amphibole + plagioclase with minor orthopyroxene ± quartz ± Fe-Ti oxides. Above $1050\text{-}1075^0C$ at 8 kb melting the amphibole is no longer stable in the residue which consists of plagioclase + clinopyroxene± olivine ± orthopyroxene (Rapp, 1990).

At pressures of 16 kb, the residual assemblages coexisting with trondhjemitic-tonalitic melts are dominated by garnet+clino pyroxene at $1025\text{-}1050^0C$ and at temperatures of $1000\text{-}1030^0C$. Plagioclase+amphibole±orthopyroxene±quartz are present in addition to garnet+clinopyroxene (Rapp et al., 1992). Similarly, they showed that melts at 22 kb co-exist with a garnet+clinopyroxene dominated residue with rutile or magnetite.

An amphibolite source (hydrous condition) leaving 60% hornblende and 40% plagioclase residue is considered as the parent and abundances of REEs in magma formed by 20% partial melting are calculated and plotted in chondrite normalized diagram (Fig6.5a).

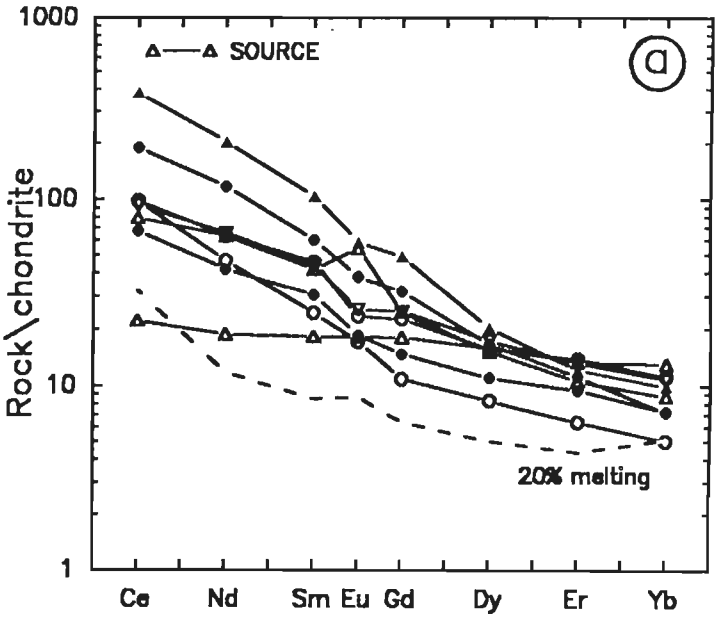

Fig. 6.5a Calculated chondrite normalized REE patterns for 20% partial melting of a tholeiite source (J-68) leaving an amphibolite residue. The REE abundances of the sanukitoids are much higher than that of calculated patterns.

The calculated patterns in diagram show substantially lower abundances in LREE (Ce_N =35) as well as, HREE (Yb_N=4.7) than the sanukitoids. After 20% partial melting the melts had Ba=1172 and 202 ppm Sr compared to average 800 ppm of Ba and 400 ppm of Sr for sanukitoids.

Similarly, a tholeiite source leaving a granulite residue consisting of 50% plagioclase, 30% ortho-pyroxene, 15% clino-pyroxene and 5% garnet is modelled for partial melting. The chondrite normalized REE patterns of the melts formed on 5%, 10% and 25% partial melting are given in Fig. 6.5b. They have a concave REE pattern with lower REE abundances than the sanukitoids.

Further, a tholeiite leaving a basic granulite residue consisting of 46.4% plagioclase, 19.4% diopside, 26.2% hypersthene, 6.5% hornblende, 0.9% opaque and 0.5% apatite (Gill, 1981) is considered for the partial melting, model. Even at 5% melting the chondrite normalized REE pattern of the melt has lower LREE abundances and higher HREE abundances than the sanukitoids. Melts formed by 10 & 25% partial melting have even lower LREE abundances than the sanukitoids (Fig. 6.5c).

Kelemen et al. (1993) suggested that partial melting of tholeiites leaving an eclogite residue (20% orthopyroxene, 45% clinopyroxene, 35% garnet) can give rise to melts of granitoid composition. One of the tholeiite (J-68) in the study area is assumed to represent source concentration for rare earth elements and other incompatible trace elements.

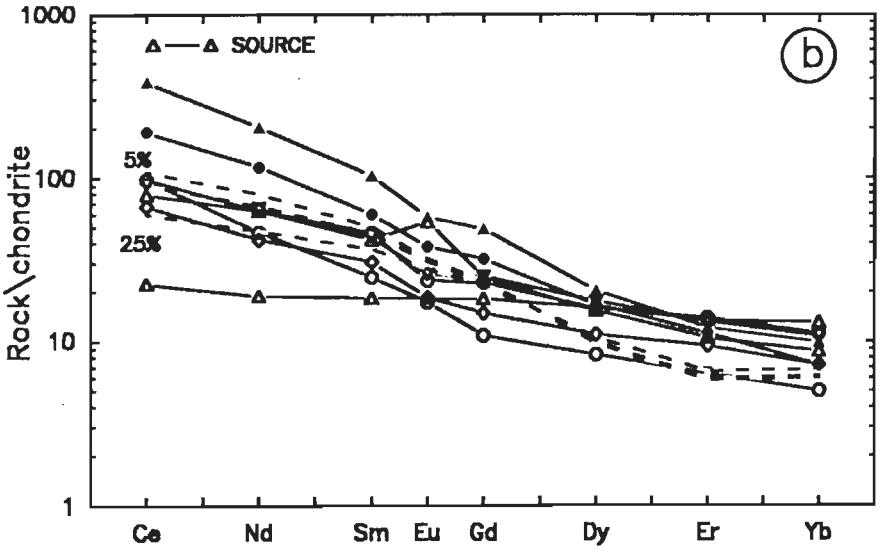

Fig. 6.5b Calculated chondrite normalized REE patterns (medium dashed lines) for 5, 10 and 25% partial melting of a tholeiite J-68 leaving a granulite residue (50% plag., 30% opx, 15% cpx and 5% garnet.

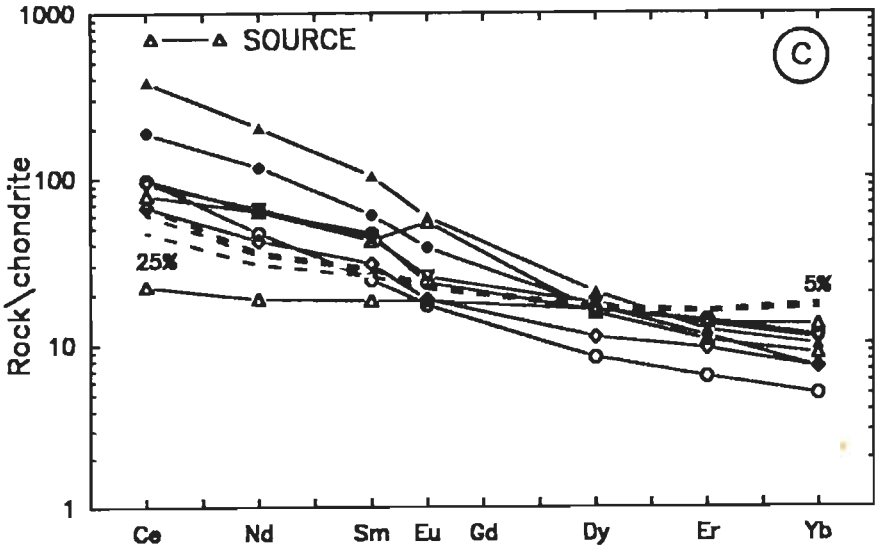

Fig. 6.5c Calculated chondrite normalized REE patterns for 5, 10 and 25% partial melting of a tholeiite (J-68) leaving a basic granulite residue (46.4% plag., 19.4% diop., 26.2% hy., 6.5% hb, 0.9% opaques, 0.5% ap.). The calculated patterns (medium dashed lines) have lower LREE and higher HREE abundances than the sanukitoid samples.

Using the batch melting equation, C_l values are calculated for 1%, 5%, 10% and 20% partial melts leaving an eclogite residue and plotted in the chondrite normalized REE diagram (Fig. 6.5d). The calculated patterns are LREE enriched and highly depleted in HREE with positive Eu anomalies. However, all the sanukitoid samples have higher HREE and some have higher LREE compared to the calculated REE patterns. Therefore, the partial melting of tholeiites under eclogite facies condition can not give rise to the magma similar in REEs and other trace element abundances as that of sanukitoid rocks in the study area. At 20% partial melting, the melt has Ba=1621 ppm and Sr=764 ppm, whereas, an average of 800 ppm Ba and 400 ppm Sr are observed in the sanukitoid samples.

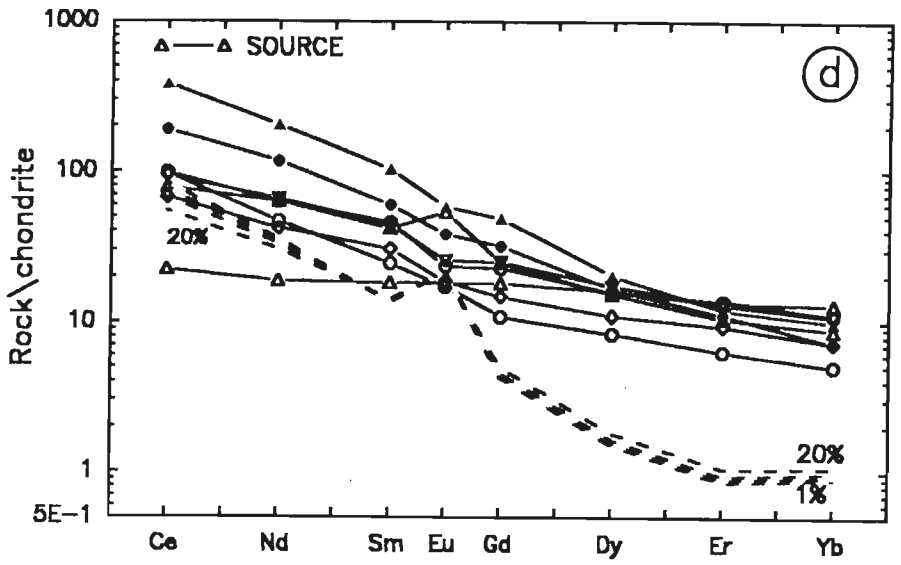

Fig. 6.5d **Calculated chondrite normalized REE patterns for 1, 5, 10 and 20% partial melting of a tholeiite (J-68) leaving an eclogite residue (45% cpx, 20% opx and 35% garnet). The calculated patterns (medium dashed lines) have lower REE abundances than the sanukitoid samples.**

The tholeiitic rocks from Masuda area have about 46 wt.% SiO_2. Residue consisting of 60% clinopyroxene + 40% plagioclase will have about 51 wt.% SiO_2. If the tholeiitic source undergoes partial melting leaving clinopyroxene, plagioclase in the residue, it can not generate magmas enriched in silica. Whereas, sanukitoid magmas are enriched in silica relative to the tholeiites. The tholeiitic amphibolites and sanukitoids have a similar range in mg #'s.

Therefore, the partial melting of gabbroic or amphibolitic sources leaving granulite or basic granulite or eclogite residue can not generate magma composition similar to that of the sanukitoids.

Partial Melting of Mantle

Several workers have considered mantle as the source for the generation of sanukitoid magma under hydrous conditions (Mysen et al.; 1974, Green, 1976). Experimental studies show that magmas with intermediate silica contents can be formed by partial melting of peridotite within a narrow pressure range of 20 kb to 10 kb (Green, 1976 and Mysen,1982). However, in dry condition the sanukitoid magmas can be generated by partial melting at pressures less than 5 kb (Jaques & Green, 1980, Takahasi and Kushiro, 1983). Experimental investigations by Tatsumi (1981,1982) on natural high magnesian andesites of the Setouchi volcanic belt demonstrated that the intermediate magma can equilibrate with mantle mineral assemblage.

Schneider and Eggler (1986) and Eggler (1987) emphasized the role of natural aqueous fluids in generating intermediate silica melts. These authors suggested that the fluids would contain significant quantities of silica, alkalis and other LIL elements. The melts which are formed initially would dissolve these fluids, as a result, the fluids with dissolved components would enhance the formation of intermediate silica melts from the peridotites compared to the melting experiments, where pure H_2O is used. Further, substantial introduction of H_2O into mantle wedge above subduction zones, would lower the solidus of peridotite relative to the melting experiments where only a small fraction of H_2O is added to the peridotite source. Therefore, one would expect an extended temperature range over which intermediate magmas could form (Wyllie, 1982). This would lead to greater diversity of magmas than produced by the experimental studies.

Thus, Sanukitoid magmas could have formed under water saturated low pressure conditions (5 to 20 kb) leaving a peridotitic residue (Mysen et al., 1974; Green, 1976). Garnet is stable under pressures greater than 20 kb (Green and Ringwood 1970; Olafsson and Eggler, 1983), Therefore, garnet might not have been a dominant mineral in the residue, because, sanukitoid magmas are considered to have formed between 10-15 kb pressure (Green, 1976). However, garnet can be expected at pressures less than 20 kb, if the mantle sources have had higher [Fe]/[Mg] values than the peridotite (Ringwood, 1975).

A primitive mantle having chondrite normalized REE abundances (1.8_N) (Taylor & McLennan, 1985) is considered as the source for the generation of sanukitoid rocks in the study area. REE abundances in the melts formed by 0.2%, 1% and 2% partial melting of the source is calculated and plotted (Fig. 6.6). It is found that even the 0.2% partial melt has lower LREE and higher HREE abundances than the sanukitoids. Further, this melt will have 162,000 ppm Ba and 18,000 ppm Sr. Hence, very low extents of partial melting of primitive mantle with a flat REE pattern can not explain the abundances of these elements in the sanukitoid magma of the Masuda area. Shirey and Hanson (1984) also derived a similar conclusion while considering petrogenesis of sanukitoids of the Rainy Lake region.

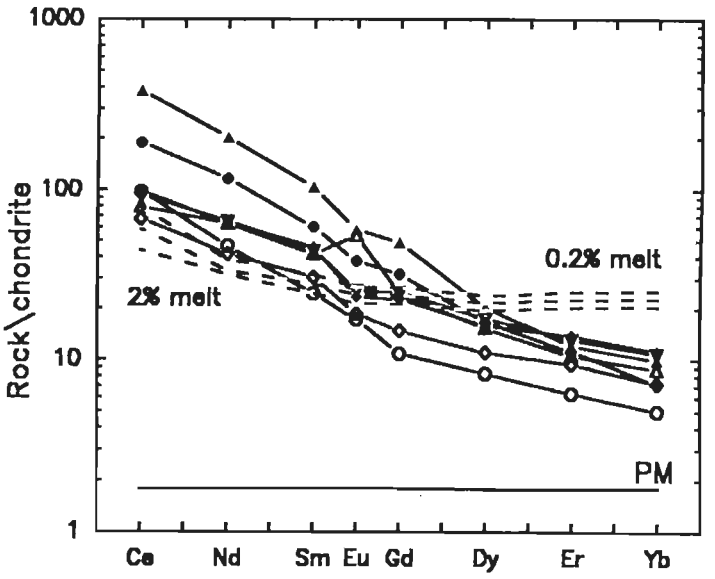

Fig. 6.6 Calculated chondrite normalized REE patterns for the partial melting (0.2, 1 and 2%) of a primitive mantle source (PM). The REE patterns of the melts (medium dashed lines) have lower abundances of LREE and higher HREE abundances than the sanukitoid samples.

6.1.4 SOURCE CHARACTERISTICS OF SANUKITOID ROCKS

In the preceding section, it was argued that the sanukitoid magmas could not have been generated by partial melting of tholeiite or fractional crystallization of basic magma with or without assimilation of upper crust. Although, partial melting of primitive mantle can yield intermediate magmas, however, it can not explain the enrichment in LREEs. This leaves the only possibility that the mantle sources for the sanukitoid magma might have been enriched in incompatible trace elements including LILEs and LREEs by some other processes. It has been suggested that the observed high abundances of LREEs and other incompatible trace elements in the sanukitoid magmas can be explained if it is derived by partial melting of enriched mantle source (Mueller et al., 1983; Shirey and Hanson, 1984; Tatsumi et al., 1986; Stern et al., 1989).

The enrichment of mantle source could be explained either selectively (in some of the incompatible trace elements) or there could be overall enrichment in all the trace elements. Mueller et al. (1983) suggested that selective enrichment of incompatible trace elements is more viable as compared to overall enrichment of all the trace elements in the mantle sources. To model generation of sanukitoid parental magmas by partial melting of the enriched mantle sources, it is assumed that the Ce is enriched 5 times and Yb 1.6 times relative to the primitive mantle. The REE abundances of primitive mantle are taken from Taylor and McLennan (1985). The enrichment factor for other REEs have been intrapolated for the calculation purposes. The enriched source on 1%, 2%, 5% and 20% partial melting produced whole range of LREE abundances comparable to that of sanukitoid suites and have higher HREE abundances than the sanukitoids (Fig. 6.7)

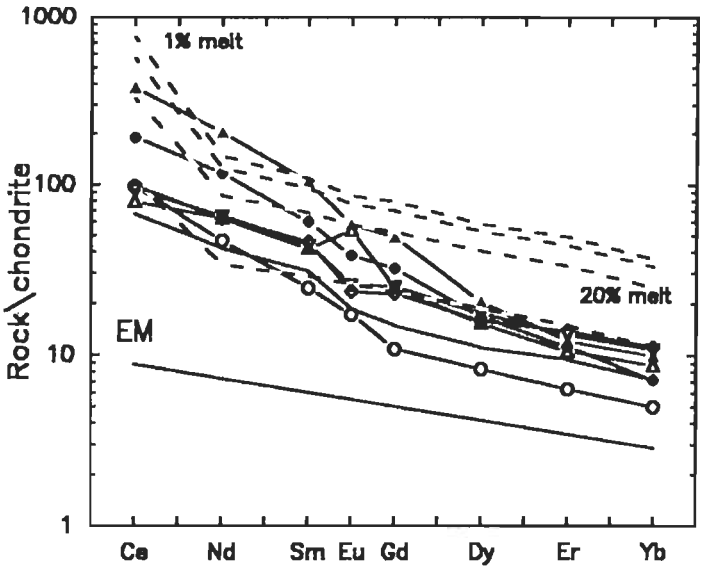

Fig. 6.7 Calculated chondrite normalized REE patterns for the partial melting (1, 2, 5 and 20%) of an enriched mantle (EM) source (Ce=5 times and Yb=1.6 times relative to primitive mantle). Note that the calculated melts have similar LREE but higher HREE abundances than that of the sanukitoids.

Thus, it is quite possible that the source might have undergone variable extents of enrichment with respect to LREE, HREE, and other incompatible and large ion lithophile elements. Tatsumi et al. (1986) explained selective enrichment of some of the incompatible trace elements in the source by taking examples from the Bonnin Island and Setouchi volcanic belt of Japan. They calculated enrichment factors for sources of High Magnesian Andesites (HMA) and Island Arc Basalts (IAB) as given below:

$$\text{ENRICHMENT FACTOR} = (C_X/C_{Zr})\ \text{Mantle Wedge}/(C_X/C_{Zr})\ \text{MORB source}$$

where C_X is the concentration of element under consideration for enrichment factor. Using this approach, the enrichment factors for sources of High Magnesian Andesites and Island Arc Basalts are calculated using the data given in Tatsumi et al. (1986) and presented in the Table 6.2.

In Table 6.2, the elements are arranged in the decreasing order of ionic radii. As the ionic radius decreases, the enrichment also decreases. It may be observed that Rb is enriched 125 times in case of HMA source and 26 times in IAB source from Setouchi volcanic belt with respect to MORB. Whereas, Y having the least ionic radius in the group is either depleted or slightly enriched in HMA and IAB sources relative to sources for MORB. Therefore, selective enrichment of the mantle sources for the sanukitoids and High Magnesian Andesites has been widely observed.

The enrichment for K, Ba are more in HMA compared to IAB. Ce is enriched ca.4 times in HMA as well as IAB. In general, the enrichment in incompatible and larger ionic radii elements are more in HMA source than IAB source.

Table 6.2 Enrichment factors in sources of High Magnesian Andesites and Island Arc Basalts relative to MORB source

Elements	Mantle sources for High Magnesian Andesite		Mantle sources for Island Arc basalts	
Area	Bonnin Isaind	Setouchi Volcanic Belt	Bonnin Isaind	Setouchi Volcanic Belt
Rb	71.6	125	21.6	26.1
K	23.6	18.3	11.5	6.9
Ba	17.3	20	12.72	13.63
Sr	3.75	2.5	6.8	1.25
Ce	___	3.98	___	3.86
Y	0.72	1.0	1.86	0.79

6.1.5 EXTENT OF ENRICHMENT REQUIRED IN SOURCES FOR MASUDA SANUKITOIDS

In order to estimate the extent of enrichment for the sources of the magma represented by Masuda sanukitoids inverse modelling have been carried out. One sample from each suite of sanukitoids (low- & High-Ti), that has highest mg#, is considered to have been derived by 5% partial melting of the enriched mantle source. The melt is assumed to have had equilibrated with 55% olivine, 25% orthopyroxene, 20% clinopyroxene. Sanukitoid samples J-53A and J-66 are assumed to represent parental magmas generated by 5% partial melting of enriched mantle sources. Using the batch melting equation, trace element abundances (Ba, Sr, Zr and REEs) in the mantle sources (C_0 values) are calculated (Table 6.3). These values are normalized to primitive mantle values (Taylor and McLennan, 1985) to arrive at the enrichment factors for the sources.

From Table 6.3, it is evident that the enrichment factors have a very wide range for REEs and particularly for Ba, Sr and Zr among the incompatible trace elements in the sources for the two suites of sanukitoids. The relatively high enrichment factors are observed for Ce, Nd, Sm compared to HREEs in both the cases. Whereas, there is depletion of Dy and Yb in the sources for sanukitoids. For example, the high Ti suite is enriched 20X in Ba, 14X in Ce, 9X in Nd and 5X in Sm as compared to low Ti suite of Ba=9X, Ce=3.3X, Nd=2.88X and Sm=3.14X relative to the primitive mantle. The enrichment factors calculated for the sources of the sanukitoids from Masuda area are broadly comparable to that of the sources for High Magnesian Andesites from Bonnin Island and Setouchi Volcanic Belt respectively, although the latter are normalized to MORB source (Tatsumi et al. 1986; Table 6.2). Similar selective and variable enrichment for LILEs and REEs in the mantle source for Archean sanukitoids of the Rainy Lake region have been reported by Shirey and Hanson (1984).

Table 6.3 Calculated incompatible trace element abundances and enrichment factors in the enriched source for sanukitoids

Elements	Ba	Sr	Zr	Ce	Nd	Sm	Eu	Gd	Dy	Yb
Abundances of trace elements in Source for J-53A (High-Ti suite) in ppm	100.87	62.25	35.85	19.41	9.37	1.67	0.381	1.10	0.64	0.199
Enrichment factror in r high Ti suite source	**19.78**	**3.5**	**4.32**	**13.52**	**8.78**	**4.81**	**2.91**	**2.4**	**1.12**	**0.54**
Abundances of trace elements in Source for J-66 (Low-Ti suite) in ppm	45.95	38.63	21.52	4.74	3.07	1.09	0.167	0.57	0.48	0.22
Enrichment factor in low Ti suite source	**9.01**	**2.17**	**2.59**	**3.3**	**2.88**	**3.14**	**1.27**	**1.24**	**0.84**	**0.59**
Primitive Mantle values	5.1	17.8	8.3	1.436	1.067	0.347	0.131	0.459	0.572	0.372

Therefore, the sources for sanukitoid magma might have been selectively enriched in LILEs and LREEs as indicated in the table and have a range of abundances for the above elements (Fig. 6.8). It can be concluded that the source for high-Ti suite requires greater enrichment in LILEs and LREEs than low-Ti suite.

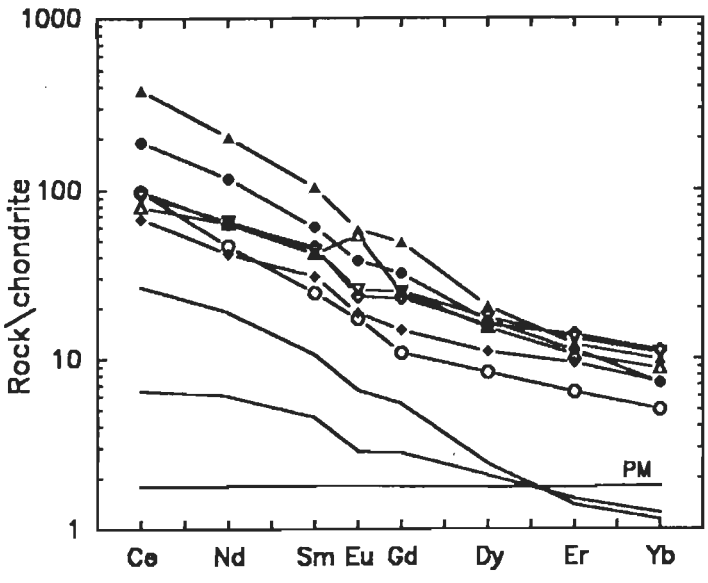

Fig. 6.8 Inverse modelling of the sources for high-Ti sanukitoid (J-53A) and low-Ti sanukitoid (J-66) assuming that their magmas were formed by 5% partial melting of shallow mantle sources leaving 55% olivine, 25% opx and 20% cpx in residue. Calculated abundances for sources of high- and low-Ti sanukitoids define a range indicated by shaded region. They have higher LREE and lower HREE abundances than the primitive mantle.

The enrichment might have taken place just prior to melting by addition of fluids or magma to already depleted sources. The fluids could have been generated from the lithosphere undergoing subduction and dehydration (Gastil, 1982; Kushiro, 1983; Tatsumi et al.,1986; Drumand and Defant, 1990). The fluids act as a carrier for Rb, K, Ba, Sr, La, Sm, Yb and Nb which enrich the depleted mantle wedge prior to melting. The migration of above elements at 12 kb pressure and 850^{0}C have been experimentally confirmed by Tatsumi et al. (1986).

6.1.6 [Mg]-[Fe] MODELLING

The low-Ti suite has mg #'s ranging from 0.52 to 0.61 which is similar to the range of Mg #'s observed for the tholeiitic amphibolites. Further, in the [Mg]-[Fe] diagram, samples of the low Ti suite fall within the field for the tholeiitic amphibolites (Fig. 6.9).

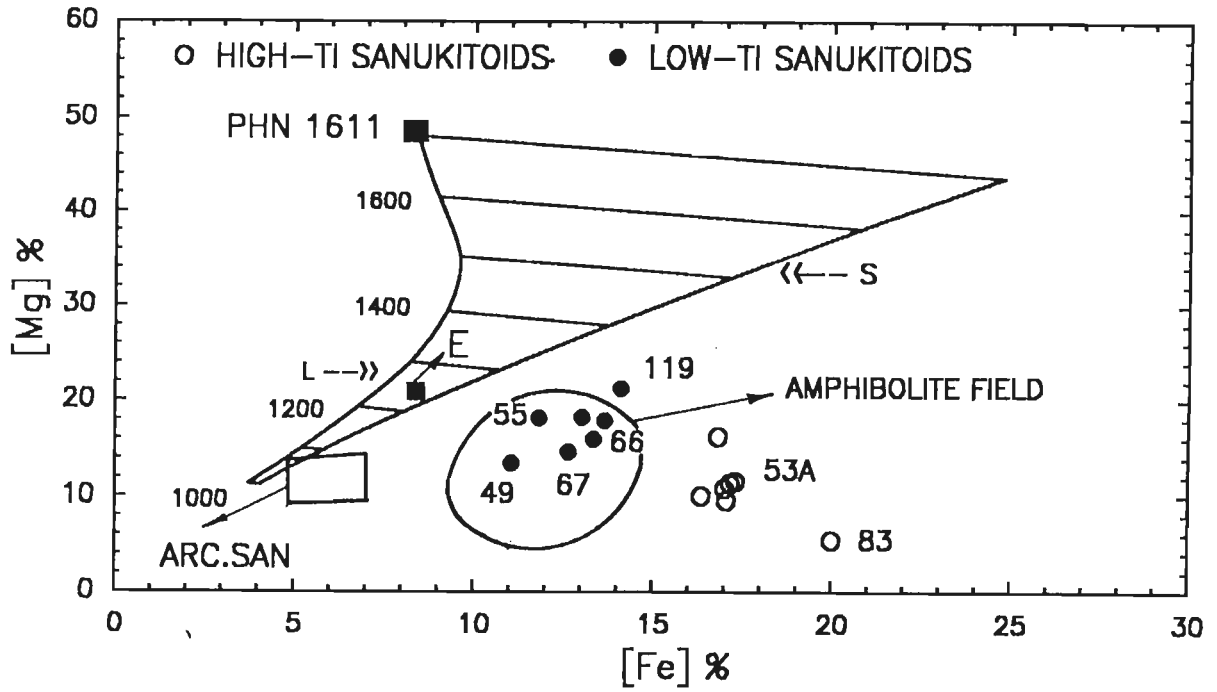

Fig. 6.9 **[Mg]-[Fe] systematics for sanukitoid suites. Details of these diagram are explained in Figure 5.4 of Chapter-V. Archaean sanukitoids (ARC.SAN) field is after Stern et al. (1989). Experimental melt composition (E) is also plotted (Table 6.1, column 9). The low- and high-Ti sanukitoids form two distinct groups. Most of the low-Ti plot within the field for amphibolites occurring in the Masuda area.**

The melt field at one atmospheric pressure for a range of temperature is constructed using peridotite as the source composition. If the sanukitoid melts were generated by partial melting of

mantle sources, then they must have been in equilibrium with olivine. The [Mg] and [Fe] are corrected composition of intermediate suite of rocks using Ford et al's (1983) equation and plotted in [Fe]-[Mg] diagram. The details of these diagram are explained in section 5.4.

The sanukitoids fall below and to the right of the solidus line. The low-Ti and high-Ti suite plot in two distinct groups (Fig. 6.9). The samples of low-Ti suite have variation in [Fe] contents by more than 3 mole %. Such a variation can not be explained by the fractionation from a single parental magma. And also fractionation of olivine and pyroxene will reduce the MgO contents without much change in FeO contents in the residual magma. If fractionation of plagioclase is considered to explain the variations in FeO abundances, then it is expected that Sr abundance decreases and negative Eu anomaly appears in residual magmas. For example, J-66 falls to right of J-55 and magma represented by J-55 could have undergone fractionation of plagioclase ± clino pyroxene to give rise to residual magma similar in composition to J-66. In this case it is expected that the residual melt (sample # J-66) should have lower Sr abundances and negative Eu anomaly. However, the sample has higher Sr contents without any Eu anomaly.

During adiabatic melting the [Fe] contents change while the [Mg] contents remain nearly constant in the melt generated by various extents of melting as the temperature remain nearly constant. Hence, the melt path will be sub-parallel to FeO axis (Fig.6.9), and will produce significant variation in FeO contents. Adiabatic melting over a pressure range from 10-15 kb could explain up to 2 mole % variation in FeO contents in the liquids (Rajamani et al., 1985).

For example, the sample # J-66 has higher [Fe] values than J-49 and therefore, its magma could represent relatively lower extents of partial melting. The sample # J-66 has high TiO_2 and Zr contents consistent with these observation. However, it also has higher Ni and lower Ba than the sample # J-49 which are not in conformity with the above suggestion.

Decoupling of some of the trace element abundances with the other trace and major elements could be as a result of source heterogeneity. If the sources were enriched variably in incompatible trace elements, such heterogeneity could be expected (Langmuir and Hanson, 1980; Stern et al., 1989).

By partial melting of peridotite in water saturated conditions, Green (1976) reported that melts of sanukitoid composition could be generated. The melt is plotted in Fig. 6.9 along with some of the Archaean Sanukitoids. The low-Ti suite has higher [Fe] and [Mg] values than the Archaean sanukitoids as well as the experimentally generated melt (Table 6.1). This indicates that the source for low-Ti suite must have had higher [Fe]/[Mg] ratio than the peridotite and undergone partial melting at higher temperature and pressure conditions (see Fig. 6.9).

The high-Ti suite falls further to right of the low-Ti suite and also has lower [Mg] values and mg# (0.29-0.463) and a very narrow range in [Fe] contents except sample no. J-83. The samples of low-Ti suite have high mg# which varies from 0.516-0.606.

Therefore, it may be possible that the high-Ti sanukitoids could be derived from low-Ti sanukitoids by fractional crystallization process. It is assumed that the high-Ti sanukitoid magma represented by sample J-53A (mg#=0.372) had been derived by olivine fractional crystallization from low-Ti sanukitoid parental magma similar in composition to sample J-66 (mg#=0.535). Mass balance calculations indicate that on 38% olivine (Fo_{80}) fractional crystallization from J-66 residual magma similar in mg# to that of J-53A can be generated.

Trace element abundances have been calculated in the residual melt on 38% fractional crystallization of olivine from a parent magma similar to J-66 in composition. These are listed along with the observed values for J-53A, a high-Ti sanukitoid sample, in Table 6.4. Except for Sr and Zr, all other trace elements are much higher in abundances in the high-Ti sanukitoids than the calculated values. Thus, the olivine fractional crystallization can not relate the low-Ti and high-Ti sanukitoid magmas. Similarly, fractional crystallization of pyroxenes or amphiboles with or without plagioclase from low-Ti sanukitoid magmas can not increase the LREEs and Ba abundances to the extent observed in high-Ti sanukitoid suite.

Table 6.4 Comparison of calculated and observed trace element abundances in the sample # J-53A

Elements	Ba	Sr	Zr	Ce	Nd	Sm	Yb
Calculated in ppm	1469	751	540	121	63	13.6	3.6
Observed in ppm	2438	751	558	309.6	121.2	19.8	2.05

It is likely that the two suites may be related by liquid immiscibility process. The investigations by Watson (1976) and Ryerson and Hess (1978) indicate that Fe, Mg, Ti, Ba and Sr go into the basic melt whereas, Si, Al and alkalis go into the felsic melt. Therefore, the decrease in MgO and increase in FeO and TiO_2 contents in the high-Ti suite relative to the low-Ti suite can not be explained by this process either.

This leaves the only possibility of deriving the high-Ti sanukitoid suite magmas by partial melting of sources with higher [Fe]/[Mg] and Ti/Mg ratio than that of the low-Ti suite. The source for high-Ti suite must have had higher enrichments in LREEs, Ba, Nb, Sr, Zr than that of low-Ti suite as already discussed in the "section 6.1.5". The high as well as low-Ti sanukitoids require variable enrichment of their mantle sources in Fe, Ti and other incompatible trace elements. The enrichment of mantle source in Fe and Ti can not be brought about by fluid metasomatism (Eggler 1987 and Menzies et al., 1987) but require metasomatism by melt addition.

As discussed earlier, the Fe and Ti abundances and [Fe]/[Mg] and Ti/Mg ratio in the mantle sources are much less than what is required to generate the sanukitoid magma. Abundances of Fe, Ti and other trace elements can be increased in the mantle if melts of tholeiitic or sanukitoid composition are introduced into the source region for the sanukitoids.

For example, a mantle source consisting of 80% primitive mantle and 20% tholeiite (Source-I) will have higher [Fe]/[Mg] and Ti/Mg ratio, as well as, incompatible trace element abundances as calculated and shown in the Table 6.5.

TABLE 6.5 Calculated elemental abundances and ratios during melt addition process

Ratios and Elements (in ppm)	Ti/Mg	Fe/Mg	Nb	Ba	Sr	Zr	Ce	Nd	Sm	Yb
Mantle	0.0045	0.294	0.56	5.1	17.8	8.3	1.436	1.067	0.35	0.37
Tholeiite (Avg. values)	0.231	2.465	8.4	304	178	84.5	16.45	11.2	3.49	2.56
Low Ti Magma (Avg. values)	0.186	2.31	11.5	748	493	233	72.2	32.37	6.94	1.77
High Ti Magma (Avg. values)	0.78	4.26	81.5	1798	565.4	362.5	176	76.07	13.11	1.786
80%M+20% Th (Source-I)	0.0498	0.7282	2.13	64.88	49.84	23.54	4.44	3.09	0.98	0.81
Calculated Source for Low Ti J-66			0.53	45.95	38.63	21.52	4.74	3.07	1.09	0.22
80%M+20% Low Ti (Source-II)	0.0408	0.6972	2.748	153.7	112.84	53.24	15.59	7.33	1.67	0.65
Calculated Source for High Ti J-53A			4.89	100.87	62.25	35.85	19.41	9.37	1.67	0.19

* Nb value calculated using the Nb value of J-67 which is similar in composition with sample J-66

Assuming that typical parent magmas for sanukitoids (low- and high-Ti suites) represent 5% partial melts the abundances of trace elements in their mantle sources have been modelled using appropriate 'D' values and batch melting equation. The sample J-53A represents the most primitive magma of the high-Ti sanukitoid suite, sample J-66 represents the most primitive magma of the low-Ti series. The calculated values for their respective mantle sources are also given in the Table 6.5.

The trace element abundances calculated for low-Ti sanukitoid sources are comparable with that of Source-I model. Whereas, calculated trace element abundances for the high-Ti sanukitoid source is much higher than the Source-I.

From [Mg] - [Fe] modelling, it was inferred that the magmas represented by low-Ti sanukitoids must have been derived from higher P & T conditions than the high-Ti sanukitoids. Therefore, it is possible that the low-Ti sanukitoid magmas might have been added to primitive mantle and thus enriching in incompatible trace elements.

Hence, a source model consisting of 80% primitive mantle + 20% low-Ti (Source-II) sanukitoids have been assumed. When it is compared with the calculated abundances of trace elements in sources for high-Ti sanukitoids, it had slightly higher Ba, Sr, Zr, Yb abundances (Table 6.5). The high-Ti sanukitoid source values for the trace elements Ba, Sr and Zr lie in between

Source-I and Source-II models. Therefore, it is possible that their sources might have been enriched in the trace elements by addition of sanukitoid and to a minor extent of tholeiitec melt.

Further, it may be noted that HREE (Yb) values calculated for the mantle sources of sanukitoids are lower than the enriched mantle sources (source-I and source-II). This may be because, the mantle sources might have been depleted in HREE prior to metasomatism. If sufficient garnet was present in the residue it will also cause HREE depletion in the melt. It may not be possible to resolve between these two possibilities, with the existing data.

6.2 GRANODIORITE PETROGENESIS

Tonalite, trondhjemite, granodiorite and their deformed counterparts are reported to have occupied a significant volume of the Archaen Crust (Glikson, 1979 and Barker, 1981). In Masuda area, the granodiorite gneiss occurs in significant volume and is spatially associated with sanukitiods and amphibolites.Therefore, it is important to understand their petrogenesis.

6.2.1 GEOCHEMICAL CHARACTERISTICS OF GRANODIORITE SUITE

The granodiotites have ca.70 wt% SiO_2, ca. 14 wt% Al_2O_3, ca.3.5 wt.% total Fe as FeO and MgO content range from 0.3 to 1.75 wt%. Among the trace elements, Ba and Sr contents have a very wide range in abundances (92-1271 ppm) and (29-497 ppm) respectively. The average Ni content is ~ 40 ppm and Cr > 200 ppm. The chondrite normalized REE patterns have a fractionated trend {i.e. $(Ce/Yb)_n$ = 10-32}. Two of the samples (J-74 & J-77) show prominent negative Eu anomalies and have higher abundances of REEs relative to rest of the samples.

Major and Trace Elements Constraints

In plots of SiO_2 vs Ba, P_2O_5 and Sr (Fig. 6.10a, b, c) the garanodiorite suite of rocks define a chemical continuum with sanukitoid rocks. It indicates that K- feldspar, plagioclase feldspar and apatite could have played a role in evolution of magmas represented by the granodiorites from their parental magmas. Similarly, the chemical continuum of granodiorite suite with the intermediate sanukitoid rocks in the plots of MgO vs TiO_2, Ba vs Sr and FeO vs TiO_2 (Fig. 6.10d, e, f) indicates that petrogenetic processes similar to that of the sanukitoids might have played a role in the origin of granodiorite suites.

It is considered that partial melting of peridotite mantle source can not generate granodiorite magmas (Green,1973, 1976). Further, experimental investigations by Helz (1976); Rapp and Watson (1988) indicate that granodiorite magmas could be generated by partial melting of mantle derived basaltic rocks and/or its differentiates. Therefore, the generation of granodioritic magmas by a two

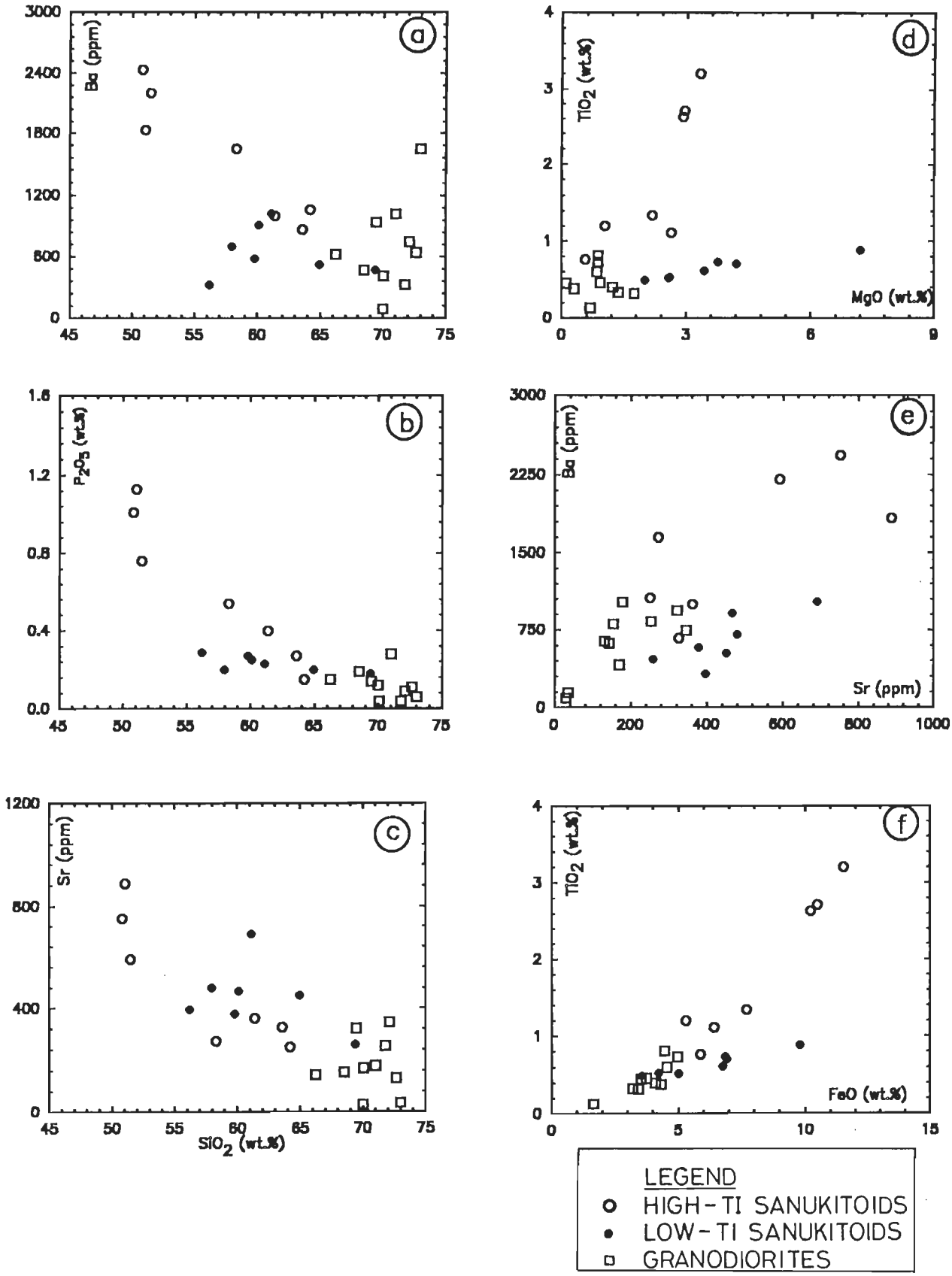

Fig. 6.10 (a-c) Harker's variation diagram for different major element oxides and some trace elements. (d-f) MgO-TiO_2, Ba-Sr and FeO_T relationship for the granodiorites and sanukitoids. The square represents granodiorites whereas, the filled and open circles represent low- and high-Ti sanukitoids respectively. Note that the granodiorites define a chemical continuum with the sanukitoids.

stage partial melting process involving mantle and mantle derived basaltic rocks is the most favoured model.

In the study area, the granodiorite suite of rocks are closely associated with intermediate sanukitoid suite and the granodiorites fall in a chemical continuum with the sanukitoid suite also. The following questions may resolve the petrogenetic modelling of the granodiorite suite:

i) whether different extents of either partial melting of a common source or fractional crystallization from a common parent can explain the variation in chemistry from sanukitoids to granodiorites?

ii) alternatively, whether granodiorite suite is derived from distinct source (s) and is not related to the sanukitoid suite?

In the field, granodioritic rocks are interbanded with amphibolites and sanukitoids. There is a possibility that the granodiorite magmas could have been generated by partial melting of tholeiitic amphibolites. Trace element abundances have been calculated assuming a tholeiitic amphibolite source which had undergone 5 to 20% partial melting leaving 60% hornblende and 40% plagioclase in the residue. The calculated REE abundances are plotted in Fig. 6.11a along with the chondrite normalized abundances of the samples. The chondrite normalised REE abundances of the amphibolite parent is also plotted in the Figure 6.11a represented by sample # J-68. It is evident from the plot that the LREE abundances of the melt are less than the samples and HREE abundances of the partial melts show a slight concave upward HREE pattern compared to the fractionated trend of the samples.

Similarly, the possibility of a tholeiitic amphibolite under eclogite facies condition as the parental source is being investigated. The residual mineralogy is represented by 45% clinopyroxene, 20% orthopyroxene and 35% garnet. The partial melting (1-20%) of the source gave rise to a LREE enriched REE patterns with a positive Eu anomaly (Fig. 6.11b). It may be noted that the chondrite normalized LREE abundances of the 10% partial melt is comparable with some of the samples. However, the HREE abundances show a concave upward chondrite normalized REE pattern and much lower in abundances than what is observed in the samples. If 10% partial melting of a tholeiitic amphibolite (sample J-68) is considered leaving an amphibolite residue, the melt would have Ba content of 1673 ppm and 205 ppm Sr. Whereas, the granodiorite samples have 92-1271 ppm Ba and 29-497 ppm Sr. Alternatively, if 10% partial melting of the tholeiite leaving an eclogite residue is considered, then the melts would have 3016 ppm Ba and 1290 ppm Sr which are about 4 times higher than what is observed in the granodioritic samples.

Therefore, partial melting of basaltic rocks leaving amphibolite or eclogite residues can not give rise to magmas having Sr, Ba and REEs abundances similar to that of the granodioritic rocks.

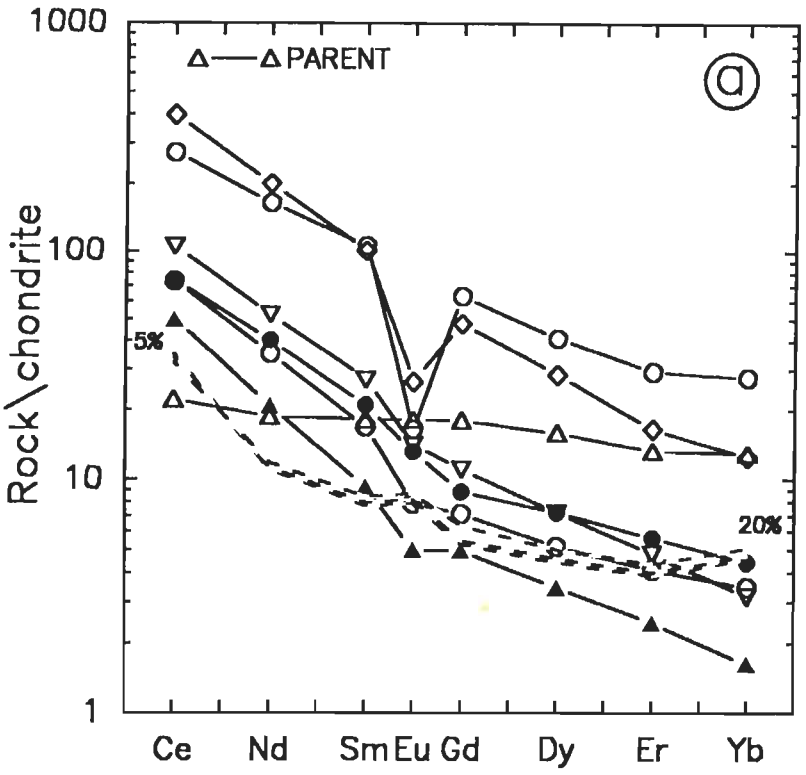

Fig. 6.11a Calculated chondrite normalized REE patterns for the partial melting (5, 10 & 20%) of an amphibolite source leaving 60% hornblende and 40% plagioclase in the residue. The calculated abundances (medium dashed lines) are lower in REE abundances than the samples and have concave upward chondrite normalized REE patterns with positive Eu anomalies.

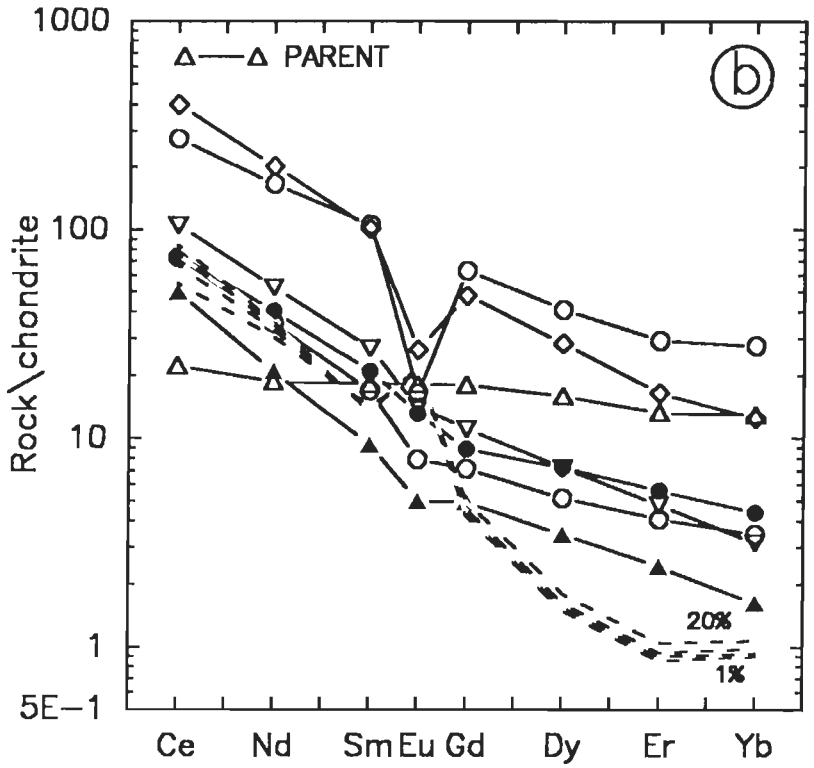

Fig. 6.11b Calculated chondrite normalized REE patterns for 1, 5, 10, and 20% partial melting of a tholeiite source leaving an eclogite residue. Only the LREE abundances of the 10% melt is comparable to the samples of granodiorite suite-II.

In granodioritic suite, two of the samples (J-74 & J-77) have higher LREEs, HREEs and prominent negative Eu anomalies from the rest of the samples. Therefore, it is likely that the two suites may have distinct sources or the petrogenetic history. Out of these two samples, J-74 has higher LREE and lower HREE abundances. It may be possible that the low-Ti sanukitoid (J-66) might have been the source to generate the magma similar to J-74 in REE abundances. The residual mineralogy of J-66 is represented by 50% plagioclase, 30% clino-pyroxene and 20% K-feldspar. The k_d values for clinopyroxene are used from the basalt melt system (Hanson, 1980) and plagioclase, K-feldspar k_d values are taken from Henderson (1982) for andesitic melt system. At 10% partial melting of J-66 source, the chondrite normalized REE abundances calculated for melts are comparable to granodiorite samples J-74 (Fig. 6.11c). However, Ce and HREE abundances in calculated melts are slightly higher than that of sample J-74. Similarly, at 10% partial melting the calculated Ba and Sr abundances will be 712 ppm as compared to observed 622 ppm of Ba and 312 ppm of Sr as compared to observed abundances of 143 ppm. It is likely that the source for J-74 might have had higher Ce, HREE and lower Sr as compared to sample J-66.

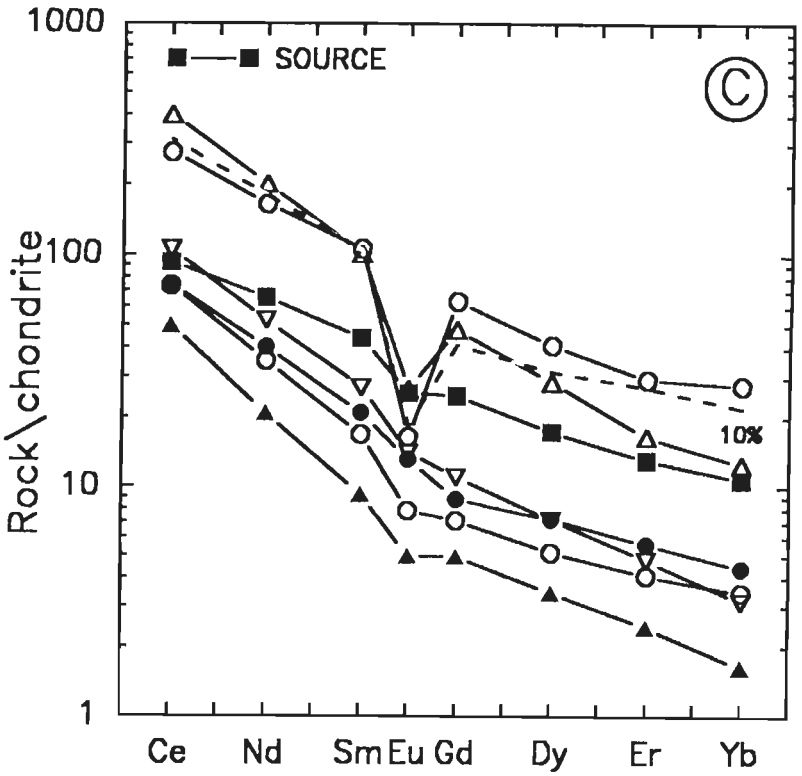

Fig. 6.11c Calculated chondrite normalized REE patterns for the 10% melt of a sanukitoid source. Note that REE patterns of the 10% melt is generally comparable with the REE abundances of sample# J-74.

Sample J-77 might have been derived from J-74 by fractionation of plagioclase and K-feldspar. This will result in higher REE abundances in the residual magma relative to the parent magma, as observed for HREEs in sample # J-77. However, the lower LREE abundances may be explained by fractionation of minor or trace phase such as allanite which is ubiquitous in sample # J-74. Fractional crystallization of plagioclase and K-feldspar would also deplete Sr and Ba abundances in residual magma as observed in sample # J-77.

The rest of the granodiorite samples having sub-parallel chondrite normalized REE patterns and no Eu anomaly may be related to low-Ti sanukite J-66 by fractionation processes. A two stage fractionation may explain the abundances of REEs, Ba and Sr found in these granodiorite samples.

The stage-I fractional crystallization involves 58% plagioclase, 20% hornblende, 20% biotite and 1% each of K-feldspar and sphene. After 40% fractional crystallization, the residual liquids had a sub-parallel REE pattern which had higher LREE and HREE abundances than the granodiorite samples (Fig. 6.12a). Therefore, a second stage fractionation from the 60% residual liquid involving the crystallizing phases 25% hornblende, 43.9% plagioclase, 20.9% K-feldspar, 10% biotite and 0.1% each of sphene and apatite has been considered. At 10%, 30%, 40%, and 50% fractional crystallization the chondrite normalised REE patterns of the residual liquid could not match with observed REE patterns of all the samples (Fig. 6.12b). However, some samples having relatively high REE abundances have comparable REE patterns to that of the calculated residual magmas formed from the second stage of fractional crystallization.

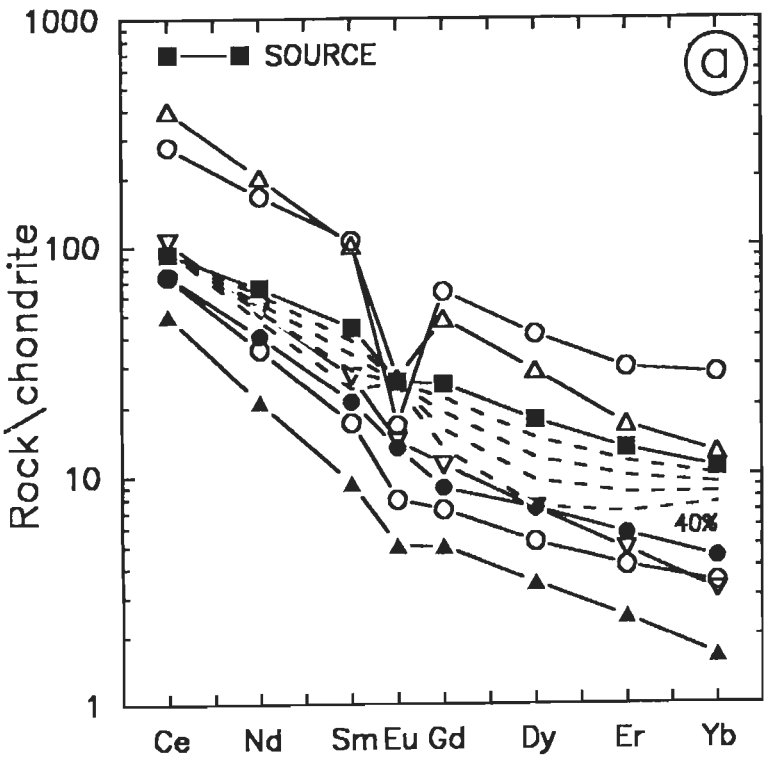

Fig. 6.12a Calculated chondrite normalized REE patterns (medium dashed lines) for residual melts on 10, 20, and 40% fractional crystallization of plagioclase, hornblende, biotite, K-feldspar and sphene from a source similar to low-Ti sanukitoids in stage I. Even on 40% fractional crystallization, the residual melt has higher REE abundances than the samples of granodiorite suite II. The solid square symbol represents the REE patterns of the parent.

6.2.2 LIQUID IMMISCIBILITY MODEL

The importance of liquid immiscibility as one of the fractionation process has been well illustrated by the studies of terrestrial as well as lunar rocks (Roeder & Wieblen, 1972; Wieblen & Roedder, 1973). Further, the experimental work carried out by Greig (1927), Bowen (1928) and Roedder (1956) have shown the immiscibility gap in silicate melts. The silicate melt have two end members : iron rich basic liquid and a silica rich quartzo-feldspathic liquid. The Fe-rich liquids are

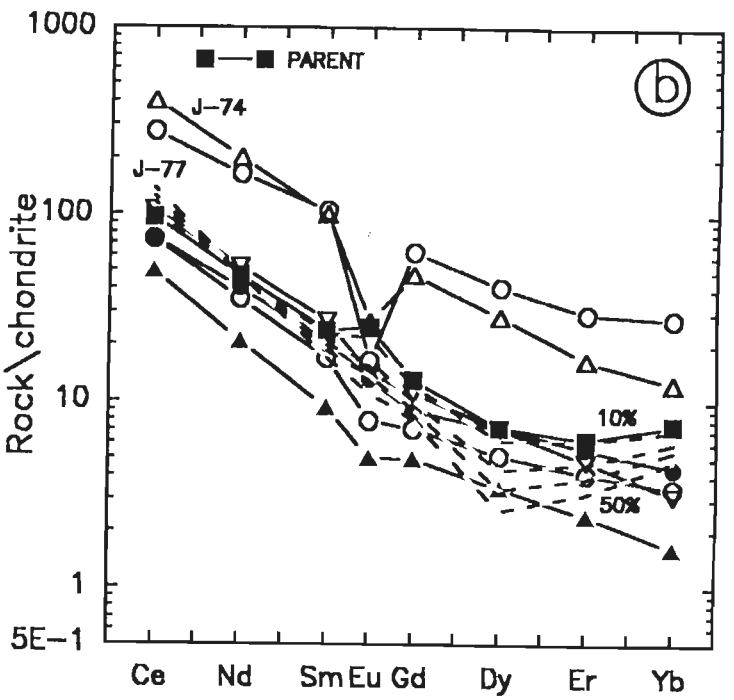

Fig. 6.12b Calculated chondrite normalized patterns (medium dashed lines) for residual melts on 10, 20, 40 & 50% fractional crystallization (stage 2) of different mineral phases (see text) from the residual liquid formed on 40% of fractional crystallization in stage I. The calculated REE patterns in the residual melts of stage II fractional crystallization are somewhat comparable to a few samples of granodiorite suite II.

enriched in CaO, MgO, FeO, TiO_2, and P_2O_5 (McBirney, 1975; Ryerson & Hess, 1978). From the two liquid partition experiments carried out by Watson (1976), Ryerson & Hess (1978) and Danekwerth and Ryerson (1980) indicate that iron rich liquid end member have more abundances of REEs, P, Zr compared to the co-existing quartzo-felspathic liquid. Thus, it may be worth considering the liquid immiscibility as a potential fractionation process for the evolution of some of the granodiorite magmas from sanukitoid magmas. The sanukitoids and granodiorites are plotted in a Greig pseudo-ternary phase diagram (Fig. 6.13). From this figure it can be observed that the sanukitoids define the basic end member while the granodiorites define felsic end member. The samples however, plot in a field which is parallel to the two liquid field.

There is a possibility that, if the crystallizing mineral phases are common to the co-existing liquid, then some similarity in chemistry of the mineral phases are expected (Bowen, 1928). For example, the amphiboles have Fe/(Fe+Mg) range of 0.52 to 0.556 in sanukitoids as compared to 0.47 to 0.62 in granodiorites. Fe/(Fe+Mg) ratio of biotites have a very remarkable similarity between sanukitoids (0.45-0.47) to that of granodiorites (0.44-0.47; Appendix III).

Immiscibility can also account the difference in trace elements and REEs. The basic liquids represented by sanukitoids in the study area have higher Ba, Sr and Zr compared to granodiorites. The REE abundances of granodiorites are less than the sanukitoids. The distribution of REEs between the two liquids will depend upon the two liquid partition coefficients. If the two liquids are related by liquid immiscibility to a common parent, it is expected that the chondrite normalized REE patterns of the immiscible liquids will be parallel or sub-parallel to each other with

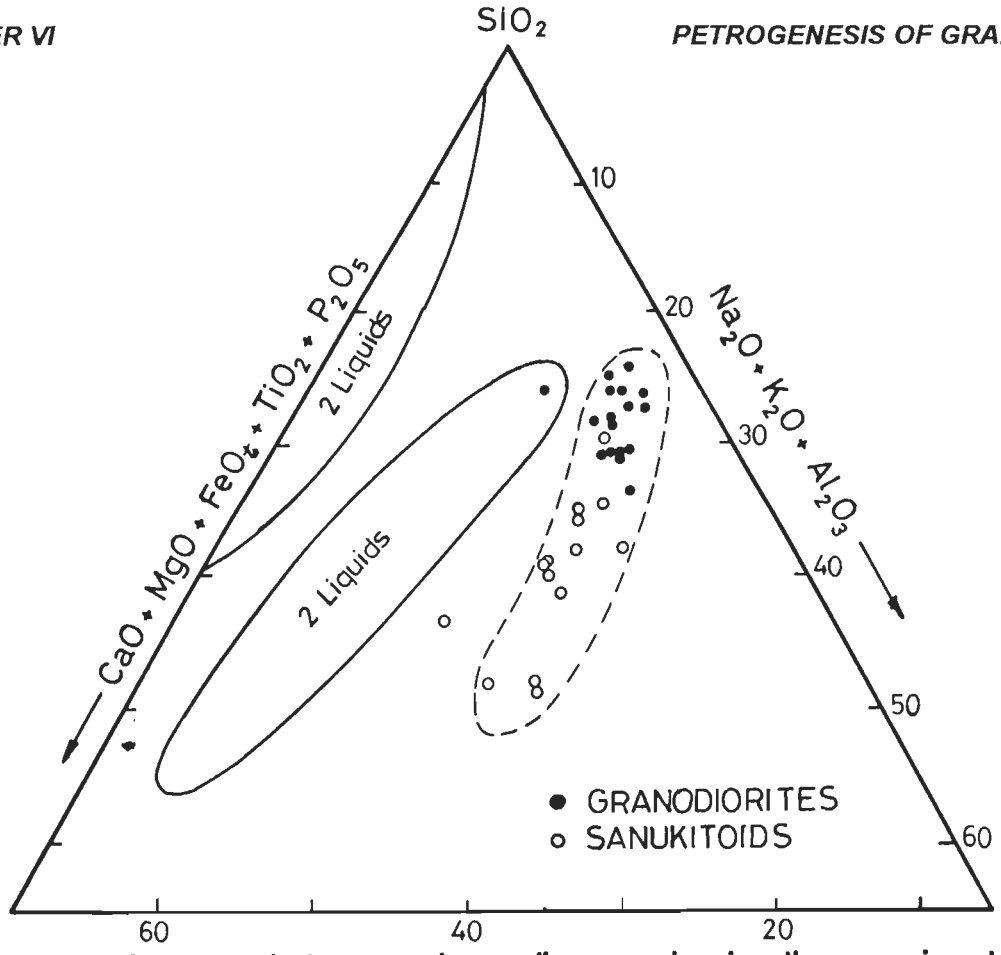

Fig. 6.13 **Greig's pseudo-ternary phase diagram showing the experimentally determined two liquid fields. The sanukitoids and granodiorite samples plot towards right of the two liquid field. The granodiorites are more evolved than the sanukitoids.**

more felsic magmas having low REE abundances {i.e. D=5 for all trivalent REEs and 3.5 for Eu, Hanson (1981)}. Some of the granodiorite samples and sanukitoids of Masuda area form parallel or sub-parallel chondrite normalised REE patterns (Fig. 6.14).

The liquid immiscibility process can be further strengthened if field as well as petrographic evidences can be coupled with chemical data. However, absence of ocelli in the thin sections of sanukitoids or granodiorite rocks might be due to separation of conjugate liquids in a larger scale and time frame (cf. Bender et. al., 1982).

In summary, there are two types of granodiorite suites based on REE abundances. One suite have higher abundances of LREEs, HREEs and negative Eu anomalies while, the other group have lower LREEs, HREEs abundances than the former and have no Eu anomaly. Sample J-74 might have been derived by partial melting of a sanukitoid source which had higher REE abundances than the sample J-66. Sample # J-77 might have been derived from magmas similar to sample # J-74 by fractionation of equal amounts of plagioclase and K-felspar and trace amount of allanite. The rest of the samples of granodiorite, which have parallel to sub-parallel chondrite normalized REE patterns to that of sanukitoids could have been derived by fractionation processes, including fractional crystallization and liquid immiscibility from intermediate sanukitoid parent magmas.

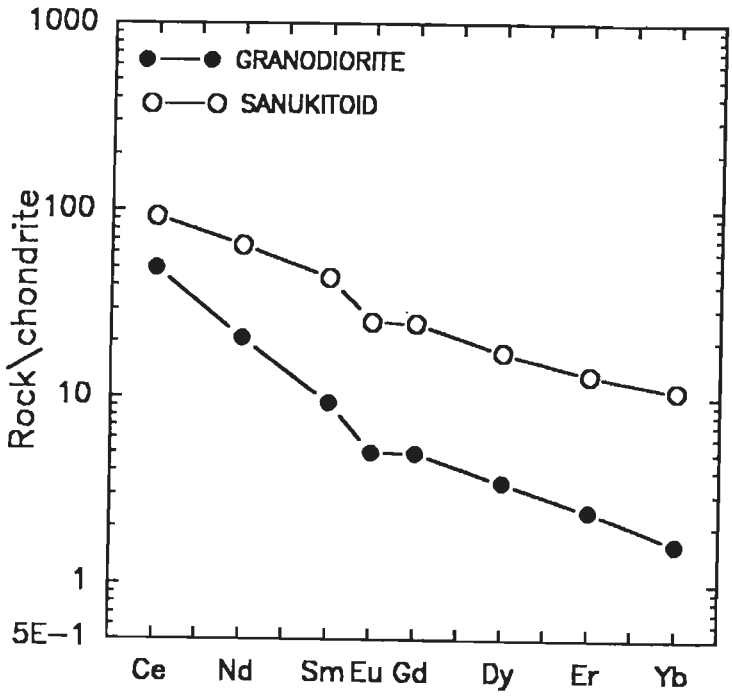

Fig. 6.14 **The chondrite normalized REE patterns for the suite II granodiorites with sanukitoids. Note that the REE patterns are subparallel to each other.**

6.3 PETROGENESIS OF GRANOPHYRES AND APLITE

In the study area, the high silica rocks such as, granophyres and aplites, occur as concordant bands and dicordant veins respectively. Their spatial distribution is insignificant when compared with granodiorite gneisses and intermediate suite of rocks. Subsolidous textures are widely observed and hence, the terminology granophyre is used to describe such rocks (Nabelek, 1986). Therefore, the petrogenetic study of granophyres and aplite may provide an insight into late stage magmatic and crustal processes.

6.3.1 GEOCHEMICAL CHARACTERISTICS

The aplite and granophyres show meta-aluminous character. The aplite (J-65) has SiO_2 content of ~73 wt.% whereas, the granophyres have more than 77 wt.%. The former has more TiO_2, FeO_t contents as compared to granophyres. The granophyre sample, J-113, has highest Ba (1830 ppm) and Sr (355 ppm) among the granophyres. The highly sheared granophyre sample # J-69 has lowest REE abundances whereas, the aplite has highest REE concentrations. The granophyres have parallel sloping chondrite normalized REE patterns. These rocks invariably show positive Eu anomalies and the extent of positive Eu anomaly (Eu/Eu^*) is highest for the sheared granophyre whereas, the aplite shows comparatively the lowest extent of positive Eu anomaly. This indicates that variably f_{O2} conditions may have prevailed during evolution of magmatic/metamorphic fluids from which rocks crystallized (Nabelek, 1986).

The granophyres and aplite samples are plotted in quartz-orthoclase-albite ternary plot along with water saturated minimum melt compositons (Luth et al., 1964) for a range of pressures from 0.5 to 10 kb (Fig. 6.15). All the granophyre samples plot well above the minimum melt

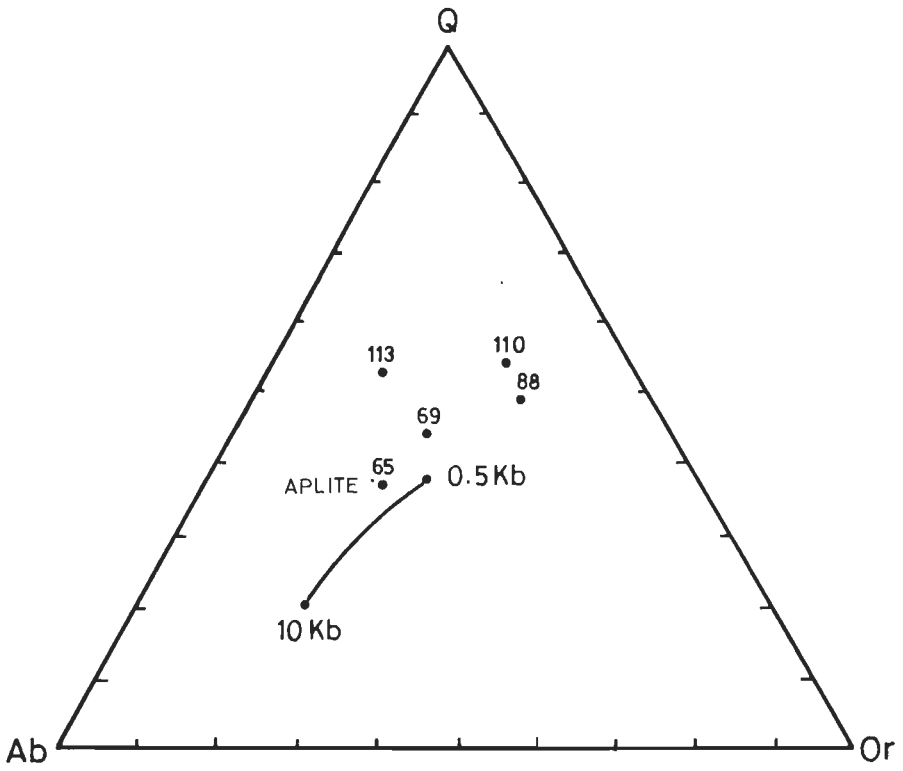

Fig. 6.15 **Quartz - Albite - Orthoclase ternary plot for 0.5 to 10 kb water pressure (after Luth et al. 1964). Note that none of the samples plot along the minimum melt composition curve.**

compositon at 0.5 kb water pressure whereas, aplite sample plot to left of the minimum melt. Similarly, in the Harker's diagram SiO_2 vs Na_2O and K_2O plot (Fig. 6.16 a&b), the granophyre samples form a group and plot below the melting range for 0.5 kb to 10 kb water pressure except the sample# J-88 which plots above the said melting range. However, the aplite in all these plots have separate identity therefore, an alternate hypothesis may be required to explain its origin.

The chondrite normalized REE patterns of granophyres (Fig. 6.17) in the Notch Peak granite stock, Utah is similar to the observed chondrite normalized patterns for granophyre samples of the study area. On the basis of trace element modelling, Nabelek (1986) suggested that the granophyres fromed by 2-13% fractional crystallization from an aqueous fluid that exsolved from granitoid magma during its emplacement. Further, he stated that the enrichment of Ba, Sr is due to large alkali feldspar/fluid partition coefficients and the depletion of certain LIL elements is due to their small solubility in aqueous fluids.

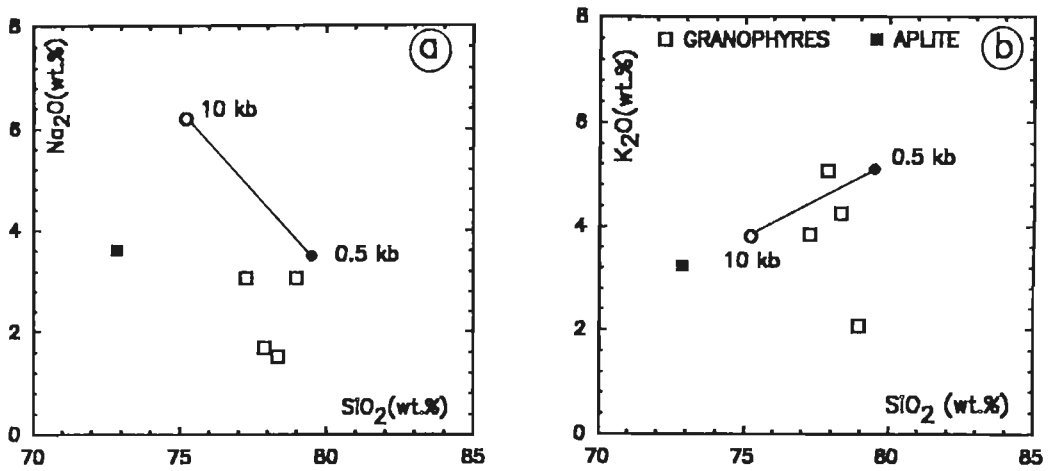

Fig. 6.16 (a & b) Harker's variation diagram for granophyres and aplite. The solid and open circles in the diagram represents the composition of minimum melt compositions at 0.5 and 10 kb water pressure respectively (Luth et al. 1964).

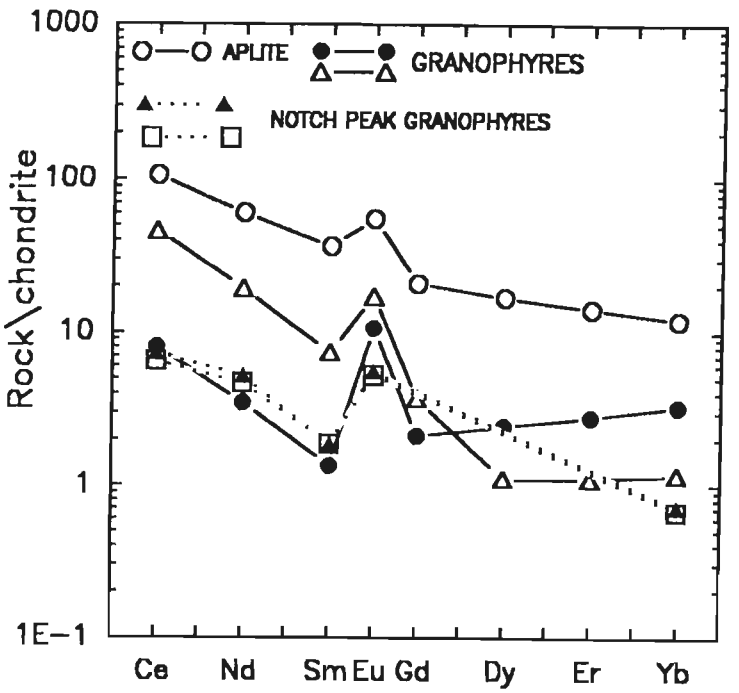

Fig. 6.17 The chondrite normalized REE patterns of granophyres and aplite of Masuda area compared with granophyres of Notch peak (Nabelek, 1986). The granophyres samples of these two areas have similar REE patterns.

There are three possible scenarios from which granophyres can be derived. They might have crystallized from (a) anhydrous melt, (b) fluids or (c) in the presence of fluids (Carron and Legache, 1980; Nabelek, 1986). As none of the samples represent the minimum melt compositions (Fig. 6.15); therefore, crystallization from melt is an unlikely process. The two granophyre samples have variable LREE, HREE and positive Eu anomalies and the granophyre sample # J-69 has lowest REE abundances and crosses the HREE pattern of sample # J-113. This indicates variable temperatures or H_2O activities resulting in different f_{O2} condition in the fluids. Granophyres crystallized from such fluids will have highly variable trace element and REE abundances and Eu anamolies, as observed in sample # J-69 and J-113. High abundances of Ba in the granophyres samples may be due to large alkali feldspar/fluid partition coefficients for Ba (Nabelek, 1986).

The aplite is post-tectonic and has lower SiO_2, highest FeO_T, TiO_2 and REE abundances in this group. It also plots close to the trace of minimum melt composition in quartz-albite-orthoclase ternary plot (Fig. 6.15). It is possible that the aplite represents hydrous melt generated during high grade metamorphism. If it represents a low percent melt derived by melting of continental crust (dominated by sanukitoids and granodiorites) leaving a feldspar dominated residue then a prominent negative Eu anomaly will be expected in it.

However, the aplite has the highest LREE and HREE abundances among the group and has positive Eu anomaly. This is possibly due to dominance of CO_2 in fluids from which the aplite might have crystallized. Because, CO_2 rich metamorphic fluid will have similar REE characteristics (cf. Hanson, 1981) as described for the aplite.

In summary, it can be inferred that the granophyres and aplite could have been derived from the crystallization of residual hydrous melts and metamorphic fluids/melts respectively, under variable f_{O2} conditions.

6.4 GEOCHEMICAL CHARACTERISTICS OF GRANOLITES

The high grade (granulite?) terrain is represented by granolitic rocks that occur to the east and south of amphibolite grade rocks of the study area. These rocks have distinct field and textural characteristics. A number of enclaves are also found within the high grade terrane which have variable size, shape and mineralogical compositions. In the present study preliminary geochemical information on these rocks have been generated.

The granolitic rocks are classified into two different suites on basis of SiO_2 contents. The first suite defines a silica range from 59-63 wt.% which is comparable to the sanukitoids. Whereas, the second suite has higher SiO_2 contents (68-71 wt.%) and are comparable to the granodiorite

gneisses. The first suite has higher TiO_2, FeO_T, MgO, Nb, Y and lower Na_2O, Sr, Ni, Zr and comparable Ba contents to that of low-Ti sanukitoids. The second suite has higher TiO_2, FeO_T, MgO, Ba, Ni, Y and lower Na_2O, Al_2O_3 abundances compared to the average abundances of these elements in the granodiorites. Remarkably, lower Zr abundances in granolites than the amphibolite facies rocks of the Masuda area is observed (Fig. 6.18).

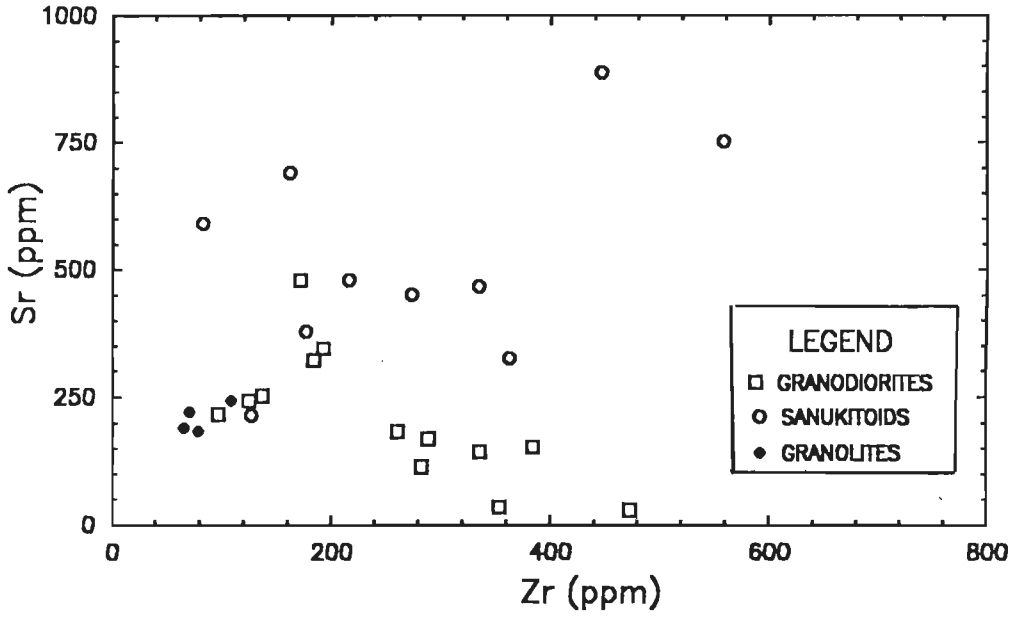

Fig. 6.18 **Zr-Sr relation for the granolites, sanukitoids and granodiorites. Note that the granodiorite samples have lower Zr contents compared to others.**

Enclaves occur abundantly within high grade granolitic rocks. One such enclave (J-81) occurring within host (J-82) is analyzed. The major and trace element abundances of these two samples are identical within analytical uncertainty. The REE abundances of these two samples are distinct but they have sub-parallel LREE enriched sloping chondrite normalized REE patterns with negative Eu anomalies (Fig. 4.7, Chapter IV). The enclave has slightly higher REE abundances than the host. A more detailed geochemical study of these rocks is required in order to understand their petrogenesis, as well as, their relationship with amphibolite grade rocks of the study area.

CHAPTER VII

DISCUSSION

The study area falls in the northern BGC terrane of the Aravalli Craton which consists of amphibolites, low and high-Ti sanukitoids, granodiorite suite and minor volumes of granophyres and aplites. Each of these rock types have distinct geochemical characteristics and petrogenetic histories. Other predominant rock types are calc-gneiss and highly mylonitized biotite-garnet migmatized gneiss. The rocks of the BGC in the study area have been metamorphosed up to upper amphibolite facies and subjected to at least four phases of folding and two episodes of shearing (Srivastava et al., 1995). The different litho-units are inter banded and co-folded and the contact relation appears to be tectonic. The amphibolite-facies terrane (study area) is surrounded by high grade granolitic terrane to the south as well as east and to the west by the Delhi Supergroup of rocks (Fig. 3.1).

7.1 AMPHIBOLITES

Geochemically, the amphibolites are Fe-rich tholeiites with a few samples having high-Mg characteristics. Magmas represented by the high-Mg amphibolites could have been derived by partial melting of garnet-lherzolite source as indicated by [Mg]-[Fe] modelling (Balakrishnan et al., 1995; Sahoo et al., 1995). Whereas, the magmas represented by tholeiitic amphibolites could not have been derived by partial melting of garnet-lherzolite source. Neither it is possible to derive the tholeiitic magmas by fractionation of olivine nor clinopyroxene from a parental magma similar to the high-Mg amphibolites. Further, the assimilation of granitoids coupled with fractionation is ruled out as a viable model for the generation of Fe-rich tholeiitic amphibolites. Therefore, the source for the tholeiitic amphibolites might have had higher [Fe]/[Mg] ratio compared to garnet-lherzolite.

The lower abundances of Ni in the tholeiitic amphibolites of Masuda may be attributed to several possibilities. For example, Hart and Davies (1978) suggested that the partial melting of mantle source under water saturated condition can generate melts with lower Ni abundances. Presence of minerals in which Ni is compatible, such as, olivine in the residual mantle can buffer

continuously the Ni abundances in the melt and hence the melt would have lower concentrations of Ni (Bougault et al., 1980). Kelemen et al. (1990) suggested that when mantle derived primitive magma passes through a large column of residual mantle, depletion of compatible element (Ni) in the melt could result, as a result of melt-rock interaction. Alternatively, partial melting of the primitive mantle with 2000 ppm Ni could not have given rise to magmas represented by the tholeiitic amphibolites. The low abundances of Ni observed in tholeiitic amphibolites could be generated from a mantle source, if it had Ni abundances in the range of 600-900 ppm.

The higher abundances of K_2O observed in some of the amphibolites of Masuda is not due to crustal contamination. Thin section study reveals the presence of biotite at places, wherever, the amphibolites are inter-banded with granitoids, the presence of biotite is observed. Therefore, higher abundances of K_2O may be due to small scale diffusion of K, perhaps, during deformation and metamorphism.

From the quantitative modelling of REE data, it is inferred that the primitive mantle having residue similar to the spinel-lherzolite could generate the magmas represented by tholeiitic amphibolites upon 5 to 20% partial melting.

It may be worth mentioning that the source for the tholeiitic amphibolites might have had similar rare earth element abundances to that of primitive mantle. Whereas, higher [Fe]/[Mg] ratio and lower Ni abundances than the primitive mantle have been inferred for their sources.

Using the REE data, it was found that the tholeiites of Masuda area define a field intermediate to N-and P- type MORBs and can be classified as transitional MORB. Further, the REEs and other trace elements (Nb, Zr) are very much akin to marginal basin basalts. It may be possible that the tholeiitic magmas represented by amphibolites might have been emplaced in a marginal basin environment.

The tholeiitic amphibolites of Masuda and the basal Aravalli meta-volcanics of Nathdwara area (occurring in southern part of Aravalli Craton) are Fe-rich tholeiites. Ahmad and Rajamani (1991) contended that the enrichment of the source in Fe (to increase [Fe]/[Mg] ratio) might have taken place by addition of melts derived from deep mantle plumes. The Fe-enrichment of mantle sources by a similar mechanism have also been proposed by Jahn et al. (1980) for the Archaean tholeiites of Finnish greenstone belt and Horan et al. (1987) for the 1800 Ma old tholeiites in east central Minnesota, Rajamani et al. (1989) for petrogenesis of tholeiitic amphibolites of Kolar Schist Belt, Dharwar Craton in south India and Sahoo and Balakrishnan (1994) for dolerite dykes of Kolar area. Thus, Fe-enrichment by melt addition appears to be a pre-requisite for generation of magmas representing tholeiitic rocks from different areas.

The Nathdwara meta-volcanics have higher Ni abundances and LREE enriched patterns (Ahmad and Rajamani, 1991). In contrast, the tholeiites of Masuda have lower Ni contents and flat REE patterns. Ahmad and Rajamani (1991) suggested that the source for Aravalli tholeiites could have been a LREE enriched shallow lithospheric source. Whereas, magmas representing the Masuda amphibolites are considered to have been derived from a flat to slightly light REE depleted lithospheric mantle source. Therefore, the basal Aravalli metavolcanics of Nathdwara and tholeiitic amphibolites of Masuda have distinct geochemical and characteristics petrogenetic histories.

Some of the mafic enclaves occurring at Jhamarkotra (near Udaipur) have comparable chondrite normalized REE patterns (Gopalan et al., 1990) with that of tholeiites of the Masuda area. According to Ahmad and Tarney (1994) there are two suites of mafic enclaves within the BGC in Nathdwara area. They suggested that the larger mafic bodies could have been the feeder to the Aravalli tholeiites. Whereas, the smaller size mafic enclaves represent either rift related basalts or tectonically accreted fragments of oceanic-island basalts.

Geochemical similarities and petrogenetic considerations suggest that the magmas parental to the amphibolites of Masuda were emplaced in marginal basin setting. The amphibolites of Masuda area might have evolved by distinct petrogenetic processes, sources and tectonic environment from that of the basal Aravalli volcanics and various types of mafic enclaves of the BGC reported from southern Aravalli Craton.

7.2 SANUKITOIDS

The higher abundances of Ba, Sr, Zr, LREEs and alkalis observed in the sanukitoids might have been inherited from their sources. On the basis of geochemical modelling, it was argued that the sanukitoid suite of rocks could neither be derived by partial melting of basalt at different metamorphic facies conditions nor by fractional crystallization with or without crustal assimilation. It was suggested that the sanukitoids must have been derived by partial melting of incompatible element enriched mantle sources under low P, water saturated hydrous conditions. The mantle source could have been enriched in large ion lithophile elements and LREEs by addition of fluids (White and Patchet, 1984; Tatsumi et al., 1986; You et al., 1996) or melts (Kelemen et al., 1993; Yogodzinski et al., 1995) or both (Eggler, 1987; Erlank et al., 1987; Smith et al., 1996).

Yogodzinski et al. (1995) reported that the Adak type of Mg-andesites are predominantly outcome of melting of the subducting slab at eclogite facies condition. They suggested that if a small percentage of melt is added to the overlying depleted arc magma source, it can be enriched in LREEs and LIL elements. It may be emphasized here that the enrichment of the source requires

an additional component from sediments (Kay, 1980), because, the mixture of subducted MORB with peridotite alone can not enrich the source in incompatible elements (Yogodzinski et al., 1995). White and Patchet (1984) considered that even a small (~1%) percent of the sediment can enrich the source in incompatible elements. Tatsumi et al. (1986), Morris et al. (1990) argued that the sediment component as fluids can be admixtured with mantle sources. However, Kay and Kay (1994) argued that the elements like Ba and Th have different solubilities under hydrothermal conditions. Therefore, transportation of large ion lithophile elements to the mantle wedge dominantly by hydrothermal fluids remain ambiguous (Kay and Kay, 1988).

Yogodzinski et al. (1995) assigned a major role to the slab melting and relatively a minor role to the subducted sediment in enriching the source for Adakite type of magnesian andesites (analogous to the sanukitoids) in Aleutian region. These authors considered that during subduction of the oceanic crust the sediments will be melted more easily than the basaltic portion of the slab. Further, they attributed insignificant role of sediments causing enrichment of overlying mantle wedge, if the subduction is oblique which results in long subduction path that carries the slab into the mantle, without undergoing any melting.

The sanukitoids in the study area have no significant Eu anomaly. The Archaean sediments generally do not have significant Eu anomalies (Taylor and McLennan, 1985). Kay (1980) observed that the Ba/Ce ratio (12.5) can be used to assess the role of subducted sediments in the sanukitoids source. However, the sanukitoids of the study area have average Ba/Ce ratio ~4. Therefore, the role of sedimentary component in the source mixture for the sanukitoids must be negligible.

From the [Mg]-[Fe] systematic it was found that the sanukitoids have variable Mg #s. The low-Ti sanukitoids have invariably lower LREEs, Ba, Sr, Zr compared to the high-Ti sanukitoids. Therefore, the mantle sources for the two suites of sanukitoids must have been heterogeneous in Mg#s, Ti/Mg ratio, Ba/Sr ratio and trace element abundances. Geochemical modelling suggests that the sources for high-Ti sanukitoids (lower Mg#) have been more affected by enrichment processes compared to low-Ti sanukitoids (higher Mg#).

From the petrogenetic considerations, it can be inferred that the melt addition process is much more relevant in causing enrichment of the sources for sanukitoids of Masuda area as compared to the fluids. The variable Ti and other incompatible trace element abundances can be explained if the parental magmas were derived by partial melting of mantle sources that had undergone prior melt addition. The composition of the melt that might have been added to the sources was constrained to vary from tholeiitic to low-Ti sanukitoids.

7.3 GRANODIORITE GNEISSES

The granodiorites define a chemical continuum with sanukitoid rocks. Geochemically, there are two distinct granodiorite suites. The first suite has higher Ba, Sr, LREE and HREE abundances compared to the second suite and also has prominent negative Eu anomalies. Geochemical modelling suggests that the magmas parental to the first suite of granodiorites might have been derived by partial melting of rocks similar to the sanukitoids.

The second suite of granodiorites have no Eu anomaly and have lower REE abundances than the first suite of granodiorites and sanukitoids. These rocks have sub-parallel sloping REE patterns and could represent residual magmas formed as a result of fractionation processes, including liquid immiscibility. Stern and Hanson (1991) suggested that the high-Mg granodiorites have been derived by fractional crystallization (up to 90%) of the diorite cumulate whereas, Bender et al. (1982) suggested liquid immiscibility model to explain the geochemical variations observed in the granodiorites of the Rose Town Complex, New York.

Some of the granodiorites and Sanukitoids of Masuda area have overlapping biotite compositions, major and trace element abundances which are characteristics of silicate magma unmixing. It appears that liquid immiscibility process must have played a significant role in evolution of granodioritic magmas from more primitive mantle derived sanukitoid magmas.

The sanukitoid-granodiorite suites are the dominant components of the exposed regions of the Precambrian continental crust (e.g. Shirey and Hanson, 1984; Balakrishnan and Rajamani, 1987; Stern et al., 1989; Stern and Hanson, 1991). It implies that the melting of the enriched mantle sources at shallow depths was a significant process in continental crustal evolution throughout Precambrian. On the basis of geochemical characteristics of the sanukitoids it may be suggested that the mantle sources were enriched by addition of melt and addition that were formed as a result of subduction of oceanic slab. Thus, the petrogenesis of Precambrian sanukitoid-granodiorite suites are quite analogous to that of Phanerozoic intermediate-felsic magmatism developed along the arcs.

7.4 SANUKITOID-GRANODIORITE PETROGENESIS : PRECAMBRIAN vs MODERN ANALOGS

The Archaean tectonics and magma genesis are thought to be different from that of Phanerozoic. For example, komatiites are mostly found in the Archaean greenstone belts and have extrusion temperature of ca.1650^{0}C while, for the modern MORB's the extrusion temperature is 1400^{0}C (Sleep, 1979). It implies that temperature of the Archaean mantle was probably hotter

than that of present day mantle by 200 to 300^{0}C (Richter, 1985). During Archaean, the production of oceanic plates was six times faster than the present day (Bickle, 1978) and also the mean age of the subducting lithosphere in the Archaean is estimated to be 20 Ma relative to 60 Ma for the present day (Martin, 1986) resulting in subduction of a plate twice hotter during Archaean than today (Parson and Sclater, 1977). Therefore, the subduction of young, warm oceanic lithosphere is believed to be the most important control over slab melting in modern subduction systems (Drummand and Defant, 1990; Kay et al., 1993; Sajona et al., 1996). However, it is also considered that slow, oblique subduction also results in partial melting of even the older (>25 Ma) down going slab (Peacock et al., 1994; Yogodzinski et al., 1995).

The sanukitoids of Masuda area are comparable to the Archaean sanukitoids of the south-west Superior Province and analogous to the modern day high-magnesian andesites of Setouchi Volcanic Belt of Japan; Adak type magnesian andesite of Aleutian arc (Miocene) and quaternary andesitic amphibolites of Montanna area (Mueller et al., 1983). Shirey and Hanson (1984) and Stern and Hanson (1991) have suggested that the parental magmas to the sanukitoids of the Superior Province were derived at low pressure by partial melting of mantle peridotite, that had been enriched by fluids or melts released by subducting slab. On the basis of Sr and Nd isotope systematics of the sanukitoids, these authors argued that the enrichment of the mantle sources and subsequent melting were discrete events and the enrichment of the source might have preceded melting by not more than 100-200 my.

High-Mg andesites which are analogous to sanukitoids are generated only under conditions of unusually high heat flow at shallower levels in the mantle wedge (Tatsumi and Maruyama, 1989). Cenozoic high-Mg andesites of the Setouchi Volcanic Belt of Japan (Tatsumi and Ishizaca, 1982a; Ishizaca and Tatsumi, 1982b) and of Baja, California (Bajaites; Saunder et al., 1987) have pronounced enrichment of LREEs, Sr and P_2O_5 abundances. These authors have suggested that they might have been formed by melting of metasomatized (by fluids/melt) mantle wedge.

From the geochemical and petrogenetic considerations of sanukitoids, it appears that the sanukitoid magmas were derived from mantle sources that had undergone enrichment of incompatible elements prior to melting. The enrichment of mantle sources might have been caused by addition of melts or fluids released by subducting slab. Thus, the sanukitoid magmatism might have occurred in arc-type tectonic settings.

7.5 GRANOPHYRES AND APLITE

The granophyres and aplites occur locally within the study area. The granophyres are inter banded with amphibolites and granitoid rocks. The geochemical characteristics of granophyres

suggest that they might have crystallized from magmatic residual fluids formed on crystallization of sanukitoid or granodiorite magmas.

The aplites crosscut the foliation and are post-tectonic. They might have crystallized from hydrothermal fluids associated with high grade metamorphic event.

7.6 GRANOLITES

The high grade granolitic rocks form a separate terrane adjacent to the study area on south and east and have distinct textural characteristics. Geochemically, the granolites define a wider range and have granodiorite to sanukitoid affinities. The enclaves which occur in these rocks are distinguishable from the host rocks in a limited number of samples. The granolitic host as well as, enclave have sub-parallel chondrite normalized REE patterns and negative Eu anomalies. The enclave has slightly higher REE abundances than the host rock. A detailed geochemical study of the granolites is needed to understand their petrogenesis which is beyond the scope of this study.

7.7 TECTONIC SETUP

The Masuda amphibolites have geochemical characteristics similar to tholeiitic basalts found in back-arc basin environment. Granodioritic rocks represent magma that were derived by fractionation processes including liquid immiscibility from parental sanukitoid magmas or by partial melting of sanukitoid rocks. Geochemical modelling reveals that the magmas representing Masuda sanukitoids were derived by partial melting of enriched shallow hydrous mantle sources similar to that of mantle wedge above subducting slab in modern arc systems. The sanukitoid-granodiorite suite is also characteristic of magmatism in arc environments, as found in Japan and Aleutian islands. The amphibolites and both types of sanukitoids were thus derived from distinct sources and tectonic settings.

Whereas, these rock types that predominantly constitute the Banded Gneissic Complex, are closely associated in space and are inter banded with each other and co-folded. They might have been brought together by accretionary processes, as suggested by Kushiro (1987) for Japanese island arcs. Later, they might have been folded and sheared to attain the present day configuration.

The Banded Gneissic Complex constitute the major lithological unit of the Aravalli Craton. The sanukitoids and granodiorite suites make up nearly 70% of the Banded Gneissic Complex. In the foregoing discussion, it was suggested that the sanukitoids and granodiorite magmas were derived from enriched mantle sources. Thus, significant additions to the Aravalli Craton from mantle in the form of granitoid magmas might have taken place during early Proterozoic. Further, it has been suggested that the continental growth in the Aravalli Craton is probably dominated by accretionary processes.

7.8 SUMMARY AND CONCLUSIONS

- Geochemically, the tholeiites show Fe - enriched trend and the source(s) for the thoeliites might have had different [Fe]/[Mg] ratio and lower Ni abundances than garnet-lherzolite.
- The tholeiites can be generated from a source similar to spinel lherzolite by 5 to 20% partial melting.
- Trace and Rare Earth Element geochemistry suggests that the thoeliites are akin to marginal basin basalts.
- The sanukitoids are calc - alkaline in nature and are classified as low - and high - Ti sanukitoids based on TiO_2/MgO and Ba/Sr ratio.
- The low - Ti sanukitoids have lower LREEs, Ba, Sr, K, Zr, and Nb compared to high-Ti sanukitoids.
- The low - Ti sanukitoids might have been derived from a mixed source consisting of 80% primitive mantle and 20% tholeiitic melt components.
- The source(s) for high - Ti sanukitoids might have varying proportion of primitive mantle, tholeiitic and low-Ti sanukitoid melt components.
- The low - Ti sanukitoid magmas might have been derived at higher P and T conditions than the high-Ti sanukitoids.
- A suite of granodiorites might have been derived by partial melting of a source similar to low-Ti sanukitoids.
- The other granodiorite suite II were derived by fractionation processes including liquid immiscibility from sanukitoid magmas. They may represent the felsic end member of immiscible silicate magmas : in which iron - rich end members are represented by magmas similar to sanukitoids.
- Granophyres could have been precipitated from residual magmatic fluids. Post - tectonic aplite vein that cross cut all rock types might have precipitated from metamorphic fluids.
- Mantle derived sanukitoid and granodiorite magmas might have played a dominant role in evolution and growth of continental during early Proterozoic in the northern Aravalli craton.
- Amphibolites and sanukitoids that were derived from distinct sources and tectonic environments were brought together by accretionary processes to attain the present spatial association in the Masuda area of the Aravalli Craton.

REFERENCES

Ahmad, T. and Rajamani, V. 1988 Geochemistry and petrogenesis of mafic inclusion within the Banded Gneissic Complex, near Nathdwara : Implication to BGC-Aravalli relationship. Mem. Geol. Soc. India, v.7, pp. 327-340.

Ahmad, T. and Rajamani, V. 1991 Geochemistry and petrogenesis of the basal Aravalli volcanics near Nathdwara, Rajasthan, India. Precamb. Res., v.49, pp. 185-204.

Ahmad, T. and Tarney, J. 1994 Geochemistry and petrogenesis of late Archean Aravalli volcanics, basement enclaves and granitoids, Rajasthan. Precambrian Research, v.65. pp.1-23.

Allegre, C.J., Couttilot, V., et 32 al., 1984 Structure and evolution of the Himalaya-Tibet orogenic belt. Nature, v.307, pp.17-22.

Arculus, R.J. and Wills, K.J.A. 1980 The petrology of plutonic blocks and inclusions from the Lesser Antilles island arc. Jour. of Petr., v.21, pp.743-799.

Arkani-Hamed, J. and Jolly, W.T. 1989 Generation of Archaean tonalites. Geology, v.17, pp.307-310.

Arth, J.G. 1972 Quartz diorites derived by partial melting of eclogite or amphibolite at mantle depths. Contrib. Min.Pet., v.37, pp161-174.

Arth, J.G. and Hanson, G.N. 1975 Geochemistry and origin of the early Precambrian crust of northeastern Minnesota. Geochem. et. Cosmochim Acta, v.4, pp. 325-362.

Arth, J.G.F., Barker, F., Peterman, Z.E. and Friedman, I. 1978 Geochemistry of the gabbro-diorite-tonalite-trondhjemite suite of southwest Finland and its implications for the origin of tonalitic and trondhjemitic magmas. Jour. of Petrol., v.19, pp.289-316.

Balakrishnan, S. and Rajamani, V. 1987 Geochemistry and petrogenesis of granitic gneisses around the Kolar Schist Belt, South India: constraints for the evolution of the crust in the Kolar area. Jour. of Geol., v.95, pp. 219-240.

Balakrishnan, S., Hanson, G.N. and Rajamani, V. 1990 Pb and Nd isotope constraints on the origin of high Mg and Tholeiitic amphibolites, Kolar Schist Belt, South India. Contrib.Min.Petro. v.107, pp.279-292.

Balakrishnan S., Sahoo, J., Giritharan,T.S. and Rajamani, V. 1995: Is BGC an Ancient Accreted Complex ? DCS News Letter, vol.5, No.1, pp.18-21.

Balasubrahmanyam, M.N. and Chandy, K.C. 1976 Lead isotope studies of Galena from some occurrences in India. Rec.Geol.Surv.Ind. v.107, pp.141-148.

Banerjee, D.M. 1971 Precambrian stromatolitic phosphorites of Udaipur, Rajasthan, India. Geol. Soc. Am. Bull., v.82, pp.2319-2330.

Barker, F. and Arth, J.G. 1976 Generation of trondhjemitic-tonalitic liquids and Archaean bimodal trondhjemite-basalt suites. Geology, v.4, pp.596-600

Barker, F. 1981 Tonalites in crustal evolution. Phil. Trans. R. Soc. Lond., v.301, pp.293-303.

Basaltic Volcanism Study Project 1981 Basaltic Volcanism on the terrestrial planets. New York, Pergamon Press, pp. 1286.

Beard, J.S. and Lofgren, G.E. 1991 Dehydration melting and water saturated melting of basaltic and andesitic greenstones and amphibolites at 1, 3, and 6.9 kb. Jour. of Petr. v.32, pp. 365-401.

Bender, J.F., Hanson, G.N. and Bence, A.E. 1982 The Cortland Complex : evidence for large-scale liquid immiscibility involving granodiorite and diorite magmas. Earth Planet. Sci. Lett., v.58, pp.330-344.

Beswick, A.E. 1982 Some geochemical aspects of alteration and genetic relations in komatiite suites. In: Arndt,N.T. and Nisbet, E.G.(Eds.) Komatiites. London: Allen and Unwin, pp.283-308.

Bhaskar Rao, Y.J., Beck, W., Rama Murthy, V., Nirmal Charan and Naqvi, S.M. 1983 Geology, geochemistry and age of metamorphism of Archaean grey gneisses around Channaraya-patna, Hassan Distt., Karnataka, South India, Mem. Geol.Soc.India, v.4, pp.309-328.

Bhattacharaya, T., Sengupta, S. and Mukhopadhyay, D. 1995 Tectonic status of the Delhi-pre-Delhi contact, east of Beawar, central Rajasthan. Mem. Geol. Soc. Ind., v.31, pp.217-230.

Bienvenu,P., Bougault,H., Joron, J.L. Treuil, M. and Dmitrievl, L. 1990 MORB alteration: Rare earth element/non-rare-earth hygromagmaphile element fractionation. Chemical Geology, v.82, pp.1-14.

Bougault, H., Joron, J.L., Monchoux, P., Treuil, M. and Walgenwitz, F. 1980 The primordial chondritic nature and large scale heterogeneities in the mantle: Evidence from the high and low partition coefficient elements in the oceanic basalts. Phil. Trans. R. Soc. Lond, v-297A, pp.115-122.

Bowen, N.L. 1928 The Evolution of Igneous rocks. Princeton Universtiy Press, Princeton, N.J.

Briqueu, L., Bougault, H. and Joron, J.L. 1984 Quantification of Nb, Ta, Ti and anomalies associated with subduction zones: petrogenetic implications. Earth Planet. Sci. Lett., V-68, pp.297-308.

Burnham, C.W. 1979b The importance of volatile constituents. In: Yorder, H.S. (Ed.) The evolution of Igneous rocks: Fiftieth Anniversary Perspectives. Princeton, NJ:Princeton university Press, pp439-482.

Carron, J.P. and Legache, M. 1980 Etude experimentale du fractionnement des elements Rb, Cs, Sr, et Ba entre feldspaths alkalins, solutionshydrothermales et liquides silicates dans le systeme Q. AB. Or.H_2O a 2 kb entre 700 et 800^{0}C. Bulletin de Mineralogie, v.103, pp.571-578.

Chaudhary, A.L., Gopalan, K. and Sastry, C.A. 1984 Present status of geochronology of the Precambrian rocks of Rajasthan. Tectonophysics, v. 105, pp. 131-140.

Condie, K.C. 1981 Archaean greenstones. Elsevier, Amsterdam, pp.434.

Condie, K.C. 1986 Origin and early growth rate of continents. Precamb. Res., v.32, pp.261-278.

Cox. K.J., Bell. J.D. and Pankhurst. R.J. 1987 The Interpretation Of the Igneous Rocks. George Allen & Unwin, pp.449.

Crawford, A.R. 1970 The Precambrian geochronology of Rajasthan and Bundelkhand, Rajasthan. Can. J. Earth. Sci. v. 7, pp. 91-110.

Crawford, A.R. 1970 and Compston, W. 1970 The age of Vindhyan System of Peninsular India. Q. J. Geol. Soc. London, v.125, pp.351-372.

Crawford, A.R. 1975 Rb-Sr age determinations for the Mount Abu granite and related rocks of Gujarat. J. Geol. Soc. India, v. 16, pp.20-28.

Crock, J.G., Lichte, F.E. and Wildeman, T.R. 1984 The group separation of the rare earth elements and Yttrium from geologic materials by cation exchange chromatography. Chem. Geol., v.45, pp. 149-163.

Crookshank 1948 Minerals of the Rajputana pegmatites. Trans. Min. Geol. Met. Inst. India, v.42, pp. 105-189.

Daneckwerth, P.A. and Ryerson, F.J. 1980 REE partitioning between coexisting silicate liquids. EOS. Trans. Am. Geophys. Union, v.61, pp.398.

Dasgupta, S.P. 1964 Structural evolution of the Khetri copper belt, Rajasthan, India. Rep. 22nd Int. Geol. Congr., New Delhi, v. 4, pp. 357-373.

Dasgupta, S.P. 1968 The structural history of the Khetri copper belt, Jhunjhunu and Sikar districts, Rajasthan. Mem. Geol. Surv. India, v.98, pp. 1-170.

Deb, M. 1980 Genesis and metamorphism of two stratiform massive sulphide deposits at Ambaji and Deri in the Precambrian of western India. Econ.Geol., v.75, pp. 572-591.

Deb, M. 1982 Crustal evolution and Precambrian metallogenesis in western India. Revista Brasileira de Geosciências, v.12, pp. 94-104.

Deb, M. 1987 Lithogeochemistry around Rampura-Agucha massive sulphide ore-body, Proterozoic Aravalli-Delhi orogenic belt, NW India : Implications on the evolution of the Archaean crust of western India. In: Proterozoic geochemistry. IGCP conference, Abstr. Pap. Lund. Sweden, pp. 28-29.

Deb, M., Thorpe, R.I., Cumming, G.L. and Wagner, P.A. 1989 Age,sorce and stratigraphic implications of Pb isotope data for conformable, sediment hosted, base metal deposits in the Proterozoic Aravalli-Delhi orogenic belt, northwestern India. Precamb. Res., v. 43, pp. 1-22.

Deb, M. and Sarkar, S.C. 1990 Proterozoic evolution and matallogenesis in the Aravalli-Delhi orogenic complex, northwestern India. Precamb. Res., v.46, pp.115-137

Deb, M. 1992 Lithogeochemistry of rocks around Rampura-Agucha massive zinc sulphide ore-body, NW India- implications for the evolution of a Proterozoic "aulacogen". In: metallogeny related to tectonics of the Proterozoic mobile belts S.C. Sarkar (Ed.) Oxford & IBH Publ. Co., New Delhi, pp. 398.

Drummond, M.S. and Defant, M.J. 1990 A model for trondhjemite-tonalite-dacite genesis and crustal growth via slab melting : Archean to modern comparisons. Jour. Geophy. Res., v. 95, pp.21503-21521.

Eggler, D.H. 1987 Solubility of major and trace elements in mantle metasomatic fluids : experimental constraints. In: Mantle metasomatism. Edited by M.A.Menzies and C.J. Hawkesworth. Academic Press, London, pp.21-41.

Eiichi, Takahashi and Christopher, M.Scarfe 1985 Melting of peridotite to 14GPa and the genesis of Komatiites. Nature, v. 315, pp.566-568.

Erlank, A.J., Waters, F.G., Hawkesworth, C.J., Haggerty, H.L., Allsopp, R.S., Rickard, R.S. and Menzies, M.A. 1987 Evidence for mantle metasomatism in peridotite nodules from the Bultfontein Floors, Kimberly, South Africa, In: Mantle Metasomatism (Eds. M.A.Menzies and C.J.Hawkesworth) Academic Press, London, pp.221-311.

Ford, C.E., Russel, D.G. and Frisk, M.R., 1983 Olivine-liquid equilibria: temperature, pressure and composition dependence of the crystal/liquid partition coefficients for Mg, Fe, Ca and Mn. Jour. of Petrology, v.24. pp. 256-265.

Gandhi, S. M., Paliwal, H.V. and Bhatnagar, S.N. 1984 Geology and ore reserve estimates of Rampura-Agucha zinc-lead deposit, Bhilwara Distt., Rajasthan. Jour. Geol. Soc. India, v.25, pp.689-705.

Gangopadhyay, P.K. and Lahiri, A. 1988 Anjna granite and associated rocks of Deogarh, Udaipur district, Rajasthan. Mem. Geol. Soc. India, v.7, pp. 307-316.

Gangopadhyay, A. and Mukhopadhyay, D. 1987 Structural geometry of Delhi Supergroup near Sendra- an example of the impress of granite diapirism on tectonic structures. In: Geological evolution of Peninsular India, petrological and structural aspects. Recent Researches in Geology, v.13, Hindustan Publ. Corp., Delhi, pp. 45-60.

Gastil, G. 1982 Symposium on subduction of oceanic plates: Summary. GSA Bulletin, v.93, pp. 464-467.

Gilbert, M.C., Heltz, R.T., Popp, R.K. and Spear, F.S. 1982 Experimental studies of amphibole stability. In: Velblen, D.R. and Ribbe, P.H. (Eds.) Amphiboles: Petrology and experimental Phase relations. Miner. Soc.Am.Rev.Miner. v.9b, pp229-354.

Gill, J.B. 1981 Orogenic andesites and plate tectonics. Springer-Verlag, New York, pp. 385

Glikson, A.Y. 1979 Early Precambrian tonalite-trondhjemite sialic nuclei. Earth-Sci. Rev, v.15, pp.1-73.

Goel, O.P. 1988 Petrogenesis of basal Aravalli metabasites east of Udaipur, Rajasthan. Mem. Geol. Soc. India, v.7, pp. 317-326.

Gopalan, K., Macdougall, J.D., Roy, A.B. and Murali, A.V. 1990 Sm-Nd evidence for 3.3 Ga old rocks in Rajasthan, northwestern India. Precamb. Res. v.48, pp. 287-297.

Govindraju, K. 1989 Compilation of working values and sample description for 272 geostandards. Geostandard Newsletter, v. 13, pp. 1-113.

Green, 1973 Experimental melting studies on a model upper mantle composition at high pressure under water-saturated and water-undersaturated conditions. Earth Planet. Sci. Lett. v.19, pp.37-57.

Green, 1976 Experimental testing of "equilibrium" partial melting of peridotite under water-saturated, high pressure conditions. The Canadian Mineralogist, v.14, pp.255-268.

Green, D.H. and Ringwood, A.E. 1970 Mineralogy of peridotitic compositions under upper mantle conditions. Physics of the Earth and Planetary Interiors, v.3, pp. 359-371.

Greig, J.W. 1927 Immiscibility in silicate melts. Am. J. Sci., 5th ser., XIII(73): pp.1-44 and XIII(74): pp.133-154.

Gromet, L.P. and Silver, L.T. 1983 Rare earth element distributions among minerals in a granodiorite and their petrogenetic implications. Geochim. Cosmochim. Acta, v-47, pp.925-39.

Guha, D.B. and Bhattacharaya, A.K. 1993 Metamorphic evolution and high grade reworking of the Sandmata complex granulites. Mem. Geol. Soc. India, v. 31, pp. 163-198.

Gupta, B.C. 1934 The geology of central Mewar, Rajputana. Mem. Geol. Surv. India, v. 65, pp. 1107-1169.

Gupta, S.N., Arora, Y.K., Mathur, R.K., Iqbaluddin, Prasad, B., Sahai, T.N. and Sharma, S.B. 1980 Lithostratigraphic map of Aravalli region, southern Rajasthan and northern Gujarat. Geol.Surv. India, Calcutta.

Hanson, G.N.and Langmuir, C.H. 1978 Modelling of major elements: in mantle-melt system using element approaches. Geochemica Comochemica Acta., v.42, pp. 725-741.

Hanson, G. N., 1980 Rare earth elements in petrogenetic studies of igneous systems. Ann. Rev. Earth Planet Sci., v.8, pp. 371-406.

Hanson, G.N. 1981 Geochemical constraints on the evolution of the early continental crust. Philos. Trans. R. Soc. London, v-1430, pp.423-442.

Hart, S.R. and Davis, K.E. 1978 Nickel partitioning between olivine and silicate melt. Earth Planet. Sci. Lett., v.40, pp.203-219.

Helz, R.T. 1976 Phase relations of basalts in their melting ranges at P_{H2O} = 5 kb. Part II Melt compositions. Jour. of Petr. v.17, pp.139-193.

Henderson, P. 1982 Inorganic geochemistry. Pergamon Press, Oxford, pp.353.

Heron, A.M. 1917 The Blana-Lalsot hills in eastern Rajputana. Rec. Geol. Surv. India, v. 48(4), pp. 181--203.

Heron, A.M. 1935 Synopsis of the Pre-Vindhyan geology of Rajputana. Trans. Nat. Inst. Sci. India, v. 1, pp. 17-33.

Heron, A.M. 1953 The geology of central Rajputana. Mem. Geol. Surv. India, v. 79 (1), 389 pp.

Herzberg, C.T. and O' Hara, M.J. 1985 Origin of peridotite and Komatiite by partial melting. Geophys. Res. Lett., v.12. pp.541-544.

Hofmann, A.W. 1988 Chemical differentiation of the earth: relationship between mantle, continental crust and oceanic crust. Earth Planet. Sci. Lett. v.90, pp. 297-314.

Horan, M.F., Hanson, G.N. and Spencer, K.J., 1987 Pb Nd isotope and trace element constraints on the origin of basic rocks in an early Proterozoic igneous complex, Minnesota. Precambrian Research, v. 37, pp. 323-342.

Irving, A. J. 1978 A review of experimental studies of crystal /liquid trace element partitioning. Geochimica et Cosmochimica Acta, v.42, pp.743-770.

Jahn, B.M., Auvray, B., Blais, S. Capdevila, R., Cornichet, J., Vidal, P. and Hameurt, J. 1980 Trace element geochemistry and petrogenesis of Finnish green stone belt. Jour.Petrol., v.21, pp.221-244.

Janardan, A.S., Newton, R.C. and Hansen, E.C. 1982 The transformation of Amphibolite facies to charnockite in southern Karnataka and tamilnadu, India. Contrib.Miner.Petr., v.79, pp.139-149.

Jaques, A.L. and green, D.H. 1980 Anhydrous melting of peridotite at 0-15 kb pressure and genesis of the tholeiitic basalts. Cotrib. Miner. Petr., v.73, pp.287-310.

Jayananda, M., Martin, H., Peucat, J. J. and Mahabaleswar. B. 1995 Late Archaean crust-mantle interactions: geochemistry of LREE enriched amntle derived magmas. Example of the Closepet Batholith of southern India. Contrib.Mineral.Petr., v.119, pp.314-329.

Jenson, L. S. 1976 A new method of classifying sub-alkaline volcanic rocks. Ontario division of mines. Misc.Paper No.66, p.22.

Joshi, M. 1985 Sandmata paragneiss complex : its structural and petrological analysis (district Udaipur, Rajasthan). Unpublished Ph.D. thesis, Banaras Hindu University, 1984.

Kataria, P. 1981 Petrological and minerological studies of rock around Amet, Udaipur, Rajasthan. Unpublished Ph.D. thesis, Rajasthan University, pp. 123-162.

Kataria, P., Chaudhury, M.W. and Althaus. E. 1988 Petrochemistry of Amphibolites from the Banded Gneissic Complex of Amet, Rajasthan, NW India. Chem. Erde., v.48, pp. 89-111.

Kay, R.W. 1978 Aleutian magnesian andesites: melts from subducted Pacific Ocean crust. Jour. of Vulcanology and Geothermal Research, v.4, pp.117-132.

Kay, R.W. 1980 Volcanic arc magma genesis: implications for element recycling in the crust-upper mantle system. Jour. of Geol., v.88, pp.497-522.

Kay, R.W. and Kay, S.M. 1988 Crustal recycling and Aleutian arc. Geochim.et Cosmochim Acta, v.52, pp. 1351-1359.

Kay, S.M. and Kay, R.W. 1994 Aleutian magmas in space and time. In: (Eds. Plafker, G. and Berg, H.C.) The geology of Alaska: Boulder, Colrado, GSA, Geology of North America, v.G-1, pp.687-722.

Kay, S.M., Ramos, V.A. and Marquez, Y.M. 1993 Evidence in Cerro Pampa volcanic rocks for slab melting prior to ridge-trench collision in southern south America. Jour. Geol., v.101, pp.703-714.

Kelemen, P.B., Johnson, K.T.M., Kinzler, R.J. and Irving, A.J. 1990 High field strength element depletions in arc basalts due to mantle-magma interaction. Nature, v.345, pp.521-524.

Kelemen, P.B., Shimizu, N. and Dunn, T. 1993 Relative depletion of niobium in some arc magmas and the continental crust: partitioning of K, Nb, La, Ce during melt / rock interaction in the upper mantle. Earth Planet. Sci. Letters, v.120, pp.111-134.

Khandelwal, N.M. and Pandya, M.K. 1988 Petrochemistry and genesis of the Precambrian amphibolites from Masuda-Ramgarh region of central Rajasthan. Mem. Geol. Soc. India, v.7, pp. 297-306.

Kostopoulos, D.K. 1991 Melting of the Shallow Upper Mantle: A New Perspective. Jour.of Petr. V.32, pp.671-699.

Kostopoulos, D.K. and James, S.D. 1992 Parametrization of the Melting Regime of the Shallow Mantle and the Effects of Variable Lithospheric Stretching on Mantle Modal Stratification and Trace Element Concentrations in Magmas. Jour.of Petr. v.33, pp.665-691.

Kramers, J.D. 1988 An open-system fractional crystallisation model for very early continental crust formation. Precambrian Res., v.38, pp.281-95.

Krogstad, E.J., Balakrishnan, S., Mukhopadhyay, D.K., rajamani, V. and Hanson, G.N. 1989 Plate Tectonic 2.5 billion years ago : Evidence at Kolar, South India. Science, v.243, pp. 137-1340

Kushiro, I. 1987 A petrological model of the mantle wedge and lower crust in the Japanese island arcs. In Magmatic Processes : Physico-chemical principles (Ed. B.O.Mysen) The Geochemical Society Special Publication, v.1, pp. 165-181.

Lal, R.K. and Shukla, R.S. 1975 Low pressure regional metamorphism in the northern portion of Khetri copper belt of Rajasthan, India. Neues Jb. Mineral. Abh., v.124, pp. 294-325.

Langmuir and Hanson 1980 An evaluation of major element heterogeneity in the mantle sources of Basalts. Phil. Trans. R. Soc. Lond, v.297A, pp.383-407.

Le Bas, M.J. and Streckeisen, A.L. 1991 The IUGS systematics of igneous rocks. Jour. Geol. Soc., London, v.148, pp. 825-833.

Luth, W.C., Jahns, R.H. and Tuttle, O.F. 1964 The granite system at pressures of 4 to 10 kbar. Jour.Geophs.Res., v.69, pp. 759-773.

Macdougall, J.D., Gopalan, K., Lugmair, G.W. and Roy, A.B. 1983 An ancient depleted mantle source for Archaean crust in Rajasthan, India Lunar Planet.Inst. Tech. Rep., v.,83, pp. 55-56.

MacGregor, I.D. and Manton, W.I. 1986 Roberts Victor Eclogites: ancient oceanic crust. Jour. of Geophys.Res., v.91, pp.14063-14079.

Martin, H. 1986 Effect of steeper Archaean geothermal gradient on geochemistry of subduction zone magmas. Geology, v.14, pp.753-756.

Martin, H. 1987 Petrogenesis of Archaean trondhjemites, tonalites and granodiorites from eastern Finland : major and trace element chemistry. Jour. of Petr. v.28, pp.921-953.

Masuda, A., Nakamura, N. and Tanaka, T. 1973 Fine Structures of mutually normalized rare-earth patterns of chondrites. Geochim. Cosmochim. Acta, v.37, pp.239-48.

McBirney, A. 1975 Differentiation of the Skaergaard intrusion. Nature (London), V-253, pp.691-694.

McCulloh, M.T. and Gamble, J.A. 1991 Geochemical and geodynamical constraints on subduction zone magmatism. Earth Planet. Sci. Lett., v.102, pp.358-374.

Menzies, M., Rogers, N., Tindle, A. and Hawkesworth, C. 1987 Metasomatic and enrichment processes in lithospheric peridotites, an effect of asthenosphere-lithosphere interaction. In: Mantle metasomatism. Edited by M.A.Menzies and C.J. Hawkesworth. Academic Press, London, pp.313-352.

Mishra, D.C., Lakshman, G., Rao, M.B.S.V. and Gupta, S.B. 1995 Analysis of the gravity-magnetic data around Nagaur-Jhalawar geotransect. Mem. Geol. Soc. India, v.31, pp. 345-352.

Mohanty, S. 1982 Structural studies around Kathar, Udaipur Distt., Rajasthan. Jour. Geol. Soc. India, v.23, pp.209-218.

Mohanty, S. and Naha, K. 1986 Stratigraphic relations of the Precambrian rocks in the Salumbar area, southeastern Rajasthanb. Jour. Geol. Soc. India, v. 27, pp. 479-493.

Moorbath, S. and Taylor, P.N. 1982 Isotopic evidence for continental growth in Precambrian: In Kroner, A. (Ed.) Precambrian plate tectonics, Elsevier.

Morris, J.D., Leeman, W.P. and Tera, F. 1990 The subducted component in island arc lavas: constraints from Be isotopes and B-Be systematics. Nature, v.344, pp.31-35.

Mueller, P.A., Wooden, J.L., Schulz, K. and Bowes, D.R. 1983 Incompatible -element -rich andesitic amphibolites from the Archaean of Montana and Wyoming : evidence for mantle metasomatism. Geology, v.11, pp.203-206.

Mukhopadhyay, D. and Dasgupta, S. 1978 Delhi-pre-Delhi relations near Badnor, central Rajasthan. Indian Jour. Earth Sci., v. 5(2), pp. 183-190.

Mysen, B.O. 1979 Trace element partitioning between garnet peridotite minerals and water rich vapour: experimental data from 5 to 30 kb. The American Mineralogist, v.64, pp.274-287.

Mysen, B.O. 1982 The role of mantle anatexis. In andesites. Edited by R.S.Thorpe, John Willey & Sons, New York, pp.489-522.

Nabelek, P.I. 1986 Trace element modelling of the petrogenesis of granophyres and aplites in the Notch Peak granitic stocks, Utah. Am. Miner., v. 71, pp.460-471.

Naha, K., Chaudhri, A.K. and Mukherji, P. 1967 Evolution of the Banded Gneissic Complex of Central Rajasthan, India. Contr.Miner.Petrl., v. 15, pp. 191-201.

Naha, K., Chaudhuri, A.K. and Bhattacharaya, A.C. 1966 Superposed folding in older precambrian rocks around Sangat, central Rajasthan, India. N. Jb. Geol. Palaeont. Abh., v. 126, pp. 205-231.

Naha, K. and Chaudhuri, A.K. 1968 Large scale fold interference in a metamorphic migmatitic complex. Tectonophysics, v. 6(2), pp. 127-142.

Naha, K.and Mukherji, P. 1969 Analysis of a large superposed folding in a migmatite terrain. Geol. en Mijnbouw, v. 48 (1), pp. 9-34.

Naha, K., Venktasubramanyam, C.S. and Singh, R.P. 1969 Upright folding of varying intensity on isoclinal folds of diverse orientation : A study from the early Precambrian of western India. Geol. Rundsch., v. 58, pp. 929-950.

Naha, K. and Majumdar, A. 1971a Structure of the Rajnagar marble band and its bearing on the early Precambrian stratigraphy of central Rajasthan, India. Geol. Rundsch., v. 60, pp. 1550-1571.

Naha, K. and Majumdar, A. 1971b Reinterpretation of the aravalli basal conglomerate at Morchana, Udaipur district, Rajasthan, western India. Geo. Mag., v. 108, pp. 111-114.

Naha, K., Chaudhri, A.K. and Mukherji, P. 1973 The "Hammer-Head Syncline" between Sangat and Kelwa in the Udaipur District, Rajasthan : A structural synthesis. Jour. Geol. Soc. India, v. 14, pp. 394-407.

Naha, K. and Halyburton, R.V. 1974a Early precambrian stratigraphy of central and southern Rajasthan, India. Precamb. Res., v. 4, pp. 55-73.

Naha, K. and Halyburton, R.V. 1974b Late stress systems deduced from conjugate folds and kink bands in the " Main Raialo Syncline", Udaipur district, Rajasthan, India. Geol. Soc. Am. Bull., v. 85, pp. 251-256.

Naha, K. and Halyburton, R.V. 1977a Structural pattern and strain history of a superposed fold system in the Precambrian of central Rajasthan, India. I structural pattern in the " Main Raialo syncline", central Rajasthan. Precamb. Res., v. 4, pp. 39-84.

Naha, K. and Halyburton, R.V. 1977b Structural pattern and strain history of a superposed fold system in the Precambrian of central Rajasthan, India. II Strain history. Precamb. Res., v. 4, pp. 85-111

Naha, K. 1983 Structural-stratigraphic relations of the pre-Delhi rocks of southcentral Rajasthan : A summary. In S. Sinha Roy (ed.). Structure and tectonics of the Precambrian rocks. Recent researches in geology, Hindustan Publ. Corp., Delhi, v. 10, pp. 40-52.

Naha, K. and Roy, A.B. 1983 The problem of Precambrian basement in Rajasthan, western India. Precamb. Res., v. 19, pp. 217-223.

Naha, K., Mukhopadhyay, D.K., Mohanty, R., Mitra, S.K. and Biswal, D.K. 1984 Significance of contrast in the early stages of the structural history of the Delhi and the Pre-Delhi rock groups in the Proterozoic of Rajasthan, western India. Tectonophysics, v. 105, pp. 193-206.

Naha, K. and Mohanty, S. 1988 Response of basement-cover rocks to multiple deformations : A study from the Precambrian of Rajasthan, Western India, Precamb. Res., v. 42, pp. 77-96.

Naha, K. and Mohanty, S. 1990 Structural studies in the pre-Vindhyan rocks of Rajasthan : A summary of the work of last three decades. In: Special issue on Structure and Tectonics : The Indian scene (eds K. Naha, S.K. Ghosh & D. Mukhopadhyay). Proc. Ind. Acad. Sci., v. 99, pp. 279-290.

Naqvi, S.M. and Rogers, J.J.W. 1987 Precambrian geology of India. Oxford University Press, 223 pp.

Niyogi, D. 1965 Stratigraphy and structure of the area around Kishangarh, Rajasthan. Trans. Min. Geol. Matall. Inst. India (Wadia Commem. volume), pp. 458-479.

O'Hara, M.J. 1968 The bearing of phase equilibria studies on the origin and evolution of basic and ultrabasic rocks. Earth Sci.Rev. v.4 pp.69-133.

O' Hara, M.J. 1985 Importance of the 'shape' of the melting regime during partial melting of the mantle. Nature, v.314. pp. 58-61.

Olafsson, M. and Eggler, D.H. 1983 Phase relations of amphibole, amphibole-carbonate and phlogopite -carbonate peridotite: petrologic constraints on the asthenosphere, Earth Planet. Sci. Lett., v.64, pp.305-315.

Paliwal, B.S. 1988 Deformation pattern in the rocks of the Aravalli Supergroup around Udaipur city, Rajasthan. Mem. Geol. Soc. India, v.7, pp.153-168.

Pandya, M.K. 1967 Contribution a `l` etude des amphibolites de la region de Kankroli, Rajasthan (India). Annales de la Soclete Geologique de Belgique. Tom., 90-1966-67, Bull. No. 4-6, pp. 431-460.

Pandya, M.K. and gyani, K.C. 1970 Granulitic rocks from the Banded Gnessic complex of Bandanwara region, Ajmer district, Rajasthan. Proc. 2nd Symp. Upp. Mantle Project, Hyderabad, pp. 339-348.

Parson, B.A. and Sclater, J.G. 1977 An analysis of the variation of ocean floor bathymetry and heat flow with ages. Jour. of Geophys.Res., v.82, pp.802-827.

Peackok, S.M. 1990 Fluid processes in subduction zones. Science, v.248, pp.329-337.

Peacock, S.M., Rushmer, T. and Thompson, A.B. 1994 Partial melting of subducting oceanic crust. Earth Planet. Sci. Lett., v.121, pp.227-244.

Pearce, J.A. 1983 Role of sub-continental lithosphere in magma genesis at active continental margins. In : Hawkesworth, C.J. and Norry, M.J. (Eds.) Continental basalts and mantle xenoliths, Shiva Nantwich, pp.230-249.

Pearce, J.A. and Cann, J.R. 1973 Tectonic setting of baic volcanic rocks determined using trace element analyses. Earth Palnet. Sci. Lett., v.19, pp.290-300.

Peucat, J.J., Vidal, P.H., Bernad-Griffths, J. and Condie, K.C. 1989 Sr, Nd and Pb Isotopic systematics in the Archaean low-to-high grade transition zone of south India. Synaccretion vs.post accretion granulites. Jour. Geol., v.97, pp.537-550.

Poddar, B.C. 1966 An example of contrasted tectonic regimes from the Precambrians of Udaipur district, Rajasthan, Ind. Min., v. 20, pp. 192-194.

Pyne, T.K. and Bandhopadhyay, A. 1985 Structure of Banded Gneissic Complex at and around Bandanwara, Ajmer district, Rajasthan. Indian Jour. Earth Sci., v. 12, pp. 9-20.

Radhakrishna, B.P. and Naqvi, S.M. 1986 Precambrian continental crust of India and its evolution. Jour. Geol. v.94, pp.145-166.

Raja Rao, C.S. 1970 Sequence, structure and correlation of the metasediments and gneissic complex of the Rajasthan. Rec. Geol. Surv. India, v. 98 (2), pp. 122-131.

Raja rao, C.S., Poddar, B.C., Basu, K.K. and Dutta, A.K. 1971 Precambrian stratigraphy of Rajasthan : A review. Rec. Geol. Surv. India, v. 101, pp. 60-79.

Rajamani, V., Shivkumar,K., Shirey, S.B. and Hanson, G.N. 1985 Geochemistry and petrogenesis of amphibolites, Kolar Schist Belt, South India : Evidence for komatitic magma derived by low percentages of melting of the mantle. J. Petrology, v.26, pp. 92- 123.

Rajamani, V., Shirey, S.B. and Hanson, G.N. 1989 Fe-rich Archaean tholeiites derived from melt enriched mantle sources: evidence from the Kolar Schist Belt, south india. Jour.Geology, v.97, pp.487-501.

Rajamani.V., Balakrishnan, S. and Hanson, G.N. 1993 Komatite Genesis: Insights provided by Fe-Mg Exchange Equilibria. Jour. of Geol. v.101, pp.809-819.

Ranawat, P.S., Bhatnagar, S.N. and Sharma, N.K. 1988 Metamorphic character of Rampur-Agucha lead-zinc deposit, Rajasthan. Mem. Geol. Soc. India, v.7, pp. 397-410.

Rapp, R.P. and Watson, E. B. 1988 Partial melting of amphibolite/eclogite and the origin of tonalitic-trondhjemitic magmas. EOS, v.69, pp.521.

Rapp, R.P. 1990 Vapour-absent melting of Amphibolite/Eclogite at 8-32 kbar: Implications for the origin and growth of continental crust. Ph.D. dissertation, Rensselaer Polytechnic Institute, Troy, New York, 318pp.

Rapp, R.P., Watson, E.B. and Miller, C.F. 1991 Partial melting of amphibolite/eclogite and the origin of Archaean trondhjemites and tonalites. Precamb.Res., v.51, pp.1-25.

Rapp, R.P. and Watson, E.B. 1995 Dehydration melting of metabasalt at 8-32 kbar:Implications for continental growth and crust-mantle recycling. Jour. of Petrol., v.36, pp.892-931.

Rapp, R.P., Wasserburg, G.J. and Kennedy, A. 1992 Ion and X-ray microprobe measurements of trace elements in tonalitic melts in equilibrium with garnet and clino-pyroxene. EOS, Transactions of the American Geophysical Union, v.73, pp.607.

Rathi, M.S., Khanna, P.P. and Mukherjee, P.K. 1991 Determination of ten rare-earth elements and yttrium in silicate rocks by ICP-AES without separation and preconcentration. Talanta, v-38, pp.329-332,

Rathi, M.S., Khanna, P.P., Mukherjee, P.K. , Purohit, K.K. and Saini, N.K. 1994 Working values for major, minor and trace elements for meta-basic reference sample (MB-H). Jour.Geol.Soc.India, v.43, pp.295-303.

Reddy, P.R., Prasad, B.R., Rao, V.V., Khare, P., Rao,G.K., Murty, A.S.N., Sarkar, D., Raju, S., Rao, G.S.P. and Sridher, V. 1995 Deep seismic reflection profiling along Nandsi-Kunjer section of Nagaur-Jhalawar transect : Preliminary results. Mem. Geol. Soc. India, v. 31, pp. 353-372.

Richter, F.M. 1985 Model for the Archaean thermal regime. Earth Planet. Sci. Lett., v.73, pp.352-360.

Ringwood, A.E. 1975 Composition and petrology of the earth's mantle. New York, McGrawhill, pp.618.

Roday, P.P. 1979 Structural pattern in the Ajabgarh rock around Anakhor, district Ajmer. Jour. Geol. Soc. India, v. 20, pp. 441-449.

Rode, K.P., Pandya, M.K. and Deshmukh, M.G. 1969 On the Charnockites and other granulitic rocks of Bhim-Karera region. Jour.Indian Geol. Soc. Acc., v.2, pp.21-26.

Roedder, E. 1956 The role of liquid immiscibility in igneous petrogenesis: a discussion. J. Geol., v-64, pp.84-88.

Roedder, E. and Weiblen, P.W. 1972 Petrographic features and petrologic significance of melt inclusions in Apollo 14 and 15 rocks. Proc. 3rd Lunar Sci. Conf. Geochim. Cosmochim. Acta. Suppl., v-3, pp.251-279.

Roeder, P.L. and Emsile, R.F. 1971 Olivine- liquid equilibrium. Contrib. Miner. Petro., v.22, pp. 275-289.

Roy, A.B. and Bejarniya, B.R. 1984 A tectonic model for the early Proterozoic Aravalli (Supergroup) rocks from North of Udaipur, Rajasthan. In crustal evolution and orogeny (Ed.S.P.H. Sychanthavang) Oxford & IBH Publishing Co. pp.252-273

Roy, A.B., Paliwal, B.S. and Goel, O.P. 1971 Superposed folding in the Aravalli rocks of the type area around Udaipur, Rajasthan. Jour. Geol. Soc. India, v. 12, pp. 342-348.

Roy, A.B. 1973 Nature and evolution of subhorizontal cleavage in the type Aravalli rocks around Udaipur, Rajasthan. Proc. Nat. Inst. Sci. India, v. 39, pp. 119-131.

Roy, A.B., Nagori, D.K., Golani, P.R. and Chaudhri, R. 1980 Structural geometry of the rock phosphate -bearing Aravalli rocks around Jhamarkota mines area, Udaipur district, Rajasthan. Indian Jour. Earth Sci., v. 7 (2), pp. 191-202.

Roy, A. B. and Paliwal, B.S. 1981 Evolution of Lower Proterozic epicontinental deposits : Stromatolite-bearing Aravalli rocks of Udaipur, Rajasthan, India. Precamb. Res., v. 14, pp. 49-74.

Roy, A. B., Somani, M.K. and Sharma, N.K. 1981 Aravalli, Pre-Aravalli relationship : A study from the Bhinder region, southern Rajasthan. Indian Jour. Earth Sci., v. 8 (2), pp. 119-130.

Roy, A.B., Paliwal, B.S. and Bejarniya, B.R. 1984 The Aravalli rocks : An evolutionary model and metallogenic trends. Indian Jour. Earth Sci., CEISM seminar, pp. 73-83.

Roy, A.B., Golani, P.R. and Bejarniya, B.R. 1985 The Ahar river granite, its stratigraphic and structural relations with the early Proterozoic rocks of southeastern Rajasthan. Jour. Geol. Soc. India, v. 26, pp. 315-325.

Roy, A.B. 1988 Stratigraphic and tectonic framework of the Aravalli mountain range. Mem. Geol. Soc. India, v.7, pp. 3-31.

Roy, A.B., Paliwal, B.S., Shekhawat, S.S., Nagori, D.K., Golani, P.R. and Bejarniya, B.R. 1988 Stratigraphy of the Aravalli Supergroup in the type area. Mem. Geol. Soc. India, v.7, pp. 121-138.

Roy, A.B. and Nagori, D.K. 1990 Influence of differential basement mobility on contrasting structural styles in the cover rocks : An example from early Precambrian rocks east of Udaipur, Rajasthan. In: Special issue on Structure and Tectonics : The Indian scene (eds K. Naha, S.K. Ghosh & D. Mukhopadhyay). Proc. Ind. Acad. Sci., v. 99, pp. 291-308.

Rudnick, R.L. 1990 Growing from below. Nature, v.347, pp.711.

Rudnick,R.L. and Taylor, S.R. 1986 Geochemical constraints on the origin of tonalitic-trondhjemitic rocks and implication for lower crustal composiion. In: Dawson, J.B., Carswell, D.A., Hall, J. and Wedepohl, K.H. (eds). The nature of the lower Continental Crust. Geol. Soc. Spec. Publ. v.24, pp.179-91.

Rudnick, R.L. and Taylor, S.R. 1987 The composition and petrogenesis of the lower crust: a xenolith study. Jour. Geophy. Res. v.92, pp. 13981-14005.

Ryerson, F.J. and Hess, P.C. 1978 Implications of liquid distribution coefficients to mineral-liquid partitioning. Geochem.et Cosmochim Acta, v.42 pp.921-932.

Saha, A.K. and Ray, S.L. 1984 The structural and geochemical evolution of the Singhbhum granite batholithic complex, India. Tectonophysics, v.105, pp.163-176.

Sahoo, J. and Balakrishnan, S. 1994 Geochemistry and Petrogenesis of Kolar Dolerite Dykes in and around Kolar Schist Belt, south India Jour. Geol.Soc.Ind. v.43, pp.511-528.

Sahoo J, Balakrishnan S, Giritharan, T.S. and Rajamani, V. (1995). Geochemical evidence for Island arc type tectonic settings in Precambrian rocks of the Banded Gneissic Complex, Rajasthan, India. International Conference on Precambrian tectonics and Metallogeny, Montreal, Sept. 1-3, 1995.

Sajona, F.G., Maury, C.R., Bellan, H., Cotton, J. and Defant, M. 1996 High field strength element enrichment of Pliocene-Plistocene Island Arc basalts, Zamboanga Peninsula, Western Mindanno (Philippines). Jour. of Petrol., v.37, pp.693-726.

Saleeby, J.B. 1983 Accretionary tectonics of the North American Cordillera. Ann.Rev. Earth Planet Sci., v.15, pp.45-73.

Sarkar, G. Ray Barman, T. and Corfu, F. 1989 Timing of continental arc type magmatism in northwest India : evidence from U-Pb zircon geochronology. Jour. Geol. v. 97, pp. 607-612.

Sarkar, S.C., Bhattacharya, P.K. and Mukherjee, A.D. 1980 Evolution of sulphide ores of Saladipura, Rajasthan, India. Econ. Geol., v.75, pp. 1152-1167.

Sarkar, S.C. 1973 Some observations on the geology in the Khetri copper belt, Rajasthan. Quart. Jour. Geol. Min. Metall. Soc. India, v. 45, pp. 223-226.

Satyanarayana, K., Srinivasan, G., Malhotra, R.K. and Tikoo, B.N. 1989 Determination of rare-earth elements and yttrium in some uranium and thorium rich geological materials by inductively coupled plasma emmision spectrometry. Expl. Res. Ato. Min, v.2, pp.235-245.

Saunder, A.D., Rogers, G., Marriner, G.F., Terrel, D.J. and Verma, S.P. 1987 Geochemistry of Cenozoic volcanic rocks, Baja California, Mexico:Implication for the petrogenis of the post subduction magmas. Jour.Volcan.Geotherm.Res., v.32, pp.223-245.

Schilling, J.G. , Zajac, M., Evans, R., Johnston,T.,White, W., Devine, J.D. and Kingsley, R. 1983 Petrologic and geochemical variations alon the Mid-Atlantic Ridge from 27 ^{0}N to 73^{0} N. Am. J. Sci. v.283. pp.510-586.

Schneider, M.E. and Eggler, D.H. 1986 Fluids in equilibrium with peridotitic minerals: implications for mantle metasomatism. Geochim.et Cosmochim. Acta, v.50, pp.711-724.

Sen, S. 1970 Some problems of Precambrian geology of central and southern Aravalli range, Rajasthan. Jour. Geol. Soc. India, v. 11, pp. 217-231.

Sen, S. 1981 Proterozoic palaeotectonics in the evolution of crust and location of mettaliferrous deposits, Rajasthan. Quart. Jour. Geol. Min. Met. Soc. India, v. 53, pp. 162-185.

Sen, S. 1983 Stratigraphy of the crystalline Precambrian of central and northern Rajasthan : A review. In S. Sinha Roy (ed.). Structure and tectonics of the Precambrian rocks. Recent researches in geology, Hindudstan Publ. Corp., Delhi, v. 10, pp. 26-39.

Sengupta, S. 1976 structures and stratigraphic relations of the Aravallis, southeastern Rajasthan, India. Jour. Geol. Soc. India, v. 17, pp. 461-470.

Shapiro, L. and Brannock, W.W. 1962 Rapid analyses of silicate, carbonate and phosphate rocks. Bull. USGS, v. 1144A.

Sharma, R.S. and Upadhyay, T.P. 1975 Multiple deformation in the Precambrian rocks to the southeast of Ajmer, Rajasthan, India. Jour. Geol. Soc. India, v. 16, pp. 428-440.

Sharma, R.S. 1977 Deformational and crystallization history of the precambrian rocks of north-central aravalli mountain, Rajasthan, India. Precamb. Res., v. 4, pp. 133-162.

Sharma, R.S. and Roy, A.K. 1979 On the polymineralllic paragenesis from Karera, district Bhilwara, Rajasthan, 1. Petrography and Mineralogy. Indian Jour. Earth Sci., v. 6, pp. 67-81.

Sharma, R.S. 1983a Basement-cover rocks relation in north-central Aravalli range : A tectonic and metamorphic synthesis. In S. Sinha Roy (ed.). Structure and tectonics of the Precambrian rocks. Recent researches in geology, Hindudstan Publ. Corp., Delhi, v. 10, pp. 53-71.

Sharma, R.S. 1983b On the polymineralllic paragenesis from Karera, district Bhilwara, Rajasthan, NW India. Geophy. Jour. Royal Astr. Soc. London, v. 73, pp. 291.

Sharma, R.S. and Joshi, M. 1984 Sandmata granulites : A case of deep level exposure of Precambrian crust in NW Indian shield. In Seminar volume on "Crustal evolution of the Indian Shield and its beraing on Metallogeny", Calcutta (Abstr), pp. 35-36.

Sharma, R.S. 1990 Metamorphic evolution of the rocks from the Rajasthan Craton, NW Indian Shield. In: S.M.Naqvi (Ed.) Precambrian Continental crust and its economic resources. Developments in Precambrian Geology, v.8 Elsevier, Amsterdam, pp.349-366.

Sharma, R.S. and Narayan, B. 1975 Petrology and polymetamorphic schists from an Archaean Complex terrane, SE of Beawar, Rajasthan, India. Neues. Jahrb.Mineral. Abh., v.124, pp.190-222.

Sharma, R.S. 1988 Patterns of metamorphism in the Precambrian rocks of the Aravalli mountain belt. Mem. Geol. Soc. India, v.7, pp. 33-76.

Shirey, S.B. and Hanson, G.N. 1984 Mantle-derived Archaean monzodiorites and trachyandesites Nature, v. 310, pp. 222-224.

Shirey, S.B. 1986 Mantle heterogeneity and crustal recycling in Archaean granite-greenstone belts : evidence from Nd isotopes and trace elements in the Rainy Lake area, Superior Province , Ontario, Canada, Geochim. et Cosmochim. Acta, v.50, pp.2631-2651.

Singh, S.P. 1988 Stratigraphy and sedimentation pattern in the Proterozoic Delhi Supergroup, nortwestern India. Mem. Geol. Soc. India, v.7, pp. 193-206.

Sinha Roy, S. 1988 Proterozoic Wilson cycles in Rajasthan. Mem. Geol. Soc. India, v.7, pp. 95-108.

Skjerlie, K.P. and Johnston, A.D. 1996 Vapour absent melting from 10 to 20 kbar of crustal rocks that contain multiple hydrous phases: implications for anatexis in deep continental crust and active continental margins. Jour. of Petrol., v.37, pp.661-691.

Sleep, N.H., 1979 Thermal histrory and degassing of earth: some simple calculations. Jour. Geol., v.87, pp.671-686.

Smith, T.E., Thirlwall, M.F. and Macpherson C. 1996 Trace element and isotope geochemistry of the volcanic rocks of Bequia, Grenadine Islands, Lesser Antilles Arc: a study of subduction enrichment and intra-crustal contamination. Jour. of Petrol., v.37, pp.117-143.

Sparks, R.S.J. 1986 The role of crustal contamination in magma evolution through geologic time, Earth Planet. Sci. Lett., v.78, pp.211-223.

Spear, F.S. 1981 An experimental study of hornblende stability and compositional variability in amphibole. Am. Jour. Sci. v.281, pp.697-734.

Srivastava, D.C., Yadav, A.K., Nag, S. and Pradhan, A.K. 1995 Deformation style of the Banded Gneissic Complex in Rajasthan : A critical evaluation. Mem. Geol. Soc. India, v.31, pp. 199-216.

Srivastava, R.K. 1988 Magmatism in the Aravalli mountain ranges and its environs. Mem. Geol. Soc. India, v.7, pp. 77-94.

Srivastava, D.C. and Yadav, A.K. 1994 Deformation and fluid evolution history in deep crustal segments of the Banded Gneissic Complex around Sandmata, Rajasthan. DCS News Letter, v.4, pp.19-21.

Stern, R.A., and Hanson, G.N. 1991 Archaean high Mg Granodiorite : a derivative of Light Rare Earth Element enriched Monzodiorite of mantle origin. Jour. of Petr. v.32, pp. 201-238

Stern, R.A., Hanson, G.N. and Shirey, S.B. 1989 Petrogenesis of mantle-derived Archaean monzodiorites and trachyandesites (sanukitoids) in southwestern Superior Province. Can. J. Earth Sci. v.. 26, pp.1688-1712.

Sugden, T.J. and Windley, B.F. 1984 Geotectonic framework of the early-mid Proterozoic Aravalli-Delhi orogenic belt, NW India. Geol. Mineral. Assoc. Can., v.94, pp. 68 9 (Abstract).

Sugden, T.J., Deb, M. and Windley, B.F. 1990 The tectonic setting of Mineralisation in the Proterozoic Aravalli-Delhi orogenic belt, NW India. In : Developments in Precambrian geology 8 : Precambrian continental crust and its economic resources (ed. S.M. Naqvi), Elsevier, Amsterdam, pp. 367-390.

Sun, S.S. 1980 Lead isotopic study of young volcanic rocks from mid ocean ridges, ocean islands and island arcs. Phil. Trans. Soc. London, v.297A, pp.313-345.

Sun, S.S. and McDonough, W.F. 1989 Chemical and isotopic systematics of oceanic basalts: Implications for mantle composition and processes. In A.D. Sanders and M.J. Norry. (ed), Magmatism in the ocean basins. Geol. Soc. Lond. Spe. Publ., v-42, pp.313-345.

Sychanthavong, S.P. and Desai, S.D. 1977 proto-plate tectonics controlling the Precambrian deformations and metallogenetic epoch of northwestern peninsular India. Minerals Sci. Engg., v. 9, pp. 218-236.

Takahasi, E. and Kushiro, I. 1983 Melting of a dry peridotite at high pressures and basalt magma genesis. The American Mineralogist, v.68, pp.850-879.

Takahasi, E. and Scarfe, C.M. 1985 Melting of Peridotite to 14 GPa and the genesis of komatiite. Nature, v.315, pp.566-568.

Tatsumi, Y., Hamilton, D.L. and Nesbit, R.W. 1986 Chemical characteristics of fluid phase released from a subducted lithosphere and origin of arc magmas: Evidence from high pressure experiments and natural rocks. J.Volcano.Geoth.Res. v.29, pp.293-309.

Tatsumi, Y. and Ishizaca, K. 1982a Magnesian andesite and basalt from Shodo Shima Island, southwest Japan, and their bearing on calc-alkaline andesites. Lithos, v.15, pp.161-172.

Tatsumi, Y. 1982b Origin of high magnesian andesites in the Setouchi volcanic belt, southwest Japan, I. Petrological and chemical characteristics. Earth Planet. Sci. Lett., v.60, pp.293-304.

Tatsumi, Y. and Maruyama, S. 1989 Bonninites and high-Mg andesites: Teconics and petrogenesis. In: (Ed. A.J.Crawford) Bonninites, Unwin Hyman, London, pp.50-71.

Tatsumi, Y. 1981 Melting experiments on a high magnesian andesite. Earth Planet. Sci. Lett., v. 54, pp.357-365.

Tatsummi, Y. 1982 Origin of high magnesian andesites in the Setouchi volcanic belt, southwest Japan, II. Melting phase relations at high pressures. Earth and Planet. Sci. Lett., v.60, pp.305-317.

Kelemen, P.B., Johnson, K.T.M., Kinzler, R.J. and Irving, A.J. 1990 High field strength element depletions in arc basalts due to mantle-magma interaction. Nature, v.345, pp.521-524.

Taylor, S.R. 1967 The origin and growth of continents. Tectonophysics, v.4, pp.67.

Taylor, S.R. 1989 Growth of planetary crusts. Tectonophysics, v.161, pp. 147-156.

Taylor, S.R. and Mclennan, S.M. 1981 The composition and evolution of the continental crust: Rare earth element evidence from sedimentary rocks. Phil. Trans. R. Soc. Lond., v.301A, pp.381-399.

Taylor, S. R. and Mc lennan, S.M., 1985 The continental crust : it's composition and evolution .Blackwell Scientific publication,Oxford. pp. 302.

Thompson, G. 1984 Basalt-Seawater interaction. In: Rona, P.A. and Bostrom, K. (Eds.) Hydrothermal processes at seafloor spreading centres. New York, Plenum Press.

Thompson,R.N., Morrison, M.A., Hendry, G.L. and Parry,S.J. 1984 An assessment of the relative roles of crust and mantle in magma genesis. Phil.Trans.R.Soc.Lond. v.A310, pp.549-590.

Thompson, R.N., Morrison, M.A., Hendry, G.L. and Parry, S.J. 1984 An assessment of the relative roles of crust and mantle in magma genesis: An elemental approach. Phil. Trans. R. Soc. Lond. v.310A, pp.549-590.

Thompson, A.B. 1992 Water in the earth's upper mantle. Nature, v.358, pp. 295-302.

Thomson, R. N. 1982 Magmatism of the British Tertiary Volcanic Province. Scott. J. Geol. v. 18. pp.49-107.

Tobisch, O.T., Collerson, K.D., Bhattacharaya, T. and Mukhopadhyay, D. 1994 Structural relationships and Sr-Nd isotope systematics of polymetamorphic granitic gneisses and granitic rocks from central Rajasthan, India : implication for the evolution of the Aravalli Craton. Precamb. Res., v.65, pp. 319-339.

Viljoen, M.J. and Viljoen, R.P. 1969 The geochemical evolution of the granitic rocks of Barberton region. Geol.Soc., South Africa, Spl.Publ. v.2, pp.189-219.

Vinogradov, A.P. and Tugarinov, A.I. 1964 Geochronology of the Indian Precambrian. In : M.R. Subramanyam and A.K. Saha (eds.), Archaean and Precambrian geology. Rep. Int. Geol. Congr., 22nd, New Delhi.

Vinogradov, A.P., Tugarinov, A.I., Zhykov, C., Stapnikova, N., Bibikova, E. and Khorre, K. 1964 Geochronology of Indian Precambrian. Rep. Int. Geol. Congr. Sect. 10, pp.553-567.

Vocke, R.D., Hanson. G.N. and Gruenenfelder, M. 1979 The effects of low temperature metasomatism on REE distributions in Roffna Gneiss, Switzerland. EOS, Trans.Am.Geophys.Union v.60 pp.425.

Volpe, A.M. and Macdougell, J.D. 1990 Geochemistry and isotopic characteristic of the mafic (Phulad ophiolite) and related rocks in the Delhi Supergroup, Rajasthan, India : Implications for rifting in the Proterozoic. Precamb. Res., v.48, pp. 167-191.

Voshage, H., Hofmann, A.W., Mazzucchelli, M., Rivalenti, G., Sinnigoi, S., Raczek, I. and Demarchi, G. 1990 Isotopic evidence from the Ivrea zone for a hybrid lower crust formed by magmatic underplating. Nature, v.347, pp.731-736.

Walker, R.J., Shirey, S.B., Hanson, G.N., Rajamani, V. and Horan, M.F. 1989: Re-Os, Rb-Sr and O isotopic systematics of the Archean Kolar schist belt, Karnataka, India. Geochim. Cosmochim. Acta, v.52, pp.3005-3013.

Walsh, J.N., Buckley, F. and Barker, J. 1981 The simultaneous determination of the rare earth elements in rocks using inductively coupled plasma source spectrometry. Chem. Geol., v.33, pp.141-153.

Watson, E.B. 1976 Two liquid partition coefficients: experimental data and geochemical implications. Contrib. Min. Petr., v.56, pp.119-134.

Watson, E.B. 1982 Melt infiltration and magma evolution. Geology, v.10, pp.236-240.

Weiblen, P.W. and Roedder, E. 1973 Petrology of melt inclusions in Apollo samples 5598 and 62295, and of clasts in 67915 and several lunar soils. Proc. 4th Lunar Sci. Conf. Geochim. Cosmochim. Acta. Suppl., v.4, pp.681-703.

White, W.M. and Patchett, J. 1984 Hf-Nd-Sr isotopes and incompatible element abundances in Island arcs: Implications for magma origins and crust-mantle evolution. Earth Planet.Sc. Lett., v.67, pp.167-185.

Wiedenbeck, M. and Goswami, J.N. 1994 $^{207}Pb/^{206}Pb$ zircon geochronology using a small ion microprobe. Geochemioca et Cosmochimica Atca, v.58, pp.2135-2141.

Wienschenk, E. 1891 Beitrage zur petrographie Japans. Neues Jahrbuch fur Mineralogie, Geologie, und Palaontologie, Abhand-lungen, Abteilung B: Geologie, Palaontologie, v.7: pp.133-151.

Wilson, M., 1989 Igneous Petrogenesis- A global tectonic approach, Unwin Hyman Ltd. pp 466.

Wilson, M., Downes, H. and Cebria, J. 1995 Contrasting fractionation trends in co-existing continental alkaline magma series; Cantal, Massif Central, France. Jour. of Petrl. v.36, pp. 1729-1753.

Wood, D.A., Tarney, J., Saunders,A.D., Bougault, H., Joron, J.L., Treuil, M. and Cann, J.R. 1979 Geochemistry of basalts drilled in the north Atlantic by IPOD Leg 49: implications for mantle heterogeneity. Earth Planet. Sci. Lett. v.42 pp. 77-97.

Wyllie, P. J. 1982 Subduction products according to experimental prediction Geol. Soc.Am.Bull. v.93, pp. 468-476.

Yardely, B.W.D. 1990 An introduction to metamorphic petrology. English Language Book Society, pp.248.

Yogodzinski, G.M., Kay, R.W., Volynets, O.N., Koloskov, A.V. and Kay, S.M. 1995 Magnesian andesites in the western Aleutian Komandorsky region: Implication for slab melting and processes in the mantle wedge. GSA Bulletin, v.107, pp.505-519.

You, C.F., Castillo, P.R., Gieskes, J.M, Chan, L.H. and Spivack, A.J. 1996 Trace element behaviour in hydrothermal experiments: Implications for fluid processes at shallow depths in subduction zones. Earth Planet.Sci.Lett. v.40, pp.41-52.

Zachariah, Z.K. 1992 Geochemistry and Petrogenesis of amphibolites of Ramagiri gold fields, South India. Unpublished Ph.D Thesis, JNU, New Delhi, pp.187.

APPENDIX I

Table 1 The mineral chemistry of amphiboles which are coexisting with the plagioclase feldspars in amphibolites.

Sample #	J-29		J-35		J-68	
	Rim	Core	Rim	Core	Rim	Core
SiO_2	46.089	45.756	44.543	43.749	44.841	43.065
Al_2O_3	10.869	10.378	10.955	11.405	10.865	10.591
FeO	17.615	16.267	19.309	19.375	17.61	17.757
MgO	9.843	9.522	8.556	7.736	10.108	10.539
MnO	0.307	0.307	0.362	0.284	0.292	0.274
CaO	12.0	12.035	12.01	11.77	11.895	11.692
K_2O	0.338	0.349	0.559	0.511	0.912	1.105
Na_2O	1.194	1.309	1.496	1.365	1.296	1.392
TiO_2	0.441	0.525	0.671	0.635	0.358	0.606
Total	98.690	96.449	98.461	96.831	98.178	97.023
Cation based on 23 Oxygen						
Si	6.7976	6.874	6.6807	6.6702	6.6945	6.5533
Al	1.8885	1.8376	1.9366	2.0495	1.1912	1.8997
Fe	2.1727	2.0438	2.422	2.4705	2.1988	2.2599
Mg	2.1642	2.1325	1.913	1.7583	2.2496	2.3907
Mn	0.0383	0.0391	0.046	0.0367	0.0369	0.0353
Ca	1.18965	1.9373	1.9302	1.9227	1.9028	1.9064
K	0.0636	0.0669	0.1069	0.0995	0.1738	0.2146
Na	0.3415	0.3814	0.4352	0.4036	0.3753	0.4102
Ti	0.0489	0.0593	0.0757	0.0728	0.0402	0.0694
Total	15.4118	15.3720	15.5463	15.4838	15.5838	15.7401

Table 2 The mineral chemistry of 3 clinopyroxene grains of a meta-gabbro sample

Samp.#	Clinopyroxene-I		Clinopyroxene-II		Clinopyroxene-III	
J-18A	Rim	Core	Rim	Core	Rim	Core
SiO_2	52.572	53.230	52.837	52.474	53.142	53.430
Al_2O_3	0.843	0.198	0.671	0.8111	0.815	0.616
FeO	6.905	6.581	6.349	6.187	6.756	6.439
MgO	13.683	14.067	13.638	13.194	14.222	14.090
MnO	0.239	0.213	0.232	0.266	0.274	0.186
CaO	23.595	24.818	24.563	24.286	24.303	24.457
K_2O	---	---	---	0.020	0.014	---
Na_2O	0.407	0.266	0.310	0.579	0.359	0.400
TiO_2	0.063	0.031	0.053	---	0.069	0.011
Total	98.308	99.403	98.653	98.539	99.953	99.628
Cation based on 6 Oxygen for Pyroxene						
Si	1.9866	1.9916	1.9889	1.9786	1.9766	1.9899
Al	0.0375	0.0088	0.0298	0.0361	0.0357	0.0270
Fe	0.2182	0.2059	0.1999	0.1951	0.2102	0.2005
Mg	0.7708	0.7846	0.7653	0.7821	0.7886	0.7822
Mn	0.0076	0.0067	0.0074	0.0085	0.0086	0.0059
Ca	0.9554	0.9950	0.9907	0.9812	0.9686	0.9760
K	---	---	---	0.0010	0.0007	---
Na	0.0298	0.0193	0.0226	0.0423	0.0259	0.0289
Ti	0.0018	0.0009	0.0015	---	0.0019	0.0003
Total	4.0078	4.0128	4.0060	4.0250	4.0168	4.0108

Table 3 **Mineral chemistry of plagioclase co-existing with the amphiboles of Table 1 and clinopyroxene.**

Samp. #	J-18A		J-29		J-35		J-68	
	Rim	Core	Rim	Core	Rim	Core	Rim	Core
SiO_2	62.711	61.614	58.708	58.201	59.429	59.899	60.604	61.239
Al_2O_3	23.722	23.282	27.172	26.851	26.110	26.190	24.139	24.090
CaO	5.076	4.999	8.423	8.221	7.622	7.533	5.399	5.735
K_2O	0.118	0.125	0.053	0.037	0.083	0.061	0.115	0.118
Na_2O	9.84	8.989	7.416	7.165	7.694	8.375	9.362	9.617
Total	101.467	99.010	101.772	100.745	100.937	102.057	99.620	100.799
Cations based on 8 Oxygen								
Si	2.7502	2.7607	2.5847	2.5917	2.6310	2.6281	2.7112	2.7125
Al	1.2262	1.2296	1.4101	1.4093	1.3625	1.3544	1.2729	1.2577
Ca	0.2385	0.2400	0.3947	0.3922	0.3616	0.3541	0.2588	0.2722
K	0.0066	0.0072	0.0030	0.0021	0.0047	0.0034	0.0066	0.0066
Na	0.8367	0.7810	0.6381	0.6187	0.6605	0.7125	0.8121	0.8260
Total	5.0583	5.0185	5.0282	5.0140	5.0203	5.0526	5.0616	5.0750
ab mol %	77.34	75.96	61.60	61.08	64.33	66.59	75.37	74.72
an mol %	22.05	23.34	38.11	38.72	35.21	33.09	24.02	24.62
or mole%	0.61	0.80	0.29	0.20	0.46	0.32	0.61	0.66

APPENDIX II

Table 1 **Mineral chemistry of Feldspar Phenocryst of J-53A at different points along a line.**

Points	1	2	3	4	5	6	7	8
SiO_2	63.136	63.037	63.006	63.600	63.633	64.378	64.097	64.193
Al_2O_3	22.298	18.264	23.396	18.204	23.248	18.353	23.093	18.764
CaO	3.260	0.048	4.407	---	4.567	0.053	4.276	0.294
K_2O	0.148	16.090	0.128	16.005	0.171	16.099	0.118	15.032
Na_2O	9.948	0.781	9.850	0.732	9.512	0.871	9.928	1.332
Total	98.790	98.220	100.848	98.542	101.132	99.754	101.512	99.615
Cation (Based on 8 Oxygen)								
Si	2.8229	2.9763	2.7744	2.9876	2.7879	2.9878	2.7974	2.9726
Al	1.1751	1.0164	1.2132	1.0079	1.2006	1.0040	1.1879	1.0242
Ca	0.1562	0.0024	0.2077	---	0.2144	0.0026	0.2000	0.0146
K	0.0084	0.9692	0.0072	0.9592	0.0096	0.9532	0.0065	0.8881
Na	0.8624	0.0715	0.8402	0.0667	0.8081	0.0784	0.8401	0.1196
Total	5.0250	5.0358	5.0427	5.0214	5.0206	5.0260	5.0320	5.0191
ab mol %	83.97	6.85	79.63	6.50	78.30	7.58	80.27	11.70
an mol %	15.21	0.23	19.68	------	20.77	0.25	19.11	1.43
or mol %	0.82	92.91	0.68	93.50	0.93	92.17	0.62	86.87

Table 2 Average mineral chemistry of different feldspar phenocrysts of different sizes of sample #. J-53A.

Feldspar	Phenocryst I	Phenocryst II	Phenocryst III
SiO_2	63.494	62.629	64.356
Al_2O_3	20.557	20.335	18.232
CaO	2.193	1.875	0.003
K_2O	7.631	8.408	15.346
Na_2O	4.405	4.030	0.577
FeO	0.121	0.104	0.003
MgO	0.017	0.000	0.019
TiO_2	0.038	0.094	0.000
BaO	0.612	0.699	0.897
Total	99.068	98.173	99.430
Cation (Based on 8 Oxygen)			
Si	2.8985	2.8963	2.9991
Al	1.1061	1.1084	1.0015
Ca	0.1073	0.0929	0.0001
K	0.4444	0.4961	0.9124
Na	0.3899	0.3614	0.0521
Fe	0.0046	0.0040	0.0008
Mg	0.0012	0.0000	0.0000
Ti	0.0013	0.0033	0.0000
Ba	0.0110	0.0127	0.0164
Total	4.9643	4.9750	4.9824
ab mole %	41.41	38.03	5.4
an mole %	11.40	9.78	0.01
or mole %	47.19	52.19	94.59

APPENDIX III

Table 1 Comparison of biotite chemistry between low- and high-Ti sanukitoids (J-53A) and granodiorites (J-41).

Sample/ Mineral →	J-53/Biotite	J-66/Biotite I		J-66/Biotite II		J-41/Biotite I		J-41/Biotite II		J-66/Amphibole	
Element ↓	Average	Rim	Core	Rim	Core	Rim	Core	Rim	Core	Rim	Core
SiO_2	36.274	38.474	37.242	37.420	37.904	35.387	35.067	35.245	36.115	43.031	43.652
Al_2O_3	15.606	14.424	13.778	14.690	14.779	17.362	17.403	17.706	17.299	10.363	10.227
FeO	21.245	16.831	17.121	16.771	16.276	16.378	16.393	17.186	16.53	18.126	18.149
MgO	8.629	11.384	11.593	12.069	12.379	11.725	11.672	12.038	10.978	9.555	9.186
MnO	0.107	0.306	0.179	0.253	0.253	0.171	0.153	0.156	0.171	0.539	0.656
CaO	0.032	0.081	0.093	0.153	0.131	0.051	0.053	0.045	0.029	11.559	11.895
K_2O	10.276	9.854	9.907	9.407	8.437	9.797	9.554	10.000	10.018	1.118	1.100
Na_2O	0.087	------	0.136	0.041	0.113	-------	0.160	0.109	0.098	1.165	1.129
TiO_2	3.239	2.261	2.338	2.275	2.237	1.856	1.74	1.688	1.428	0.654	0.628
Total	95.495	93.616	92.387	93.055	92.510	92.728	92.195	94.173	92.665	96.112	96.623
Cation (Based on 22 oxygen for biotite and 23 oxygen for amphibole)											
Si	5.6041	5.8972	5.8246	5.7712	5.8226	5.4868	5.4689	5.4103	5.6026	6.622	6.6799
Al	2.8412	2.6060	2.5400	2.6704	2.6760	3.1731	3.1991	3.2037	3.1632	1.8797	1.8447
Fe	2.7454	2.1576	2.2394	2.1632	2.0910	2.1238	2.1381	2.2063	2.1447	2.3329	2.3228
Mg	1.9866	2.6011	2.7030	2.17448	2.8347	2.7101	2.7135	2.7546	2.5387	2.1920	2.0955
Mn	0.0140	0.0398	0.0237	0.0330	0.0330	0.0225	0.0202	0.0203	0.0225	0.0703	0.0850
Ca	0.0053	0.0134	0.0156	0.215	0.0215	0.0084	0.0089	0.0074	0.0048	1.9060	1.9505
K	2.0257	1.9269	1.9768	1.8509	1.6535	1.9380	1.9009	1.9583	1.9828	0.2196	0.2147
Na	0.0264	------	0.0412	0.0124	0.0338	-------	0.0483	0.0324	0.0294	0.3477	0.3351
Ti	0.3763	0.2606	0.2750	0.2639	0.2585	0.2165	0.2041	0.1949	0.1666	0.0757	0.0723
Total	15.6250	15.5026	15.6394	15.5613	15.4246	15.6792	15.7019	15.7883	15.6553	15.6460	15.6004
Fe/Fe+Mg	0.5802	0.4534	0.4531	0.4381	0.4245	0.4393	0.4407	0.4447	0.4579	0.97	0.5257